

PION DOUBLE CHARGE EXCHANGE FORMALISM

by

MAHER OMAR ELGHOSSAIN, B.Sc., M.Sc.

A DISSERTATION

IN

PHYSICS

Submitted to the Graduate Faculty  
of Texas Tech University in  
Partial Fulfillment of  
the Requirements for  
the Degree of

DOCTOR OF PHILOSOPHY

Approved

May, 1996

110  
801  
T3  
1996  
NO. 12  
Cop. 2

## ACKNOWLEDGEMENTS

FEB 6 11 00  
(11-25)

Praise be to God, the Cherisher and the Sustainer of the Worlds for giving me the power and patience to finish my doctoral research and to overcome the challenges along the way.

My great thanks and appreciation to my advisor Dr. M. A. K. Lodhi for his guidance, cooperation, understanding and advice to get this work completed. I am indebted to my research advisor Dr. W. R. Gibbs for his support, advice, numerous suggestions about additional work to be done, and the time he spent to check it and revise it. I would like to thank the other members of the committee for their advice, and the time they spent on reading this dissertation.

I would like to thank the Islamic University of Gaza for their support. Finally, my gratitude and appreciation to my family: my wife, Magdoleen, my children, Rasha, Reem, Rana, Luay, and my parents for their patience, understanding, care, encouragement, and moral support.

# TABLE OF CONTENTS

ACKNOWLEDGEMENTS	ii
ABSTRACT	v
LIST OF TABLES	vii
LIST OF FIGURES	viii
CHAPTER	
I. INTRODUCTION	1
1.1 The Pion	1
1.2 Pions In Search Of Dibaryons	2
1.3 Charge Exchange Reactions	3
1.4 Correlations	6
1.5 Objective	11
1.6 Motivation	15
II. THE PION DOUBLE CHARGE EXCHANGE OPERATOR	22
2.1 DCX Operator Using Plane Wave	22
2.2 General Formulation	24
2.3 Spin-independent Contribution	30
2.4 Double-spin-flip Term	31
2.5 Projected Operator	32
III. DOUBLE CHARGE EXCHANGE REACTIONS ON CALCIUM AND CARBON NUCLEI	36
3.1 Historical Background and Nuclear Structure	37
3.1.1 The Shell Model	38
3.1.2 The Seniority Model	39
3.1.3 DCX Operator Using Double Scattering	41
3.2 DCX Cross Section	43
3.3 Pion Optical Potential and Treatment of Distortions	44
3.4 Pion Absorption Correction	49
IV. REMOVING THE $\delta$ FUNCTION FROM THE DCX AMPLITUDE	54
4.1 The Appearance of the $\delta$ -function	56
4.2 The Correction for the $\delta$ Function	57
4.3 The Correction In Distorted Waves	60
V. RESULTS AND DISCUSSION	70

VI. CONCLUSIONS	92
REFERENCES	96
APPENDIX	
A. SPIN REDUCTION FOR THE DOUBLE-SPIN-FLIP TERM	99
B. CALCIUM CODE	101
C. SAMPLE OUTPUT RESULTS OF CALCIUM CODE	136
D. CARBON CODE	150
E. SAMPLE OUTPUT RESULTS OF CARBON CODE	173

## ABSTRACT

The behavior of the operator responsible for sequential pion double charge exchange (DCX) on nuclei has been investigated in the plane wave limit in order to study its extension in space especially the short-range part.

The DCX cross sections were calculated for Ca isotopes up to an incident pion energy of 300 MeV as two single-charge exchanges, using both the shell model and the seniority model. The effects of previously proposed modifications to the mechanism have been investigated at low energy, where a resonance-like structure in the energy dependence has been observed. One of the modifications that has been studied is the inclusion of pion true absorption in the pion optical potential, by extracting the coefficients which correspond to the calcium and carbon nuclei from existing data of pion absorption. The second effect studied is the removal of the delta function from the DCX amplitude (which originated from the idea of point-like pion-nucleon coupling), where the interaction extends over a finite region of space. This work was restricted to the sequential pion double charge exchange mechanism, which is generally believed to be dominant in many cases. These corrections have been studied in the plane wave and distorted wave modes.

The results of these calculations for calcium agree with the data for the energies above 200 MeV and partially agree below 200 MeV. The calculations were done for different pion-nucleon ranges ( $\alpha = 800, 600, 300$  MeV/c). The DCX cross sections were calculated for  $^{14}\text{C}$  up to 300 MeV of pion energy using two single

charge exchange (SCX) scattering steps on the valence nucleons and at different ranges  $\alpha$ . The results give a reasonable fit with data.

## LIST OF TABLES

1.1	Physical Properties of Pions and Other Related Hadrons	17
2.1	Table of $\lambda$ 's Calculated from the Phase Shifts of Reference [28]	35
4.1	Table of $g_L(r_1, r_2)$ Calculated from the Analytic and Numerical forms (Trapezoidal (t) and Simpson (s) rules).	68
4.2	Table of DCX Cross Sections, experimental from [24], and from this calculation for $^{42,44}\text{Ca}$ Analog State at $\alpha = 300$ MeV/c.	69

## LIST OF FIGURES

1.1	Isospin Selection Rule for Charge Exchange.	16
1.2	Sequential DCX Mechanism (SEQ).	16
1.3	Meson Exchange Current (MEC).	18
1.4	Six-Quark Bags (SQB).	18
1.5	Delta Resonance Interaction (DINT).	18
1.6	The $0^\circ$ cross sections as a function of energy for SCX transitions to analog states from $^{14}\text{C}$ (top crosses), and DCX transitions to analog states from $^{14}\text{C}$ and $^{18}\text{O}$ , the data (close and open circles at different time) from [24] and theoretical curves from [25, 26].	19
1.7	The DCX transition cross sections in $^{44}\text{Ca}$ as a function of energy [24] and the fit (open circles) from [9].	20
1.8	The DCX transition cross sections in $^{48}\text{Ca}$ as a function of energy [24] and the fit from [9].	21
5.1	Comparison of the classical and quantum-mechanical double - scattering cross sections at 100 MeV. The solid line represents the QM cross section with the $\delta$ -function included and the dash-dot curve the same quantity without it. The dashed line is the classical cross section.	74
5.2	Non-spin-flip and double-spin-flip DCX operators at $x=0$ ( $90^\circ$ ) as a function of energy at an internucleon spacing 1 fm. The solid line corresponds to the total, the dashed line to the DSF operator and the dash-dot line to NSF operator.	75
5.3	Absolute value of projected operator with (solid curve) and without(dotted curve) the inclusion of the double spin flip amplitude. The dash-dot curve is the absolute value of the sum without the $\delta$ -function.	76
5.4	Behavior as a function of energy of the two coefficients in Eq 2.38 as well as of the $\delta$ -function. $C^\pm \equiv  \lambda_0 \pm \lambda_1 k^2 ^2$ .	77



- 5.5 Behavior of the real and the imaginary part of  $r^2Q^\pm(r)$  as a function of  $r$  at 200 MeV. The oscillatory behavior of  $Q^+$  (dash-dot) and the total operator (solid) is apparent while  $Q^-$  (dash) is nearly constant. 78
- 5.6 Absolute value of the integrated operator  $\bar{Q}(R)$  from 1 fm at energies a) 200 MeV and b) 50 MeV as a function of  $R$ . The dotted curve gives  $\bar{Q}^+(R)$ , the dash-dot curve  $\bar{Q}^-(R)$  and the solid curve is the sum of the two. 79
- 5.7 Values of the coefficient of  $\rho^2$ ,  $W$ , which represent pion true absorption versus energy. 80
- 5.8 The DCX cross sections calculations for Ca isotopes to the isobaric analog state at  $10^\circ$ . The curves shown are obtained from full DWIA calculations (solid curve), DWIA calculations with non-spin-flip amplitudes (small and large dashes), pion energy up to 300 MeV, and  $\alpha = 800$  MeV/c. The data are from ref. [24]. 81
- 5.9 The DCX cross sections calculations for Ca isotopes to the ground state at  $10^\circ$ . The curves shown are obtained from full DWIA calculations (solid curve), DWIA calculations with non-spin-flip amplitudes (dash-dot), pion energy up to 300 MeV, and  $\alpha = 800$  MeV/c. The data are from ref. [24]. 82
- 5.10 The DCX cross sections calculations for Ca isotopes to the isobaric analog state at  $10^\circ$ . The curves shown are obtained from full DWIA calculations (solid curve), DWIA calculations with non-spin-flip amplitudes (dot-das), pion energy up to 300 MeV, and  $\alpha = 600$  MeV/c. The data are from ref. [24]. 83
- 5.11 The DCX cross sections calculations for  $^{44}\text{Ca}$  isotopes to the ground and analog state at  $10^\circ$ . The curves shown are obtained from full DWIA calculations (solid curve), DWIA calculations with non-spin-flip amplitudes (dot-dash), pion energy up to 300 MeV, and  $\alpha = 300$  MeV/c. The data are from ref. [24]. 84
- 5.12 The DCX cross sections calculation for the reaction  $^{14}\text{C}(\pi^+, \pi^-)^{14}\text{O}$  DIAS at  $5^\circ$ . The curves shown are obtained from full DWIA calculations (solid curve), DWIA calculations with non-spin-flip amplitudes (dot-dash), pion energy up to 300 MeV and  $\alpha = 300$  MeV. The data are from ref. [24]. 85

- 5.13 The DCX cross sections calculation for the reaction  $^{14}\text{C}(\pi^+, \pi^-)^{14}\text{O}$  DIAS at  $5^\circ$ . The curves shown are obtained from full DWIA calculations (solid curve), DWIA calculations with non-spin-flip amplitudes (dot-dash), pion energy up to 300 MeV and  $\alpha = 500$  MeV. The data are from ref. [24]. 86
- 5.14 The DCX cross sections calculation for the reaction  $^{14}\text{C}(\pi^+, \pi^-)^{14}\text{O}$  DIAS at  $5^\circ$ . The curves shown are obtained from full DWIA calculations (solid curve), DWIA calculations with non-spin-flip amplitudes (dot-dash), pion energy up to 300 MeV and  $\alpha = 800$  MeV. The data are from ref. [24]. 87
- 5.15 DCX cross sections for  $^{48,44}\text{Ca}$  ground state (g) at  $10^\circ$ . The curves shown are obtained from full DWIA and shell model (Sh) calculations, total (solid), no  $\delta$ -function (dash-dot), seniority model (Sn) total (dash), and (Sn) no  $\delta$ -function (dot), with  $\alpha=300$  MeV/c. The data are from ref. [24]. 88
- 5.16 DCX cross sections for  $^{48}\text{Ca}$  both analog (an) and ground state (g) at  $10^\circ$ . The curves shown are obtained from full DWIA and seniority (Sn) model calculations, total (solid), no  $\delta$ -function (dash-dot), no DSF (dot), no DSF and no  $\delta$ -function (dash), and with  $\alpha= 800$  MeV/c. The data are from ref. [24]. 89
- 5.17 DCX cross sections for  $^{44}\text{Ca}$  both analog (an) and ground state (g) at  $10^\circ$ . The curves shown are obtained from full DWIA and seniority (Sn) model calculations, total (solid), no  $\delta$ -function (dash-dot), no DSF (dot), no DSF and no  $\delta$ -function (dash), and with  $\alpha=300$  MeV/c. The data are from ref. [24]. 90
- 5.18 DCX cross sections for  $^{42}\text{Ca}$  analog (an) state at  $10^\circ$ . The curves shown are obtained from full DWIA and seniority (Sn) model calculations, total (solid), no  $\delta$ -function (dash-dot), no DSF (dot), no DSF and no  $\delta$ -function (dash), and with  $\alpha=300$  and 600 MeV/c. The data are from ref. [24]. 91

# CHAPTER I

## INTRODUCTION

The study of nuclear structure using different particles as probes is very important in nuclear physics. These particles include electrons, protons, neutrons, and pions. For this work only the pion will be used to study the double charge exchange (DCX) operator and to calculate the corresponding cross sections for calcium and carbon nuclei.

### 1.1 The Pion

Pions can carry electric charges of  $+e$ ,  $-e$ ,  $0$  and are thus denoted by  $\pi^+$ ,  $\pi^-$ ,  $\pi^0$ . The  $\pi^+$ ,  $\pi^-$  are antiparticles to each other and  $\pi^0$  is its own antiparticle. One of the most important properties of the pion which makes it (see Table 1.1) attractive as a nuclear probe is its light mass. The mass of the charged [1] pion is  $m_{\pi^\pm} = 139.6$  MeV and that of the neutral pion is  $m_{\pi^0} = 135.0$  MeV. This makes the pion the lightest of the strongly-interacting particles having about  $1/7$  of the mass of the nucleons. As a result, a nucleon in the nucleus remains nearly stationary during the scattering process. The charged pion has a relatively long lifetime (26 ns) which allows beams of charged pions to be transported over reasonable distances. The dominant decay mode of the charged pion is  $\pi^\pm \rightarrow \mu^\pm \nu_\mu$  (100%). A rough estimate of the mean decay length  $\lambda$  of the charged pion is given by  $\lambda = \frac{pc}{mc^2} c\tau = 5.56$  p cm where  $p$  is the pion laboratory momentum

in MeV/c,  $mc^2$  is the pion rest energy in MeV and  $\tau$  is the mean life time in sec.

The neutral pion has a lifetime of  $0.83 \pm 0.06 \times 10^{-16}$  s and a dominant decay mode of  $\pi^0 \rightarrow \gamma\gamma$  (99%).  $\pi^0$  has lifetime which is too short to be used as a beam. The pion is a spin  $J^\pi = 0^-$  boson, (pseudoscalar), total isospin,  $I=1$  (isovector). The fact that it has spin zero simplifies the algebra of the basic  $\pi$ -n interaction.

There are several features of  $\pi$ - nucleus interaction that are different from nucleon-nucleus interaction. Pion absorption has a drastic effect on the nucleus, because it deposits 140 MeV in the nucleus. The three charge states allow the pion to undergo double charge exchange in pion nucleus scattering. The single charge exchange reaction can be also studied in addition to elastic and inelastic scattering. Another useful feature about the pion as a probe is that the  $\pi$ - n interaction is simple to describe theoretically in the isospin  $I= 3/2$  state (i.e.,  $\pi^+p$  or  $\pi^-n$  interaction). In addition, the  $I= 3/2$  state is much stronger than the  $I=1/2$  state in the energy range from 50 to 400 MeV.

### 1.2 Pions In Search Of Dibaryons

The search for dibaryons started with nucleon-nucleon elastic scattering, then it quickly spread to include every reaction which involves two baryons, especially pion double charge exchange. Dibaryons have the baryon number,  $B=2$ , which includes  $NN$ ,  $N\Delta$ ,  $NN^*$ ,  $\Delta\Delta$ , .. . Of the dibaryons, we know only the deuteron. So, the discovery of a new dibaryon would be of great significance. Pion DCX was one of the tools which was used to search for dibaryons. In experiments [2] with

high statistics and good resolution (FWHM=1.5MeV), the measurement of the reaction  $d(\pi^-, \pi^+)\pi^- nn$ , shows no evidence of any resonant structure in the region 2000 MeV to 2070 MeV.

### 1.3 Charge Exchange Reactions

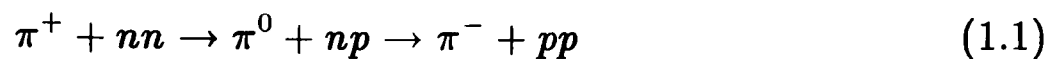
The isospin  $I=1$  of the pion permits two types of charge exchange reactions on nuclei:

1. Single-charge exchange (SCX) processes  $A(\pi^\pm, \pi^0)X$  with a change  $\Delta I_3 = \pm 1$  of the nuclear isospin.
2. Double-charge exchange (DCX) processes  $A(\pi^+, \pi^-)X$  and  $A(\pi^-, \pi^+)X$  with a  $\Delta I_3 = \pm 2$  of the nuclear isospin.

A diagram of the isospin states that can be reached by SCX and DCX reactions is shown in Figure 1.1 illustrating the selection rules in these processes. In the  $\Delta$ -resonance region at  $T_\pi=180$  MeV (the lowest nucleon excited state with spin and isospin equal to  $3/2$  and a mass of 1232 MeV) the ratios  $\sigma_r:\sigma_{SCX}:\sigma_{DCX}$  between reaction, single and total charge exchange cross-sections are typically 100:10:1.

The double-charge-exchange process is one of the rarer forms of pion reaction. The particular interest in this reaction is a consequence of its second order nature. For example, if a positive pion, entering the nucleus, is to emerge as a negative pion by exchanging its charge with the nucleons, then the process must take place in at least two stages, converting the two different neutrons into protons. Interest

in the reaction, as a nuclear structure tool, originated in the early 1960's. This interest can be related to the fact the DCX changes the charges of two nucleons. The simplest mechanism for this process is two successive SCX scatterings, for example



The isobaric-analog state (IAS) and Double-isobaric analog state (DIAS) in SCX and DCX, respectively, have a special role in pion charge exchange reactions since the initial and the final nuclear wave functions for these states are identical except for isospin projection. IAS are states which have the same total isospin, spin structure, and spatial structure, but a different third component of isospin  $I_z$ . They are states in different nuclei of the same  $A$ , but different  $N$  and  $Z$ , which have the same number of nucleons in each shell-model orbit. Since  $\pi N$  elastic scattering cross sections are generally much larger than inelastic cross sections at low energy, it is natural to assume that nucleons on which charge exchange has occurred remain in the same orbit is more likely than inelastic charge exchange in which the charge exchanged nucleon changes orbits. The analog states are generated by applying the isospin raising operator to the initial state.

The IAS is generated with  $I_+$  and the DIAS is generated with  $(I_+)^2$ . Since the final wave function is almost identical to the initial wave function, the charge exchange reactions to analog states behave very much like elastic scattering and the use of the optical potential for the reactions is suggested. Since the types of

calculations are generally straightforward, most theoretical approaches try to calculate DCX using the impulse approximation, and add the second-order terms to try to fit the data.

The second-order terms describe mechanisms such as correlations, scattering from deltas and mesons-exchange currents, and pion absorption. There are two regions where the double charge exchange reaction has been studied:

1. The low-energy region:

At low energy the mean free path of a pion in the nucleus is large. Each single-charge exchange in this process is dominated by the spin-averaged s- and p-wave amplitude proportional to:

$$\lambda_0 + \lambda_1 \mathbf{q} \cdot \mathbf{k} \quad (1.2)$$

where  $\mathbf{k}$  is the intermediate momentum in the two-step process, and  $\lambda_0$  and  $\lambda_1$  are the coefficients of s-wave and p-wave for pion nucleon scatterings.

The particularly interesting energy region is  $T_\pi=50$  MeV. At this energy the  $\pi N$  forward single-charge exchange amplitude nearly vanishes due to the destructive interference between s- and p-wave components. One of the interesting facts about the DCX at 50 MeV is that the double-charge exchange analog cross-section is very nearly constant as a function of the nuclear mass number  $A$  [3]. For analog transitions the DCX process is expected to take place on the two valence neutrons. This process is controlled

by the correlation properties of the valence pair at a typical distance of about 1 fm [4] which is a common feature of a variety of  $I=1$  nuclei.

## 2. The $\Delta$ (1232) region:

In this energy region ( $T_\pi = 180$  MeV), the double-charge exchange process generally exhibits strong diffractive features as a consequence of the short pion mean free path. The pion-nuclear elastic scattering in the  $\Delta$  region can be considered as scattering from a black disc. On the other hand, the DCX process shows the characteristic pattern associated with coherent emission from the diffuse edge of a disc. The dependence of the DCX cross-sections on the nuclear mass number has qualitatively similar geometric features. One expects for uncorrelated nucleons that the forward DCX cross-section to the analog states falls off with nuclear mass number  $A$  as in [5]:

$$\frac{d\sigma(\theta = 0^\circ)}{d\Omega} \propto (N - Z)(N - Z - 1)A^{-\frac{10}{3}} \quad (1.3)$$

The DCX can be calculated by considering the  $\Delta$ -dominated sequential charge exchange as in Figure 1.5 of the next section.

### 1.4 Correlations

The distribution of the nucleons relative to each other is a critical element in the description of the nuclear structure of the nucleus. The study of short-range two-body correlations is a very important subject which can not be carried out by reactions which involve only a single nucleon. There have to be at least two



nucleons in order to know about the correlation characteristics of the two nucleons involved (position, spin, isospin and angular momentum). One type of correlation can be explained as interdependence of the coordinates of a pair of nucleons (i.e., the spin, isospin and the spatial coordinates). It is difficult to measure these correlations by any direct means even though there are many aspects of nuclei, such as their spectra, which depend critically on the relative separation of the nucleons. Other than the spectra themselves there are several techniques to measure the nucleon correlations using different kinds of probes, some of which are described below.

### 1. Electron Scattering:

The electromagnetic probe has been used to study nucleon-nucleon short range correlations. For example, considering the reaction  ${}^3\text{He}(e,e'pp)n$  [6], a two-body correlation function in  ${}^3\text{He}$  can be extracted. The kinematics where the two protons are emitted symmetrically with respect to the virtual photon in the laboratory allows the the extraction of the correlation function in the initial state after correcting for the final state interactions.

### 2. Pion Absorption:

Pion absorption or pion production can be another tool for studying nucleon-nucleon correlations [7]. Following the absorption of a low energy pion on a pair of a nucleons, they recoil with relative momentum  $p_r = \sqrt{M} = 1.8 \text{ fm}^{-1}$ . This implies that nucleon pair separation distances as of the order 0.54 fm can

be studied by analysis of the absorption process. The short-range correlations in  $^3\text{He}$  [7] can be investigated by extending the calculation of total absorption rates for negative pions in  $^3\text{He}$  to the three-body spectrum of nucleons in the final state. Some information about short-range nucleon-nucleon correlations in the ground state of He has been obtained in this manner.

### 3. Two-Nucleon Transfer Reaction:

The (p,t) and (t,p) reaction mechanism has been studied by considering both the simultaneous two-nucleon transfer (SIM) (p-t or t-p) and the sequential (SEQ) (p-d-t or t-d-p) mechanisms. For example, in the reactions  $^{22}\text{Ne}(p,t)^{20}\text{Ne}$  and  $^{40}\text{Ca}(t,p)^{42}\text{Ca}$  [8], the sequential was found to be dominant or comparable to the SIM mechanism. The information extracted from these reactions is unreliable because of the uncertainty in the reaction mechanism.

### 4. Pion DCX Reactions:

Pion double charge exchange (DCX) offers one of the most promising possibilities for studying correlations among nucleons in nuclei since it requires at least two interactions for the process to take place. There have been a number of studies [9, 10], and it has now been demonstrated [11] that the reaction is indeed sensitive to nucleon-nucleon correlations. There are several possibilities offered for pion double charge exchange reaction mechanisms which can be classified as:

## 1. Optical Potential:

The general isospin structure of the optical potential is:

$$U = U_0 + (I_\pi \cdot I_A)U_1 + (I_\pi \cdot I_A)^2U_2 \quad (1.4)$$

where  $I_\pi$  is the isospin of the pion and  $I_A$  is isospin of the nuclear target.  $U_0$ ,  $U_1$ , and  $U_2$  are referred to as the isoscalar, isovector, and isotensor components of the optical potential.  $U_0$  is determined by elastic scattering,  $U_1$  is sensitive to IAS cross sections,  $U_2$  is sensitive to DIAS cross sections. The optical potential given above has been used to perform an analysis at 164 MeV data for elastic, IAS, and DIAS scattering. The results [12] are quite sensitive to short-range correlations.

## 2. Sequential Mechanism (SEQ):

Sequential mechanism means that an incident  $\pi^+$  exchanges its charge with a neutron to produce a  $\pi^0$ , which propagates to another neutron where it exchanges its charge to produce a  $\pi^-$ , that then leaves the nucleus. This picture for sequential scattering is illustrated in Figure 1.2. The sequential scattering process discussed above has both long and short-range components [13]. The correlations contained within the shell model [4, 14] wave functions are adequate to give a satisfactory account of much of the data for both IAS and DIAS transitions at 50 MeV.

### 3. Meson Exchange Current (MEC):

In this mechanism, the incident  $\pi^+$  knocks out a virtual pion from the pion cloud of a neutron and is absorbed on a second neutron [15] as shown in Figure 1.3.

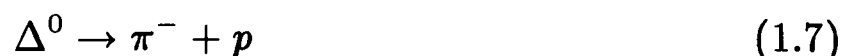
### 4. Six-Quark bags (SQB):

A  $\pi^+$  is absorbed by an up (u) (in a bag having the quantum numbers of the two neutrons) quark and a  $\pi^-$  emitted by a down quark (d) as shown in Figure 1.4. The calculations agree with the small angle data for the 50 MeV DCX reaction on  $^{14}\text{C}$  and  $^{18}\text{O}$  [16], but the 6-quark bag model is generally not as successful as the sequential mechanism.

### 5. Delta Interaction (DINT):

In the  $\Delta$ -interaction (DINT) a neutron from the target nucleus absorbs an incoming  $\pi^+$  and subsequently emits  $\pi^+$  which is absorbed by another neutron to become a proton by interacting with the  $\Delta^+$  in the intermediate state.

The final  $\Delta^0$  emits a  $\pi^-$  leaving a proton behind. This is shown in Figure 1.5.



In this, case the cross section is very sensitive to the incoming pion energy in the resonance region. It is therefore argued that DINT is energy dependent

because of the  $\Delta$  propagator in it. The DINT proceeds entirely through the  $\Delta$  and is purely P-wave while the SEQ has contributions from both the S-wave and P-wave pion-nucleon scattering amplitudes. The isovector S-wave amplitude is moderately large in the resonance region and interferes destructively with the P-wave amplitude below resonance and constructively above resonance. The DINT mechanism has been found to be dominant in non-analog transitions (nuclei with  $N=Z$ ), which cause nucleons in the final state to change orbit from the initial state [17]. This implies a likely change in the angular momentum between the initial and final state.

### 1.5 Objective

This work presents a study of the DCX reaction in the intermediate energy range up to 300 MeV, which will include the following:

#### 1. The DCX Operator:

The behavior of the operator responsible for pion DCX in nuclei will be investigated in the plane wave limit, and the effect of spin-flip and non spin-flip will be studied. The aim of this study will be to gain a qualitative understanding of the sequential DCX operator, which will be useful for those who want to see how sensitive DCX is to particular models of nuclear structure.

In addition to a knowledge of the dependence of the cross section on the correlation structure, the DCX operator itself is of interest in order to know

at what internucleon distances the nuclear wave functions are being tested.

In Chapter II, only the sequential operator will be considered. This study does not treat those based on  $\Delta$  interactions[18] or mesonic interactions with virtual mesons[19] although both of those mechanisms may be important in certain cases. There are several reasons for studying the DCX (or more generally, the double scattering) operator:

- (a) The range of the operator is not well known.
- (b) The form of the operator has never been explicitly given. The normal calculation is done by performing the integrals over the nuclear wave function first and then doing the integral over intermediate momentum of the neutral pion. It is useful to have approximate formulas for the operator to test the shell and other models of nuclear structure. DCX is very sensitive to correlation structure of the nuclear wave functions. Although implicit in many specific calculations, the explicit form of the DCX operator, including processes in which both nucleons flip their spins, has not, to our knowledge, been given. The operators are particularly simple for forward DCX. These forms will be useful for those who want to see how sensitive DCX is to particular models.
- (c) It has been observed in both distorted wave and plane wave calculations that the introduction of the double-spin-flip amplitude decreases the cross section. This reduction seems to be present independent of the

distortion (and some other factors, such as nuclear size). Because of the robustness of the destructive-interference effect, it is natural to suspect that the cancellation is inherent in the DCX operator itself. Thus, in order to obtain some understanding of this cancellation, a simple model can be examined.

- (d) The plane-wave DCX operator resembles the one-pion-exchange potential since the dominant (or only) coupling to the nucleon is p-wave in nature. In both operators there is a  $\delta$ -function present in the relative spatial coordinate. The debate regarding the removal of the  $\delta$ -function from the DCX operator is no doubt similar to that of the case of nucleon-nucleon potential. However, for pion double charge exchange the possibility of a test by the direct measurement of cross sections exists, giving an alternative to inferences from nucleon-nucleon scattering.

## 2. The Calculation Of DCX Cross Sections For Calcium and Carbon Nuclei:

In Chapter III, the pion double charge exchange in the nuclear shell and seniority model will be studied. One of the problems that will be treated in the chapter is the variation of the DCX cross section to the double isobaric analog states (DIAS) with the number of excess neutrons in a given shell (see Eq. 1.3) [9]. The DCX cross sections will be calculated in both the shell model and seniority model for  $^{42,44,46,48}\text{Ca}$  up to 300 MeV of pion energy. The ground state and the Double Isobaric Analog State (DIAS) are included in the calculations[9].

A computer code (Appendix B) is used for the calculation of the cross sections for Ca isotopes which solves for the final state wave function of the pion using a finite range nonlocal potential which describes the propagation of the pion. The same technique is used in another code for  $^{14}\text{C}$  which calculates the DCX cross sections.

Correction has been included for pion true absorption by including a purely imaginary term in the optical potential [20]. The values of the absorption coefficient  $W$  for Ca have been determined by comparison of the predicted true absorption cross sections with the experimental values of nearby nuclei [21, 22, 23].

For this purpose, the code has been modified to calculate the absorption cross section and reproduce the one which is expected from the experimental results. From this the values of  $W$  will be determined. Also, the  $W$ 's corresponding to  $^{14}\text{C}$  are determined by scaling those for calcium.

The cross section is calculated in the code for DIAS as a function of the number of excess neutrons for any shell-model orbit  $j$  up to  $j=13/2$  for excess neutrons only. There are only two amplitudes regardless of the size of the shell. One of these amplitudes corresponds to monopole transitions while the second amplitude corresponds to the short range part (quadrupole) and it is identified as a measure of the correlated part of the shell-model wave function. The sequential reaction mechanism in which the pion undergoes two single charge exchange



scatterings on valence neutrons has been used. This two-step process has no restriction on the angular momentum and is believed to be the dominant.

The calculations of the DCX cross sections for carbon (Appendix D) and calcium nuclei will be performed in the plane wave impulse approximation (PWIA) as a check, and the distorted wave impulse approximation (DWIA).

### 1.6 Motivation

The main reason for studying the mechanism is to increase our knowledge about nucleon-nucleon correlations, especially the short range part, and to get more information about the nuclear structure of calcium and carbon. One of the objectives of the study is to see if the resonance-like structure around 50 MeV can be explained without the assumption of dibaryons. Most of the data which are already available on DCX reaction for Ca and C show the energy dependence of both DIAS and ground state for  $f^{7/2}$ -shell nuclei, where the cross sections have peaks at energies below 70 MeV and are almost flat at energies above 200 MeV. For  $^{42}\text{Ca}$  a sharp peak at 50 MeV is evident (see Figures 1.6, 1.7, and 1.8 taken from [24]).

The normal assumption gives a peak in the general area but precise quantitative agreement is lacking. The removal of the delta function may change that (for the better or for the worse). Modifications to the above calculations will be included, like pion true absorption correction, and delta function removal from

the DCX amplitude which originated from the idea of point-like pion-nucleon interaction, since it extends over short region of space.

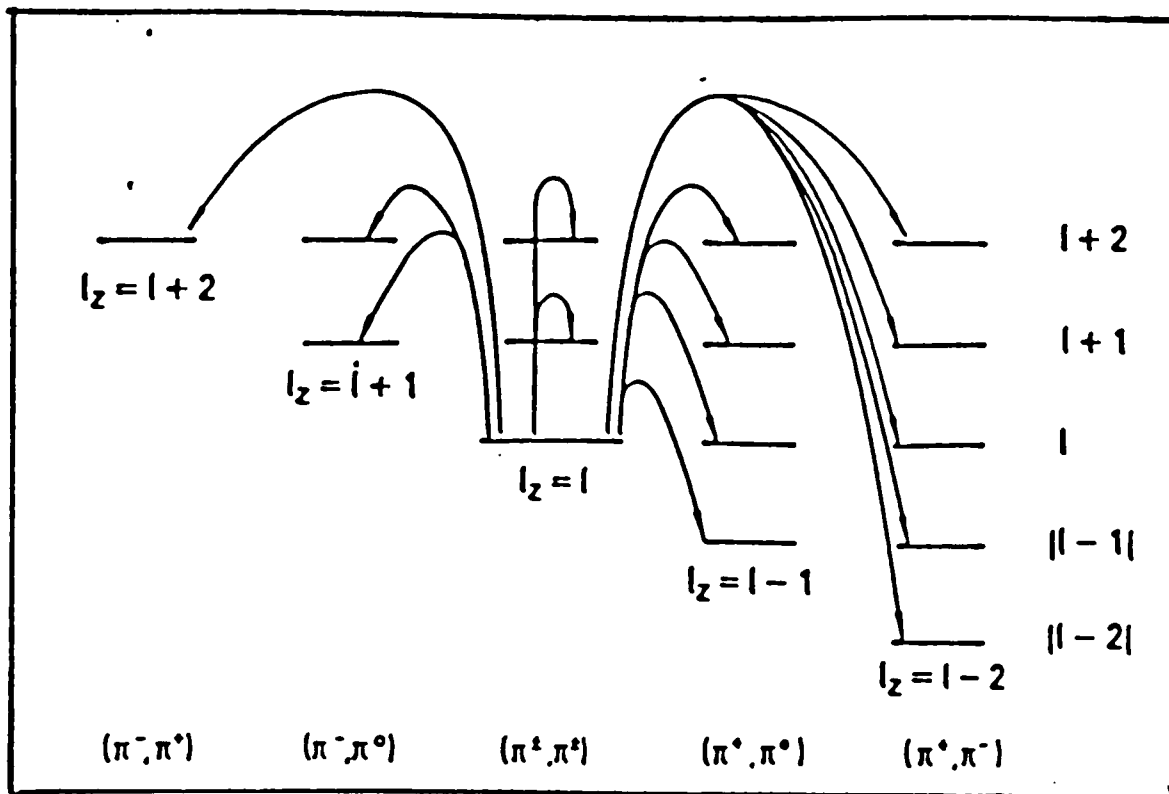


Figure 1.1: Isospin Selection Rule for Charge Exchange.

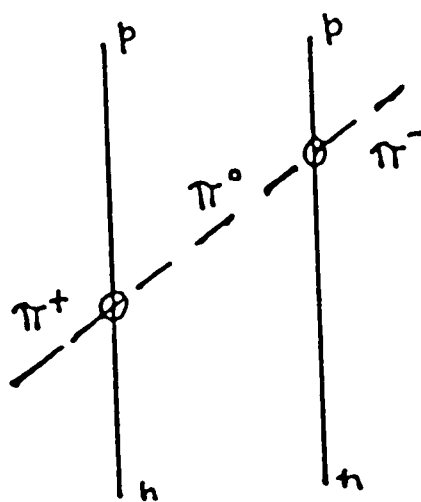


Figure 1.2: Sequential DCX Mechanism (SEQ).

Table 1.1: Physical Properties of Pions and Other Related Hadrons

Particles	MASS	$J^\pi$	Mean Life	Decay Mode	Quarks content
$\pi^+, \pi^-$	139.56	$0^-$	$2.603 \times 10^{-8} \text{ s}$	$\pi^\pm \rightarrow \mu^\pm \nu_\mu$	$\pi^+(u\bar{d}), \pi^-(\bar{u}d)$
$\pi^0$	135.0	$0^-$	$0.83 \times 10^{-16} \text{ s}$	$\pi^0 \rightarrow \gamma\gamma$	$(u\bar{u} - d\bar{d})/\sqrt{2}$
Proton(p)	938.3	$1/2^+$	$> 10^{31} \text{ y}$	-	(uud)
neutron(n)	939.6	$1/2^+$	898 s	$n \rightarrow e^- \bar{\nu}$	(udd)
$\rho$	770	$1^{--}$	$\Gamma(\rho)=153 \text{ MeV}$	$\rho \rightarrow \pi\pi$	$\rho^+(ud), \rho^-(\bar{u}d)$
$\omega$	783	$1^{--}$	$\Gamma(\omega)=9.8 \text{ MeV}$	$\omega \rightarrow \pi\pi\pi$	$\omega^0(u\bar{u} + d\bar{d})/\sqrt{2}$

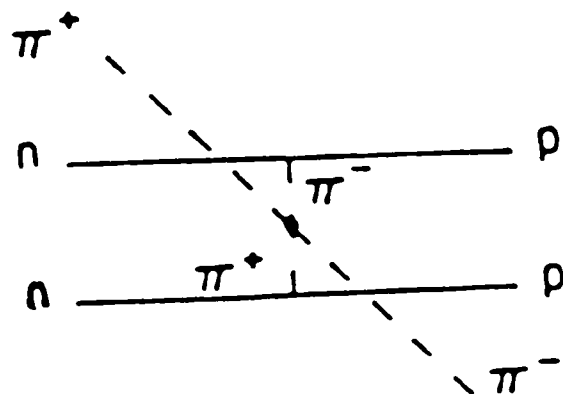


Figure 1.3: Meson Exchange Current (MEC).

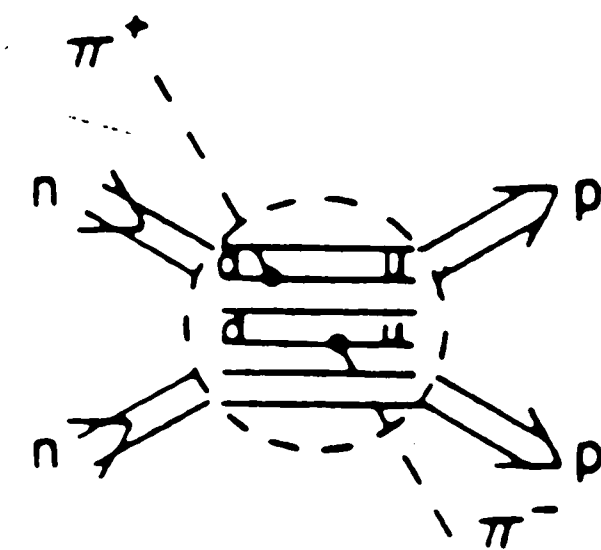


Figure 1.4: Six-Quark Bags (SQB).

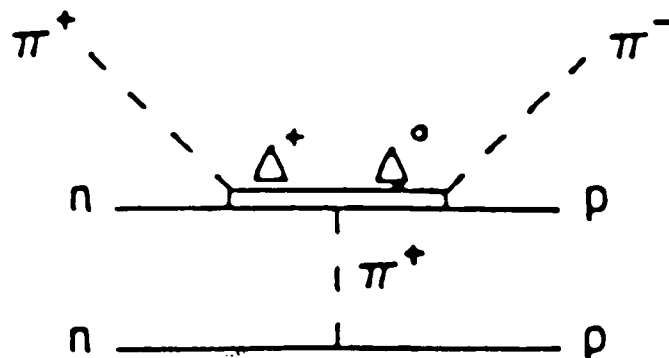


Figure 1.5: Delta Resonance Interaction (DINT).

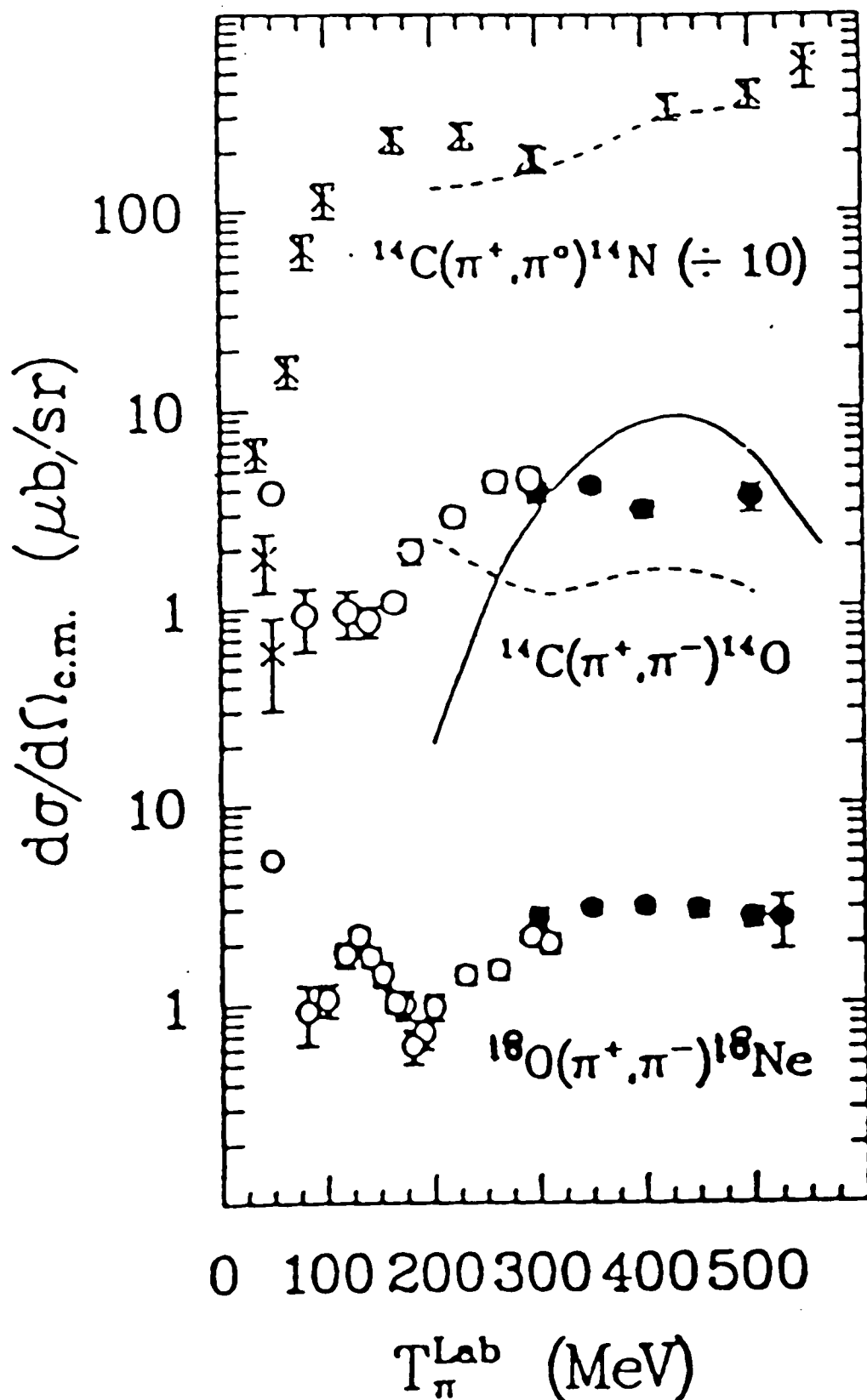


Figure 1.6: The  $0^\circ$  cross sections as a function of energy for SCX transitions to analog states from  $^{14}\text{C}$  (top crosses), and DCX transitions to analog states from  $^{14}\text{C}$  and  $^{18}\text{O}$ , the data (close and open circles at different time) from [24] and theoretical curves from [25, 26].

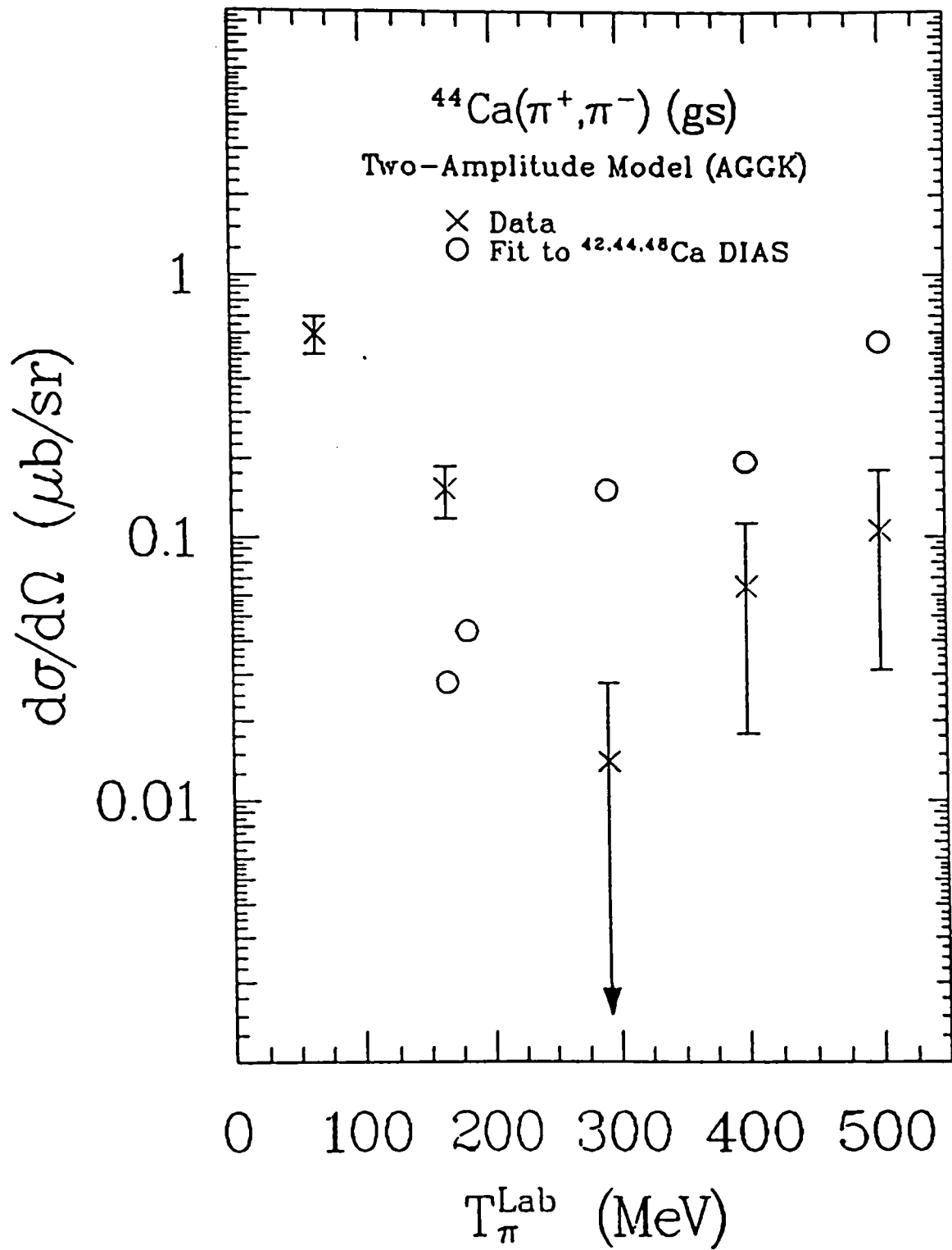


Figure 1.7: The DCX transition cross sections in  $^{44}\text{Ca}$  as a function of energy [24] and the fit (open circles) from [9].

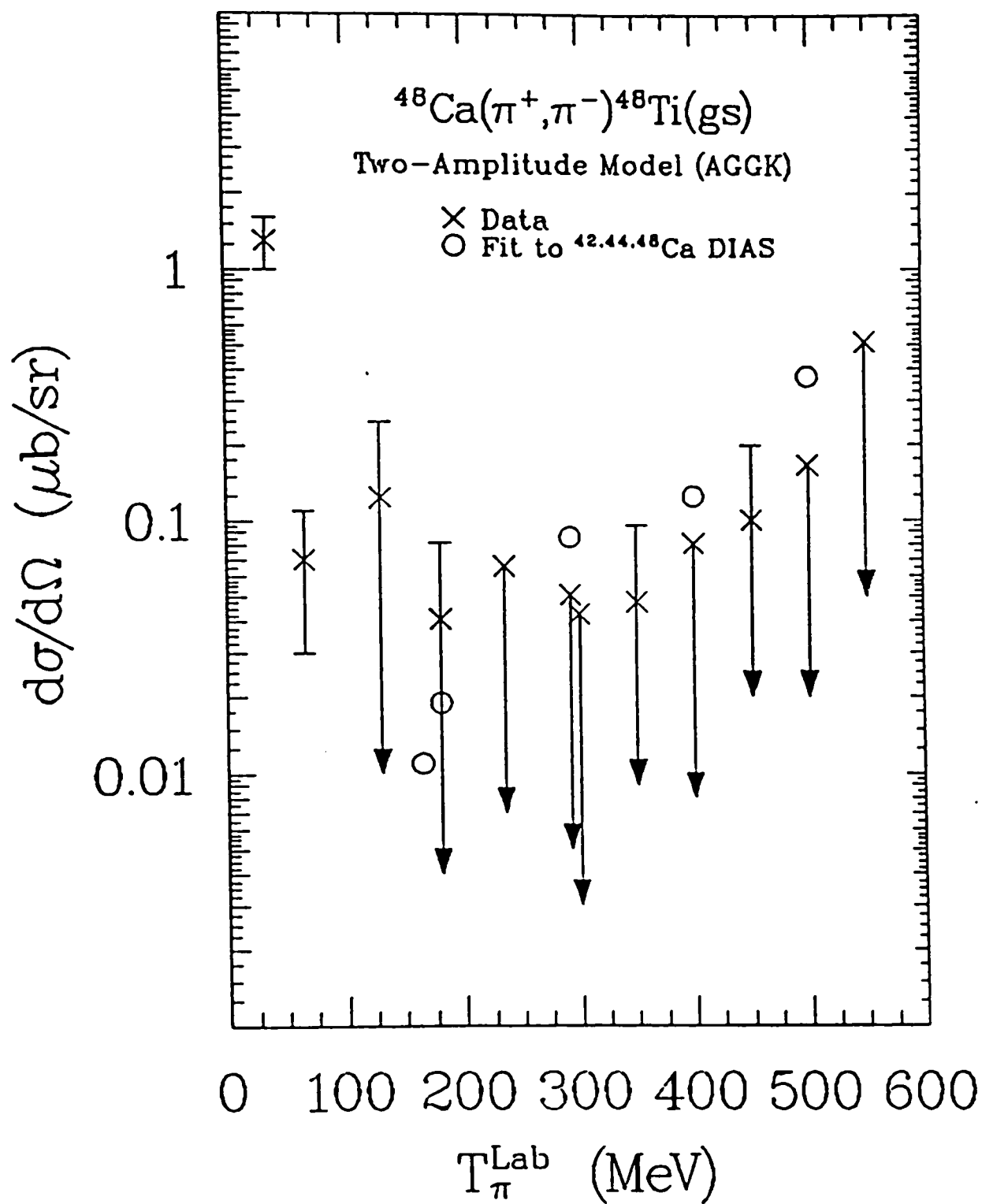


Figure 1.8: The DCX transition cross sections in  $^{48}\text{Ca}$  as a function of energy [24] and the fit from [9].

CHAPTER II  
THE PION DOUBLE CHARGE EXCHANGE  
OPERATOR

2.1 DCX Operator Using Plane Wave

This chapter contains a summary of the results from this work published in [27]. We concentrate here primarily on the reaction which takes place on two active neutrons external to an inert core. If their angular momentum is non-zero, they may be coupled to other external neutrons (as in the case of the calcium isotopes) to form a spin-zero ground state.

From somewhat indirect arguments it has been inferred [13, 4] that the principal internucleon spacing being sampled is the order of 1 fm. This range is determined by the following three elements.

1. The intrinsic coordinate dependence of the DCX operator,  $\tilde{F}$ , itself. This operator is an intricate function of the coordinates of the active nucleons.
2. The nuclear wave function or two-body density matrix: The correlations, even in a simple shell model, strongly affect the number of close neutron pairs, and therefore greatly influence the DCX cross section. The DCX cross section is obtained, in the impulse approximation, by integrating  $\tilde{F}$  over the nuclear wave function.
3. The pion-nuclear optical potential: The pion wave function is distorted by the nuclear medium. For example, the absorptive nature of the potential



tends to suppress DCX for configurations in which the nucleons are widely spaced; conversely, a pion-nucleon resonance in the optical potential might enhance DCX from widely-spaced pairs.

A completely clean description of  $\tilde{F}$  independent of the nuclear wave function and the optical distortions is not possible. To make progress in this area we invoke two approximations. First, we adopt the closure approximation on the nuclear intermediate wave function so that  $\tilde{F}$  becomes a local function of the nucleon coordinates. This approximation could be improved by applying binding corrections to the active nucleons. Second, within the sequential mechanism, we will ignore the optical distortion of the intermediate  $\pi^0$  meson. This is, unfortunately, only a rough approximation, although it may be partially softened by a choice of the effective energy of  $\pi^0$ . Although our results are strictly valid only within the plane-wave impulse approximation (PWIA), optical distortions of the incident  $\pi^+$  and outgoing  $\pi^-$  may, in principle, be included by (a) replacing the exponential factor in front of equation (2.3) by the overlap of the incident and outgoing pionic (distorted) wave functions, and (b) treating the initial and final pion momenta,  $\mathbf{k}$  and  $\mathbf{k}'$ , as derivative operators on the incoming and outgoing pion distorted waves, respectively. Consequently, certain aspects of our results hold in the distorted-wave case. The advantage of our approach is that the operator  $F$  (which is  $\tilde{F}$  with the external pion waves removed) is then a function of the *relative* coordinates of the two neutrons rather than of the coordinates of

both neutrons. Consequently, we will be able to express the results in terms of a single central function and its derivatives.

In this way one can explicitly examine certain features of the problem, such as the vanishing of the “long-range term” for the two nucleons aligned along the  $z$  axis at the same energy, so that the  $0^\circ$  single charge exchange cross section has a deep minimum, or so that the “double spin-flip” part of the amplitude is of “near-zero” character, i.e., gives no contribution to the amplitude at long range. Because the farther the intermediate  $\pi^0$  travels the more its propagation is affected by the nuclear medium, we expect that the model is more reliable for DCX from close neutron pairs. The longer-range results might be also expected to be relevant, at least qualitatively, at low pion energies, for which the nucleus is relatively transparent.

Although the emphasis in this work is on the DCX process, the same general formulas will also apply to any double-scattering process of a spin 0 particle on a pair of nucleons for which the  $s$ - and  $p$ -wave elementary amplitudes dominate.

## 2.2 General Formulation

The sequential (double-scattering) operator for the pion DCX amplitude in the plane wave limit and assuming closure over the intermediate nuclear states is

$$\tilde{F}(\mathbf{k}, \mathbf{k}'; \mathbf{r}_1, \mathbf{r}_2) = \frac{1}{2\pi^2} \int d\mathbf{q} \frac{e^{-i\mathbf{k}' \cdot \mathbf{r}_2} f(\mathbf{q}, \mathbf{k}') e^{i\mathbf{q} \cdot (\mathbf{r}_2 - \mathbf{r}_1)} f(\mathbf{k}, \mathbf{q}) e^{i\mathbf{k} \cdot \mathbf{r}_1}}{q^2 - \kappa^2 - i\epsilon} \quad (2.1)$$

$$= \frac{e^{-i(\mathbf{k}' \cdot \mathbf{r}_2 - \mathbf{k} \cdot \mathbf{r}_1)}}{2\pi^2} \int d\mathbf{q} \frac{f(\mathbf{q}, \mathbf{k}') e^{i\mathbf{q} \cdot \mathbf{r}} f(\mathbf{k}, \mathbf{q})}{q^2 - \kappa^2 - i\epsilon} \quad (2.2)$$

$$= e^{-i(\mathbf{k}' \cdot \mathbf{r}_2 - \mathbf{k} \cdot \mathbf{r}_1)} F(\mathbf{k}, \mathbf{k}', \mathbf{r}). \quad (2.3)$$

The DCX operator is a function of the coordinates  $\mathbf{r}_1, \mathbf{r}_2$  and spin variables  $\sigma_1, \sigma_2$  (implicit in the two single charge exchange operators  $f$ ) of the two nucleons.  $\tilde{F}$  is the lowest-order two-nucleon DCX operator, and since it changes two neutrons (protons) into two protons (neutrons), it represents the isotensor part of the general two-nucleon operator. Here  $\mathbf{r} (\equiv \mathbf{r}_2 - \mathbf{r}_1)$  is the radial vector between the two nucleons. It is precisely the dependence of  $F$  on this variable which is of interest. The quantity  $f$ , the pion-nucleon charge-exchange (off-shell) amplitude, is an operator in the nucleon spin space. We shall use the form

$$f(\mathbf{q}, \mathbf{q}', E) = \lambda_0(E)v(q)v(q') + \lambda_1(E)v(q)v(q')\mathbf{q} \cdot \mathbf{q}' + i\lambda_f(E)v(q)v(q')\boldsymbol{\sigma} \cdot \mathbf{q} \times \mathbf{q} \quad (2.4)$$

where  $\lambda_0, \lambda_1$  and  $\lambda_f$  are the coefficients of s-wave, p-wave, and spin-flip amplitudes which are taken from the phase shifts analysis (see Table 2.1) [28], and  $v(q)$  is the off-shell form factor for pion-nucleon interaction. While many of the results which follow are independent of the particular choice of  $v(q)$ , a form must be chosen when calculations are made. In these cases we will use

$$v(q) = \frac{\alpha^2 + k^2}{\alpha^2 + q^2}, \quad (2.5)$$

which has a single parameter  $\alpha$  to describe the range of the pion-nucleon interaction. For the figures of this chapter we use  $\alpha = 800$  MeV/c.  $k$  is the on-shell momentum corresponding to the center-of-mass energy  $E$ .

Since we have used the closure approximation to sum over all intermediate nuclear states, we have introduced the intermediate momentum  $\kappa$ , usually taken to be the on-shell momentum of the intermediate  $\pi^0$ . It could also include an effective excitation of the nucleus, chosen to improve the closure approximation. The reaction amplitude is given by the matrix element of this operator taken between the initial and final nuclear wave functions.

In general, all cross terms from the two occurrences of the SCX operators and the three terms in Eq. 2.4 interfere, but for a double-analog transition between shell-model wave functions made up of orbitals all with the same parity, the spin-dependent and spin-independent terms do not interfere, i.e., there are non-spin-flip (NSF) and double-spin-flip (DSF) terms only. We shall assume that this is the case for this examination of the structure of the operator. Thus, we have two terms:

$$F_{NSF}(\mathbf{k}, \mathbf{k}', \mathbf{r}) = \frac{1}{2\pi^2} \int d\mathbf{q} \frac{[\lambda_0 + \lambda_1 \mathbf{q} \cdot \mathbf{k}'] [\lambda_0 + \lambda_1 \mathbf{k} \cdot \mathbf{q}] v^2(q) e^{i\mathbf{q} \cdot \mathbf{r}}}{q^2 - \kappa^2 - i\epsilon} \quad (2.6)$$

and

$$F_{DSF}(\mathbf{k}, \mathbf{k}', \mathbf{r}) = -\frac{\lambda_f^2}{2\pi^2} \int d\mathbf{q} \frac{[\boldsymbol{\sigma}_1 \cdot \mathbf{k} \times \mathbf{q}] [\boldsymbol{\sigma}_2 \cdot \mathbf{q} \times \mathbf{k}'] v^2(q) e^{i\mathbf{q} \cdot \mathbf{r}}}{q^2 - \kappa^2 - i\epsilon}. \quad (2.7)$$

By replacing the vector  $\mathbf{q}$  in the amplitudes by  $-i\nabla$ , we can write the operators in terms of the function  $g(\mathbf{r})$  (considered by Glauber[14]) and its derivatives.

$$F_{NSF}(\mathbf{k}, \mathbf{k}', \mathbf{r}) = (\lambda_0 - i\lambda_1 \mathbf{k} \cdot \nabla)(\lambda_0 - i\lambda_1 \mathbf{k}' \cdot \nabla)g(\mathbf{r}) \quad (2.8)$$

$$F_{DSF}(\mathbf{k}, \mathbf{k}', \mathbf{r}) = \lambda_f^2 (\boldsymbol{\sigma}_1 \cdot \mathbf{k} \times \nabla) (\boldsymbol{\sigma} \cdot \nabla \times \mathbf{k}') g(r) \quad (2.9)$$

where

$$g(r) = \frac{1}{2\pi^2} \int d\mathbf{q} \frac{v^2(q) e^{i\mathbf{q}\cdot\mathbf{r}}}{q^2 - \kappa^2 - i\epsilon} \quad (2.10)$$

$$g(r) = \frac{-2\pi}{2\pi^2} \int_0^\infty q^2 dq \int_0^\pi d(\cos(\theta)) \frac{v^2(q) e^{iqr \cos(\theta)}}{q^2 - \kappa^2 - i\epsilon} \quad (2.11)$$

$$g(r) = \frac{i}{\pi} \int_0^\infty q dq \frac{v^2(q) (e^{-iqr} - e^{+iqr})}{r(q^2 - \kappa^2 - i\epsilon)} \quad (2.12)$$

substitutes from eq. 2.5 then:

$$g(r) = \frac{i(\alpha^2 + k^2)(\alpha^2 + k^2)}{r} \frac{1}{\pi} \int_0^\infty q dq \frac{(e^{-iqr} - e^{+iqr})}{(q^2 - \kappa^2 - i\epsilon)(\alpha^2 + q^2)^2} \quad (2.13)$$

By doing the contour integration of the last equation which has singularities at  $q = \pm i\alpha$  and  $q = \pm ik$ , using Cauchy's theorem, the integral can be considered as sum over the residues of the function contained within the contour.

$$\oint f(z) dz = 2\pi i \sum_i Rf(a_i) \quad (2.14)$$

where  $R$ , is the residue and is defined as:

$$Rf(a_i) = \lim_{z \rightarrow a_i} [(z - a_i) f(z)] \quad (2.15)$$

and the result is:

$$g(r) = \frac{e^{i\kappa r} - e^{-\alpha r}}{r} - \frac{(k^2 + \alpha^2)(k'^2 + \alpha^2)}{2\alpha(\kappa^2 + \alpha^2)} e^{-\alpha r}. \quad (2.16)$$

For large  $r$ ,  $-i\nabla g(r) = \kappa \hat{r} g(r)$  so that, for  $\mathbf{r} \parallel \mathbf{k}$  or  $\mathbf{r} \parallel \mathbf{k}'$  and  $|\mathbf{k}| = |\mathbf{k}'| = \kappa$  the amplitude contains a factor  $\lambda_0 + \lambda_1 k^2$  and hence is small at 50 MeV where the single charge exchange is nearly zero. For short ranges the reaction still proceeds even for  $\mathbf{r}$  aligned along the momenta.

In the case  $|\mathbf{k}| = |\mathbf{k}'| = \kappa$  we have, for small  $r$ ,

$$g(r) \rightarrow C_0 + \frac{1}{2}C_2 r^2 + \frac{1}{3}C_3 r^3 + \dots, \quad (2.17)$$

where

$$C_0 = \frac{(\alpha + ik)^2}{2\alpha}; \quad C_2 = -(2ik^3 + \alpha^3 + 3k^2\alpha)/6; \quad C_3 = (\alpha^2 + k^2)^2/8. \quad (2.18)$$

Note that for a function  $v(q)$  with a stronger suppression for large  $q$  (such as a Gaussian), all odd coefficients would be zero.

For  $|\mathbf{k}| = |\mathbf{k}'| = \kappa$  the needed derivatives are given by:

$$g'(r) = \frac{ike^{ikr} + \alpha e^{-\alpha r}}{r} - \frac{e^{ikr} - e^{-\alpha r}}{r^2} + \frac{1}{2}(\alpha^2 + k^2)e^{-\alpha r} \quad (2.19)$$

$$g''(r) = -\frac{k^2 e^{ikr} + \alpha^2 e^{-\alpha r}}{r} - 2\frac{ike^{ikr} + \alpha e^{-\alpha r}}{r^2} + 2\frac{e^{ikr} - e^{-\alpha r}}{r^3} - \frac{1}{2}\alpha(\alpha^2 + k^2)e^{-\alpha r}. \quad (2.20)$$

We note the appearance of three types of terms:

1. those of short range ( $e^{-\alpha r}$ ),
2. those of radiation (long) range ( $e^{ikr}/r$ ),
3. and those of "near-zone" type ( $e^{ikr}/r^2$  and  $e^{ikr}/r^3$ ).

This last class of terms is due entirely to the p-wave nature of the pion-nucleon interaction.

Two combinations of these functions which turn out to be useful are

$$g^+(r) \equiv g''(r) + \frac{2}{r}g'(r) = \nabla^2 g(r) = -k^2 \frac{(e^{ikr} - e^{-\alpha r})}{r} - \frac{\alpha(\alpha^2 + k^2)}{2} e^{-\alpha r} \quad (2.21)$$

and

$$g^-(r) \equiv g''(r) - \frac{1}{r}g'(r). \quad (2.22)$$

Note that,  $g^+(r)$  contains a function which limit to a  $\delta$  function, so that:

$$\lim_{\alpha \rightarrow \infty} g^+(r) = -k^2 \frac{e^{ikr}}{r} - \frac{\delta(r)}{4\pi r^2} \quad \text{or} \quad \lim_{v(q) \rightarrow 1} (q^2 - k^2)g(r) = \frac{\delta(r)}{4\pi r^2}. \quad (2.23)$$

It is often argued that the  $\delta$ -function should not appear in the analogous case of the one-pion-exchange contribution to the nucleon-nucleon potential. The extraction of this term in the same manner as is done in the nucleon-nucleon problem [29] leads to the result that  $g^+(r)$  becomes simply  $-k^2 g(r)$ . While it can be argued that the  $\delta$ -function is inappropriate here as in the nucleon-nucleon case (all DCX calculations to date have included it to our knowledge), we will restrict ourselves to simply considering the two possibilities, i.e., with and without its inclusion.

While each of  $g''(r)$  and  $g'(r)/r$  contain a  $\delta$  function,  $g^-(r)$  is exactly the combination in which the  $\delta$  functions cancel, in fact,  $g^-(r)$  satisfies the condition,

$$g^-(0) = 0. \quad (2.24)$$

Thus, for large  $\alpha$ , we expect that,  $g^+(r)$  is large and  $g^-(r)$  is small for small  $r$ .

### 2.3 Spin-independent Contribution

Evaluating Eq. 2.6

$$F_{NSF}(\mathbf{k}, \mathbf{k}', \mathbf{r}) = \lambda_0^2 g(r) - i\lambda_0 \lambda_1 (\mathbf{k} \cdot \hat{\mathbf{r}} + \mathbf{k}' \cdot \hat{\mathbf{r}}) g'(r) \quad (2.25)$$

$$- \lambda_1^2 \left[ \frac{1}{3} \mathbf{k} \cdot \mathbf{k}' g^+(r) + (\mathbf{k} \hat{\mathbf{r}} \mathbf{k}' \hat{\mathbf{r}} - \frac{1}{3} \mathbf{k} \cdot \mathbf{k}') g^-(r) \right].$$

Notable in this last form is the “tensor operator”  $S_{12}(\mathbf{r}) \equiv \mathbf{k} \cdot \mathbf{r} \mathbf{k}' \cdot \mathbf{r} - \frac{1}{3} \mathbf{k} \cdot \mathbf{k}'$ , so familiar in the nucleon-nucleon problem. In fact this last term has the same form as the one-pion-exchange potential (with replacement by the corresponding  $g^+(r)$  and  $g^-(r)$ ) except the spin operators have been replaced by momenta.

The radiation (large  $r$ ) limit of this expression is:

$$(\lambda_0 + \lambda_1 \boldsymbol{\kappa} \cdot \mathbf{k})(\lambda_0 + \lambda_1 \mathbf{k} \cdot \boldsymbol{\kappa}') \frac{e^{i\boldsymbol{\kappa} r}}{r} \quad (2.26)$$

where we have set  $\boldsymbol{\kappa} = \hat{\mathbf{r}} \boldsymbol{\kappa}$ .

The classical expression for the cross section for double charge exchange from two nucleons is simply the cross section for a single charge exchange on the first particle  $[\sigma(\mathbf{k}, \mathbf{k})]$  multiplied by the probability that another charge exchange occurs on the second nucleon  $[\sigma(\mathbf{k}, \mathbf{k}')/r^2]$ . This product is equal to the absolute square of the radiation limit of the quantum-mechanical operator given in Eq. 2.25. Since it is the classical expression which is used in modeling nuclear reactions with intranuclear cascades, it is of interest to compare the two expressions over the range of  $r$  of importance in the nucleus, see the results of Chapter V.



For  $0^\circ$  DCX to the double analog state ( $\mathbf{k}' = \mathbf{k}$ ) and  $\kappa = k$  we find:

$$F_{NSF}(\mathbf{k}, \mathbf{k}, \mathbf{r}) = \sum_{L=0,1,2} g_L(r) P_L(x) \quad (2.27)$$

where  $x = \hat{\mathbf{k}} \cdot \hat{\mathbf{r}}$  and

$$g_0(r) = \lambda_0^2 g(r) - \frac{\lambda_1^2 k^2}{3} g^+(r); \quad g_1(r) = -2i\lambda_0 \lambda_1 k g'(r); \quad g_2(r) = -\frac{2}{3} \lambda_1^2 k^2 g^-(r). \quad (2.28)$$

#### 2.4 Double-spin-flip Term

For the NSF part of the operator the spin structure was irrelevant but for the DSF it is necessary to assume something about the singlet-triplet decomposition of the two-nucleon wave function. Appendix A develops the equations necessary to treat the general case, but here we assume the pure singlet case for which the operator is:

$$\mathbf{e}_1 \cdot \mathbf{e}_2 = -(\mathbf{k} \times \mathbf{q}) \cdot (\mathbf{k}' \times \mathbf{q}) = -\mathbf{k} \cdot \mathbf{k}' q^2 + (\mathbf{k} \cdot \mathbf{q})(\mathbf{k}' \cdot \mathbf{q}), \quad (2.29)$$

which in coordinate space is

$$\mathbf{k} \cdot \mathbf{k}' \nabla^2 - (\mathbf{k} \cdot \nabla)(\mathbf{k}' \cdot \nabla). \quad (2.30)$$

The DSF operator becomes

$$F_{DSF}(\mathbf{k}, \mathbf{k}', \mathbf{r}) = \lambda_f^2 \left[ \frac{2}{3} \mathbf{k} \cdot \mathbf{k}' g^+(r) + (\mathbf{k} \hat{\mathbf{r}} \cdot \mathbf{k}' \hat{\mathbf{r}} - \frac{1}{3} \mathbf{k} \cdot \mathbf{k}') g^-(r) \right]. \quad (2.31)$$

At  $\mathbf{k} = \mathbf{k}'$ ,

$$F_{DSF}(\mathbf{k}, \mathbf{k}, \mathbf{r}) == \sum_{L=0,2} s_L(r) P_L(x), \quad (2.32)$$

where

$$s_0(r) = \frac{2}{3} \lambda_f^2 k^2 g^+(r); \quad s_2(r) = -\frac{2}{3} \lambda_f^2 k^2 g^-(r). \quad (2.33)$$

The cancellation between DSF and NSF amplitudes is exact (as it must be) in the far zone, since for  $x=1$   $F_{DSF}$  is proportional to  $g^+(r) - g^-(r) = 3g'(r)/r$  which falls as  $1/r^2$ .

### 2.5 Projected Operator

An important case for double charge exchange is that in which the reaction takes place on two identical nucleons in a relative s state [30] clearly involving only the singlet component of the spin state. By including the exponential factor multiplying the integral in Eq. 2.3 and projecting onto the s-wave part of the relative-motion wave function, we have, for  $\mathbf{k} = \mathbf{k}'$ ,

$$Q(r) \equiv \frac{1}{2} \int_{-1}^1 dx e^{-i\mathbf{k}\cdot\mathbf{r}} [[g_0(r) + s_0(r)] P_0(x) + g_1(r) P_1(x) + [g_2(r) + s_2(r)] P_2(x)] \quad (2.34)$$

$$= j_0(kr) [g_0(r) + s_0(r)] - ij_1(kr) g_1(r) - j_2(kr) [g_2(r) + s_2(r)]. \quad (2.35)$$

$$= j_0(kr) \lambda_0^2 g(r) - \frac{k^2}{3} j_0(kr) (\lambda_1^2 - 2\lambda_f^2) g^+(r)$$

$$-2\lambda_0\lambda_1kg'(r)j_1(kr) + \frac{2k^2}{3}j_2(kr)(\lambda_1^2 + \lambda_f^2)g^-(r). \quad (2.36)$$

The short-range part of this operator contains a  $\delta$ -function in the limit of large  $\alpha$ :

$$\lim_{\alpha \rightarrow \infty} Q(r) = -\frac{k^2}{3}(\lambda_1^2 - 2\lambda_f^2)\delta(r)/r^2 + \dots \quad (2.37)$$

Here the explicit cancellation between the NSF and DSF terms is evident. For  $\Delta_{33}$  dominance (DINT),  $\lambda_f = \frac{1}{2}\lambda_1$  so that the short-range part of the operator is decreased by a factor of two by the inclusion of double spin flip.

It is interesting to consider the large  $r$  limit of Eq. 2.36,

$$\lim_{r \rightarrow \infty} Q(r) = \frac{-i}{2kr^2} [(\lambda_0 - \lambda_1k^2)^2 e^{2ikr} - (\lambda_0 + \lambda_1k^2)^2]. \quad (2.38)$$

This limit is most useful at low energies, for which the pion mean-free-path within the nucleus is large. The double-spin-flip contributions do not appear, they have cancelled exactly.

Also noteworthy is that the coefficient of the non-oscillating part of the expression is proportional to the square of the forward single-charge-exchange operator, which is very small near 50 MeV.

What remains is an operator proportional to  $\frac{e^{2ikr}}{r^2}$ . The expectation value of this residual operator will tend toward zero as  $k$  becomes large. Thus we see again that the long-range part of the DCX amplitude is small near 50 MeV to the extent that the form factor constrains each individual single charge exchange to take place in the forward direction.

Of course Eq. 2.38 represents only the large  $r$  limit, and we must look at the complete expression to observe the rest of the dependence. To this end we write the operator as the sum of two terms, one representing the part that oscillates at long range and the other which goes as  $1/r^2$  for large  $r$ :

$$Q = Q^+ + Q^-. \quad (2.39)$$

This can be done in a simple (non-unique) fashion by writing the Bessel functions in Eq. 2.36 in terms of spherical Hankel functions.

$$Q^\pm(r) = \frac{h_0^\pm(kr)[g_0(r) + s_0(r)] - ih_1^\pm(kr)g_1(r) - h_2^\pm(kr)[g_2(r) + s_2(r)]}{2} \quad (2.40)$$

To reveal the difference in the “range” of the oscillating part and the “ $1/r^2$ ” part, the total operator has been integrated over a Gaussian sample function with a radial extent  $R$  by multiplying by  $\psi^2(R, r)$ , where

$$\psi(R, r) = Ne^{-\frac{3r^2}{4R^2}}; \quad N^2 = \frac{3}{R^3} \sqrt{\frac{6}{\pi}}, \quad (2.41)$$

and  $R^2 = \langle r^2 \rangle$ .

$$\bar{Q}^\pm(R) \equiv \int_{r_{min}}^{\infty} r^2 dr \psi^2(R, r) Q^\pm(r). \quad (2.42)$$

The results of this Chapter will be presented in the figures of Chapter V (5.1, 5.2, 5.3, 5.4, 5.5, and 5.6).

Table 2.1: Table of  $\lambda$ 's Calculated from the Phase Shifts of Reference [28]

$T_{lab}(\text{MeV})$	$P_{CM}(\text{MeV}/c)$	$\lambda_0(\text{fm})$		$\lambda_1(\text{fm}^3)$		$\lambda_f(\text{fm}^3)$	
		Real	Imag.	Real	Imag.	Real	Imag.
20	66.3	-0.187	-0.006	0.615	0.013	0.282	0.007
40	95.3	-0.185	-0.007	0.631	0.041	0.300	0.021
60	118.6	-0.184	-0.007	0.651	0.089	0.321	0.045
80	138.9	-0.183	-0.005	0.669	0.162	0.340	0.081
100	157.3	-0.181	-0.003	0.674	0.270	0.353	0.134
120	174.4	-0.180	0.000	0.640	0.415	0.345	0.206
140	190.5	-0.179	0.003	0.527	0.575	0.298	0.285
160	205.7	-0.177	0.006	0.321	0.680	0.203	0.337
180	220.3	-0.176	0.010	0.087	0.665	0.094	0.329
200	234.3	-0.175	0.014	-0.083	0.555	0.016	0.275
220	247.8	-0.173	0.018	-0.168	0.424	-0.020	0.210
240	260.9	-0.172	0.021	-0.195	0.312	-0.029	0.155
260	273.6	-0.170	0.025	-0.195	0.229	-0.024	0.116
280	285.9	-0.169	0.028	-0.184	0.169	-0.015	0.070

# CHAPTER III

## DOUBLE CHARGE EXCHANGE REACTIONS ON CALCIUM AND CARBON NUCLEI

The next section of this chapter will summarize the formalism of Aurbach, Gibbs, Ginocchio, and Kaufmann (AGGK) [9] which is based on the studies of the pion double charge exchange reaction for the Ca isotopes where the DCX reaction can be a means for probing the short range part of the nucleon-nucleon correlations in the nucleus. This can be done by including various degrees of correlations in the wave function.

The DCX reactions on various nuclides in the same shell can be compared, the simplest cases being  $^{42}\text{Ca}$ ,  $^{44}\text{Ca}$ ,  $^{48}\text{Ca}$ . If the reaction proceeds by a long-range process then all excess neutron pairs will take part, and the cross section is expected to be proportional to the total number of such neutron pairs, giving a ratio of 1:6:28 for the three isotopes given above.

As we shall see in the following section, the DCX amplitude can be written as the sum of two amplitudes in this model. The first amplitude favors the long-range process and has the property that the cross sections due to it alone obey the excess-neutron-pair rule. The second amplitude corresponds to a shorter internucleon range, and its dependence on the number of excess neutrons is different but can still be expressed simply.

The study of the reaction operator is of interest in order to know the region of contribution of the "short-range" amplitude so that it is known at what internucleon distances the nuclear wave functions are being tested. The relationship among DCX reactions to both analog and ground states are reviewed. A reaction model calculation is used to calculate the DCX cross sections using both the seniority model and the realistic shell model. The results are compared to the existing data.

The calculations are performed in the plane impulse approximation (PWIA) (as a check) and the distorted wave impulse approximation (DWIA). The DCX operator in the shell model and the seniority model will be reviewed and the pion absorption correction for calcium isotopes which is new to this work, will be discussed.

### 3.1 Historical Background and Nuclear Structure

The Double Charge Exchange operator,  $F$ , is, in the lowest order, a two-nucleon operator since it changes two neutrons (protons) into two protons (neutrons);  $F$  is an isotensor operator. The second-order process considered in  $F$  will also contribute to both elastic and inelastic scatterings as well as double and single charges exchange. However, in those reactions the lowest-order operator is a one-nucleon operator which, in general, will dominate over the second order process which makes the DCX a unique probe in nuclear physics. The DCX

operator will be a function of the coordinate  $r_1, r_2$ , spin variables  $\sigma_1, \sigma_2$  and the isospin variables  $\tilde{\tau}_-(1), \tilde{\tau}_-(2)$  of the two nucleons.

$$F_{12}(\mathbf{k}, \mathbf{k}') = [F_0(\mathbf{r}_1, \mathbf{r}_2) + F_1(\mathbf{r}_1, \mathbf{r}_2)(\sigma_1 \cdot \sigma_2)] \tilde{\tau}_-(1) \cdot \tilde{\tau}_-(2). \quad (3.1)$$

### 3.1.1 The Shell Model

Within the shell-model space, only the matrix elements of this operator with respect to the wave functions of two nucleons in the valence shell will be needed. These can be determined by the two-nucleon density of the many-nucleon wave functions. The complex amplitude  $F_L$  for even  $L$  involves only the spin-independent  $\tilde{F}_0$ :

$$F_L = G^{Llj} \sum_M \int d^3\mathbf{r}_1 d^3\mathbf{r}_2 \tilde{F}_0(\mathbf{r}_1, \mathbf{r}_2) Y_{LM}^*(\hat{r}_1) Y_{LM}(\hat{r}_2) \rho_{nlj}(r_1, r_2) \quad (3.2)$$

where

$$G^{Llj} = \frac{(2l+1)^2(2j+1)}{4\pi} [C_{1/2jj}^{Ll} (C_{000}^{llL})]^2 \quad (3.3)$$

$$\rho_{nlj}(r_1, r_2) = \Psi^{(\pi)}_{nlj}(r_1) \Psi^{(\pi)}_{nlj}(r_1) \Psi^{\nu}_{nlj}(r_1) \Psi^{\nu}_{nlj}(r_2). \quad (3.4)$$

The single-neutron (proton) radial wave functions are  $\Psi^{(\nu)}(r)$  ( $\Psi^{(\pi)}(r)$ ) with orbital angular momentum,  $l$ , radial quantum number,  $n$ , and  $Y_{LM}(\hat{r})$  as the



spherical harmonics. The complex amplitude for odd  $L$  involves only the spin-dependent  $\tilde{F}_1$  operator [9]:

$$F_L = \sum_{\lambda\lambda'} D_{\lambda L l j} D_{\lambda' L l j} \int d^3\mathbf{r}_1 d^3\mathbf{r}_2 \tilde{F}_1(\mathbf{r}_1, \mathbf{r}_2) Y_{\lambda L}(\hat{\mathbf{r}}_1) \cdot Y_{\lambda' L}(\hat{\mathbf{r}}_2) \rho_{nlj}(\mathbf{r}_1, \mathbf{r}_2) \quad (3.5)$$

where  $D_{\lambda L, l, j}$  contains 3- $j$  and 6- $j$  coefficients. The DCX operator  $F_L(\mathbf{k}, \mathbf{k}')$  depends on the pion-nucleon dynamics, the pion energy, and the single-nucleon wave function. It can be seen from Eq. 3.1 and Eq. 3.5 that if the pion interaction is spin independent, only the even multipoles will contribute; if there is spin dependence the odd multipoles will also appear. The two neutrons and two protons are coupled to angular momentum  $J$  and, because of the Paul principle, only even values of  $J$  are allowed  $J=0, 2, \dots, 2j-1$ . So there are only  $j+1/2$  independent complex amplitudes.

The monopole part of the DCX operator is involved only in the double-analog charge exchange transition. Hence, for non-double-analog charge exchange transitions, there are  $j-1/2$  complex amplitudes.

### 3.1.2 The Seniority Model

The fundamental basic assumptions of the seniority model are (1) the dominant effective interaction between valence nucleons occurs for nucleons coupled to angular momentum zero and isospin one and (2) the single-nucleon energies are degenerate or quasidegenerate. The two nucleon matrix elements of  $F$  are:

$$\langle j^2 T = 1, J | F | j^2 T = 1, J \rangle = 2\sqrt{5}G_J, \quad (3.6)$$

where the factor  $\sqrt{5}$  is the three-J symbol involved in going to isospin double-barred matrix elements. We will define the amplitudes [9]:

$$A = F_0 - \frac{1}{\Omega} \sum_{L=odd} F_L \quad (3.7)$$

$$B = \sum_{L>0} F_L - \frac{(\Omega - 1)}{\Omega} \sum_{L=odd} F_L \quad (3.8)$$

and  $\Omega=J+1/2$ . Hence, if there is no spin dependence, i.e.,  $F_L = 0$ ,  $L$  odd, then the amplitude  $A$  is the long-range (monopole) part of the DCX reaction while  $B$  is the short-range part. However, spin dependence, while not changing the number of amplitudes that DCX depends on, will alter the values of the amplitudes. If the spin dependence is dominant, then this separation into long range and short range may no longer be valid. Using Eq. 3.6, the DCX matrix element for the transition from a target with  $I_z = I = \frac{(N-Z)}{2}$ , to the double-analog state,  $I'=I$ ,  $I'_z = I - 2$

$$\langle j^n I = I_z = I - 2, I = 0 | F | j^n I, I_z, j = 0 \rangle = \sqrt{I(2I - 1)}[A + XB] \quad (3.9)$$

where

$$X = \frac{1}{(\Omega - 1)(2I + 3)(2I - 1)} [(n + 3)(\Omega + 1 - n) + \frac{(n - 2I)(n + 2I + 2)(3\Omega + 2)}{2(\Omega + 1)}]. \quad (3.10)$$

It can be seen from this expression that for a given number of valence nucleons the effect of the monopole amplitude  $A$  increases as isospin pairs coupled to isospin zero in Eq. 3.9 do not contribute to the monopole part of the DCX. However, for a fixed isospin the contribution of  $B$  with respect to  $A$  increases as the number of

valence nucleons increases. For targets with identical nucleons, only ( $I=n/2$ ) Eq.

3.9 reduces to

$$\begin{aligned} \langle j^n I = n/2, I_z/2, j = 0 | F | j^n I = I_z = n/2, j = 0 \rangle & \quad (3.11) \\ & = \sqrt{\frac{n(n-1)}{2}} \left[ A + \frac{(\Omega + 1 - n)}{(\Omega - 1)(n - 1)} B \right] \end{aligned}$$

which agrees with [9]. This formula is valid for the calcium isotopes. If B is zero, then the DCX cross section will increase in proportion to the number of neutron pairs= $I(2I - 1)$ . The DCX transition to the ground state,  $T' = T - 2$ , depends on B only because, as has been mentioned previously, the monopole term can not change isospin. This matrix element is given by

$$\langle j^n I' = I - 2, j' = 0 | F | j^n I, I_z = I, j = 0 \rangle = \sqrt{I(2I - 1)} Y B \quad (3.12)$$

where

$$\begin{aligned} Y & = \frac{\Omega}{4(\Omega - 1)(2\Omega + 1)(2I - 1)} \\ & \times \left[ \frac{(I - 1)(n + 2I + 2)(n - 2I + 4)(4\Omega + 4 - n - 2I)(4\Omega + 2 - n + 2I)}{(2I + 1)} \right]^{\frac{1}{2}}. \quad (3.13) \end{aligned}$$

This means that the DCX reactions will be the same for particle-hole related nuclei, except for the dependence of the pion dynamics on atomic mass, i.e., the mass dependence of the amplitudes A and B.

### 3.1.3 DCX Operator Using Double Scattering

The purpose of this section is to derive the double charge exchange amplitudes,  $F_L$ , using a sequential model of single charge exchanges on nucleons. In a full

multiple-scattering model, the DCX operator  $F$  is an explicit function of the pion coordinates and those of the two neutrons undergoing charge exchange. A simple and physically reasonable operator of this form arises from the double-scattering model, in which DCX proceeds through two successive single charge exchanges (SCX).

$$F(\mathbf{r}_1, \mathbf{r}_2, \mathbf{k}', \mathbf{k}) = 2\left[-\frac{1}{2\pi^2}\right] \int d\mathbf{q} \phi_{\mathbf{k}'}^-(\mathbf{r}_2) f(\mathbf{k}', \mathbf{q}) \frac{\phi_{\mathbf{q}}^+(\mathbf{r}_2) \phi_{\mathbf{q}}^-(\mathbf{r}_1)}{k_0^2 - q^2 + i\epsilon} f(\mathbf{q}, \mathbf{k}) \phi_{\mathbf{k}}^+(\mathbf{r}_1), \quad (3.14)$$

$f(\mathbf{q}, \mathbf{q}')$  is the spin-averaged amplitude for pion-nucleon charge exchange. The right-hand distorted wave  $\phi^+$  represents the incident  $\pi^+$  wave, the central distorted wave and the denominator represents the  $\pi^0$  propagator and the left-hand distorted wave represents the outgoing  $\pi^-$  wave. In the DWIA, the pion wave functions and the propagator are distorted by coulomb and optical potentials. The overall factor of 2 accounts for the process in which the first charge exchange is on neutron position  $r_2$ . The pion-nucleon charge exchange amplitude has the following form:

$$f(\mathbf{q}', \mathbf{q}) = \lambda_0(k) v_0(q') v_0(q) + v_0(q') v_0(q) \lambda_1(q) \mathbf{q}' \cdot \mathbf{q} \quad (3.15)$$

where  $v_0$  and  $v_1$  are defined by:

$$v_i(q) = \frac{k^2 + \alpha_i^2}{q^2 + \alpha_i^2}; \quad i = 0, 1 \quad . \quad (3.16)$$

A plane wave impulse approximation and distorted wave impulse approximation have been used in the calculation of the DCX operator  $F$ . The operator is integrated over the nucleon wave functions in order to get the multipole

$$F_L(\mathbf{k}, \mathbf{k}') = \int \Psi_{nlj}^2(\mathbf{r}_1, \mathbf{r}_2) F(\mathbf{r}_1, \mathbf{r}_2) \Psi_{nlj}^2(\mathbf{r}_1, \mathbf{r}_2) d^3\mathbf{r}_1 d^3\mathbf{r}_2 \quad (3.17)$$

where  $\Psi(\mathbf{r}_1, \mathbf{r}_2)$  can be expanded in terms of spherical harmonics for both the plane wave and distorted wave one. Then  $F_L(\mathbf{r}_1, \mathbf{r}_2)$  will be

$$F_L(\mathbf{k}', \mathbf{k}) = G^{Llj} \int d\mathbf{r}_1 d\mathbf{r}_2 \sum_M Y_{LM}(\hat{r}_1) Y_{LM}^*(\hat{r}_2) \Psi_{nlj}(r_1) \Psi_{nlj}(r_2) F(\mathbf{r}_1, \mathbf{r}_2, \mathbf{k}', \mathbf{k}). \quad (3.18)$$

In the seniority model, assuming a spin independent operator,  $A$  is  $F_0$ , and  $B$  is the sum of higher multipoles. For  $^{14}\text{C}$  only  $L=0, 2$  contribute and for  $\text{Ca}$   $L=0, 2, 4, 6$  will contribute, i.e.,  $B = F_2 + F_4 + F_6$ . The DCX amplitudes for the transitions from  $^{42,48}\text{Ca}$  targets to DIAS and  $\sqrt{1}(A + B)$  for  $^{42}\text{Ca}$  (DIAS and GS transition),  $\sqrt{6}(A + B/9)$  for  $^{44}\text{Ca}$  (DIAS transition), and  $\sqrt{28}(A - B/7)$  for  $^{48}\text{Ca}$  (DIAS transition). The square of the first factor represents the number of pairs of valence neutrons.

### 3.2 DCX Cross Section

Since the DCX operator is a two-nucleon operator, once the DCX reaction is known for two nucleons coupled to angular momentum  $J=0, 2, \dots, 2j-1$  in a shell model orbit  $j$ , then it can be determined for many nucleons in that orbit.

A two amplitude model based on seniority-zero shell model wave functions has been successfully applied to DCX measurements below 300 MeV. In this model differential cross sections for the transition to the DIAS and to the ground state are given as:

$$\frac{d\sigma}{d\Omega}(DIAS) = \frac{n(n-1)}{2} |A + Xe^{i\phi}|^2 \quad (3.19)$$

$$\frac{d\sigma}{d\Omega}(g.s) = \frac{n(n-1)}{2} |YB|^2, \quad (3.20)$$

where  $n=2T$  is the number of valence neutrons and

$$X = \frac{(5-n)}{3(n-1)} \quad (3.21)$$

$$Y = \frac{4}{9(n-1)} \sqrt{(n-2)(10-n)}. \quad (3.22)$$

So the cross sections for calcium isotopes are given by:

$${}^{42}\text{Ca}({}^{54}\text{Fe}): |A + B|^2 \quad (3.23)$$

$${}^{44}\text{Ca}({}^{52}\text{Cr}): 6 |A + B/9|^2 \quad (3.24)$$

$${}^{46}\text{Ca}({}^{50}\text{Ti}): 15 |A - B/15|^2 \quad (3.25)$$

$${}^{48}\text{Ca}({}^{48}\text{Ti}): 28 |A - B/7|^2. \quad (3.26)$$

### 3.3 Pion Optical Potential and Treatment of Distortions

While the technique for the solution of the pion wave functions is given in [31], a summary of the relevant material will be also presented here. In the two codes

(Appendix B and D) which calculate the DCX cross sections for Ca and  $^{14}\text{C}$ , there is a subroutine PIPOOT which calculates the potential for the pion nucleus interaction for the case in which the potential is nonlocal since the two-body scattering amplitude is not a function of the difference of the momenta. This separable form is used as a model for the potential, Since the wave function is already available in r-space, the solution of the Schrödinger equation is done in r-space. Only s and p waves are included in the two-body scattering amplitude. The non-local potential will be given in coordinate space by

$$V(\mathbf{r}, \mathbf{r}') = \frac{1}{(2\pi)^6} \int d\mathbf{q}d\mathbf{q}' V(\mathbf{q}, \mathbf{q}') e^{-i\mathbf{q}\cdot\mathbf{r}} e^{i\mathbf{q}'\cdot\mathbf{r}'}. \quad (3.27)$$

Consider first the case of an s-wave (isotropic) basic scattering amplitude with an overall strength  $b_0$ . The two body amplitude is given by:

$$f(\mathbf{q}, \mathbf{q}') = b_0 v(\mathbf{q})v(\mathbf{q}') \quad (3.28)$$

so that

$$V^s(\mathbf{q}, \mathbf{q}') = b_0 v(q)v(q') \int ds e^{i(\mathbf{q}-\mathbf{q}')\cdot\mathbf{s}} \rho(s) \quad (3.29)$$

and

$$V^s(\mathbf{r}, \mathbf{r}') = \frac{b_0}{(2\pi)^6} \int d\mathbf{q}d\mathbf{q}' ds v(q)v(q') e^{-i\mathbf{q}\cdot(\mathbf{r}-\mathbf{s})} e^{i\mathbf{q}'\cdot(\mathbf{r}'-\mathbf{s})} \rho(s) \quad (3.30)$$

where  $v(q)$  is the off-shell form factor which represents the range of the separable interaction. If  $v(q)$  is a constant then the interaction will be of zero range.

Defining

$$F(\mathbf{r}, \mathbf{s}) \equiv \frac{1}{(2\pi)^3} \int d\mathbf{q} v(q) e^{-i\mathbf{q}\cdot(\mathbf{r}-\mathbf{s})}. \quad (3.31)$$

Then, by expansion in spherical harmonics:

$$F(\mathbf{r}, \mathbf{s}) = \frac{(4\pi)^2}{(2\pi)^3} \int d\mathbf{q} v(q) \sum (-i)^l Y_l^m(\hat{\mathbf{r}}) Y_l^m(\hat{\mathbf{q}}) j_l(qr) \sum (i)^\lambda Y_{\lambda}^{\mu}(\hat{\mathbf{q}}) Y_{\lambda}^{\mu*}(\hat{\mathbf{s}}) j_{\lambda}(qs) \quad (3.32)$$

or

$$F(\mathbf{r}, \mathbf{s}) = \sum Y_l^m(\hat{\mathbf{r}}) Y_l^{m*}(\hat{\mathbf{s}}) F_l(\mathbf{r}, \mathbf{s}) \quad (3.33)$$

where

$$F_l(\mathbf{r}, \mathbf{s}) \equiv \frac{2}{\pi} \int_0^{\infty} q^2 dq v(q) j_l(qr) j_l(sr). \quad (3.34)$$

In the limit  $v(q)$  is constant (equal to one)

$$F_l(\mathbf{r}, \mathbf{s}) \rightarrow \delta(\mathbf{s} - \mathbf{r}'). \quad (3.35)$$

So, the potential can be written in  $r$ -space as a single three-dimensional integral

$$V^s(\mathbf{r}, \mathbf{r}') = b_0 \int d\mathbf{s} F(\mathbf{r}, \mathbf{s}) \rho(\mathbf{s}) F(\mathbf{s}, \mathbf{r}') \quad (3.36)$$

or

$$V^s(\mathbf{r}, \mathbf{r}') = \int s^2 ds F_l(\mathbf{r}, \mathbf{s}) \rho(s) F_l(\mathbf{s}, \mathbf{r}') b_0 \sum Y_l^m(\hat{\mathbf{r}}) Y_l^{m*}(\hat{\mathbf{r}}) V_l^S(\mathbf{s}, \mathbf{r}'). \quad (3.37)$$



The p-wave component of the two-body amplitude can be handled in a very similar manner with a simple trick. The potential can be written as before,

$$V^p(\mathbf{r}, \mathbf{r}') = \frac{b_1}{(2\pi)^6} \int d\mathbf{q} d\mathbf{q}' \mathbf{q} \cdot \mathbf{q}' v(q) v(q') e^{-i\mathbf{q} \cdot \mathbf{r}} e^{i\mathbf{q}' \cdot \mathbf{r}} e^{i(\mathbf{q}' - \mathbf{q}) \cdot \mathbf{s}} \rho(s). \quad (3.38)$$

Writing

$$\mathbf{q} \cdot \mathbf{q}' = -\frac{1}{2}[(\mathbf{q}' - \mathbf{q})^2 - q^2 - q'^2] \quad (3.39)$$

replacing  $q^2 \rightarrow \nabla_r^2$ ;  $q'^2 \rightarrow -\nabla_{r'}^2$  and  $(\mathbf{q}' - \mathbf{q})^2 \rightarrow -\nabla_s^2$  acting only on the exponential. Since there are two functions of  $s$  under the integral sign we can transfer the  $\nabla_s^2$  onto  $\rho(s)$  by integration by parts to obtain:

$$V^p = V(\mathbf{r}, \mathbf{r}') = \frac{b_1}{2} \int ds (F(\mathbf{r}, s) [\nabla_s^2 \rho(s)] \times F(\mathbf{s}, \mathbf{r}')) - [\nabla_r^2 F(\mathbf{r}, s)] \rho(s) F(\mathbf{s}, \mathbf{r}') - F(\mathbf{r}, s) \rho(s) [\nabla_{r'}^2 F(\mathbf{s}, \mathbf{r}')]. \quad (3.40)$$

Substitute for

$$\nabla_r^2 F(\mathbf{r}, s) = \sum Y_l^m(\hat{\mathbf{r}}) Y_l^{m*}(\hat{\mathbf{s}}) \tilde{F}_l(\mathbf{r}, s) \quad (3.41)$$

so that

$$V^p(\mathbf{r}, \mathbf{r}') = \sum Y_l^m(\hat{\mathbf{r}}) Y_l^{m*}(\hat{\mathbf{r}}) V_l^p(r, r') \quad (3.42)$$

where

$$V_l^p(\mathbf{r}, \mathbf{r}') = \frac{b_1}{2} [\tilde{F}_l(r, s) \rho(s) F_l(s, r') - \tilde{F}_l(r, s) \rho(s) F_l(s, r') - F_l(r, s) \rho(s) \tilde{F}_l(s, r')]. \quad (3.43)$$

Writing the two-body amplitude as

$$f(\mathbf{q}, \mathbf{q}') = \sum b_L v(q) q^L v(q') q'^L P_L(\hat{\mathbf{q}}, \hat{\mathbf{q}}')$$

$$= 4\pi \sum \frac{b_L}{2L+1} v(q)q^L v(q')q' Y_L^{M*}(\hat{\mathbf{q}}) Y_L^M(\hat{\mathbf{q}}') \quad (3.44)$$

then the  $L^{th}$  two-body partial wave can be expressed as:

$$V^L(\mathbf{r}, \mathbf{r}') = \frac{b_L}{2\pi^6} \frac{4\pi}{2L+1} \int d\mathbf{q} d\mathbf{q}' ds v(q)v(q')q'^L \sum Y_L^{m*}(\hat{\mathbf{q}}) e^{-i\mathbf{q}\cdot(\mathbf{r}-\mathbf{s})} e^{i\mathbf{q}'\cdot(\mathbf{r}'-\mathbf{s})} \rho(s). \quad (3.45)$$

Defining

$$F_L^M(\mathbf{r}, \mathbf{s}) \equiv \frac{1}{2\pi^3} \int d\mathbf{q} v(q)q^L Y_L^M(\hat{\mathbf{q}}) e^{-i\mathbf{q}\cdot(\mathbf{r}-\mathbf{s})} \rho(s) \quad (3.46)$$

which can be written as

$$F_L^M(\mathbf{r}, \mathbf{s}) = \frac{(4\pi)^2}{(2\pi)^3} \int d\mathbf{q} v(q)q^L \sum (-i)^L Y_l^m(\hat{\mathbf{r}}) Y_l^{m*}(\hat{\mathbf{q}}) j_l(qr) \sum (i)^\lambda Y_\lambda^{\mu*}(\hat{\mathbf{s}}) j_\lambda(qs) \quad (3.47)$$

then  $V$  will be written as

$$V^L(\mathbf{r}, \mathbf{r}') = \frac{4\pi b_L}{2L+1} \int ds F_L^M(\mathbf{r}, \mathbf{s}) \rho(s) F_L^{m*}(\mathbf{s}, \mathbf{r}') \quad (3.48)$$

Where

$$F_{L,\lambda,l}(r, s) \equiv \frac{2}{\pi} \int_0^\infty q^2 dq v(q)q^L j_l(qr) j_l(sr) \quad (3.49)$$

then by expanding  $V$  we get

$$V^L(\mathbf{r}, \mathbf{r}') = b_L \sum Y_l^m(\hat{\mathbf{r}}) Y_l^{m*}(\hat{\mathbf{r}}') [C_{L,l,\lambda}^{0,0,0}]^2 \int_0^\infty s^2 ds f_{L,\lambda,l}(r, s) \rho(s) f_{L,\lambda,l}(s, r'). \quad (3.50)$$

The subroutine PIPOT in the code calculates the  $V^S, V^P$  and another subroutine

VCAL calculates the total non-local potential for different values of  $r$  and  $r'$ ,

$$V_T = -\frac{A}{4\pi} [b_0 V^s(r, r') + b_1 V^p(r, r')] \quad (3.51)$$

then this potential will be included the in Schrödinger equation which can be written in the partial wave form and solved for the pion wave function.

### 3.4 Pion Absorption Correction

The pion absorption process is essentially an exclusive reaction in which no pion is left in the final state. Its study provides unique information on pion-nucleus interactions where the pion mass as well as its energy and momentum are completely converted to the energy of the nucleus in the final state. The conservation of energy and momentum does not allow the pion to be absorbed by a single bound nucleon at rest (very low probability). Since the pion transfers a large energy to the nucleon, in the final state it will have kinetic energy  $T_N = \frac{p^2}{2M} \equiv m_\pi$ , which corresponds to the momentum  $p \equiv (2m_\pi M)^{\frac{1}{2}} \equiv 500$  MeV/c. This value of p is about twice that available from the nuclear Fermi momentum distribution. Consequently, the absorption process preferentially involves two or more nucleons to distribute the momentum mismatch. Since pion absorption by a single nucleon is strongly suppressed, the leading process involves at least two nucleons. The two-body absorption is often considered to be S-wave  $\pi N$  rescattering followed by absorption, and p-wave pion absorption with formation of an intermediate  $\Delta N$  state.

For nucleons the terms reaction cross section, inelastic cross section and absorption cross section are often used to describe processes that remove flux from the elastic channel. For pions the term inelastic denotes a scattering event that

has a real pion in the final state but not elastic scattering. The term absorption refers to reactions with no real pion in the final state, which is sometimes called true absorption. The term reaction cross section refers to the sum of absorption and inelastic scattering, and total cross section is the sum of reaction and elastic one. The total nuclear absorption cross sections have been measured as a function of energy for selected nuclei through the resonance region [21, 22]. Even outside this region  $\sigma_{abs}$  is important, in particular for heavy nuclei, for which it becomes about one-third of the total cross-section at  $\Delta$ -resonance energy. The cross section for light nuclei with  $A \leq 30$  shows the typical  $\Delta$ - resonance behaviour familiar from the  $\pi$  d absorption process, but this feature is nearly absent for heavy elements. This suggests that the basic absorption process in heavy elements is proceeds by one or more quasifree scattering steps. The scattering amplitude  $f_k(\theta)$  can be written in terms of partial waves as follows:

$$f_k(\theta) = \frac{1}{k} \sum_{l=0}^{\infty} (2l+1) e^{i\delta_l} \sin \delta_l P_l(\cos \theta) \quad (3.52)$$

$$= \frac{1}{2ik} \sum_{l=0}^{\infty} (2l+1) (S_l - 1) P_l(\cos \theta) \quad (3.53)$$

where  $S_l$  is the scattering matrix. Then the total cross section can be obtained from the optical theorem:

$$\sigma_{total} = \frac{4\pi}{k} \text{Im} f(0) \quad (3.54)$$

where  $f(0)$  is the forward scattering amplitude or,

$$\sigma_{total} = \frac{2\pi}{k^2} \sum_{l=0}^{\infty} (2l+1) \text{Re}(1 - S_l). \quad (3.55)$$

Also, the integral of the elastic scattering can be written as:

$$\int \sigma(\theta)d\Omega = \frac{\pi}{k^2} \sum_{l=0}^{\infty} (2l+1)[|S_l|^2 + 1 - 2\text{Re}S_l]. \quad (3.56)$$

Subtracting the integral of the elastic cross section from the total cross section gives the reaction cross section :

$$\sigma_R = \frac{\pi}{k^2} \sum_{l=0}^{\infty} (2l+1)(1 - |S_l|^2). \quad (3.57)$$

Thus, for a real potential there is no reaction possible, the integrated elastic is complex and the mean flux is not conserved so that  $|S_l|^2 \leq 1$  replaces the elastic condition of unitarity  $|S_l|=1$ .

In the code (Appendix B), the correction for pion true absorption can be achieved (from this work) by including a purely imaginary term in the optical potential [20] of the form  $W\rho^2$ , where  $\rho$  is the nuclear density (nucleons per fm<sup>3</sup>).

The imaginary part of the optical potential is:

$$V_{abs} = iW\rho^2(r) \quad (3.58)$$

where  $\rho(r)$  is normalized, such that  $\int_0^{\infty} r^2 dr \rho(r) = 1$ , and  $W$  is the pion absorption coefficient, The total cross section (from the elastic channel containing the optical potential) can be separated into an elastic ( $\sigma_e$ ), quasi-free ( $\sigma_{qf}$ ), and true absorption ( $\sigma_a$ ) piece given by [32]

$$\sigma_e = \int \frac{d\sigma}{d\Omega} d\Omega \quad (3.59)$$

$$\sigma_a = \frac{4\pi W}{k} \sum_l (2l + 1) \int |\psi_l(r)|^2 \rho^2(r) dr \quad (3.60)$$

$$\sigma_{qf} = \frac{4\pi}{k} \sum_l (2l + 1) \int \int \psi_l^*(r') \text{Im}(V(r, r')) \psi_l(r) r^2 dr r'^2 dr' \quad (3.61)$$

where  $V$  is the first-order optical potential. Then

$$\sigma_{total} = \sigma_e + \sigma_a + \sigma_{qf}, \quad (3.62)$$

where  $\sigma_{qf}$  is giving above for a complex potential. The parameter  $W$  is adjusted to reproduce the experimental values for true absorption cross sections for both Ca and C. This can be done by running the code to calculate,  $\sigma_a$ , the absorption cross section and the reaction cross section,  $\sigma_r$ , which are supposed to be equal when the potential is real so that  $\sigma_a = \sigma_r$  and the quasifree potential will be zero. The code is run again to reproduce the experimental cross section by including the potential (real part only) and by adjusting the parameters  $W$ . For each value of  $\sigma_a$ , (which is interpolated from the experimental results [21, 22, 23] to obtain the absorption coefficients of Ca (from this work) for all the different energies), the values of  $W$  were fitted to the following formula (Breit-Wigner):

$$W = \frac{(\Gamma/2)^2}{(E - E_0)^2 + (\Gamma/2)^2}. \quad (3.63)$$

The constants  $E_0=215$  and  $\Gamma=77/2$  give the best fit. The values of  $W$  which correspond to  $^{14}\text{C}$  were determined by scaling those for Ca by  $(\frac{14}{40})^2$ .

The code (Appendix B) which is used for the calculations of the DCX cross sections for Ca isotopes is run with two data files, `ingin.dat` and `pout.dat`. The first

one has the input parameters such as core atomic number,  $Z$ , energy, alpha, and other important parameters, while the other one, which comes as output of another program rdep.for, calculates the strengths of the potential  $b_0$  and  $b_1$  using the technique of multiple scattering. Once these two files are set, then the Ca code can be run for different energies up to 300 MeV to calculate both the two parameters A, and B, consequently the DCX cross sections from the above equations (see sample results in Appendix C). The results of this Chapter will be presented in the figures of Chapter V (5.7, 5.8, 5.9, 5.10, 5.11, 5.12, 5.13 and 5.14).

CHAPTER IV  
REMOVING THE  $\delta$  FUNCTION FROM THE DCX  
AMPLITUDE

In this chapter, the delta function removal from the DCX amplitude (as developed in this work) will be treated. The DCX operator resembles the one pion exchange potential since the dominant coupling to the nucleon is p wave in nature. The appearance of the  $\delta$ -function in the DCX operator comes from the point of view of point-like pion-nucleon coupling, where the interaction actually extends over a finite region of space. The  $\delta$ -function present in the exchange of  $\pi^0$  in the relative spatial coordinates in the limit of zero range form factors, so the propagator part of the operator is:

$$\frac{q^2}{q^2 - k^2} \quad (4.1)$$

which is finite as  $q$  goes to infinity; it leads to an amplitude with a  $\delta$ -function in  $r$  space.

The general expression for the double charge exchange amplitude in the sequential approximation is:

$$A_{DCX}(\mathbf{k}', \mathbf{k}) = \int d\mathbf{r}_1 d\mathbf{r}_2 \chi^*(\mathbf{r}_1, \mathbf{r}_2) \psi_-^{(-)*}(\mathbf{k}', \mathbf{r}_2) f(\mathbf{k}_2, \mathbf{q}_2) G(\mathbf{r}_1, \mathbf{r}_2) \quad (4.2)$$

$$\psi_+^{(+)}(\mathbf{k}, \mathbf{r}_1) \chi(\mathbf{r}_1, \mathbf{r}_2)$$

where  $\chi$  represents the wave function of the two nucleons in the nucleus,  $\psi_+$  and  $\psi_-$  represent the wave functions of the incoming and outgoing pions,  $f(\mathbf{k}, \mathbf{k}')$



represents the single charge exchange amplitude discussed previously and  $G(\mathbf{r}_1, \mathbf{r}_2)$  is the Green's function for the propagation of the neutral pion from  $\mathbf{r}_1$  to  $\mathbf{r}_2$ . The quantities  $\mathbf{k}_1$ ,  $\mathbf{k}_2$ ,  $\mathbf{q}_1$  and  $\mathbf{q}_2$  are to be interpreted as operators on, respectively, the initial pion wave function, the final pion wave function, the argument  $\mathbf{r}_1$  in the Green function and the argument  $\mathbf{r}_2$  in the Green function. The  $\delta$ -function correction will arise only from the part of the double scattering amplitude which comes from the p-wave part of the product. Thus, to develop the correction we need only consider that term.

$$\begin{aligned} & \psi_-^{(-)*}(\mathbf{k}', \mathbf{r}_2) f(\mathbf{k}_2, \mathbf{q}_2) G(\mathbf{r}_1, \mathbf{r}_2) f(\mathbf{q}_1, \mathbf{k}_1) \psi_+^{(+)}(\mathbf{k}, \mathbf{r}_1) \\ \rightarrow & \psi_-^{(-)*}(\mathbf{k}', \mathbf{r}_2) \frac{(\alpha^2 + k_0^2)^2 \mathbf{k}_2 \cdot \mathbf{q}_2}{(\alpha^2 + k_2^2)(\alpha^2 + q_2^2)} G(\mathbf{r}_1, \mathbf{r}_2) \frac{(\alpha^2 + k_0^2)^2 \mathbf{k}' \cdot \mathbf{q}_1}{(\alpha^2 + k_1^2)(\alpha^2 + q_1^2)} \psi_+^{(+)}(\mathbf{k}, \mathbf{r}_1). \end{aligned} \quad (4.3)$$

Note that the factor  $\frac{1}{(\alpha^2 + k^2)}$  can be applied to the pion wave functions changing only the radial parts:

$$\frac{(\alpha^2 + k_0^2)}{(\alpha^2 + k^2)} \psi(\mathbf{r}) = \tilde{\psi}(\mathbf{r}) \quad (4.4)$$

so that we need consider only

$$(\alpha^2 + k_0^2)^2 \frac{\mathbf{k}_2 \cdot \mathbf{q}_2}{(\alpha^2 + q_2^2)} G(\mathbf{r}_1, \mathbf{r}_2) \frac{\mathbf{k}_2 \cdot \mathbf{q}_1}{(\alpha^2 + q_1^2)}. \quad (4.5)$$

In the present program, the Green's function is obtained by a numerical procedure. Since we anticipate that the correction is of very short range, we will

make (for the purposes of the correction only) the approximation that the neutral pion is undistorted in the intermediate state. So, for  $\mathbf{r}_1 \approx \mathbf{r}_2$  we write

$$(\alpha^2 + k_0^2)^2 \int \frac{d\mathbf{q}}{(2\pi)^3} \frac{\mathbf{k}_2 \cdot \mathbf{q}_2}{(\alpha^2 + q_2^2)} \frac{e^{i\mathbf{q} \cdot (\mathbf{r}_1 - \mathbf{r}_2)}}{q^2 - k_0^2 + i\epsilon} \frac{\mathbf{k}_1 \cdot \mathbf{q}_1}{(\alpha^2 + q_1^2)} \quad (4.6)$$

$$= (\alpha^2 + k_0^2)^2 \int \frac{d\mathbf{q}}{(2\pi)^3} \frac{\mathbf{k}_2 \cdot \mathbf{q}}{(\alpha^2 + q^2)} \frac{e^{i\mathbf{q} \cdot (\mathbf{r}_1 - \mathbf{r}_2)}}{q^2 - k_0^2 + i\epsilon} \frac{\mathbf{k}_1 \cdot \mathbf{q}}{(\alpha^2 + q^2)}$$

$$= (\alpha^2 + k_0^2)^2 \int \frac{d\mathbf{q}}{(2\pi)^3} \frac{\mathbf{k}_2 \cdot \mathbf{q} \mathbf{k}_1 \cdot \mathbf{q}}{(\alpha^2 + q^2)^2} \frac{e^{i\mathbf{q} \cdot (\mathbf{r}_1 - \mathbf{r}_2)}}{q^2 - k_0^2 + i\epsilon}$$

$$= (\alpha^2 + k_0^2)^2 \int \frac{d\mathbf{q}}{(2\pi)^3} \frac{\mathbf{k}_2 \cdot \hat{\mathbf{q}} \mathbf{k}_1 \cdot \hat{\mathbf{q}}}{(\alpha^2 + q^2)^2} e^{i\mathbf{q} \cdot (\mathbf{r}_1 - \mathbf{r}_2)} \frac{q^2}{q^2 - k_0^2 + i\epsilon}. \quad (4.7)$$

#### 4.1 The Appearance of the $\delta$ -function

The expansion of  $\mathbf{k}_2 \cdot \mathbf{q} \mathbf{k}_1 \cdot \mathbf{q}$  will yield an s-wave and a d-wave part as can be shown in the following:

$$\begin{aligned} \mathbf{k}_2 \cdot \mathbf{q} \mathbf{k}_1 \cdot \mathbf{q} &= \frac{1}{3}(\mathbf{k}_2 \cdot \mathbf{k}_1)q^2 + \frac{1}{3}[3(\mathbf{k}_1 \cdot \mathbf{q})(\mathbf{k}_2 \cdot \mathbf{q}) - (\mathbf{k}_1 \cdot \mathbf{k}_2)q^2] \quad (4.8) \\ &= \frac{1}{3}(\mathbf{k}_2 \cdot \mathbf{k}_1)q^2 + \frac{1}{3}S_{12} \end{aligned}$$

where the tensor operator  $S_{12}$  in the momentum space is defined as:

$$S_{12} = [3(\mathbf{k}_1 \cdot \mathbf{q})(\mathbf{k}_2 \cdot \mathbf{q}) - (\mathbf{k}_1 \cdot \mathbf{k}_2)q^2].$$

By the tensor product, this can be written as a sum of s-wave and d-wave as follows:

$$(\mathbf{k}_1 \cdot \mathbf{q}) \cdot (\mathbf{k}_2 \cdot \mathbf{q}) = \frac{4\pi}{3} \sum_{m,m'} q^2 (-1)^{m+m'} k_1^{-m'} k_2^m Y_1^m(\hat{\mathbf{q}}) Y_1^{m'}(\hat{\mathbf{q}}) \quad (4.9)$$

which can be simplified by Gaunt's integral:

$$(\mathbf{k}_1 \cdot \mathbf{q})(\mathbf{k}_2 \cdot \mathbf{q}) = \frac{4\pi}{3} \sum_{m,m'} (-1)^{m+m'} k_1^{-m} k_2^{-m'} \sqrt{\frac{(3)(3)}{4\pi(2\lambda+1)}} C_{1,1,\lambda}^{0,0,0} C_{1,1,\lambda}^{m,m',\mu} Y_{\lambda}^{\mu}(\hat{\mathbf{q}}) \quad (4.10)$$

$$= \frac{1}{3} q^2 (\mathbf{k}_1 \cdot \mathbf{k}_2) + \sqrt{\frac{8\pi}{15}} q^2 \sum_{\mu} (-1)^{\mu} \Sigma_2^{\mu} Y_2(\hat{\mathbf{q}}) \quad (4.11)$$

where

$$\Sigma_2^{\mu} = \sum_{m,m'} C_{1,1,2}^{m,m',\mu} k_1^m k_2^{m'}. \quad (4.12)$$

As can be seen, this expression has both s-wave and d-wave parts. The part we want to correct is only the s-wave portion which is the one that contains the delta function since the integral of:

$$\int_0^{\infty} q^2 dq j_0(qr) \rightarrow \delta(r) \quad (4.13)$$

is finite at  $q \rightarrow \infty$  and goes to a delta function.

#### 4.2 The Correction for the $\delta$ Function

So, the s-wave part of the pp amplitude is:

$$A_s = \frac{1}{3} \mathbf{k}_2 \cdot \mathbf{k}_1 (\alpha^2 + k_0^2)^2 \int \frac{d\mathbf{q}}{(2\pi)^3} \frac{e^{i\mathbf{q} \cdot (\mathbf{r}_1 - \mathbf{r}_2)}}{(\alpha^2 + q^2)^2} \frac{q^2}{q^2 - k_0^2 + i\epsilon} \quad (4.14)$$

which will be corrected as follow:

$$\rightarrow (\alpha^2 + k_0^2)^2 \frac{1}{3} \mathbf{k}_2 \cdot \mathbf{k}_1 \int \frac{d\mathbf{q}}{(2\pi)^3} \frac{e^{i\mathbf{q} \cdot (\mathbf{r}_1 - \mathbf{r}_2)}}{(\alpha^2 + q^2)^2} \left( \frac{q^2}{q^2 - k_0^2 + i\epsilon} - 1 \right). \quad (4.15)$$

Thus, the correction to the operator is:

$$C = -\frac{1}{3} \mathbf{k}_2 \cdot \mathbf{k}_1 (\alpha^2 + k_0^2)^2 k_0^2 \int \frac{d\mathbf{q}}{(2\pi)^3} \frac{e^{i\mathbf{q} \cdot (\mathbf{r}_1 - \mathbf{r}_2)}}{(\alpha^2 + q^2)^2}. \quad (4.16)$$

We will have to evaluate:

$$I = (\alpha^2 + k_0^2)^2 \int \frac{d\mathbf{q}}{(2\pi)^3} \frac{e^{i\mathbf{q} \cdot (\mathbf{r}_1 - \mathbf{r}_2)}}{(\alpha^2 + q^2)^2} \quad (4.17)$$

$$I = (\alpha^2 + k_0^2)^2 (4\pi)^2 \int \frac{d\mathbf{q}}{(2\pi)^3} \sum Y_L^M(\hat{\mathbf{r}}_1) Y_L^{M*}(\hat{\mathbf{q}}) Y_{L'}^{M'*}(\hat{\mathbf{r}}_2) Y_{L'}^{M'}(\hat{\mathbf{q}}) \frac{j_L(qr_1) j_{L'}(qr_2)}{(\alpha^2 + q^2)^2} \quad (4.18)$$

$$I = (\alpha^2 + k_0^2)^2 \frac{2}{\pi} \int q^2 dq \sum Y_{L'}^{M'}(\hat{\mathbf{r}}_1) Y_{L'}^{M'*}(\hat{\mathbf{r}}_2) \frac{j_{L'}(qr_1) j_{L'}(qr_2)}{(\alpha^2 + q^2)^2}$$

$$I = (\alpha^2 + k_0^2)^2 \frac{2}{\pi} \sum Y_{L'}^{M'}(\hat{\mathbf{r}}_1) Y_{L'}^{M'*}(\hat{\mathbf{r}}_2) \int_0^\infty q^2 dq \frac{j_{L'}(qr_1) j_{L'}(qr_2)}{(\alpha^2 + q^2)^2}$$

$$I = \sum Y_{L'}^{M'}(\hat{\mathbf{r}}_1) Y_{L'}^{M'*}(\hat{\mathbf{r}}_2) g_{L'}(r_1, r_2) \quad (4.19)$$

where

$$g_{L'}(r_1, r_2) \equiv (\alpha^2 + k_0^2)^2 \frac{2}{\pi} \int_0^\infty q^2 dq \frac{j_{L'}(qr_1) j_{L'}(qr_2)}{(\alpha^2 + q^2)^2} \quad (4.20)$$

$$= -(\alpha^2 + k_0^2) \frac{2}{\pi} \frac{d}{d\alpha} \frac{1}{4} \int_{-\infty}^{\infty} q^2 dq \frac{j_{L'}(qr_1)j_{L'}(qr_2)}{(\alpha^2 + q^2)} \quad (4.21)$$

$$= -\frac{(\alpha^2 + k_0^2)}{\alpha} \frac{2}{\pi} \frac{d}{d\alpha} \frac{1}{16} \int_{-\infty}^{\infty} q^2 dq \frac{[h_{L'}^{(+)}(qr_1) + h_{L'}^{(-)}(qr_1)][h_{L'}^{(+)}(qr_2) + h_{L'}^{(-)}(qr_2)]}{(\alpha^2 + q^2)}. \quad (4.22)$$

This integration can be done using the residue theorem:

$$I = \int_{-\infty}^{\infty} f(z)dz = 2\pi i \sum R \quad (4.23)$$

where R is the residue in the upper half plane equal:

$$R = \lim_{z \rightarrow z_0} (z - z_0) f(z) \quad (4.24)$$

and  $z_0 = \pm i\alpha$  are the poles in which the above integral will be evaluated. The results are:

$$g'_L(r_1, r_2) = -\frac{(\alpha^2 + k_0^2)^2}{2\alpha} \frac{d}{d\alpha} \alpha j_{L'}(i\alpha r_2) h^+_{L'}(i\alpha r_1) \quad \text{for } r_1 > r_2 \quad (4.25)$$

$$g'_L(r_1, r_2) = -\frac{(\alpha^2 + k_0^2)^2}{2\alpha} \frac{d}{d\alpha} \alpha j_{L'}(i\alpha r_1) h^+_{L'}(i\alpha r_2) \quad \text{for } r_1 < r_2. \quad (4.26)$$

By differentiating with respect to  $\alpha$  equation 4.29, we get:

$$g'_L(r_1, r_2) = \frac{(\alpha^2 + k_0^2)^2}{2\alpha} [j_{L'}(i\alpha r_2) h^+_{L'}(i\alpha r_1) + i\alpha r_2 j'_{L'}(i\alpha r_2) h^+_{L'}(i\alpha r_1)]$$

$$+ i\alpha r_1 j_{L'}(i\alpha r_2) h'_{L'}(i\alpha r_1)] \quad (4.27)$$

$$j'_{L'}(x) = \frac{1}{2L'+1} (L' j_{L'-1}(x) - (L'+1) j_{L'+1}(x)) \quad (4.28)$$

$$h'^+_{L'}(x) = \frac{1}{2L'+1} (L h^+_{L'-1}(x) - (L'+1) h_{L'+1}(x)).$$

### 4.3 The Correction In Distorted Waves

The distorted pion waves are:

$$\tilde{\psi}(\mathbf{k}, \mathbf{r}) = 4\pi \sum i^\lambda Y_\lambda^{\mu*}(\hat{\mathbf{r}}) Y_\lambda^\mu(\hat{\mathbf{k}}) \tilde{\phi}_\lambda(k, r) \quad (4.29)$$

$$C = -\frac{1}{3} (4\pi)^2 \int d\mathbf{r}_1 d\mathbf{r}_2 \chi_f^*(\mathbf{r}_1, \mathbf{r}_2) \chi_i(\mathbf{r}_1, \mathbf{r}_2)$$

$$\mathbf{k}_2 \cdot \mathbf{k}_1 \sum i^{\lambda-\lambda'} Y_\lambda^{\mu*}(\hat{\mathbf{r}}_1) Y_\lambda^\mu(\hat{\mathbf{k}}_i) \tilde{\phi}_\lambda(k_i, r_1) Y_{\lambda'}^{\mu'}(\hat{\mathbf{r}}_2) Y_{\lambda'}^{\mu'*}(\hat{\mathbf{k}}_f) \tilde{\phi}_{\lambda'}(k_f, r_2)$$

$$Y_{L'}^{M'}(\hat{\mathbf{r}}_1) Y_{L'}^{M''*}(\hat{\mathbf{r}}_2) g_{L'}(r_1, r_2). \quad (4.30)$$

For a single shell orbital and  $0^+ \rightarrow 0^+$ , the spin average of the nuclear wave

function can be written as:

$$\langle \chi_f^*(\mathbf{r}_1, \mathbf{r}_2) \chi_i(\mathbf{r}_1, \mathbf{r}_2) \rangle = \chi_\ell^2(r_1) \chi_\ell^2(r_2) \sum a_L Y_L^M(\hat{\mathbf{r}}_1) Y_L^{M*}(\hat{\mathbf{r}}_2). \quad (4.31)$$

Defining one term in the above sum as  $F_L^C(\mathbf{k}, \mathbf{k}')$ , we have

$$\begin{aligned}
 F_L^C(\mathbf{k}, \mathbf{k}') &= -\frac{1}{3}(4\pi)^2 \int d\mathbf{r}_1 d\mathbf{r}_2 \chi_\ell^2(r_1) \chi_\ell^2(r_2) \sum_M Y_L^M(\hat{\mathbf{r}}_1) Y_L^{M*}(\hat{\mathbf{r}}_2) \\
 &\quad \sum i^{\lambda-\lambda'} Y_\lambda^\mu(\hat{\mathbf{k}}_i) Y_{\lambda'}^{\mu'*}(\hat{\mathbf{k}}_f) Y_{L'}^{M'}(\hat{\mathbf{r}}_1) Y_{L'}^{M''*}(\hat{\mathbf{r}}_2) g_{L'}(r_1, r_2) \\
 &\quad \left[ \mathbf{k}_1 Y_\lambda^{\mu*}(\hat{\mathbf{r}}_1) \bar{\phi}_\lambda(k_i, r_1) \right] \cdot \left[ \mathbf{k}_2 Y_{\lambda'}^{\mu'}(\hat{\mathbf{r}}_2) \bar{\phi}_{\lambda'}(k_f, r_2) \right]. \tag{4.32}
 \end{aligned}$$

Expanding the spherical harmonics of the same argument, we have

$$\begin{aligned}
 &\sum_{M, M'} Y_L^M(\hat{\mathbf{r}}_1) Y_L^{M*}(\hat{\mathbf{r}}_2) Y_{L'}^{M'}(\hat{\mathbf{r}}_1) Y_{L'}^{M''*}(\hat{\mathbf{r}}_2) = \\
 &\sum \sqrt{\frac{(2L+1)(2L'+1)}{4\pi(2L''+1)}} C_{L, L', L''}^{0,0,0} C_{L, L', L''}^{M, M', M''} Y_{L''}^{M''}(\hat{\mathbf{r}}_1) \\
 &\quad \times \sqrt{\frac{(2L+1)(2L'+1)}{4\pi(2L''' + 1)}} C_{L, L', L'''}^{0,0,0} C_{L, L', L'''}^{M, M', M'''} Y_{L'''}^{M'''}(\hat{\mathbf{r}}_2) \\
 &= \frac{(2L+1)(2L'+1)}{4\pi} \sum_{L'', M''} \frac{[C_{L, L', L''}^{0,0,0}]^2}{(2L''+1)} Y_{L''}^{M''}(\hat{\mathbf{r}}_1) Y_{L''}^{M''*}(\hat{\mathbf{r}}_2). \tag{4.33}
 \end{aligned}$$

Using this result we can write:

$$F_L^C(\mathbf{k}, \mathbf{k}') = -(2L+1)(2L'+1) \frac{4\pi}{3} \sum i^{\lambda-\lambda'} Y_\lambda^\mu(\hat{\mathbf{k}}_i) Y_{\lambda'}^{\mu'*}(\hat{\mathbf{k}}_f) \frac{[C_{L, L', L''}^{0,0,0}]^2}{(2L''+1)}$$

$$\begin{aligned} & \times \int d\mathbf{r}_1 d\mathbf{r}_2 \chi_\ell^2(r_1) \chi_\ell^2(r_2) Y_{L''}^{M''}(\hat{\mathbf{r}}_1) Y_{L''}^{M''*}(\hat{\mathbf{r}}_2) g_{L'}(r_1, r_2) \\ & \times [\mathbf{k}_1 Y_\lambda^{\mu*}(\hat{\mathbf{r}}_1) \tilde{\phi}_\lambda(\mathbf{k}_i, r_1)] \cdot [\mathbf{k}_2 Y_{\lambda'}^{\mu'}(\hat{\mathbf{r}}_2) \tilde{\phi}_{\lambda'}(\mathbf{k}_f, r_2)] \end{aligned} \quad (4.34)$$

$$\begin{aligned} & = -\frac{4\pi}{3} \sum i^{\lambda-\lambda'} Y_\lambda^\mu(\hat{\mathbf{k}}_i) Y_{\lambda'}^{\mu'*}(\hat{\mathbf{k}}_f) (2L+1)(2L'+1) \\ & \times \frac{[C_{L,L',L''}^{0,0,0}]^2}{(2L''+1)} \int r_1^2 dr_1 r_2^2 dr_2 \chi_\ell^2(r_1) \chi_\ell^2(r_2) g_{L'}(r_1, r_2) \\ & \times \int d\Omega_1 d\Omega_2 Y_{L''}^{M''}(\hat{\mathbf{r}}_1) Y_{L''}^{M''*}(\hat{\mathbf{r}}_2) [\mathbf{k}_1 Y_\lambda^{\mu*}(\hat{\mathbf{r}}_1) \tilde{\phi}_\lambda(\mathbf{k}_i, r_1)] \cdot [\mathbf{k}_2 Y_{\lambda'}^{\mu'}(\hat{\mathbf{r}}_2) \tilde{\phi}_{\lambda'}(\mathbf{k}_f, r_2)]. \end{aligned} \quad (4.35)$$

Defining

$$a^0(\lambda, \mu) = \sqrt{\frac{(\lambda+1)^2 - \mu^2}{(2\lambda+1)(2\lambda+3)}}; \quad b^0(\lambda, \mu) = \sqrt{\frac{\lambda^2 - \mu^2}{(2\lambda-1)(2\lambda+1)}} \quad (4.36)$$

$$a^\pm(\lambda, \mu) = \sqrt{\frac{(\lambda \pm \mu + 1)(\lambda \pm \mu + 2)}{2(2\lambda+1)(2\lambda+3)}}; \quad b^\pm(\lambda, \mu) = \sqrt{\frac{(\lambda \mp \mu - 1)(\lambda \mp \mu)}{2(2\lambda-1)(2\lambda+1)}} \quad (4.37)$$

$$F(\lambda, r) = \frac{df(r)}{dr} - \frac{\lambda}{r} f(r); \quad G(\lambda, r) = \frac{df(r)}{dr} + \frac{\lambda+1}{r} f(r), \quad (4.38)$$

we can write the effect of the gradient operator on the product of a spherical harmonic times a function of  $r$  as:

$$\nabla_0 [f(r) Y_\lambda^\mu] = a^0(\lambda, \mu) F_\lambda(r) Y_{\lambda+1}^\mu(\hat{\mathbf{r}}) + b^0(\lambda, \mu) G_\lambda(r) Y_{\lambda-1}^\mu(\hat{\mathbf{r}}) \quad (4.39)$$



$$\nabla_{\pm} [f(r)Y_{\lambda}^{\mu}] = a^{\pm}(\lambda, \mu)F_{\lambda}(r)Y_{\lambda+1}^{\mu\pm 1}(\hat{\mathbf{r}}) - b^{\pm}(\lambda, \mu)G_{\lambda}(r)Y_{\lambda-1}^{\mu\pm 1}(\hat{\mathbf{r}}). \quad (4.40)$$

Note also using:

$$a^{\sigma}(\lambda, \mu) = \sqrt{\frac{\lambda+1}{2\lambda+3}} C_{\lambda, 1, \lambda+1}^{\mu, \sigma, \mu+\sigma}; \quad b^{\sigma}(\lambda, \mu) = \sqrt{\frac{\lambda}{2\lambda-1}} C_{\lambda, 1, \lambda-1}^{\mu, \sigma, \mu+\sigma} \quad (4.41)$$

we can write

$$\nabla_{\sigma} [f(r)Y_{\lambda}^{\mu}(\hat{\mathbf{r}})] = \sum_{L, M} (-1)^{\frac{L+\lambda+1}{2}} \sqrt{\frac{L+\lambda+1}{2(2L+1)}} C_{\lambda, 1, L}^{\mu, \sigma, M} F_{\lambda, L}(r) Y_L^M(\hat{\mathbf{r}}) \quad (4.42)$$

and

$$\nabla_{-\sigma} [f(r)Y_{\lambda}^{*\mu}(\hat{\mathbf{r}})] = \nabla_{-\sigma} [f(r)Y_{\lambda}^{-\mu}(\hat{\mathbf{r}})] (-1)^{\mu} \quad (4.43)$$

$$= \sum_{L, M} \sqrt{\frac{L+\lambda+1}{2(2L+1)}} C_{\lambda, 1, L}^{-\mu, -\sigma, M} (-1)^{\mu} F_{\lambda, L} Y_L^M(\hat{\mathbf{r}})$$

$$= \sum_{L, M} \sqrt{\frac{L+\lambda+1}{2(2L+1)}} C_{\lambda, 1, L}^{\mu, \sigma, M} (-1)^{\mu} F_{\lambda, L} Y_L^{-M}(\hat{\mathbf{r}})$$

$$= (-1)^{\sigma} \sum_{L, M} \sqrt{\frac{L+\lambda+1}{2(2L+1)}} C_{\lambda, 1, L}^{\mu, \sigma, M} F_{\lambda, L} Y_L^{*M}(\hat{\mathbf{r}}). \quad (4.44)$$

Using these expressions to expand the last line of Eq. 4.35, (which can be done using the tensor product), by replacing  $\mathbf{k}_1$  and  $\mathbf{k}_2$  by their momentum operators  $\nabla^1$  and  $\nabla^2$ , and the tensor product of the two operators will be:

$$\nabla^1 \cdot \nabla^2 = \nabla_0^1 \nabla_0^2 - \nabla_+^1 \nabla_-^2 - \nabla_-^1 \nabla_+^2 \quad (4.45)$$

$$\int d\Omega_1 d\Omega_2 Y_{L''}^{M''}(\hat{\mathbf{r}}_1) Y_{L''}^{M''*}(\hat{\mathbf{r}}_2) [\mathbf{k}_1 Y_{\lambda}^{\mu*}(\hat{\mathbf{r}}_1) \tilde{\phi}_{\lambda}(\mathbf{k}_i, r_1)] \cdot [\mathbf{k}_2 Y_{\lambda'}^{\mu'}(\hat{\mathbf{r}}_2) \tilde{\phi}_{\lambda'}(\mathbf{k}_f, r_2)] =$$

$$\int d\Omega_1 d\Omega_2 Y_{L''}^{M''}(\hat{\mathbf{r}}_1) Y_{L''}^{M''*}(\hat{\mathbf{r}}_2) [A_1 + A_2 + A_3 + A_4 + \dots + A_{12}]$$

where:

$$A_1 = a^0(\lambda, \mu) a^0(\lambda', \mu') F_{\lambda}(r_1) F_{\lambda'}(r_2) Y_{\lambda+1}^{\mu}(\hat{\mathbf{r}}_1) Y_{\lambda'+1}^{\mu'}(\hat{\mathbf{r}}_2)$$

$$A_2 = +b^0(\lambda, \mu) b^0(\lambda', \mu') G_{\lambda}(r_1) G_{\lambda'}(r_2) Y_{\lambda-1}^{\mu}(\hat{\mathbf{r}}_1) Y_{\lambda'-1}^{\mu'}(\hat{\mathbf{r}}_2)$$

$$A_3 = +a^0(\lambda, \mu) b^0(\lambda', \mu') F_{\lambda}(r_1) G_{\lambda'}(r_2) Y_{\lambda+1}^{\mu}(\hat{\mathbf{r}}_1) Y_{\lambda'-1}^{\mu'}(\hat{\mathbf{r}}_2)$$

$$A_4 = +b^0(\lambda, \mu) a^0(\lambda', \mu') G_{\lambda}(r_1) F_{\lambda'}(r_2) Y_{\lambda-1}^{\mu}(\hat{\mathbf{r}}_1) Y_{\lambda'+1}^{\mu'}(\hat{\mathbf{r}}_2)$$

$$A_5 = -a^+(\lambda, \mu) a^-(\lambda', \mu') F_{\lambda}(r_1) F_{\lambda'}(r_2) Y_{\lambda+1}^{\mu+1}(\hat{\mathbf{r}}_1) Y_{\lambda'+1}^{\mu'-1}(\hat{\mathbf{r}}_2)$$

$$A_6 = +a^+(\lambda, \mu) b^-(\lambda', \mu') F_{\lambda}(r_1) G_{\lambda'}(r_2) Y_{\lambda+1}^{\mu+1}(\hat{\mathbf{r}}_1) Y_{\lambda'-1}^{\mu'-1}(\hat{\mathbf{r}}_2)$$

$$A_7 = +b^+(\lambda, \mu) a^-(\lambda', \mu') G_{\lambda}(r_1) F_{\lambda'}(r_2) Y_{\lambda-1}^{\mu+1}(\hat{\mathbf{r}}_1) Y_{\lambda'+1}^{\mu'-1}(\hat{\mathbf{r}}_2)$$

$$A_8 = -b^+(\lambda, \mu)b^-(\lambda', \mu')G_\lambda(r_1)G_{\lambda'}(r_2)Y_{\lambda-1}^{\mu+1}(\hat{\mathbf{r}}_1)Y_{\lambda'-1}^{\mu'-1}(\hat{\mathbf{r}}_2)$$

$$A_9 = -a^-(\lambda, \mu)a^+(\lambda', \mu')F_\lambda(r_1)F_{\lambda'}(r_2)Y_{\lambda+1}^{\mu-1}(\hat{\mathbf{r}}_1)Y_{\lambda'+1}^{\mu'+1}(\hat{\mathbf{r}}_2)$$

$$A_{10} = +a^-(\lambda, \mu)b^+(\lambda', \mu')F_\lambda(r_1)G_{\lambda'}(r_2)Y_{\lambda+1}^{\mu-1}(\hat{\mathbf{r}}_1)Y_{\lambda'-1}^{\mu'+1}(\hat{\mathbf{r}}_2)$$

$$A_{11} = +b^-(\lambda, \mu)a^+(\lambda', \mu')G_\lambda(r_1)F_{\lambda'}(r_2)Y_{\lambda-1}^{\mu-1}(\hat{\mathbf{r}}_1)Y_{\lambda'+1}^{\mu'+1}(\hat{\mathbf{r}}_2)$$

$$A_{12} = -b^-(\lambda, \mu)b^+(\lambda', \mu')G_\lambda(r_1)G_{\lambda'}(r_2)Y_{\lambda-1}^{\mu-1}(\hat{\mathbf{r}}_1)Y_{\lambda'-1}^{\mu'+1}(\hat{\mathbf{r}}_2).$$

The integration over space for the same argument  $(r_1, r_2)$  separately will satisfy the orthonormality relation:

$$\int Y_{l'm'}^*(\hat{\mathbf{r}}_1)Y_{lm}(\hat{\mathbf{r}}_1) = \delta_{ll'}\delta_{mm'}. \quad (4.46)$$

This implies that  $L'' = \lambda \pm 1$ ,  $\lambda' \pm 1$ ,  $M'' = \mu, \mu'$ , and  $\mu \pm 1$ , so  $\lambda' = \lambda$ ,  $\mu' = \mu$  only, and  $L'' = \lambda \pm 1$ . Then all the cross terms will cancel except the first two, which are  $A_1$  and  $A_2$ . The correction will be as follows:

$$F_L^C = -\frac{4\pi}{3} \sum i^{\lambda-\lambda'} Y_\lambda^\mu(\hat{\mathbf{k}}_i) Y_{\lambda'}^{\mu'*}(\hat{\mathbf{k}}_f) (2L+1)(2L'+1) \int r_1^2 dr_1 r_2^2 dr_2 \chi_\ell^2(r_1) \chi_\ell^2(r_2) g_{L'}(r_1, r_2)$$

$$\times \left[ \frac{[C_{L,L',\lambda+1}^{0,0,0}]^2}{(2\lambda+3)} (a^0(\lambda,\mu))^2 F_\lambda(r_1)F_\lambda(r_2) + \frac{[C_{L,L',\lambda-1}^{0,0,0}]^2}{(2\lambda-1)} (b^0(\lambda,\mu))^2 G_\lambda(r_1)G_\lambda(r_2) \right] \quad (4.47)$$

which can be expressed in terms of Legendre polynomials. The result can be reduced to the following equation:

$$F_L^C = -\frac{1}{3} \sum (2\lambda+1) P_\lambda(\cos \theta) \times \left[ \frac{[C_{L,L',\lambda+1}^{0,0,0}]^2}{(2\lambda+3)} (a^0(\lambda,\mu))^2 f_{\lambda,L'} + \frac{[C_{L,L',\lambda-1}^{0,0,0}]^2}{(2\lambda-1)} (b^0(\lambda,\mu))^2 g_{\lambda,L'} \right] \quad (4.48)$$

by defining:

$$f_{\lambda,L'} = \int r_1^2 dr_1 r_2^2 dr_2 \chi_\ell^2(r_1) \chi_\ell^2(r_2) F_\lambda(r_1) F_\lambda(r_2) g_{L'}(r_1, r_2) \quad (4.49)$$

$$g_{\lambda,L'} = \int r_1^2 dr_1 r_2^2 dr_2 \chi_\ell^2(r_1) \chi_\ell^2(r_2) G_\lambda(r_1) G_\lambda(r_2) g_{L'}(r_1, r_2). \quad (4.50)$$

By substituting for the values of  $a^0(\lambda,\mu)$  and  $b^0(\lambda,\mu)$ , we get the final form of the correction which looks like:

$$F_L^C = -\frac{1}{3} \sum P_\lambda(\cos \theta) \times \left[ \frac{[C_{L,L',\lambda+1}^{0,0,0}]^2 (\lambda+1)^2}{(2\lambda+3)^2} f_{\lambda,L'} + \frac{[C_{L,L',\lambda-1}^{0,0,0}]^2 \lambda^2}{(2\lambda-1)^2} g_{\lambda,L'} \right] \quad (4.51)$$

or

$$F_L^C(\mathbf{k}, \mathbf{k}') = -\frac{4\pi}{3} (2L+1) \sum (2L'+1) \frac{[C_{L,L',L''}^{0,0,0}]^2 (L''+\lambda+1)}{2(2L''+1)(2\lambda+1)} Y_\lambda^\mu(\hat{\mathbf{k}}) Y_\lambda^{*\mu}(\hat{\mathbf{k}}') f_{\lambda,L',L''} \quad (4.52)$$

$$= -\frac{1}{3}(2L+1) \sum_{L''=\lambda\pm 1} (2L'+1) \frac{[C_{L,L',L''}^{0,0,0}]^2 (L''+\lambda+1)}{2(2L''+1)} f_{\lambda,L',L''} P_{\lambda}(\cos\theta). \quad (4.53)$$

The calculation of the delta function correction was proceeded by calculating the function  $g_L(r_1, r_2)$  both numerically using trapezoidal and Simpson rules and analytically using the residue theorem as a check (see Table 4.1). Then the analytic function  $g_L(r_1, r_2)$  included in the distorted wave code (Appendix B) was calculated at the same time as the other calculations. The functions  $f_{\lambda,L'}$  and  $g_{\lambda,L'}$  were calculated in the code by integrating over  $r_1$  and  $r_2$  using the same nuclear and pion initial and final wave functions. Then, the last equation of the delta correction was calculated and added to the rest of the DCX amplitude.

In order to check the calculation, the distorted code has been run in the plane wave mode and compared with another plane wave code. The two amplitudes agree with each other with and without delta function. The main purpose is to evaluate the DCX cross sections for Ca isotopes after adding the delta correction, the results will be shown in the figures of Chapter V (5.15, 5.16, 5.17, and 5.18) for both the ground state and analog state. In Table 4.2, the cross sections results for a few energies are shown as a result of these calculations compared with the experimental results from ref [24].

Table 4.1: Table of  $g_L(r_1, r_2)$  Calculated from the Analytic and Numerical forms (Trapezoidal (t) and Simpson (s) rules).

$r_1$ fm	$r_2$ fm	$g_L(r_1, r_2)$ Analytically	$g_L(r_1, r_2)$ Numerically	% difference
0.50000000	0.50000000	1.40080378	1.40095864 (t) 1.40080390 (s)	0.01105467 0.01104603
0.50000000	1.00000000	0.76085967	0.76085073 0.76085958	0.00117523 0.00116315
0.50000000	4.00000000	0.00877968	0.00878033 0.00877970	0.00742412 0.00727117
1.00000000	3.00000000	0.04601619	0.04601655 0.04601617	0.00078710 0.00083291
2.00000000	6.00000000	0.00104734	0.00104733 0.00104734	0.00062358 0.00076097
3.00000000	7.00000000	0.00060093	0.00060088 0.00060088	0.00792092 0.00816123
4.00000000	2.00000000	0.01872612	0.01872611 0.01872611	0.00004112 0.00003277
7.00000000	0.50000000	0.00009318	0.00009300 0.00009300	0.20033139 0.20707640
8.00000000	10.00000000	0.00188339	0.00188339 0.00188339	0.00029930 0.00034402
9.00000000	8.00000000	0.00597016	0.00597023 0.00597023	0.00106950 0.00107241
10.00000000	7.50000000	0.00111605	0.00111606	0.00099149

Table 4.2: Table of DCX Cross Sections, experimental from [24], and from this calculation for  $^{42,44}\text{Ca}$  Analog State at  $\alpha = 300 \text{ MeV}/c$ .

$T_{lab}(\text{MeV})$	$^{42}\text{Ca}$ (an) Experiment	$^{42}\text{Ca}$ (an) Theory	$^{44}\text{Ca}$ (an) Experiment	$^{44}\text{Ca}$ (an) Theory
20	$0.588 \pm 0.100$	0.6796		0.9712
25	$0.460 \pm 0.230$	0.6426	$1.185 \pm 0.307$	1.0588
30	$3.294 \pm 0.350$	0.6470		0.2370
35	$2.538 \pm 0.460$	0.7422	$2.200 \pm 0.600$	0.9822
50	$4.111 \pm 0.840$	1.8770	$1.800 \pm 0.400$	3.6855
60	$1.410 \pm 0.358$	2.847		2.8475
65	$1.410 \pm 0.358$	3.5740	$0.300 \pm 0.110$	5.788
75		5.1769		6.10576
80	$0.615 \pm 0.307$	8.8067		4.9096
125	$0.300 \pm 0.100$	3.3253	$0.850 \pm 0.300$	8.3022
162.5	$0.150 \pm 0.050$		$0.180 \pm 0.050$	
175		0.50248		1.7438
180	$0.130 \pm 0.030$	0.4290	$0.700 \pm 0.180$	1.5007
210		0.1955	$0.300 \pm 0.050$	0.7144
225		0.1381		0.5113
230	$0.180 \pm 0.030$	0.1632	$0.620 \pm 0.050$	0.6195
290	$0.400 \pm 0.060$	0.1662	$1.850 \pm 0.300$	0.6378
300		0.1545	$2.000 \pm 0.300$	0.5977

## CHAPTER V

### RESULTS AND DISCUSSION

In the following chapter, the results of the previous chapters will be mentioned. This includes both Chapter II for the pion double charge exchange operator study, Chapter III for DCX cross section calculations of calcium and carbon nuclei by including the pion absorption correction, and the DCX cross section for calcium isotopes including both corrections for pion absorption and delta removal from the DCX amplitude as found in Chapter IV.

The DCX operator was calculated as a function of energy, and the spin effect on the operator was investigated as shown in Chapter II. The results are given in Figures 5.1, 5.2, 5.3, 5.4, 5.5, and 5.6. Figure 5.1 shows the quantum and classical cross sections for  $\mathbf{k} = \mathbf{k}'$ , i.e.,  $0^\circ$  and  $|\mathbf{k}| = \kappa$ , as a function of the angle between the two nucleons (equal to the two single-charge-exchange scattering angles). It is seen that the agreement between the two is very poor in the near-zone region. This potentially significant quantum correction is due largely to the properties of the pion in the following sense: the near-zone corrections arise from the p-wave nature of the interaction; if  $\lambda_1$  were zero the expression would contain only the function  $g(r)$ , which has no near-zone components. For small  $\kappa$ , the near-zone corrections are particularly important, so it is precisely the pion, with its precocious p-wave strength due to the 3-3 resonance, which gives the strongest violation of the classical limit.



Figure 5.2 shows the non-spin-flip and DSF DCX operator at  $x=0$  ( $90^\circ$ ) as a function of energy at  $r=1$  fm. This configuration, in which the nucleons are oriented perpendicular to the beam axis, provides the most important contribution to DCX for pions of energy of approximately 50 MeV; at this energy the single-charge-exchange cross section is nearly zero in the forward direction. Figure 5.3 shows the absolute value of the projected operator with and without the inclusion of the double spin flip. It is seen that when the DSF operator is important below 300 MeV it diminishes the sensitivity of DCX to the short range part of the nucleon-nucleon wave function.

Figure 5.4 shows the behavior as a function of energy of the two coefficients in Eq. 2.38 as well as that of the  $\delta$ -function. Figure 5.5 shows the behavior of  $r^2Q^\pm(r)$  the projected operator as a function of  $r$  at 200 MeV. The oscillatory behavior of  $Q^+$  and the total operator is apparent while  $Q^-$  is nearly constant. Figure 5.6 shows the absolute integrated operator for  $r_{min} = 1$  fm at 200 and 50 MeV as a function of  $R$ . At 200 MeV the sum approaches  $\bar{Q}(R)$  for large  $r$  so the oscillating part dies out. At 50 MeV the same thing must happen eventually but because of the smaller value of  $k$  the cancellation between  $Q^+$  and  $Q^-$  dominates over the nuclear volume.

The results of Chapter III will be in the Figures 5.7, 5.8, 5.9, 5.10, 5.11, 5.12, 5.13, and 5.14 which include the absorption effect.

Figure 5.7 shows the values of  $W$  which represent pion true absorption versus energy as giving by Eq. 3.63. Figures 5.8 and 5.9 which show the DCX cross sections calculations at  $10^\circ$  for  $^{42,44,48}\text{Ca}$  to the isobaric analog state and to the ground state with  $\alpha = 800$  MeV/c and pion energy up to 300 MeV. The data are taken from [33, 34, 35]. Figures 5.10 and 5.11 are the same but at  $\alpha = 600$  and 300 MeV/c. The curves are obtained from DWIA of the seniority model calculations (solid curve) total, DWIA calculations with non-spin-flip amplitudes only (small and large dashes).

As it can be seen, the calculation fits fairly well for the energy range above 200 MeV where the cross sections of calcium isotopes are almost flat. At the energy range below 200 MeV there are resonances which partially fit as expected, for this reason the delta function has been removed from the DCX amplitude as given in Chapter IV.

Similarly, the DCX cross sections of the  $^{14}\text{C}(\pi^+, \pi^-)^{14}\text{O}$  reactions are calculated in a different code using the same optical potential but instead of calculating A and B the code calculates two SCX amplitudes to get the total DCX amplitude then the cross section can be obtained for both non-spin-flip and the total. The result of this code is shown in Figures 5.12, 5.13, and 5.14, which shows the DCX cross sections calculated for the reaction  $^{14}\text{C}(\pi^+, \pi^-)^{14}\text{O}$  (DIAS) at  $5^\circ$ . The curves shown are obtained from DWIA calculations. The pion energy up to

300 MeV and  $\alpha = 300, 500, 800$  MeV/c, respectively, data are taken from [36, 37, 38, 39, 40]. The calculations gives a reasonable fit with data.

Figure 5.15 shows the shell (Sh) and seniority (Sn) models calculations for the ground state (g) at  $10^\circ$  for  $^{44,48}\text{Ca}$  with  $\alpha = 300$  MeV/c. The results fit the data fairly well and the  $\delta$ -function corrections show a small improvement in the agreement with the cross sections of the calcium isotopes.

Figures 5.16 and 5.17 are the seniority model (Sn) calculations from DWIA for both the ground state and the analog state of  $^{44,48}\text{Ca}$ , which include total DCX cross sections, without  $\delta$ -function, no DSF, no DSF and no  $\delta$ -function and at  $\alpha = 800$  and  $300$  MeV/c. Figure 5.18 is the same but for  $^{42}\text{Ca}$  analog state with  $\alpha = 300$  and  $600$  MeV/c. The results of the DCX cross sections for Ca isotopes as can be seen from the graph are in good agreement with data for  $^{42}\text{Ca}$ , in partial agreement for  $^{44}\text{Ca}$ , and agree poorly for  $^{48}\text{Ca}$ . Notice that the peaks in the low energy region are still there even after the delta correction which leaves open the possibility for the Dibaryon's existence.

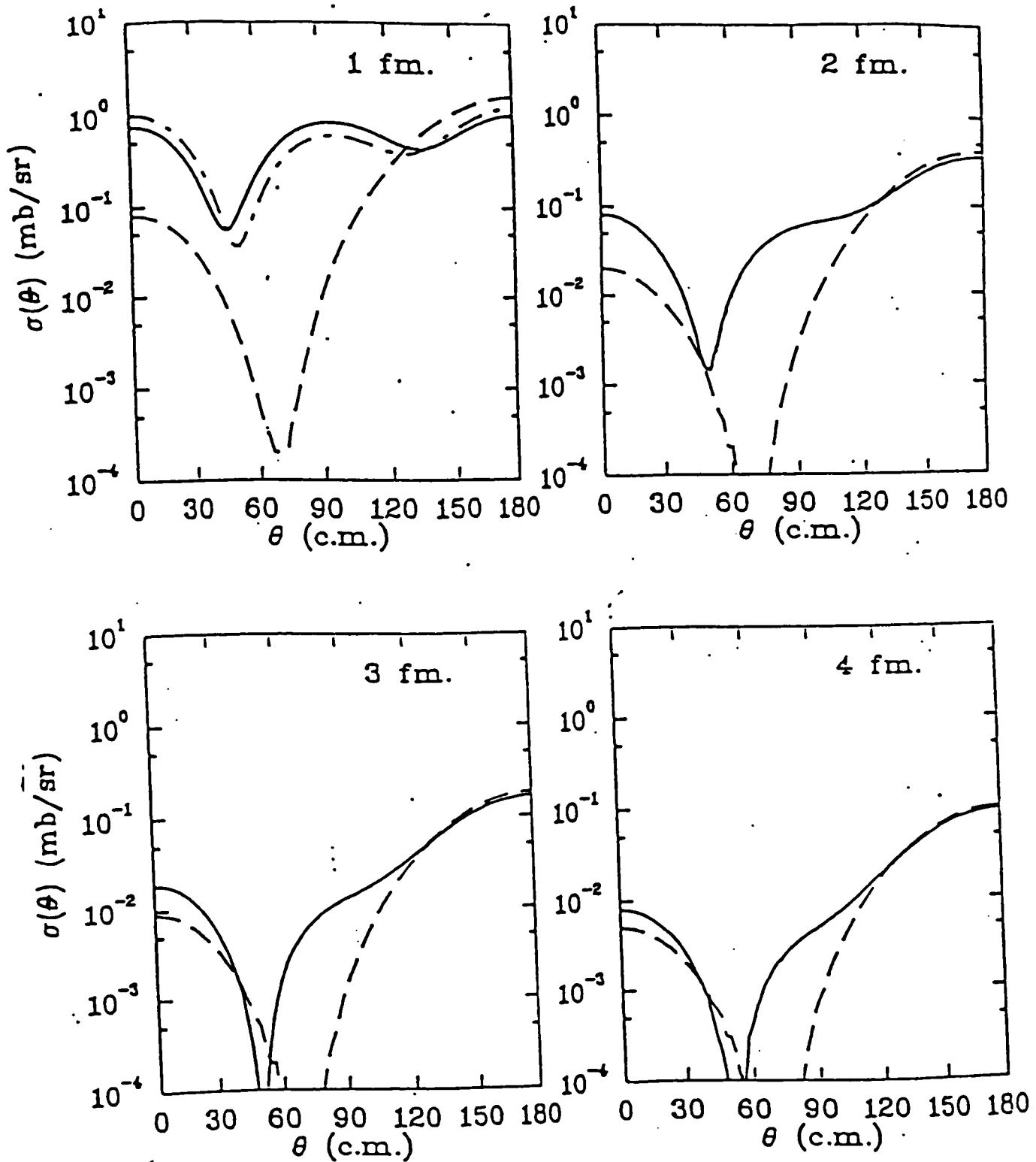


Figure 5.1: Comparison of the classical and quantum-mechanical double-scattering cross sections at 100 MeV. The solid line represents the QM cross section with the  $\delta$ -function included and the dash-dot curve the same quantity without it. The dashed line is the classical cross section.

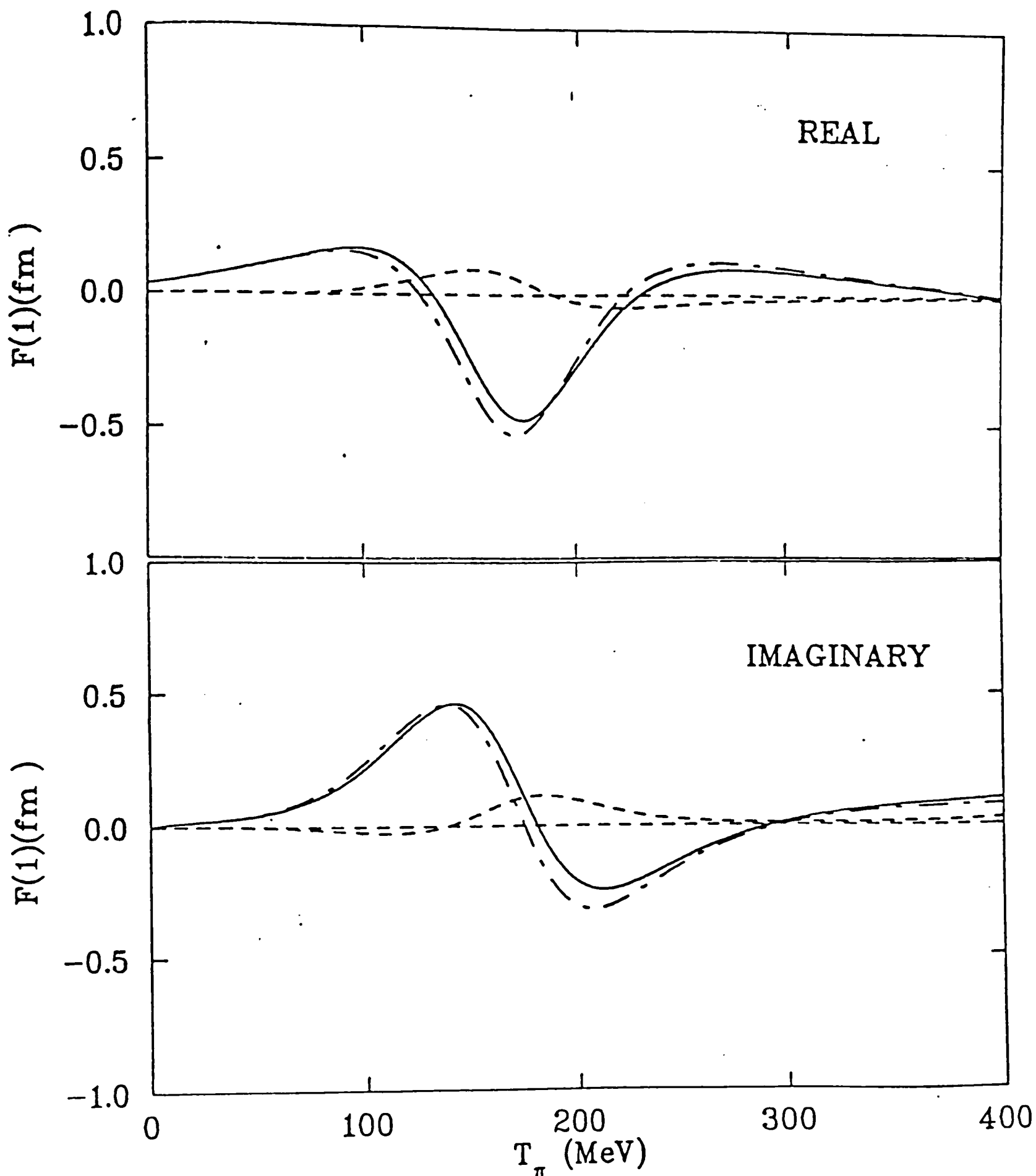


Figure 5.2: Non-spin-flip and double-spin-flip DCX operators at  $x=0$  ( $90^\circ$ ) as a function of energy at an internucleon spacing 1 fm. The solid line corresponds to the total, the dashed line to the DSF operator and the dash-dot line to NSF operator.

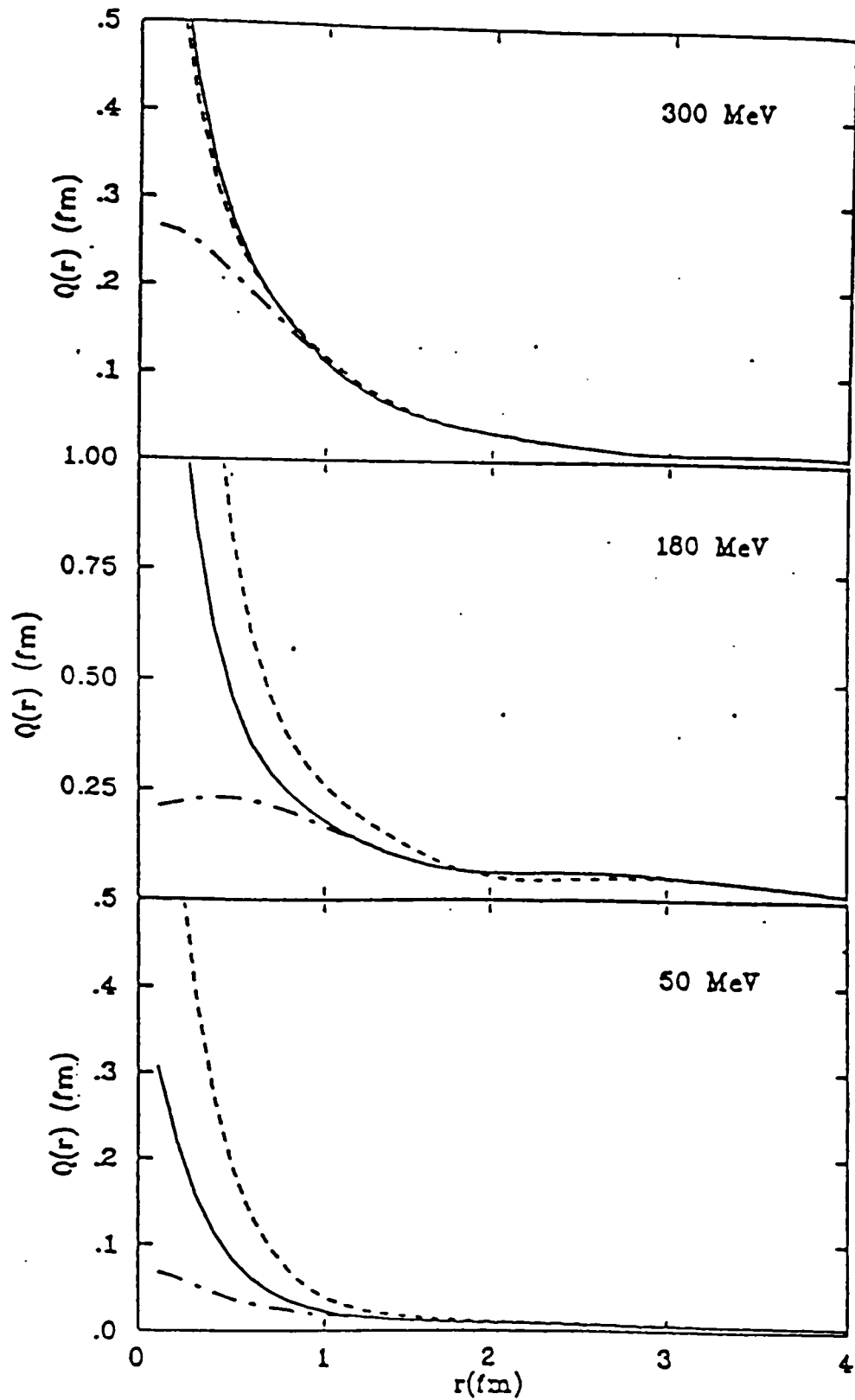


Figure 5.3: Absolute value of projected operator with (solid curve) and without (dotted curve) the inclusion of the double spin flip amplitude. The dash-dot curve is the absolute value of the sum without the  $\delta$ -function.

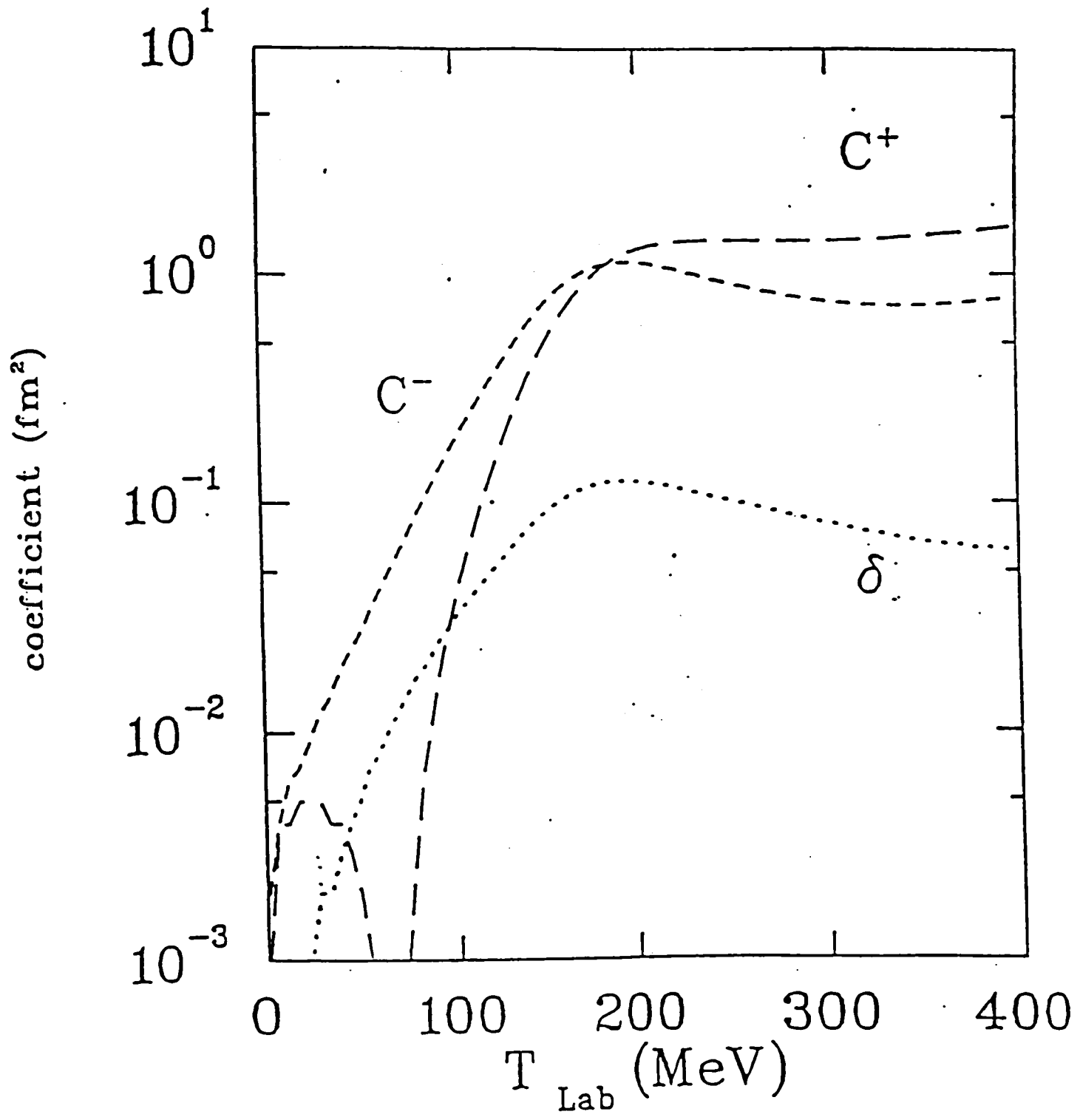


Figure 5.4: Behavior as a function of energy of the two coefficients in Eq 2.38 as well as of the  $\delta$ -function.  $C^\pm \equiv |\lambda_0 \pm \lambda_1 k^2|^2$ .

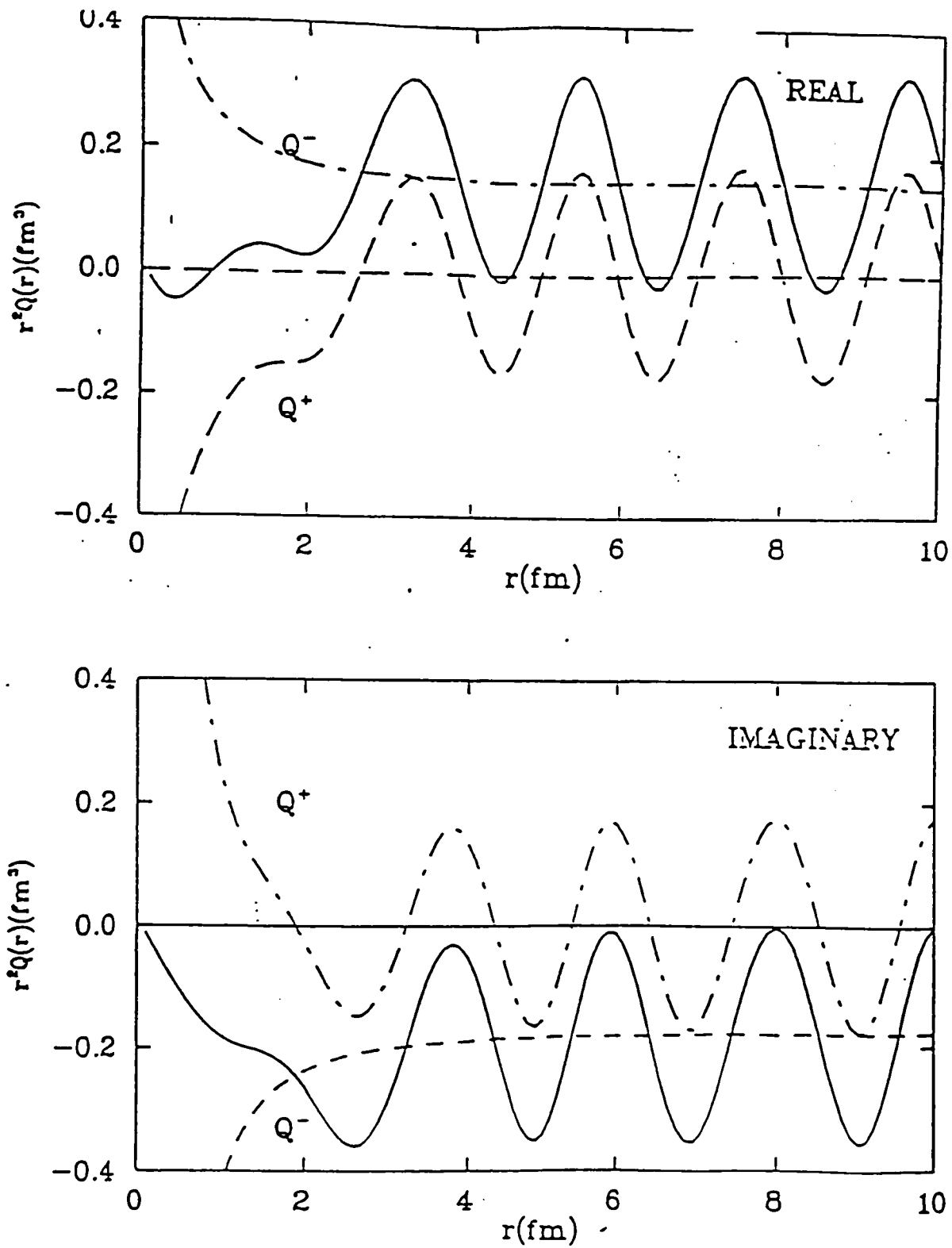


Figure 5.5: Behavior of the real and the imaginary part of  $r^2 Q^\pm(r)$  as a function of  $r$  at 200 MeV. The oscillatory behavior of  $Q^+$  and the total operator is apparent while  $Q^-$  is nearly constant.



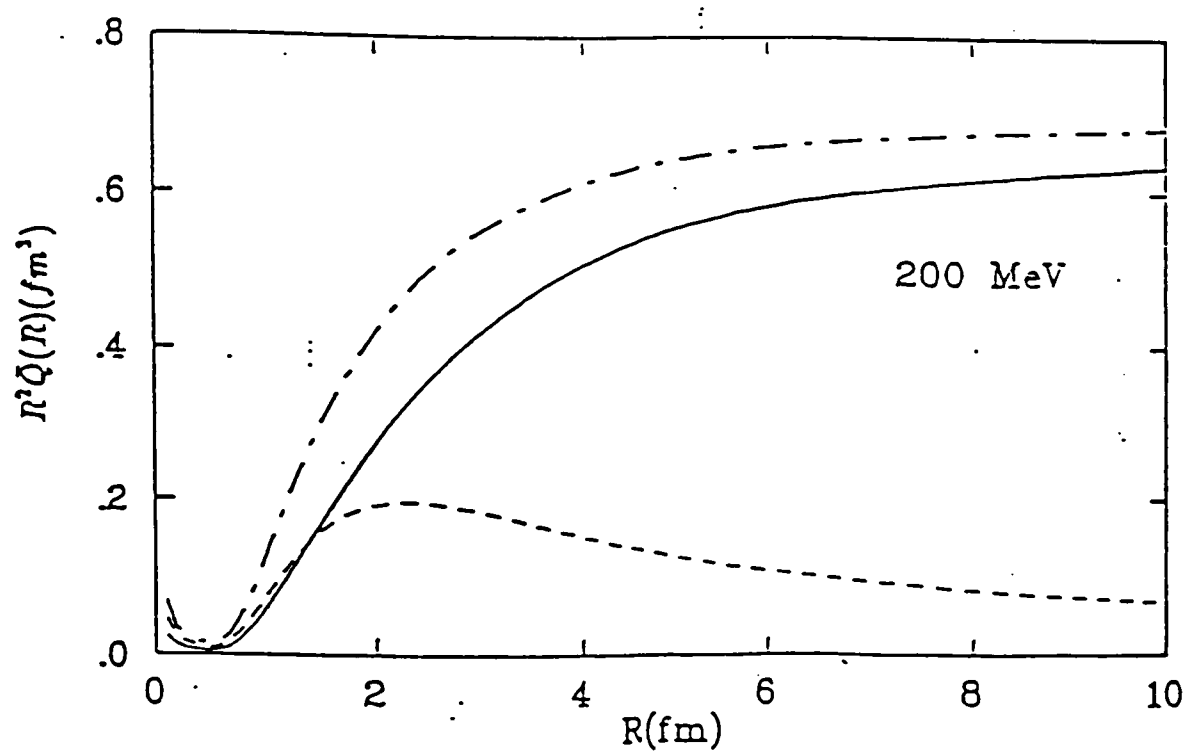
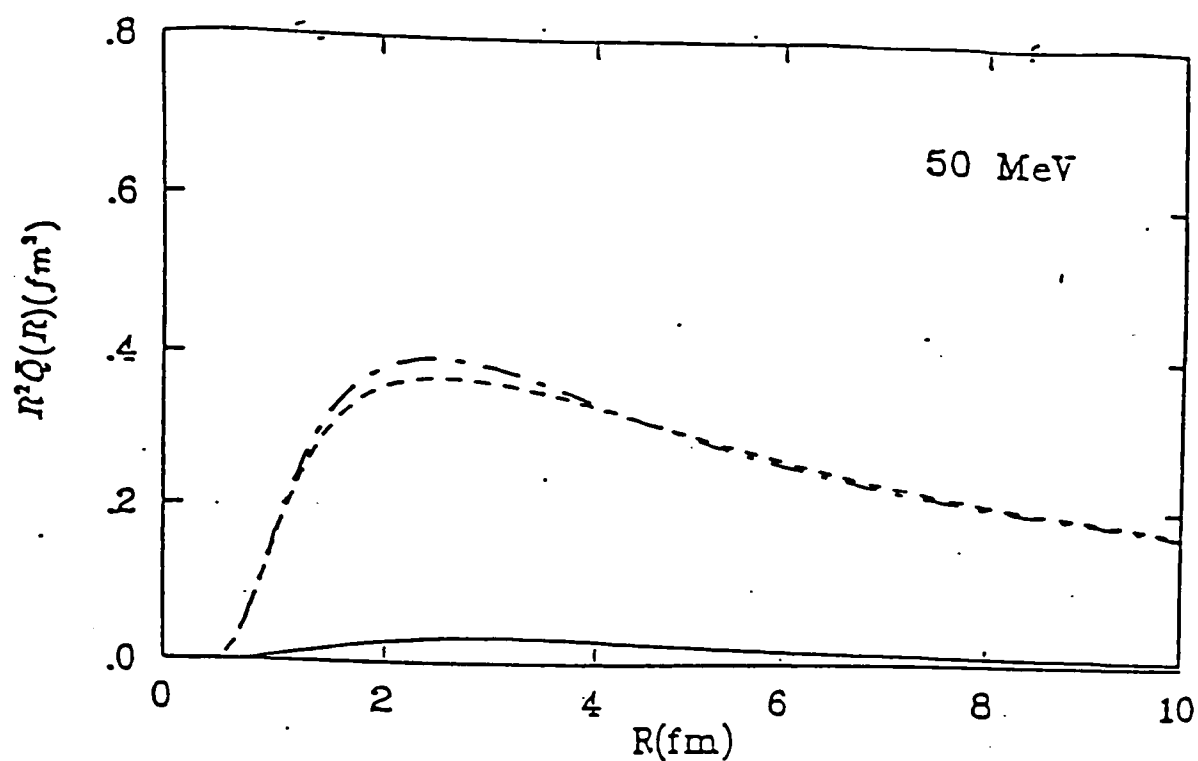


Figure 5.6: Absolute value of the integrated operator  $\bar{Q}(R)$  from 1 fm at energies a) 200 MeV and b) 50 MeV as a function of  $R$ . The dotted curve gives  $\bar{Q}^+(R)$ , the dash-dot curve  $\bar{Q}^-(R)$  and the solid curve is the sum of the two.

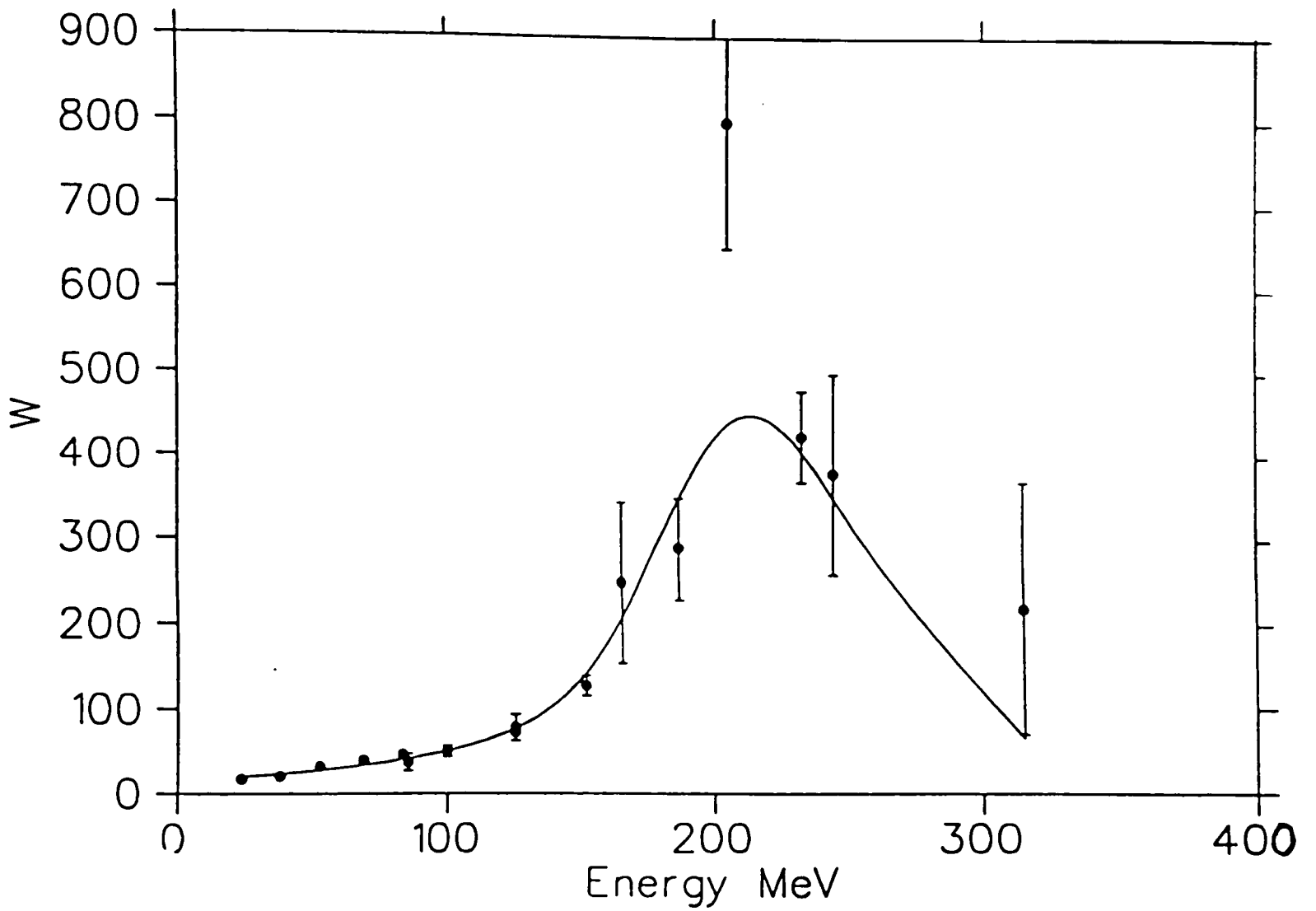


Figure 5.7: Values of the coefficient of  $\rho^2$ ,  $W$ , which represent pion true absorption versus energy.

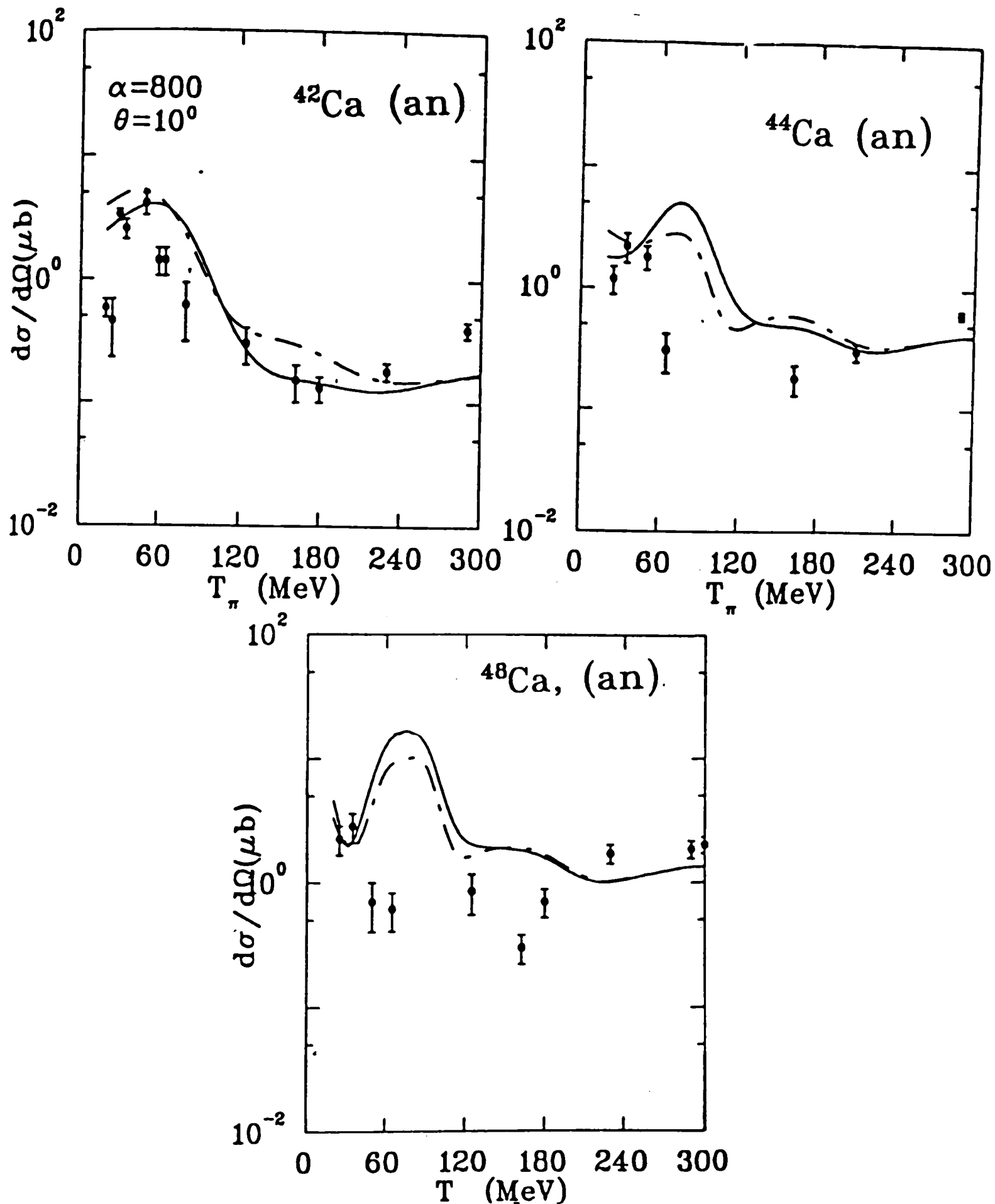


Figure 5.8: The DCX cross sections calculations for Ca isotopes to the isobaric analog state at  $10^\circ$ . The curves shown are obtained from full DWIA calculations (solid curve), DWIA calculations with non-spin-flip amplitudes (small and large dashes), pion energy up to 300 MeV, and  $\alpha = 800$  MeV/c. The data are from ref. [24].

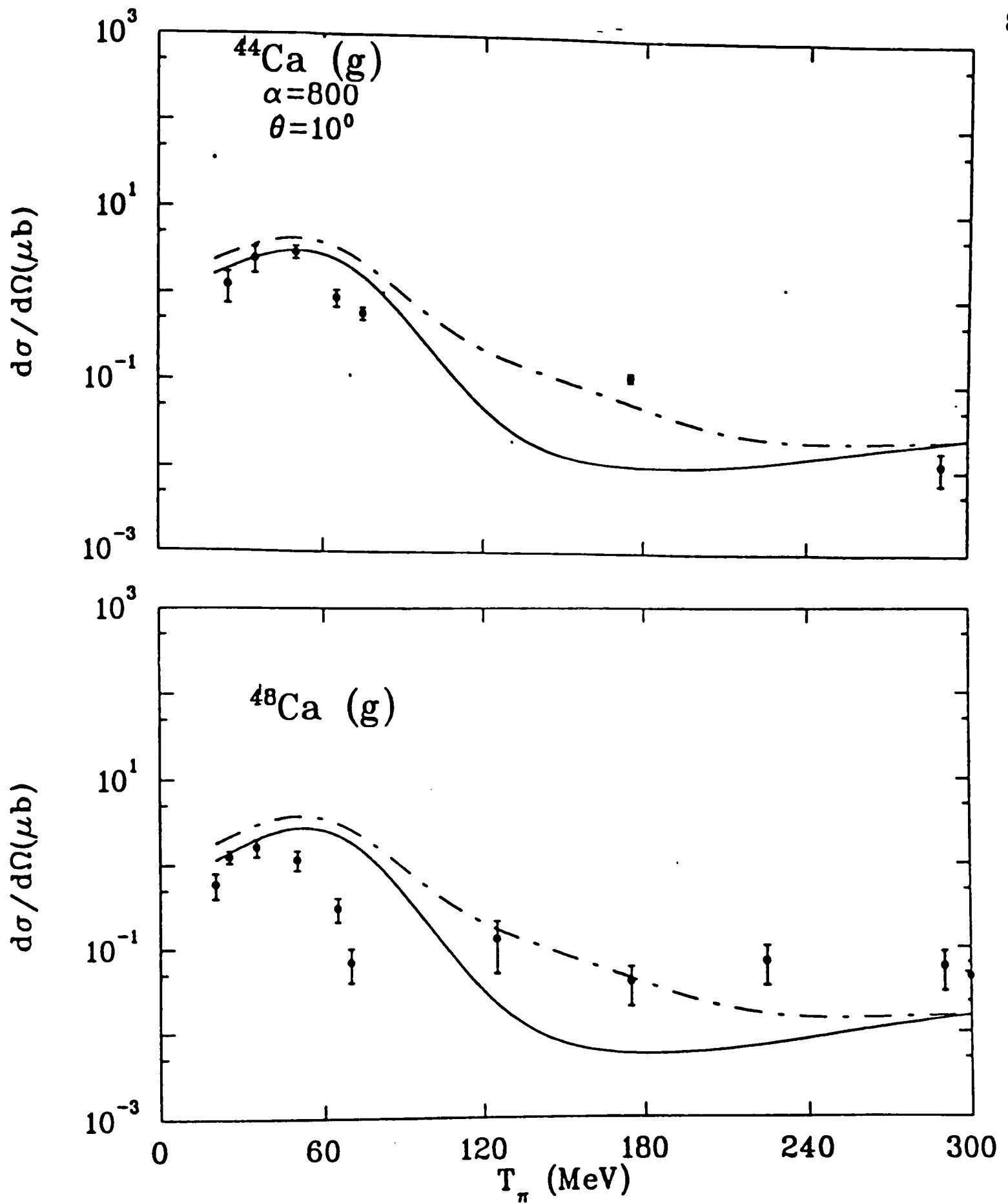


Figure 5.9: The DCX cross sections calculations for Ca isotopes to the ground state at  $10^\circ$ . The curves shown are obtained from full DWIA calculations (solid curve), DWIA calculations with non-spin-flip amplitudes (dash-dot), pion energy up to 300 MeV, and  $\alpha = 800$  MeV/c. The data are from ref. [24].

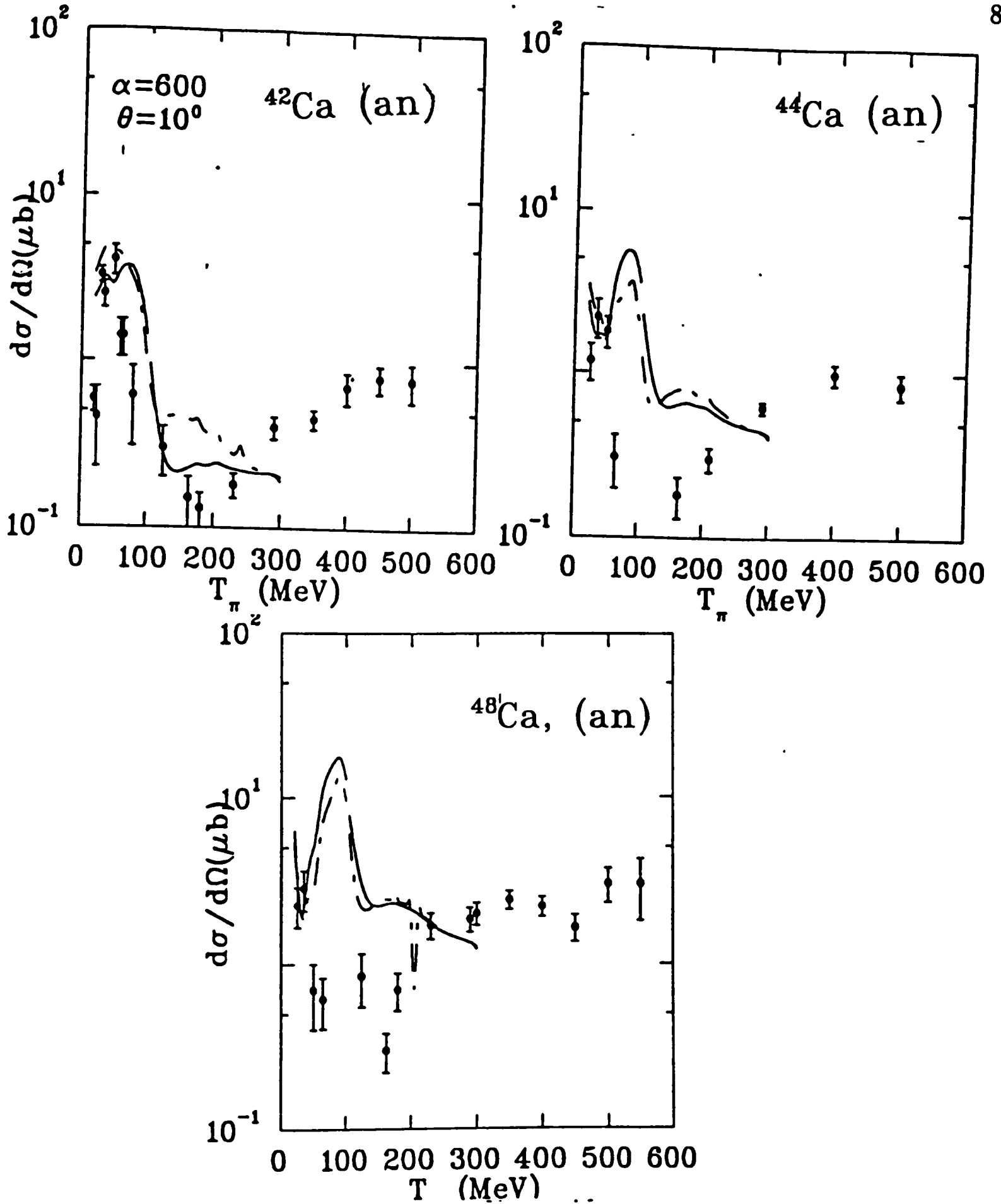


Figure 5.10: The DCX cross sections calculations for Ca isotopes to the isobaric analog state at  $10^\circ$ . The curves shown are obtained from full DWIA calculations (solid curve), DWIA calculations with non-spin-flip amplitudes (dot-das), pion energy up to 300 MeV, and  $\alpha = 600$  MeV/c. The data are from ref. [24].

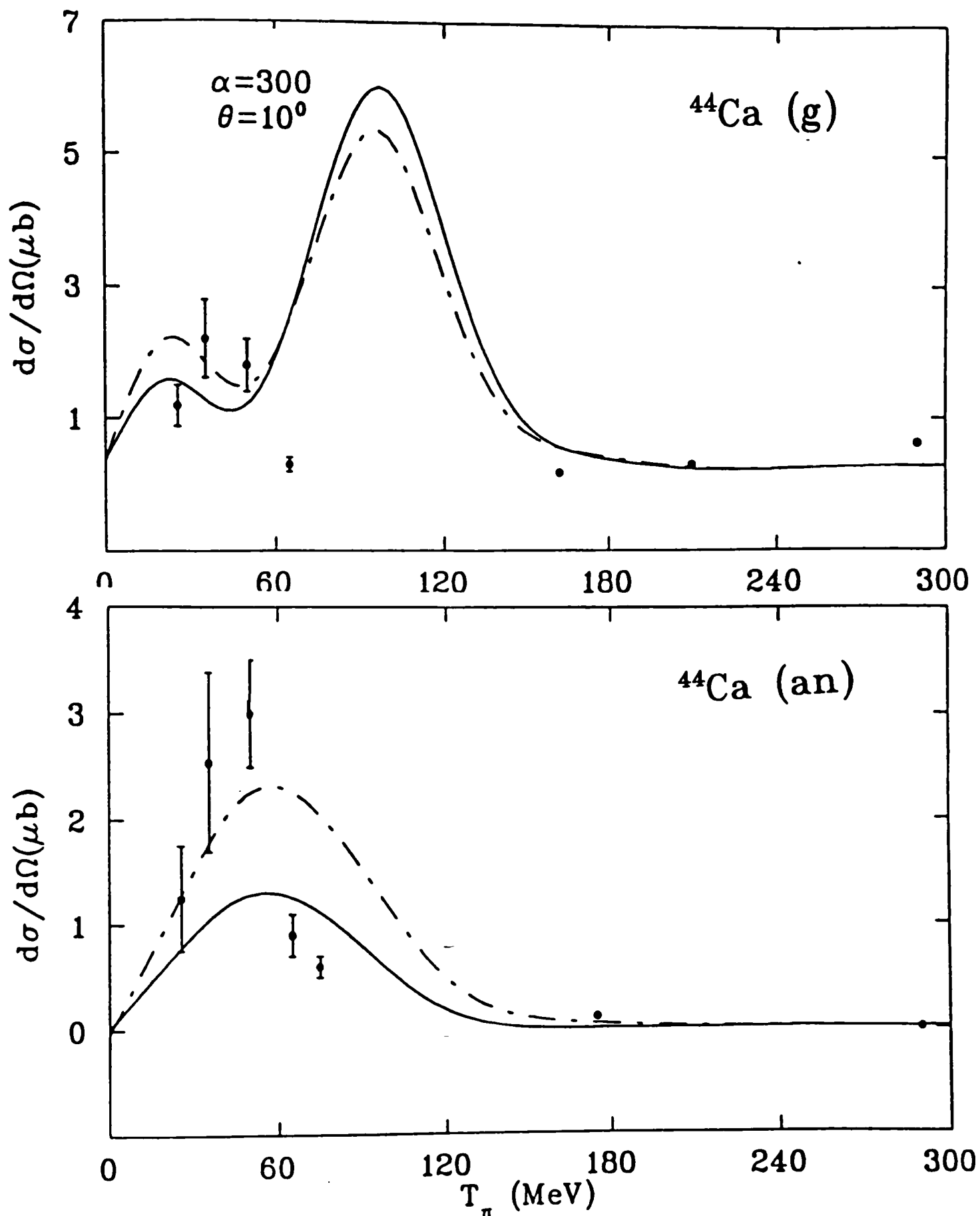


Figure 5.11: The DCX cross sections calculations for  $^{44}\text{Ca}$  isotopes to the ground and analog state at  $10^\circ$ . The curves shown are obtained from full DWIA calculations (solid curve), DWIA calculations with non-spin-flip amplitudes (dot-dash), pion energy up to 300 MeV, and  $\alpha = 300$  MeV/c. The data are from ref. [24].

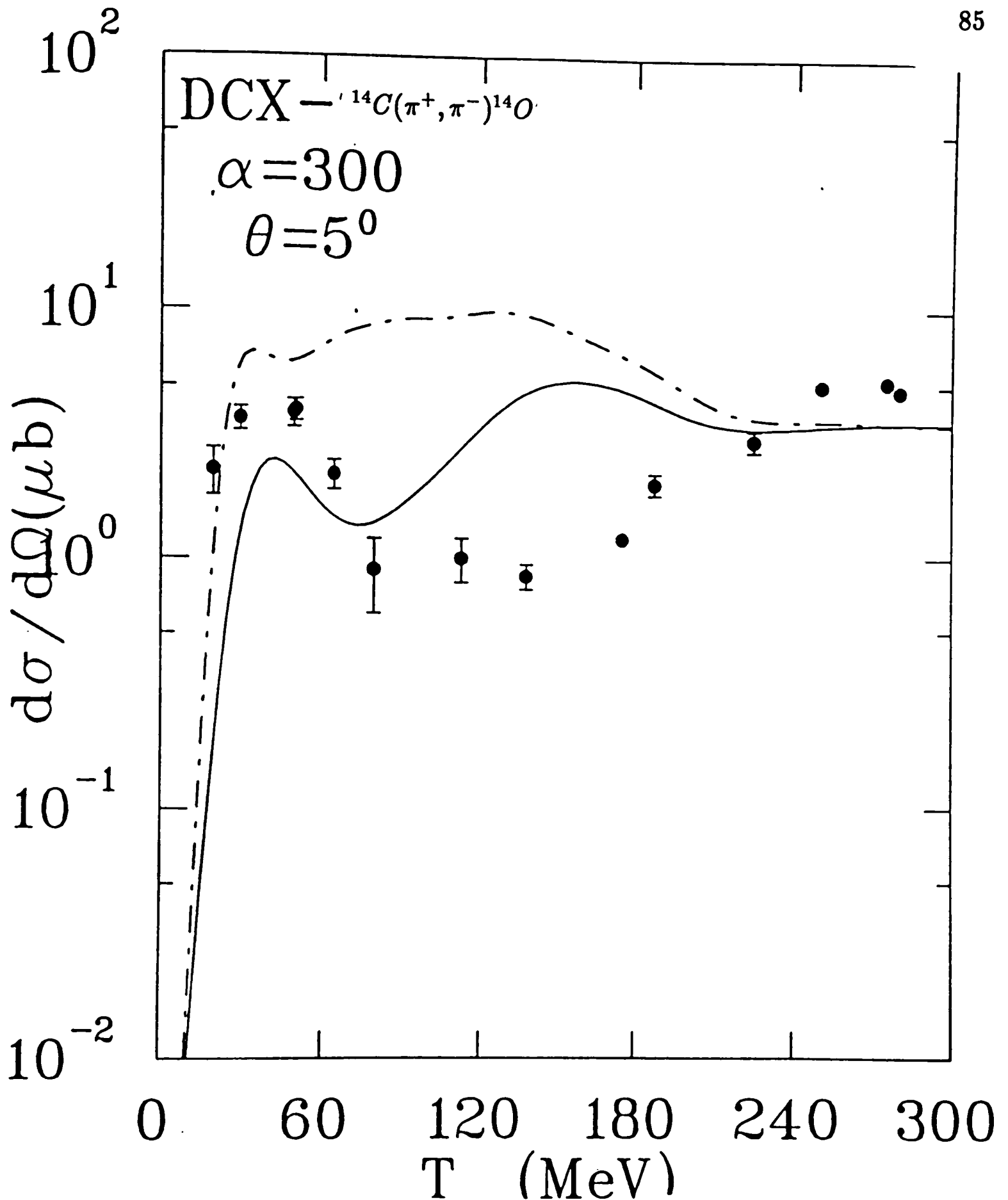


Figure 5.12: The DCX cross sections calculation for the reaction  $^{14}\text{C}(\pi^+, \pi^-)^{14}\text{O}$  DIAS at  $5^\circ$ . The curves shown are obtained from full DWIA calculations (solid curve), DWIA calculations with non-spin-flip amplitudes (dot-dash), pion energy up to 300 MeV and  $\alpha = 300$  MeV. The data from [24].

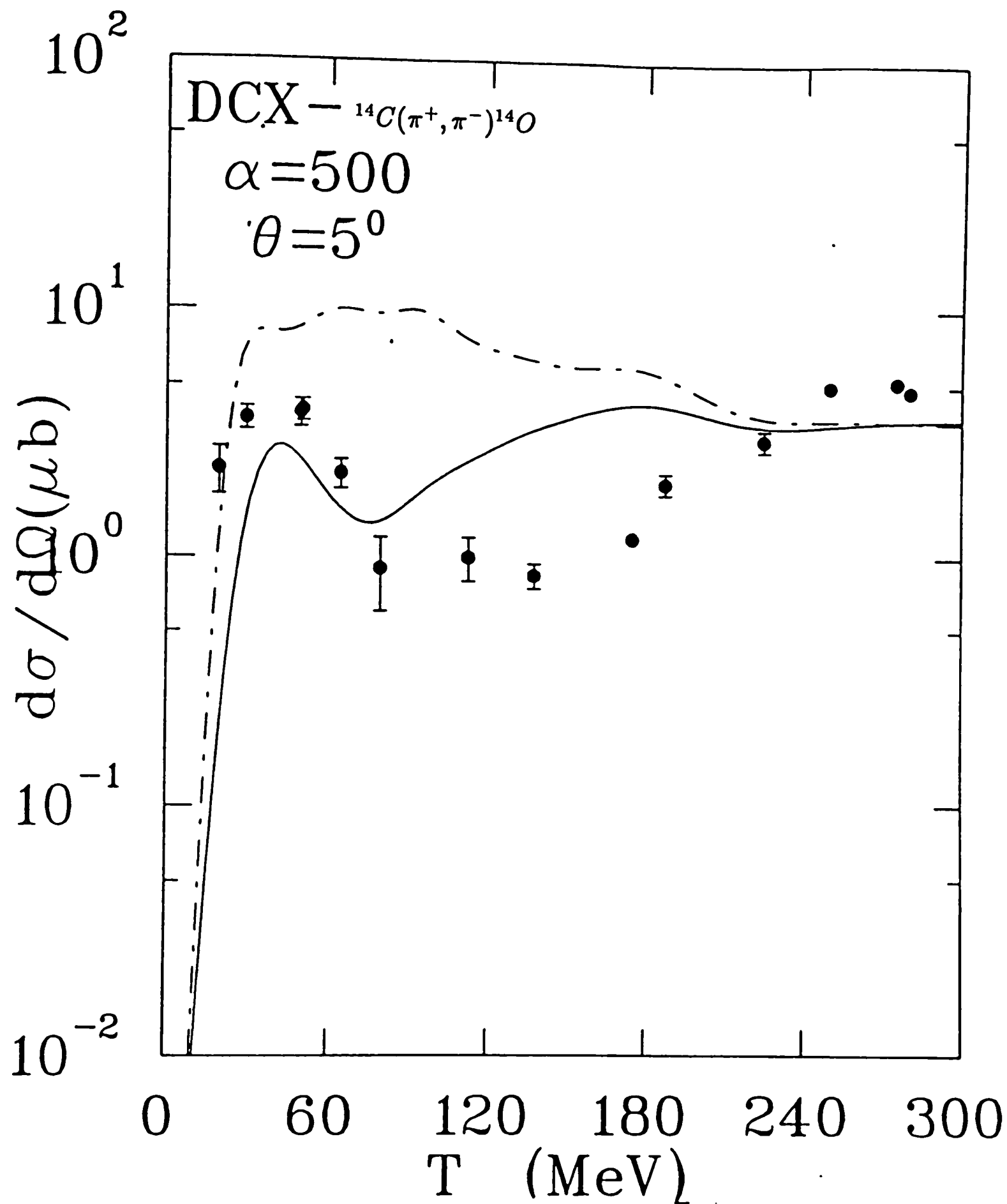


Figure 5.13: The DCX cross sections calculation for the reaction  $^{14}\text{C}(\pi^+, \pi^-)^{14}\text{O}$  DIAS at  $5^\circ$ . The curves shown are obtained from full DWIA calculations (solid curve), DWIA calculations with non-spin-flip amplitudes (dot-dash), pion energy up to 300 MeV and  $\alpha = 500$  MeV. The data from [24].



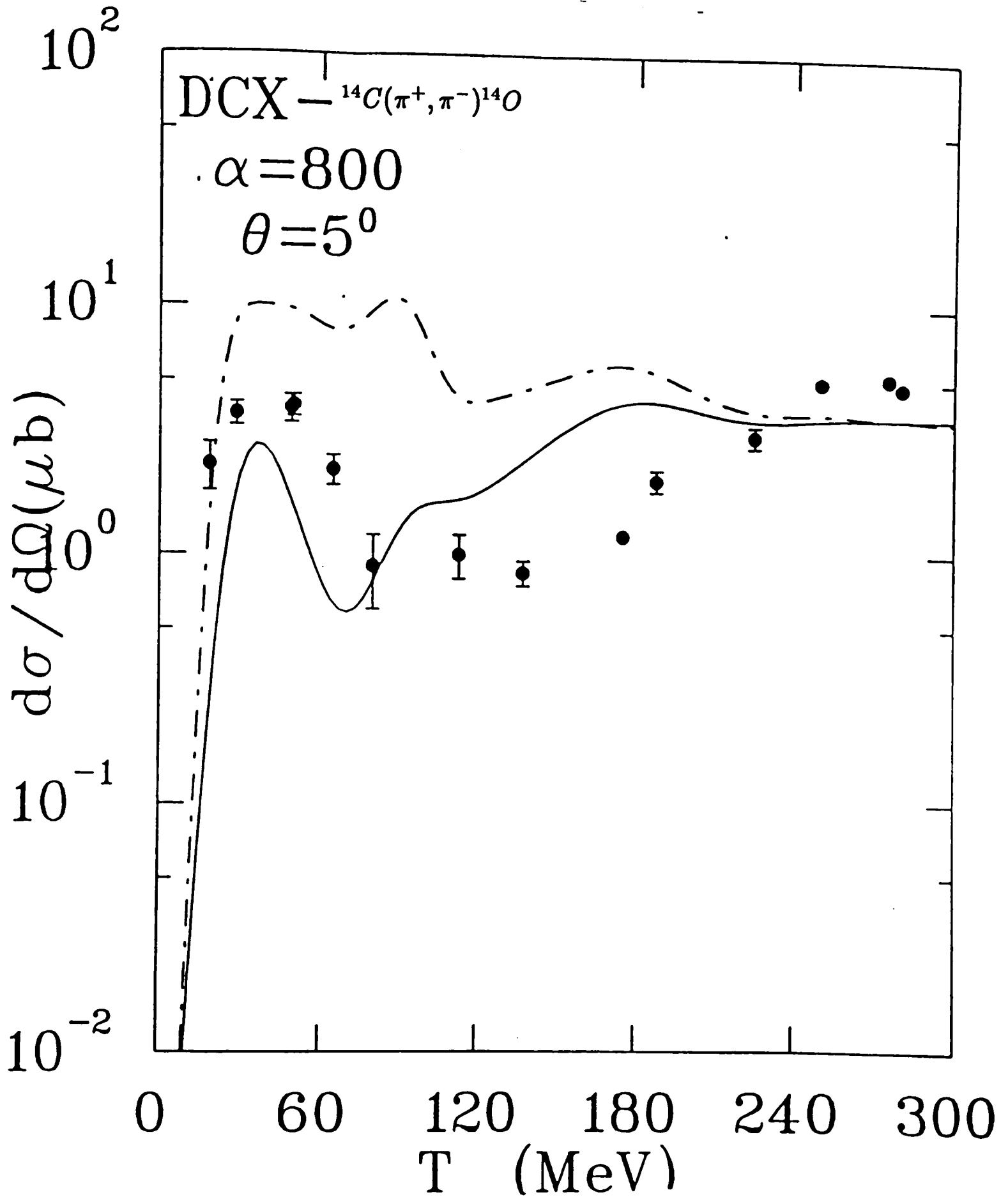


Figure 5.14: The DCX cross sections calculation for the reaction  $^{14}\text{C}(\pi^+, \pi^-)^{14}\text{O}$  DIAS at  $5^\circ$ . The curves shown are obtained from full DWIA calculations (solid curve), DWIA calculations with non-spin-flip amplitudes (dot-dash), pion energy up to 300 MeV and  $\alpha = 800$  MeV. The data from [24].

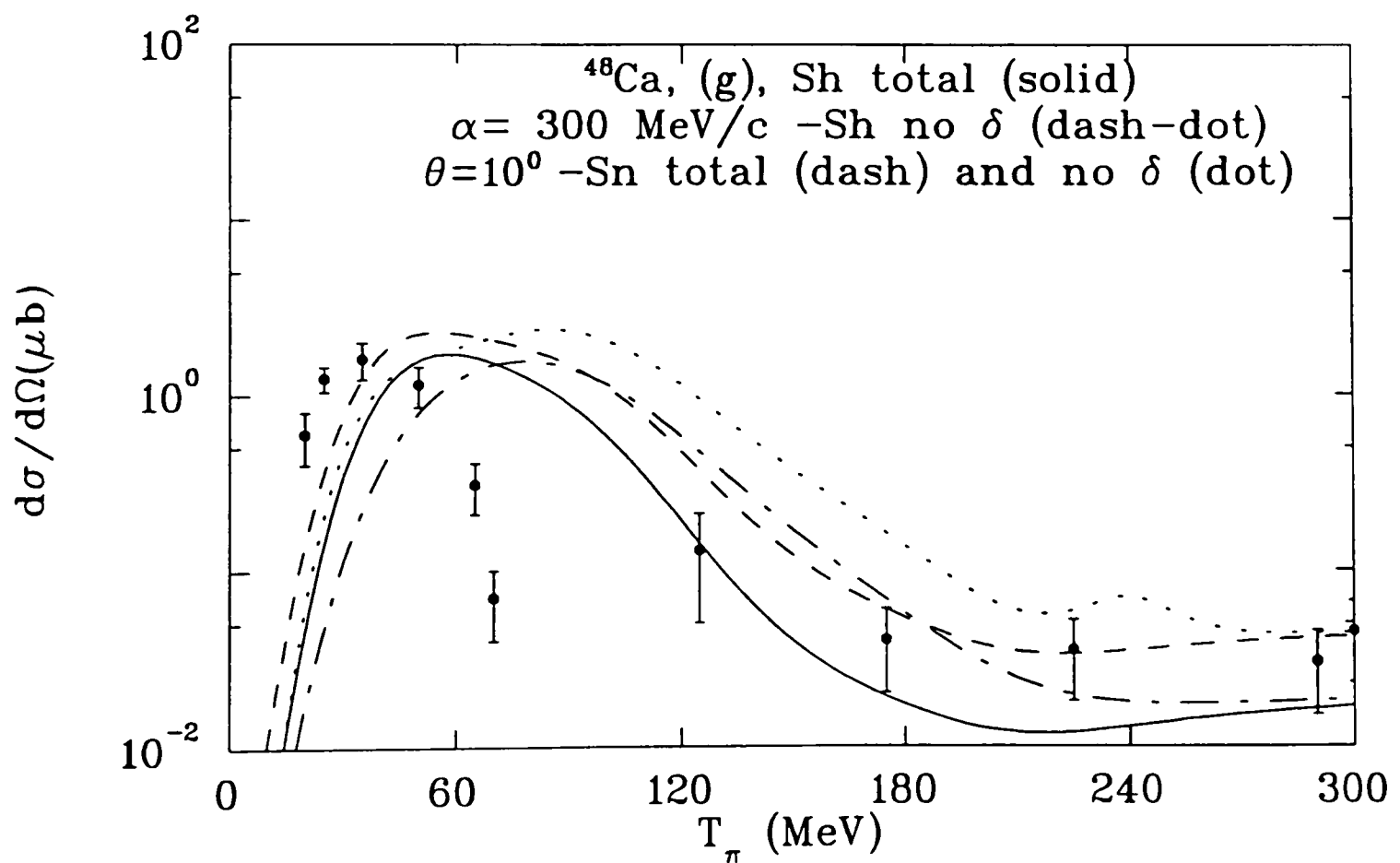
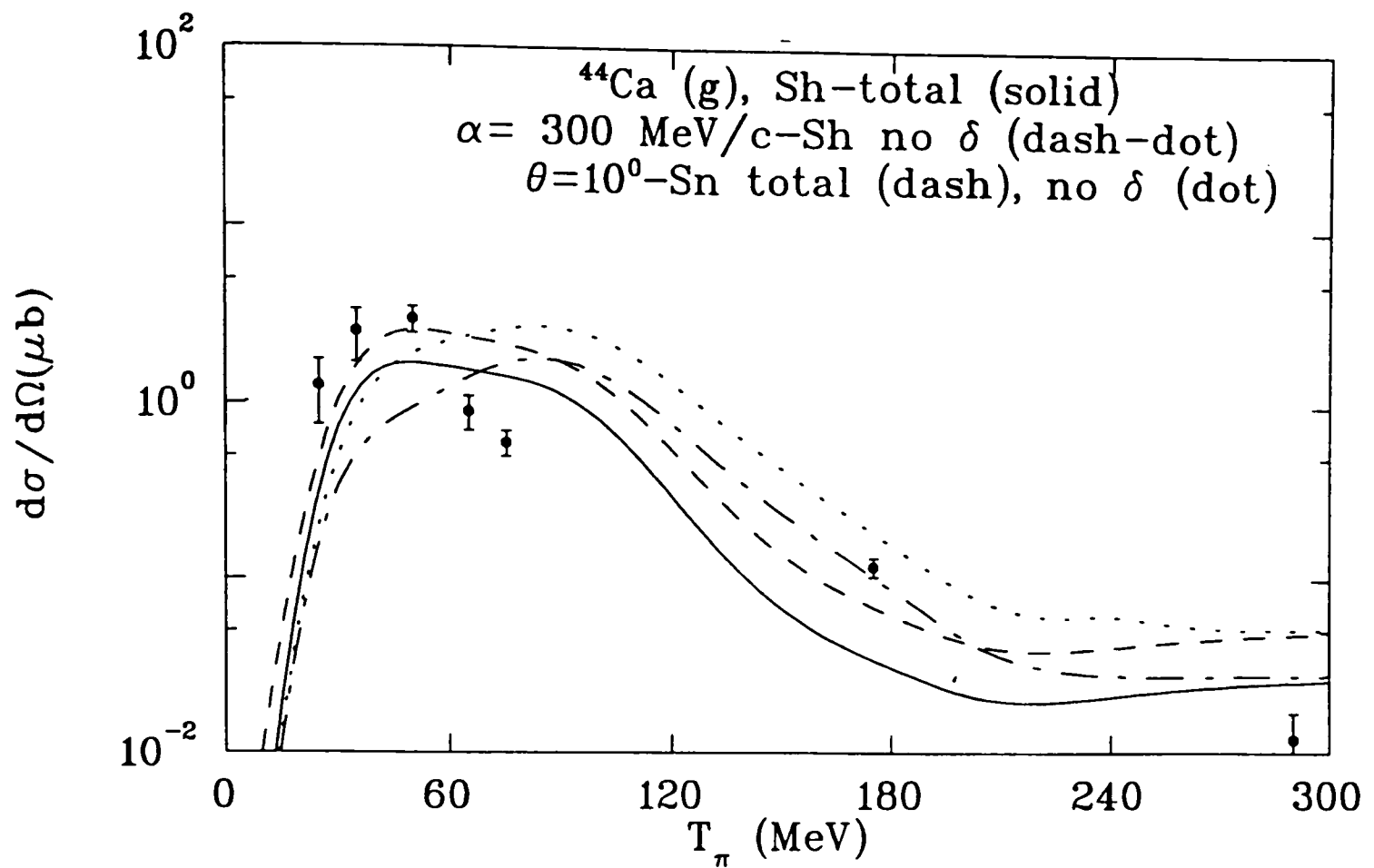


Figure 5.15: DCX cross sections for  $^{48,44}\text{Ca}$  ground state (g) at  $10^\circ$ . The curves shown are obtained from full DWIA and shell model (Sh) calculations, total (solid), no  $\delta$ -function (dash-dot), seniority model (Sn) total (dash), and (Sn) no  $\delta$ -function (dot), with  $\alpha = 300 \text{ MeV}/c$ . The data from [24].

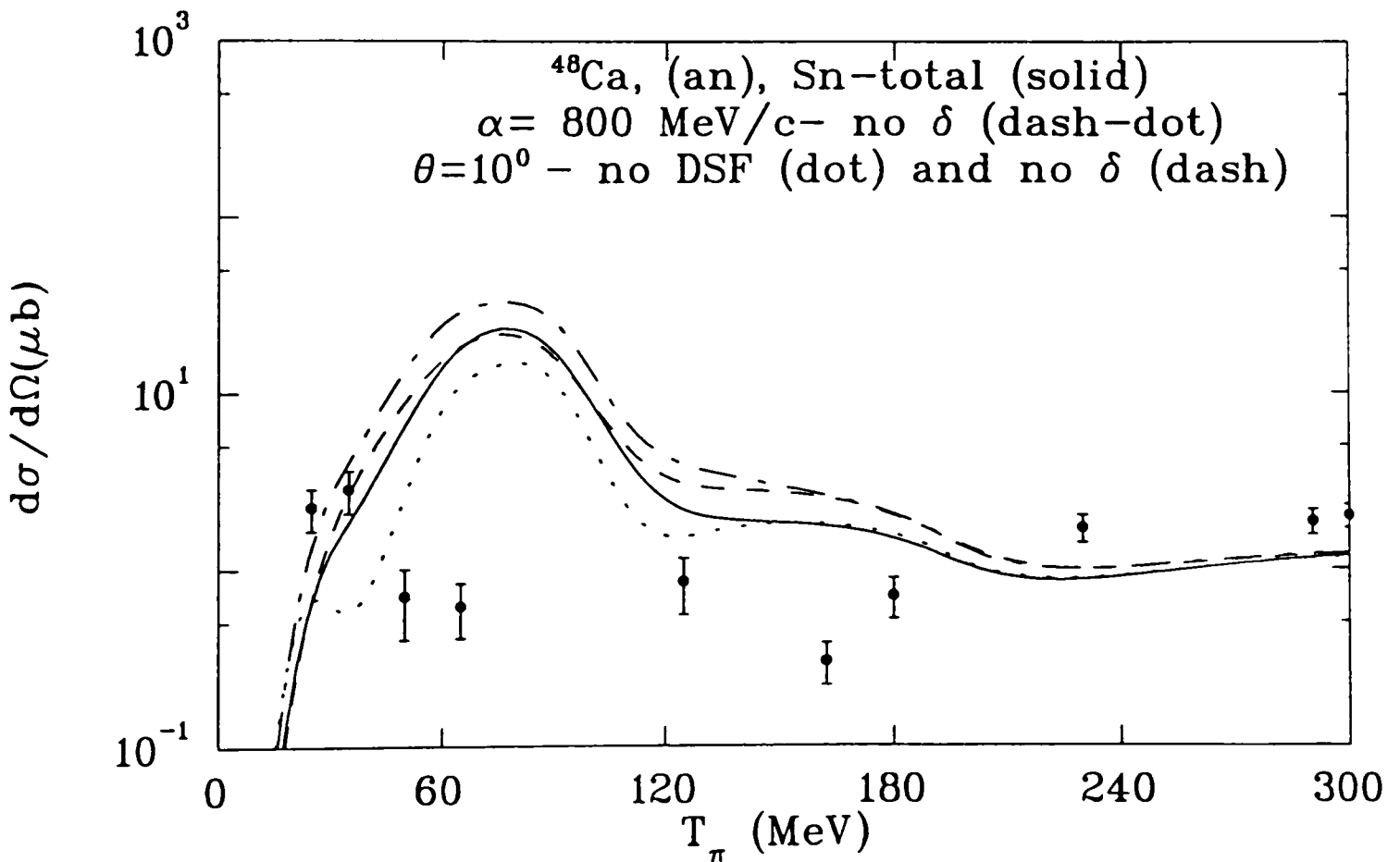
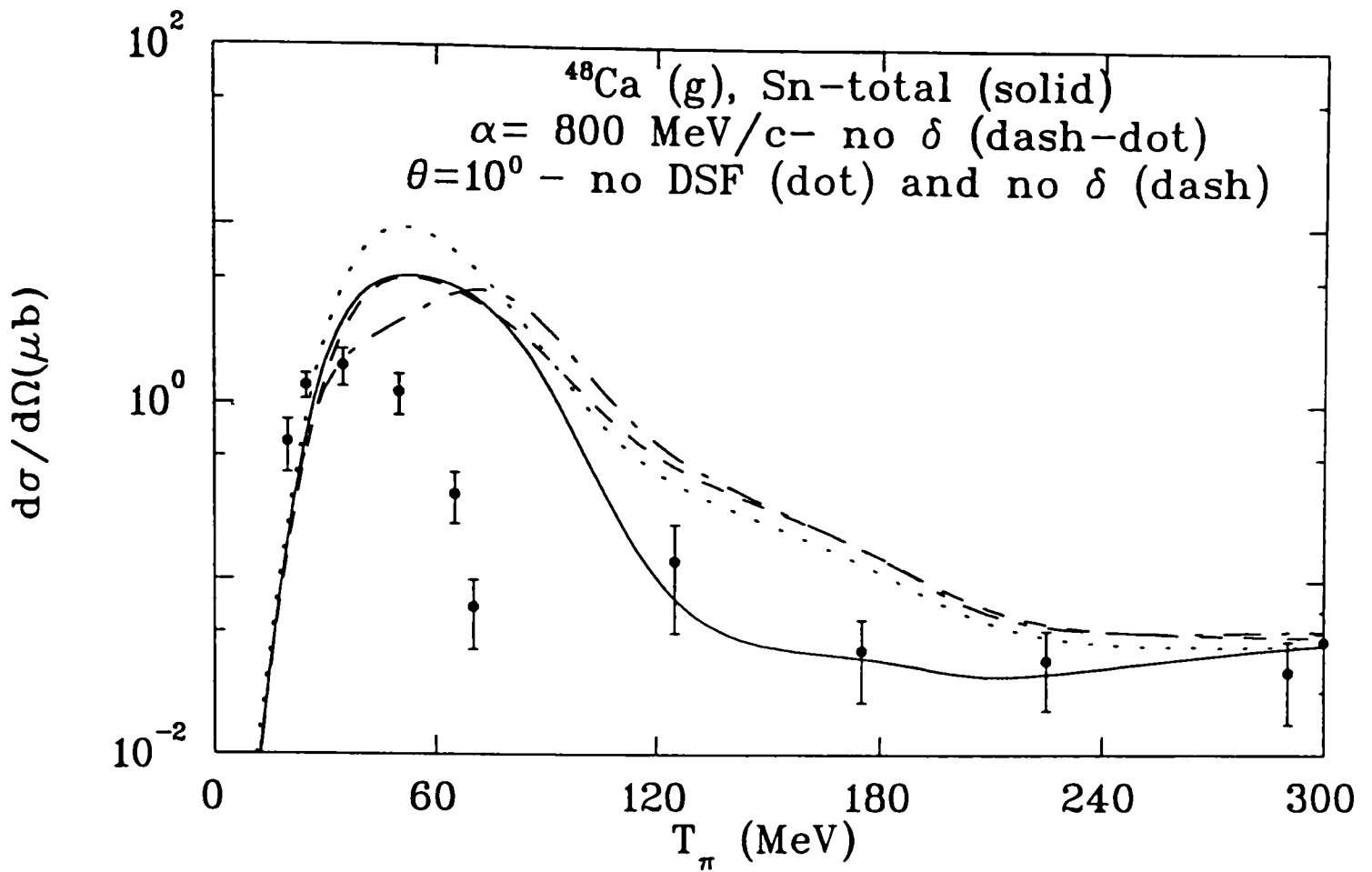


Figure 5.16: DCX cross sections for  $^{48}\text{Ca}$  both analog (an) and ground state (g) at  $10^\circ$ . The curves shown are obtained from full DWIA and seniority (Sn) model calculations, total (solid), no  $\delta$ -function (dash-dot), no DSF (dot), no DSF and no  $\delta$ -function (dash), and with  $\alpha = 800 \text{ MeV}/c$ . The data from [24].

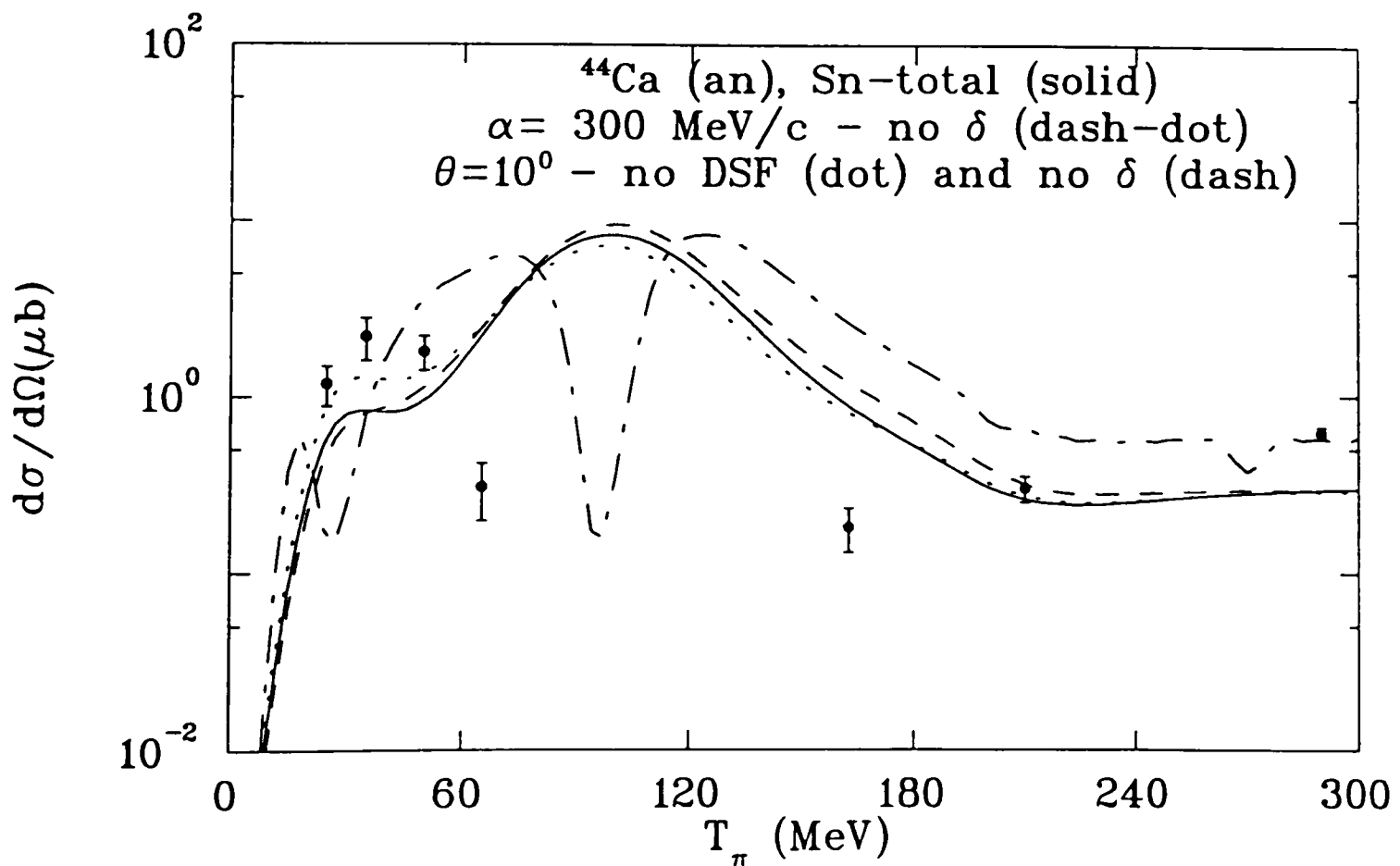
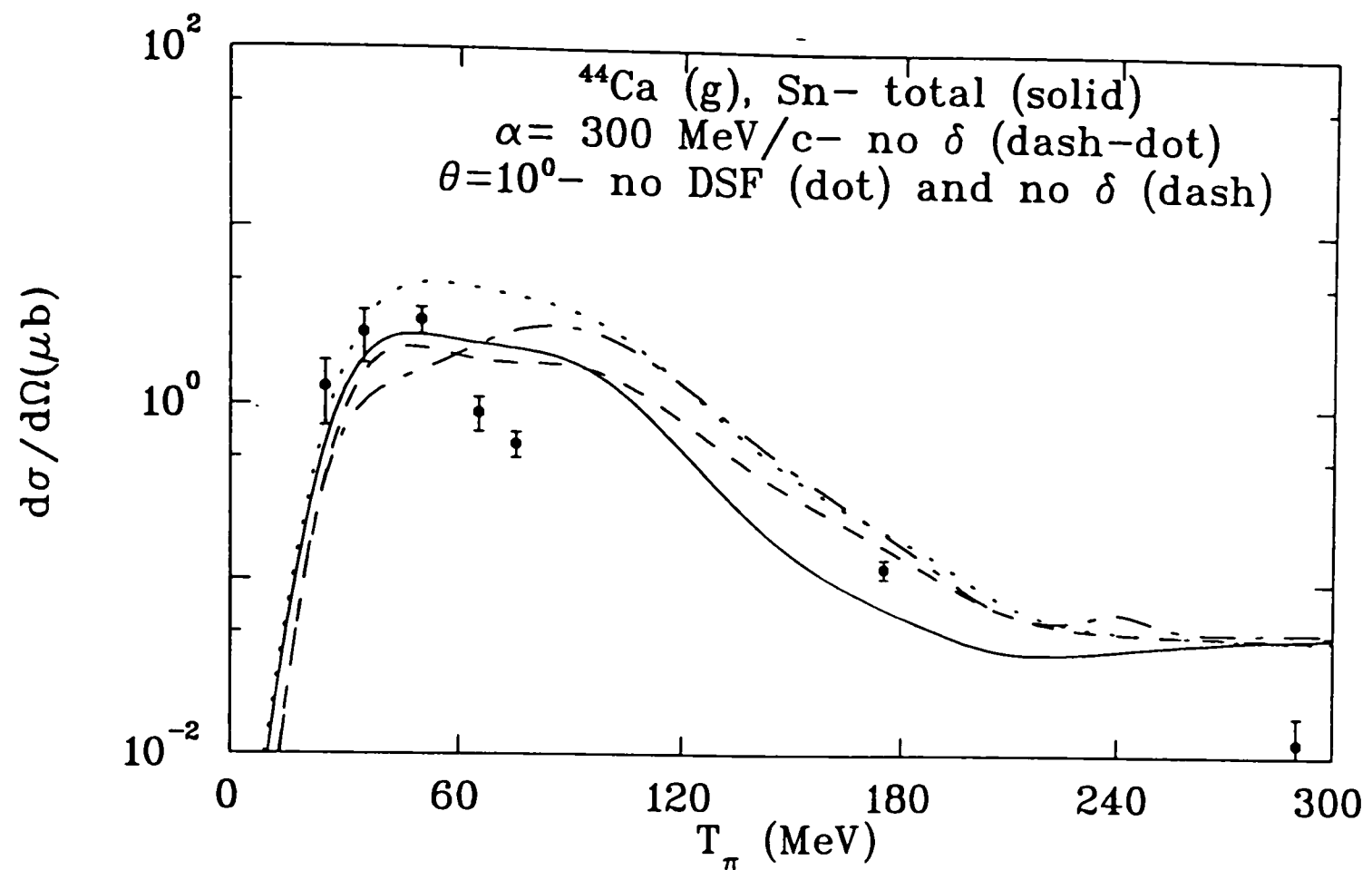


Figure 5.17: DCX cross sections for  $^{44}\text{Ca}$  both analog (an) and ground state (g) at  $10^\circ$ . The curves shown are obtained from full DWIA and seniority (Sn) model calculations, total (solid), no  $\delta$ -function (dash-dot), no DSF (dot), no DSF and no  $\delta$ -function (dash), and with  $\alpha=300 \text{ MeV}/c$ . The data from [24].

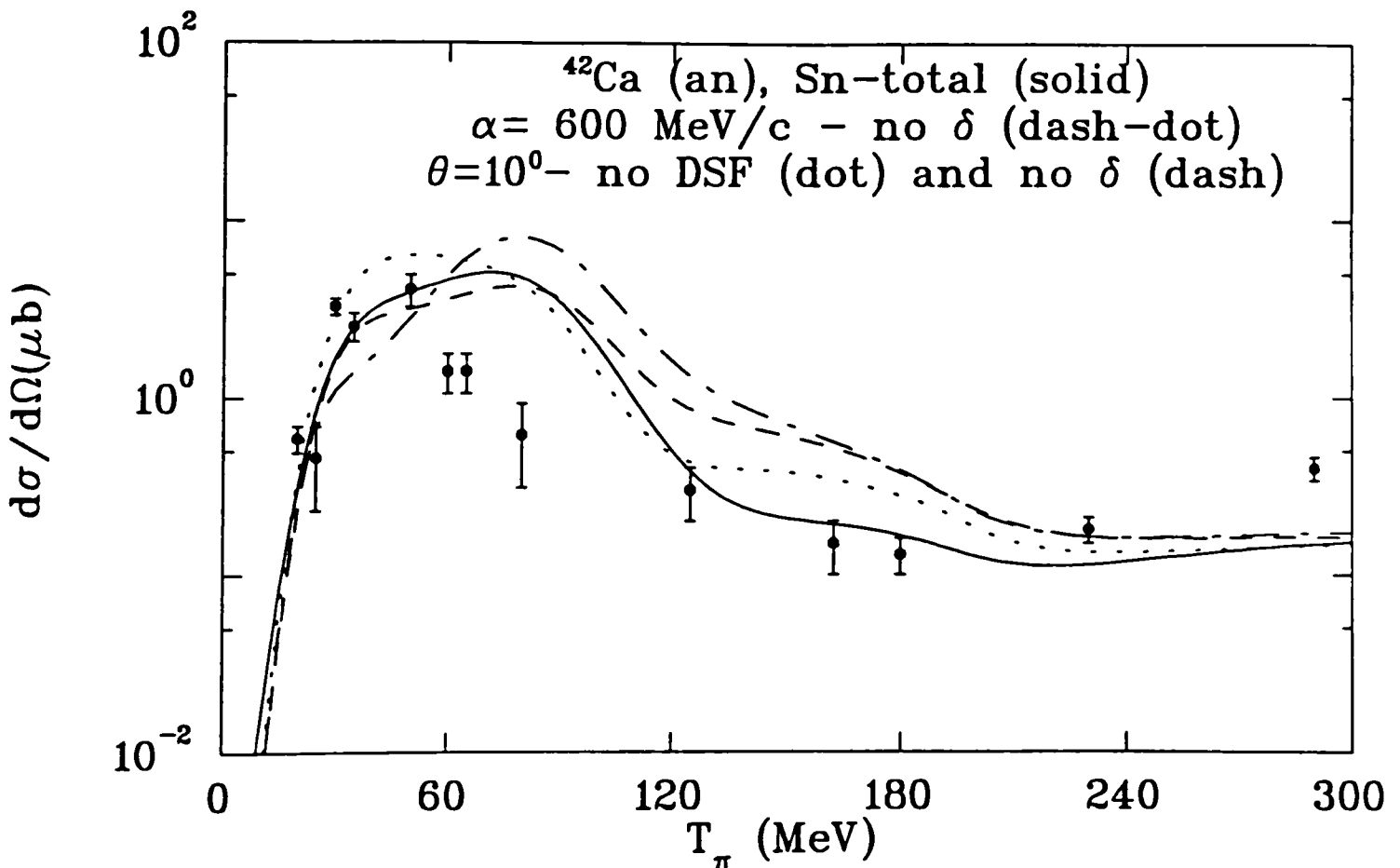
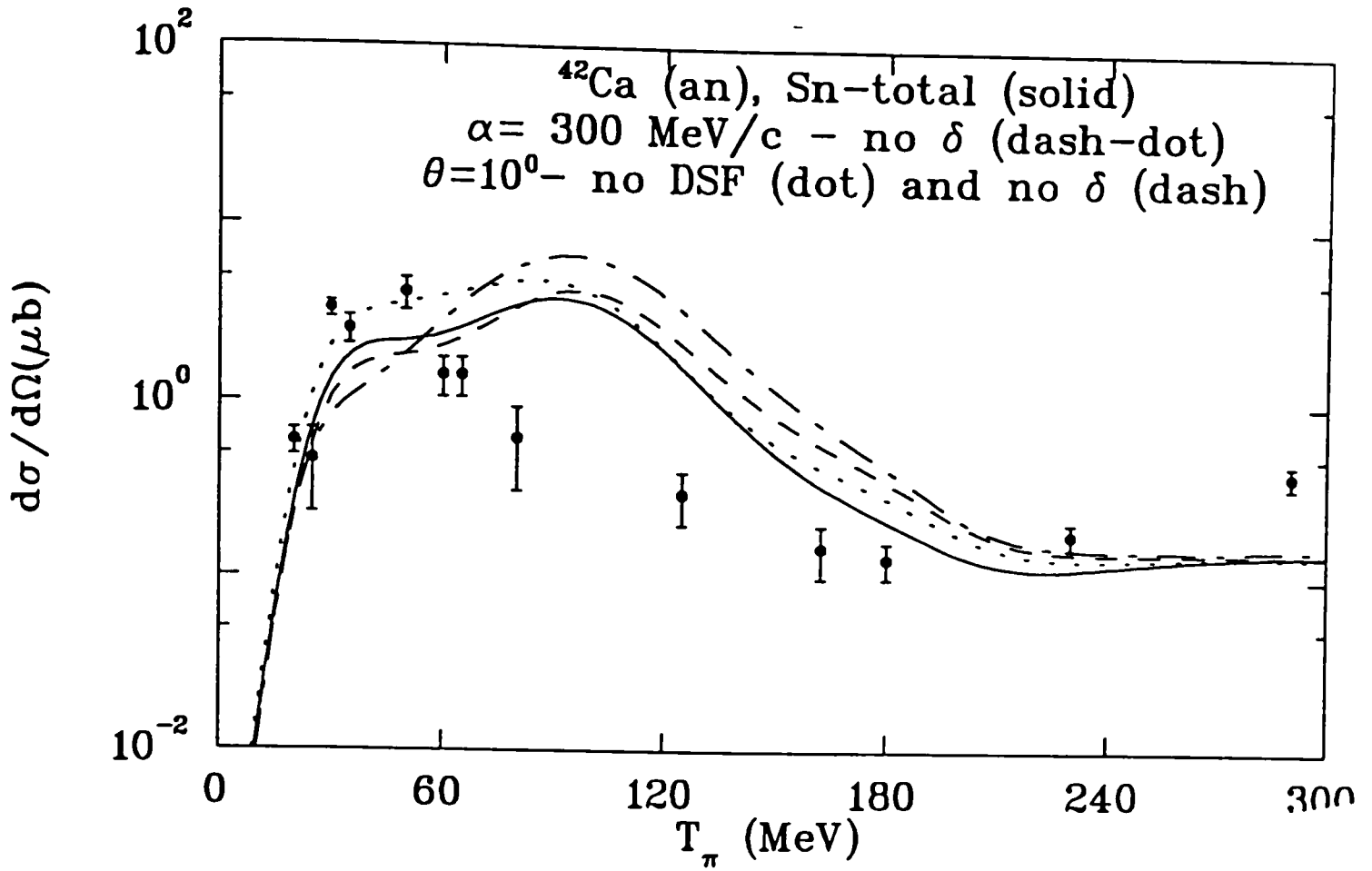


Figure 5.18: DCX cross sections for  $^{42}\text{Ca}$  analog (an) state at  $10^\circ$ . The curves shown are obtained from full DWIA and seniority (Sn) model calculations, total (solid), no  $\delta$ -function (dash-dot), no DSF (dot), no DSF and no  $\delta$ -function (dash), and with  $\alpha=300$  and  $600 \text{ MeV/c}$ . The data from [24].

## CHAPTER VI

### CONCLUSIONS

The DCX operator has three basic behaviors corresponding to three “ranges” in the internucleon spacing. The first behavior corresponds to a classical range in that it falls off with a rapid decrease after a characteristic distance (with the monopole function used for illustration it has an exponential fall off with range  $1/\alpha$ ). The form of the operator in this zone depends on the inclusion (or not) of the  $\delta$ -function. After this initial short-range phase of the operator, there is a “near-zone” range which is of varying importance depending on the energy of the reaction. In a typical case, this range falls within the nuclear volume and must be considered. The specification of the next two behavioral characteristics is not as simple. After the initial fall off of the short range and the near-zone region, the function can be separated into one part which behaves as  $e^{2ikr}/r^2$  and another which goes as  $1/r^2$ . In the mean (i.e., after integrating over a wave function) the oscillating function will decrease more rapidly than the other with the increasing size of the system. In this sense, it has a “shorter range,” the characteristic size of which is determined by  $\frac{1}{2k}$ .

Also, it has been demonstrated and clarified in the graphs of the results of Chapter III, that the DSF plays a crucial part in DCX operator, both integrated and projected one, as shown in Figures 5.2 and 5.3 that the energy dependence and

the space dependence of the operator has been affected by the inclusion of DSF or reduced, especially at energies below 200 MeV, and goes to a minimum at 50 MeV.

The general properties of the DCX operator in the shell model are studied and the matrix element of a general two-nucleon operator in the seniority model with isospin is evaluated [9]. The relationships among DCX reactions to both analog and ground states are calculated.

The calculations performed in the plane wave impulse approximation (PWIA) as a check and the distorted wave impulse approximation (DWIA), reproduce the DCX cross sections approximately on Ca isotopes for  $T_\pi \leq 300$  MeV. The lowest-order pion double charge exchange reaction has been calculated using shell-model wave functions. The distortions of incoming, intermediate, and outgoing pions are included. The closure approximation is made for the intermediate states with an average excitation energy used in the pion propagator. The double charge exchange is assumed to take place on the valence nucleons which are assumed to be in a single spherical shell-model orbital. The sequential reaction mechanism in which the pion undergoes two single charge exchange scatterings on the valence neutrons has been used. In the seniority model the DCX for all the isotopes is given in terms of two complex amplitudes. One amplitude is primarily sensitive to the short-range correlation of the valence nucleons and spin dependence of the DCX amplitude; the other amplitude to the long-range behavior. Furthermore, the relative importance of these two amplitudes

depends very much on the pion energy. In general, nuclei are relatively transparent to low-energy ( 20 to 80 MeV) pions and thus penetrate nuclei more than near resonance ( $T_\pi = 164$  MeV), where multiple scattering processes occur inside the nucleus which demonstrated in these resonances that are observed in the data and the calculations and revealed the structure of the nucleus. In particular a pion energies between 30-60 MeV, the DCX seems be dominated by the configuration when the nucleons are about 1-2 fm apart. There is a considerable improvement of the calculation after the correction for pion absorption and a slight improvement after the delta function has been removed from the DCX amplitude where the interaction of two nucleons extends over short region of space due to the delta function which has been subtracted from the rest of the total DCX amplitude. The results for the DCX cross sections for the Ca isotopes for  $T_\pi \leq 300$  MeV (see Figures 5.8 to 5.18) as can be seen from the graphs are in good agreement with the experimental result for  $^{42}\text{Ca}$ , in partial agreement for  $^{44}\text{Ca}$ , and in poor agreement for  $^{48}\text{Ca}$ .

One might explain the results as follows. First, pion absorption is very important in the DCX reaction and it does have a significant effect on the calculation. Second, the delta function correction slightly affects the DCX cross section and it does improve the results for the ground state but not the for analog state. Finally, the appearance of this peak in the low energy region might be a sign for the existence of the dibaryon.



In general, the calculations were done over the full range up to 300 MeV, where only few energies were calculated before. These calculations included a number of corrections for the DCX cross section calculations. A more sophisticated form of correlation could be added to the nuclear wave function. Finally, the calculated DCX cross sections are improved by these corrections.

## REFERENCES

- [1] Pions and Nuclei, Torleif Ericson and Wolfram Weise, Oxford University Press, New York, (1988).
- [2] E. Piasetzky et al., *Proc. Int. Conf. on Particle and Nuclei*, Kyoto, (1987), and C. Morris and D. Ashery, LAMPF proposal 1023 (1988).
- [3] K. K. Seth, *Nucl. Phys.* , **478**, 591c (1988), *Phys. Rev. C* **30**, 962 (1984).
- [4] M. Bleszynski, and R. J. Glauber, in *Proc. Intersections Between Particle and Nuclear Physics*, Lake Louise, Canada (1986) AIP 150 p. 644.
- [5] M. B. Johnson, *Phys. Rev. C* **22**, 192 (1980).
- [6] Z. E. Meziani, in *Proceedings of the second LAMPF international workshop on Pion Nucleus Double Charge Exchange*, 1989, edited by W.R.Gibbs and M.J.Leitch, Word Scientific, Singapore, p 300 (1990).
- [7] J. Roginsky, C. Werntz, in *Proceedings of the second LAMPF international workshop on Pion Nucleus Double Charge Exchange*, 1989, edited by W.R.Gibbs and M.J.Leitch Word Scientific, Singapore, p 324 (1990).
- [8] K. I. Kubo, in *Proceedings of the second LAMPF international workshop on Pion Nucleus Double Charge Exchange*, 1989, edited by W.R.Gibbs and M.J.Leitch Word Scientific, Singapore, p 281 (1990).
- [9] N. Auerbach, W. R. Gibbs, J. N. Ginocchio and W. B. Kaufmann, *Phys. Rev. C* **38**, 1277 (1988); N. Auerbach, W. R. Gibbs and E. Piasetzky, *Phys. Rev. Lett.* **59**, 1076 (1987).
- [10] E. Bleszynski, M. Bleszynski and R. J. Glauber, *Phys. Rev. Lett.* **54**, 1230 (1985)
- [11] W. R. Gibbs, J. N. Ginocchio and N. Auerbach, *Comments Nucl. Part. Phys.* **20**, 141 (1991).
- [12] S. J. Greene, C. J. Harvey, P. A. Seidl, R. Gilman, E. R. Siciliano, and M.B. Johnson, *Phys. Rev. C* **30**, 2003 (1984).

- [13] W. R. Gibbs, W. B. Kaufmann and P. B. Siegel, *Proceedings Los Alamos Workshop on DCX*, (1985) edited by H. Baer, Los Alamos Rep. LA-10550-C, p. 90.
- [14] R. J. Glauber, M. Bleszynski and E. Bleszynski, *Workshop on Pion-nuclear Physics*, August (1987) LAMPF.
- [15] D. S. Koltun, in *Proceedings of the second LAMPF international workshop on Pion Nucleus Double Charge Exchange*, (1989), edited by W.R.Gibbs and M.J.Leitch, Word Scientific, Singapore, p 3 (1990).
- [16] G. A. Miller, *Proceedings Los Alamos Workshop on DCX*, (1985) ed. H. Baer, Los Alamos Rep. LA-10550-C, p. 193.
- [17] M. B. Johnson, in *Proceedings of the second LAMPF international workshop on Pion Nucleus Double Charge Exchange*, (1989), edited by W.R.Gibbs and M.J.Leitch Word Scientific, Singapore, p 333 (1990).
- [18] M. B. Johnson, *Annals of Physics* **203** (1990).
- [19] M. F. Jiang, D. S. Koltun, *Phys. Rev. Lett.* **42**, 2662 (1990), E. Oset, D. S. Strottman, M. J. Vicente-Vacas and J. Wei-Hsing, *Nucl. Phys.* **A408**, 461 (1983), et al., *Phys. Rev. C* **39**, 2356 (1988).
- [20] M. J. Leitch, H. W. Baer, R. L. Curman and C. L. Morris et al. , *Phys. Rev. C* , **39**, 2356 (1983).
- [21] D. Ashery, I. Navon and G. Azuelos et al., *Phys. Rev. Lett.* **23**, 2173 (1980).
- [22] K. Nakai, T. Kobayashi, T. Numao, T. A. Shibata et al., *Phys. Rev. Lett.* **44**, 1446 (1980).
- [23] R. D. Ransome, C. L. Morris, M. K. Jones et al., *Phys. Rev. C* **46**, 273 (1992).
- [24] G. R. Burleson, New Mexico State University, *Workshop on Pion-nuclear Physics*, August 1987 LAMPF.
- [25] G. E. Parnell, Ph.D. dissertation, Texas A & M University, D. J. Ernst. *Workshop on Pion-nuclear Physics*, August 1987 LAMPF.

- [26] G. A. Miller, *Phys. Rev. C* **35**, 377 (1987).
- [27] W. R. Gibbs, M. O. El-ghossain, and W. B. Kaufmann, *Phys. Rev. C*, **48**, 1546 (1993).
- [28] M. Rowe, M. Solomon and R. Landau, *Phys. Rev. C* **18**, 584 (1978).
- [29] T. E. O. Ericson and M. Rosa Clot, *Nucl. Phys.* **A405**, 497 (1983).
- [30] D. D. Strottman, *Proceedings of the Los Alamos Workshop on DCX*, (1985) edited by H. Baer, Los Alamos Rep. LA-10550-C, p. 263.
- [31] W. R. Gibbs, *Computation in Modern Physics*, Word Scientific (1995).
- [32] H. Garcilazo, W. R. Gibbs, *Nucl. Phys.*, **A381**, 487 (1982).
- [33] R. Gilman, L. C. Bland, P. A. Seidl, C. F. Moore, C. L. Morris et al., *Nucl. phys.* , **A432**, 610 (1985).
- [34] L. C. Bland, R. Gilman, M. Cardchi, K. Dhuga, C. L. Morris et al., *Rhys. Rev. Lett.* **128B**, 157 (1983).
- [35] A. L. Williams, J. A. McGill and C. L. Morris et al., *phys. Rev. C* **43**, 766 (1991).
- [36] M. J. Leitch, E. Piassetky, H. W. Baer, J. D. Bowman, R. L. Burman and C. L. Morris et al., *Phys. Rev. Lett.* , **39**, 2356 (1989).
- [37] M. J. Leitch, E. Piassetky, H. W. Baer, J. D. Bowman, R. L. Burman et al., *Phys. Rev. Lett.* , **54**, 1482 (1985).
- [38] A. Ahman, R. R. Johnson, U. Wenads, N. Hessey, *Phys. Rev. Lett.* **55**, 1273 (1985).
- [39] P. A. Seidl, M. D. Brown et al., M. Barnett, B. M. Forster et al. *Phys. Rev. Lett.* **55**, 1273 (1985).
- [40] S. J. Greene, D. B. Holtkamp, W. B. Cottingame et al., *Phys. Rev. C* , **25**, 297 (1982).
- [41] W. R. Gibbs, A. T. Hess and W. B. Kaufmann, *Phys. Rev. C* **13**, 1982 (1976), C. Morris et al., *Nucl. Phys.* , **A432**, 610 (1985).

## APPENDIX A

### SPIN REDUCTION FOR THE DOUBLE-SPIN-FLIP

#### TERM

We define the basic tensor operators by

$$t^{+1} = -(t_x + it_y)/\sqrt{2}; \quad t^{-1} = (t_x - it_y)/\sqrt{2}; \quad t^0 = t_z, \quad (\text{A.1})$$

and a tensor operator made up of a bilinear combination of two of these elementary quantities  $\mathbf{t}_1$  and  $\mathbf{t}_2$  by

$$T_L^M = \sum_{\mu, \mu'} C_{\mu, \mu', M}^{1, 1, L} t_1^\mu t_2^{\mu'}. \quad (\text{A.2})$$

In this notation the dot product is

$$\mathbf{t}_1 \cdot \mathbf{t}_2 = \sum_{\mu} t_1^\mu t_2^{-\mu} (-1)^\mu = -\sqrt{3} T_0^0, \quad (\text{A.3})$$

and the inversion is given by

$$t_1^\mu t_2^{\mu'} = \sum_{L, M} C_{\mu, \mu', M}^{1, 1, L} T_L^M. \quad (\text{A.4})$$

To express the operator

$$\mathcal{O} = (\boldsymbol{\sigma}_1 \cdot \mathbf{k} \times \mathbf{q})(\boldsymbol{\sigma}_2 \cdot \mathbf{q} \times \mathbf{k}') \quad (\text{A.5})$$

in tensor form we put  $\mathbf{e}_1 = \mathbf{k} \times \mathbf{q}$ ,  $\mathbf{e}_2 = \mathbf{q} \times \mathbf{k}'$ , and write

$$\mathcal{O} = \sum_{\mu} \sigma_1^{-\mu} \mathbf{e}_1^\mu (-1)^\mu \times \sum_{\mu'} \sigma_2^{-\mu'} \mathbf{e}_2^{\mu'} (-1)^{\mu'} = \sum_{\mu, \mu'} \sigma_1^{-\mu} \sigma_2^{-\mu'} \mathbf{e}_1^\mu \mathbf{e}_2^{\mu'} (-1)^{\mu+\mu'} \quad (\text{A.6})$$

$$= \sum_{L, M} (-1)^{L+M} \Sigma_L^{-M} E_L^M \quad (\text{A.7})$$

where  $\Sigma$  and  $E$  are defined as bilinear tensor operators in terms of the Pauli matrices  $(\boldsymbol{\sigma}_1, \boldsymbol{\sigma}_2)$  and the pair  $(\mathbf{e}_1, \mathbf{e}_2)$ .

The operators  $E_L^M$  are

$$E_0^0 = -\frac{1}{\sqrt{3}} \mathbf{e}_1 \cdot \mathbf{e}_2 \quad (\text{A.8})$$

$$E_1^1 = \frac{1}{2} [e_1^z (e_2^x + ie_2^y) - (e_1^x + ie_1^y) e_2^z] = \frac{-i}{2} [(\mathbf{e}_1 \times \mathbf{e}_2)^x + i(\mathbf{e}_1 \times \mathbf{e}_2)^y] \quad (\text{A.9})$$

$$E_1^0 = \frac{i}{\sqrt{2}} (e_1^x e_2^y - e_1^y e_2^x) = \frac{i}{\sqrt{2}} (\mathbf{e}_1 \times \mathbf{e}_2)^z; \quad E_1^{-1} = E_1^{1*} \quad (\text{A.10})$$

$$E_2^2 = \frac{1}{2}(e_1^x + ie_1^y)(e_2^x + ie_2^y) \quad (\text{A.11})$$

$$E_2^1 = -\frac{1}{2}[(e_1^x + ie_1^y)e_2^z + e_1^z(e_2^x + ie_2^y)] \quad (\text{A.12})$$

$$E_2^0 = \sqrt{\frac{3}{2}}e_1^ze_2^z - \frac{1}{\sqrt{6}}\mathbf{e}_1 \cdot \mathbf{e}_2; \quad E_2^{-1} = -E_2^{1*}; \quad E_2^{-2} = E_2^{2*} \quad (\text{A.13})$$

Since for a double-analog transition the initial and final states are the same, only the symmetric combinations will enter.

$$E_2^1 + E_2^{-1} = i(e_1^ye_2^z + e_1^ze_2^y); \quad E_2^2 + E_2^{-2} = e_1^xe_2^x - e_1^ye_2^y \quad (\text{A.14})$$

For  $\hat{\mathbf{k}}=\hat{\mathbf{k}}'=\hat{\mathbf{z}}$ , since  $e_1^z = e_2^z = 0$  and  $\mathbf{e}_1 = -\mathbf{e}_2$ , then the operators  $E_L^M$  for (L= 0, 1, 2) are

$$\begin{aligned} E_0^0 &= \mathbf{e}_1 \cdot \mathbf{e}_1 / \sqrt{3} \\ E_1^M &= 0 \\ E_2^2 + E_2^{-2} &= (e_1^x)^2 - (e_1^y)^2 \\ E_2^1 = E_2^{-1} &= 0 \\ E_2^0 &= -\frac{1}{\sqrt{6}}\mathbf{e}_1 \cdot \mathbf{e}_2 \\ &= \frac{1}{\sqrt{6}}\mathbf{e}_1 \cdot \mathbf{e}_1. \end{aligned} \quad (\text{A.15})$$

We can evaluate the spin operator in the singlet-triplet basis using the Wigner-Eckhart theorem:

$$\langle S\Sigma | \Sigma_L^M | S'\Sigma' \rangle = C_{M,\Sigma',\Sigma}^{L,S',S} \langle S || \Sigma_L || S' \rangle. \quad (\text{A.16})$$

The reduced matrix elements are

$$\langle 0 || \Sigma_0 || 0 \rangle = \sqrt{3} \quad \langle 1 || \Sigma_0 || 1 \rangle = -\frac{1}{\sqrt{3}} \quad (\text{A.17})$$

$$\langle 1 || \Sigma_2 || 1 \rangle = 2\sqrt{\frac{5}{3}}; \quad \langle 0 || \Sigma_1 || 1 \rangle = \sqrt{6}; \quad \langle 1 || \Sigma_1 || 1 \rangle = 0. \quad (\text{A.18})$$

## APPENDIX B CALCIUM CODE

```

common /rhoc/ rc, as, anr,rrmax,nnmax
common /ifac/ ifac, om
common /factbl/ fac(30),dfac(28)
common /atgt/ atgt, pi, zmult, anmult, fact
common /vt/ t, ak, dw, rz
common /rhonew/ drrr, rhos, rpp, rhop,rhoin(200)
common/ampblk/e,cpl0,cpl1,cplf,czf,cz0,cz1,iat,qvalue
common/bigrho/ delta,deltai,brho(0:20000)
complex cpl0,cpl1,cplf,czf,cz0,cz1,c00,c01,c10,c11,cff
dimension rh(100),rhop(500),rhos(501),rpp(501),iv(160)
dimension fsick(160),rrs(200),mtem(160,160),rhoinc(200)
dimension tdx(0:1001),td1(201),sq(20),cf(20),dp(7),dm(7)
DIMENSION RHC(200),RHX(200),RPPC(500),RHOSX(501),FN(3),SN(3)
COMPLEX CBN0(3),CBN1(3),AD(2,4),ADSF(2,4),AF(2,4)
character *72 head
dimension sgc(51), pl(200),prp(200),RHOINX(200),RPPX(501)
complex gee(0:6,51),tv1(160),tv2(160),gsf(0:7,51)
1,uz2(0:25,161,2),uzdd(0:25,161,2),vz(200,2),vzdd(200,2),vz2(200,2)
2 ,v22(200,2),vdel(200,2),vdelp(200,2)
dimension gc(0:6,0:6),srl(3,30),stl(3,30),SAL(3,30),RHOSC(500)
complex scl(40),p1h,p3h,alsz,akc,z(0:25,100),G(0:25,160,160)
complex psip(201),ts(160,160),f(800),sumf,ahi,ahf,ahid,ahfd
complex ca2,ca4,ca6,ca8,a1(0:200),a2(0:200),ampgc
complex ca2d,ca4d,ca6d,ca8d,ampd(4,51),alowd,alofd
1 ,b2(0:200),b1(0:200),a3(0:200),a4(0:200)
2 ,b3(0:200),b4(0:200),b5(0:200),b6(0:200),a5(0:200),a6(0:200)
3 ,b7(0:200),b8(0:200),a7(0:200),a8(0:200),vzm2(200,2)
complex*16 cj(50),CH(50),AJL(50),ANL(50)
complex sl(40),fsk, fpk,uz(0:25,161,2),a(0:7,0:25),aa(0:7,51)
complex cb0, cb1,temc,temb,tembp,uzd(0:25,161,2)
common /opt/ cb0, cb1
complex b0cex,b1cex,b0v(40),b1v(40),temd(2),tema,B0VC(40),B1VC(40)
1 ,tem(2),temm2(2),tmm,tmp,tpm,tpp,xalpha,xbeta
dimension psi(160),r(160),x(160),lm(40)
1 ,rwf(1001),wfc(0:1001),td(201),wfo(0:1001),wf(0:1001),tdd(201)
2 ,qj(15,200),qh(15,200)
complex princ,b(0:7,0:25),bb(0:7,51),bbp(0:7,51),cc(0:7,51)
1 ,bp(0:7,0:25),c(0:7,0:25),amp(4,51),asf(0:7,0:25),
x alow,aodd,sf(0:7,51),alof,ccd(0:7,51),sfd(0:7,51)
COMPLEX AI,SH1,SH2,CAP,T(160,160),x,sb,psi,det,y,s
COMPLEX*8 CI,VCORE(160,160),VX(160,160),VT(160,160)

```

```

COMPLEX AS(2,4),AP(2,4),APSF(2,4)
dimension gk(0:15,160,160)
COMPLEX*16 AH(0:15,200)
COMPLEX*16 AJP(0:15,200),AHP(0:15,200),AJK(0:15,200)
COMPLEX UZZ(0:15,200,3),FK(0:15,160,3),GR(0:15,200,3)
COMPLEX FP(0:15,200,3),GP(0:15,200,3),SUMKG,SUMKF
COMPLEX GLML(0:15,0:15),FLML(0:15,0:15),DELAMP
COMPLEX DELC(0:15,51),CoR(0:15,0:15)
open (1,file='wfout.dat',status='unknown')
open (2,file='ca40den.dat',STATUS='unknown')
open (4,file='wfin.dat',STATUS='unknown')
6 open (5,file='ingin.dat',STATUS='UNKNOWN')
open (6,file='ginout.dat',STATUS='unknown')
open (8,file='pout.dat',STATUS='unknown')
open (3,file='fpndat3.dat',STATUS='UNKNOWN')
OPEN (9,FILE='INF.dat',STATUS='unknown')
c.....wfin and wfout transition densities (calculated from wsbs)
c.....ca40den
c.....ingin controls energy, distortion core, off-shell range, etc.
c.....pout comes from rdep
c.....ginout is main output file
c calculation of facs
fac(1)=1.
do i=2,30
uuu=i-1
fac(i)=fac(i-1)*uuu
enddo
dfac(1)=1.
do i=2,28
uuu=2*i-1
dfac(i)=dfac(i-1)*uuu
enddo
zer=0.
one=1.
do 1651 l=1,20
elb=l
sq(1)=sqrt(elb/(elb+1))
1651 cf(1)=cof6j(one,one,one,elb,elb-1,elb)*sqrt(2*elb+1)
x *sqrt(3*elb*(2*elb+1))
oh=0.5
omegj=4.

```



```

aj=3.5
els=3.
lls=7
do 1652 l=1,lls,2
al=1
dp(l)=cof9j(al+1,one,al,els,oh,aj,els,oh,aj)
x *cof3j(els,els,al+1.,zer,zer,zer)
x *(2*els+1)*sqrt(2*(2*aj+1)*(2*(al+1.)+1))
dm(l)=cof9j(al-1,one,al,els,oh,aj,els,oh,aj)
x *cof3j(els,els,al-1.,zer,zer,zer)
x *(2*els+1)*sqrt(2*(2*aj+1)*(2*(al-1.)+1))
1652 continue
do 1804 ii=0,6,2
gc(0,ii)=1.
1804 gc(ii,0)=1.
do 1797 ii=0,7
do 1797 jj=0,6,2
aii=ii
ajj=jj
gc(jj,ii)=-4.*cof6j(3.5,3.5,aii,3.5,3.5,ajj)
1797 continue
c write (6,333)char(15)
333 format(a2)
read (5,571) idel,imax,iat,ipi0
C IPI0=0
write(6,572) idel,imax,iat,ipi0
571 format(4i5)
572 format(' idel,imax=',2i3,' iat(=1 for angle xf)='i3,
x 'ipi0 ( =1 for pi0 distorts)='i3)
llm=6
do 41 i=1,200
read (2,42) rrs(i),rhoin(i)
c print *,rrs(i),rhoin(i)
41 continue
42 format(f7.2,e15.8)
ai=(0.,1.)
hc=197.33
pi=3.14159265358979
fac(1)=1.
fsc=1./137.035982
apm=139.57

```

```

read (5,490) ztgt,atgt,del,alz,alp1,alphap,qvalue,nsick
C alphap=800.0
write (6,490) ztgt,atgt,del,alz,alp1,alphap,qvalue,nsick
nnuc=atgt
FKMT=(ATGT-1.)/ATGT
read (5,500) npr1,npr2,npr3,npr4,npr5,npr6
write (6,500) npr1,npr2,npr3,npr4,npr5,npr6,npp
c a given npr=1 causes intermediate printing
c npr2 causes the wave function to be printed
c npr3 causes the full non-local potential to be printed
read (5,510) n,nkmt,lmax,rz,e,zpi,rq
write (6,510) n,nkmt,lmax,rz,e,zpi,rq
c n is the number of mesh points,
c rz is the matching radius, e is the incident energy and zpi the charg
c of the incident pion
c rq=radius of equivalent charged sphere
C ZPI=0.0
del=rz/n
n1=n-1
npp=n1
irowe=0
if (e.gt.80.)irowe=1
if (irowe.eq.1) write(6,777)
if (irowe.eq.0) write(6,778)
777 format(' using rowe-saloman amplitudes')
778 format(' using siegel-gibbs amplitudes')
call sgampx(irowe,nnuc)
c for test with plane wave code
c cplf=0.
c cz0=cpl0
c cz1=cpl1
c czf=0.
write (6,779) cpl0,cpl1,cplf
779 format(' cpl0=',2f9.5,' cpl1=',2f9.5,' cplf=',2f9.5)
write (6,780) cz0,cz1,czf
780 format(' cz0=',2f9.5,' cz1=',2f9.5,' czf=',2f9.5)
c create tables of spherical bessels of imag arg for finite range
C PRINT*,CPI0, CPL1, CPLF
nppp=npp+39
do 885 i=1,nppp
xx=i*del*alp1

```

```

ep=exp(xx)
call cjh(xx,ep,cj,ch,lmax)
do 886 il=1,lmax,2
qj(il,i)=-dimag(cj(il))
qh(il,i)=dimag(ch(il))
qj(il+1,i)=cj(il+1)
qh(il+1,i)=ch(il+1)
C PRINT*,IL,QJ(IL,I),QH(IL,I)
886 continue
885 continue
c do 887 il=1,lmax
c write (6,888)il
c 888 format(i5)
c do 889 i=1,nppp
c write (6,890) i*del,qj(il,i),qh(il,i)
c 889 continue
c 887 continue
c 890 format(f10.5,1p4e17.8)
c stop
do 43 i=1,800
43 read (4,44) rwf(i),wfc(i)
read (4,590) head
write (6,590) head
read (4,590) head
write (6,590) head
do 47 i=1,800
47 read (1,44) rwf(i),wfo(i)
read (1,590) head
write (6,590) head
read (1,590) head
write (6,590) head
44 format(f8.2,e15.8)
sum=0.
do 51 i=1,800
wf(i)=wfc(i)*wfo(i)
sum=sum+wf(i)*rwf(i)**2
51 continue
eps=rwf(1)
sum=sum*eps
write (6,52)sum
52 format(' transition density normalization',2f10.5)

```

```

wf(0)=0.
do 55 i=1,799
c print *,i,eps,rwf(i),wf(i)
wfo(i)=(wf(i+1)-2.*wf(i)+wf(i-1))/eps**2+(wf(i+1)-wf(i-1))
1/(eps*rwf(i))
tdx(i)=(wf(i+1)-wf(i-1))/(eps*2)
55 continue
sum=0.
do 45 i=1,n
rr=del*i
r(i)=rr
dd=rr/eps
ii=dd
if (ii.gt.798) goto 45
dd=dd-ii
td(i)=(1.-dd)*wf(ii)+dd*wf(ii+1)
tdd(i)=(1.-dd)*wfo(ii)+dd*wfo(ii+1)
tdl(i)=(1.-dd)*tdx(ii)+dd*tdx(ii+1)
sum=sum+td(i)*rr**2
45 continue
sum=sum*del
write(6,52)sum
sum=0.
acore=40.
core=acore/atgt
val=(atgt-acore)
CALL CLRHO
DO 992 I=1,200
992 RHOINC(I)=RHO(RRS(I))
C PRINT *,RHOINC(I)
DO 993 I=1,500
RHOSC(I)=RHOS(I)
RPPC(I)=RPP(I)
c print *,.02*(i-1),rhosc(i),rppc(i)
993 CONTINUE
DO 64 I=1,N
64 RHC(I)=RHO(R(I))
c 64 print *,rhc(i)
DO 931 I=1,200 !DO EXTRA NEUTRON DENSITY
931 RHOIN(I)=WF(5*(I-1))
CALL CLRHO

```

```

DO 357 I=1,200
357 RHOINX(I)=RHO(RRS(I))
DO 596 I=1,500
RHOSX(I)=RHOS(I)
RPPX(I)=RPP(I)
c print *,rhosx(i),rppx(i)
596 CONTINUE
DO 84 I=1,N
84 RHX(I)=RHO(R(I))
SUMP=0.
SUMN=0.
SUMX=0.
SUMPR=0.
SUMNR=0.
SUMXR=0.
do 782 i=1,200
SUMC=SUMC+(RHOINC(I))*RRS(I)**2
SUMPR=SUMPR+(RHOINC(I))*RRS(I)**4
C SUMN=SUMN+(RHOINN(I))*RRS(I)**2
C SUMX=SUMX+(RHOINX(I))*RRS(I)**2
C SUMNR=SUMNR+(RHOINN(I))*RRS(I)**4
C SUMXR=SUMXR+(RHOINX(I))*RRS(I)**4
rhoin(i)=core*rhoin(i)+val*wf((i-1)*5)
sum=sum+rhoin(i)*(0.05*(i-1))**2
782 continue
write(6,783) sum*.05
783 format(' norm of revised density',f10.4)
C call clrho
c do 463 i=1,200
c write (6,464) i*.05,rhoin(i),i*.02,rhos(i),rpp(i)
c 463 continue
c 464 format(f6.2,f10.5,f6.2,2f10.5)
write (6,444) rrmx,nnmx
444 format(' rrmx',f6.2,' nnmx',i5)
delta=.001
deltai=1./delta
jj=rrmx*deltai
do 471 i=1,jj
rr=delta*i
brho(i)=rho(rr)
471 continue

```

```

brho(0)=brho(1)
alpha=(alphap/hc)
aias=atgt*938.9
om=apm+e
aklab=sqrt(om**2-apm**2)/hc
epn=sqrt(139.57**2+938.9**2+2.*om*938.9)
akcmi=aklab*938.9/epn
ep=sqrt(139.57**2+aias**2+2.*om*aias)
anuc=aias+qvalue
omf=(ep**2-apm**2-anuc**2)/2./anuc
ak=sqrt(om**2-apm**2)/197.32
aky=ak
ak=ak*aias/ep
akz=ak
aki=ak
akf=sqrt(omf**2-apm**2)/hc
enpf=sqrt(139.57**2+938.9**2+2.*omf*938.9)
akcmf=akf*938.9/enpf
akf=akf*anuc/ep
rati=aki/akcmi
ratf=akf/akcmf
c for test with pw code
cpl0=cpl0*rati
cz0=cz0*ratf
cpl1=cpl1/rati
cz1=cz1/ratf
cplf=cplf/rati
czf=czf/ratf
c take out above for test with pw code
cff=cplf*czf
c00=cpl0*cz0
c01=cpl0*cz1
c10=cpl1*cz0
c11=cpl1*cz1
write(6,3333) c00,c01,c10,c11
3333 format(' c:00,01,10,11',8f8.4)
cfact=ep/anuc
read (5,580) ifac,idat,zf,rad
C ifac=0
if (ifac.eq.0) write (6,837)
837 format(' doing plane wave calculation')

```

```

if (ifac.eq.4) write (6,838)
838 format(' using l dependent optical model strengths')
write (6,580) ifac,idat,zf,rad
C read (5,570) wabs
WABS=(515.0*77.0*77.0/4.0)/((E-215.)**2+77.**2/4.0)
C WABS=0
wabs0=wabs
c wabs=wabs*(acore/12.)**2
write (6,530) wabs,aki,akf,akcmi,akcmf
read (8,590) head
write (6,590) head
read (8,600) lampx,head
write (6,600) lampx,head
read (8,610) lb,b0cex,b1cex,fsk,fpk
write (6,610) lb,b0cex,b1cex,fsk,fpk
read (8,610) lb,cb0c,cb1C
write (6,610) lb,cb0C,cb1C
cb0C=cb0c*cfact
cb1C=cb1C/cfact
do 60 lp=1,lampx
read (8,610) lm(lp),b0vc(lp),b1vc(lp)
if (lp.le.lmax) write (6,610) lm(lp),b0vC(lp),b1vC(lp)
b0vC(lp)=b0vc(lp)*cfact
b1vC(lp)=b1vc(lp)/cfact
60 continue
write (6,630) ztgt,atgt,alz,alp1,ak
if (nsick.ne.1) go to 70
call chg (acore,fsick,n,del)
write (6,620) atgt
70 continue
write (6,640) e,zpi,alphap
write (6,671) n,rz
deli=1./del
n2=n-2
ipass=1
tek=2*zpi*ztgt*fsc*sqrt(apm**2+(hc*aki)**2)/hc
c start l loop
441 sumr=0.0
sumt=0.0
SUMAB=0.0
do 440 il=1,lmax

```

```

if(ipass.eq.2)ak=akf
if(ipass.eq.3)ak=akz
eta=tek/(2.*ak)
l=il-1
al=1
if (ifac.eq.2) go to 130
if (ipass.lt.3.and.il.eq.1) write (6,661) ak,eta
if (ipass.lt.3.and.il.eq.1) write (6,660)
661 format(' k ',f10.5,' eta ',f10.5)
CB0=CB0C
CB1=CB1C
C PRINT *,IFAC
IF (IFAC.EQ.2) GO TO 130
k=1
if (ifac.eq.4) k=il
CB0=B0VC(K)
CB1=B1VC(K)
130 CONTINUE
IF (IFAC.EQ.0) CB0=0.
IF (IFAC.EQ.0) CB1=0.
AK0=1. !?
DO 582 I=1,500
RPP(I)=RPPC(I)
582 RHOS(I)=rhosc(i)
c rrrr=0.02*(i-1)
c 582 print *,rrrr,rpp(i),rhos(i),rho(rrrr),rhopp(rrrr)
938 CALL VCAL (ALPHA,Del,N,IL)
DO 568 I=1,N
DO 568 J=1,N
568 VCORE(I,J)=T(I,J)
c 568 PRINT *,VCORE(I,J)
FACT=(4.0*PI)/(AK*(AKCMI)**2)
IF (IPASS.EQ.1) THEN
CALL FPN(e,AS,AP,APSF,AD,ADSF,AF)
FN(IPASS)=AP(1,1)
SN(IPASS)=AS(1,1)
CBN0(IPASS)=FACT*AS(1,1)/(2.0*AI)
CBN1(IPASS)=3.0*FACT*AP(1,1)/(2.0*AI)
ENDIF
IF (IPASS.EQ.2) THEN
CALL FPN(e,AS,AP,APSF,AD,ADSF,AF)

```



```

FN(IPASS)=AP(2,1)
SN(IPASS)=AS(2,1)
CBN0(IPASS)=FACT*AS(2,1)/(2.0*AI)
CBN1(IPASS)=3.0*FACT*AP(2,1)/(2.0*AI)
ENDIF
IF (IPASS.EQ.3) THEN
CBN0(IPASS)=(CBN0(1)+CBN0(2))/2.0
CBN1(IPASS)=(CBN1(1)+CBN1(2))/2.0
ENDIF
c print *,cbn0(ipass),cbn1(ipass),l,ipass
IFACX=4 !?
IF(IFACX.EQ.0) GOTO 1031
C CB0=CB0C
C CB1=CB1C
IF (IFACX.EQ.2) GO TO 932
K=1
IF (IFACX.EQ.4) K=IL
CB0=B0VC(K)
CB1=B1VC(K)
932 CONTINUE
DO 983 I=1,500
RPP(I)=RPPX(I)
983 RHOS(I)=RHOSX(I)
c 983 print *,rpp(i),rhos(i)
CB0=CBN0(IPASS)
CB1=CBN1(IPASS)
CALL VCAL (ALPHA,Del,N,IL)
DO 969 I=1,N
DO 969 J=1,N
969 VX(I,J)=T(I,J)
c 969 PRINT *,VX(I,J)
1031 DO 573 I=1,N
DO 573 J=1,N
573 T(I,J)=(40.0*VCORE(I,J)+VAL*VX(I,J))
DO 556 I=1,500
RPP(I)=RPPC(I)
556 RHOS(I)=rhosc(i)
C do i=1,n1
c do j=1,n1
c t(i,j)=real(t(i,j))
c end do

```

```

c end do
if (npr3.eq.1) call potpr (r,n,il,alphap)
do 211 i=1,n1
211 t(i,i)=t(i,i)-2.*deli**2
do 212 i=1,n2
t(i,i+1)=t(i,i+1)+deli**2
t(i+1,i)=t(i+1,i)+deli**2
212 continue
c11=al*(al+1.)
do 220 i=1,n1
facc=1./r(i)
if (r(i).lt.rq) facc=(3./rq-r(i)**2/rq**3)/2.
if (nsick.eq.1) facc=fsick(i)
220 t(i,i)=t(i,i)-c11/r(i)**2-tek*facc+ai*wabs*rho(r(i))**2+ak**2
if (ipass.eq.3) goto205
do 230 i=1,n2
230 x(i)=-t(i,n1)
call cls (n2,1,t,160,x,160)
x(n1)=1.
if(npr2.ne.1)goto 241
write (6,242)(r(i),x(i),i=1,n1)
242 format(3f10.5)
241 continue
do 240 i=1,n1
c if (1.eq.10) write (6,936) r(i),x(i)
c 936 format(' r,x ',3e18.7)
240 psi(i)=x(i)
call sigcou (eta,sgc)
do 80 jl=1,lmax
80 scl(jl)=cexp(2.*ai*sgc(jl))
sh1=y(ak*r(n1),l,eta)
sh2=y(ak*r(n2),l,eta)
det=psi(n1)*sh2-psi(n2)*sh1
cap=.5*(sh2*conjg(sh1)-sh1*conjg(sh2))/det
s=-(psi(n1)*conjg(sh2)-psi(n2)*conjg(sh1))/det
939 sl(il)=s
SUMA=0.0
do 275 i=1,n1
psi(i)=cap*psi(i)
psip(i+1)=psi(i)
SIA=(cabs(Psi(I))*RHO(R(I)))**2

```

```

SUMA=(SUMA+SIA)
275 continue
do 323 jj=n1-1,nppp+1
rt=del*(jj-1)
sh1=y(ak*rt,l,eta)
psip(jj)=(conjg(sh1)+s*sh1)*.5
323 continue
STL(IPASS,IL)=2*PI*(2*aL+1)*(1-REAL(S))/AK**2
SRL(IPASS,IL)=PI*(2*aL+1)*(1-(CABS(S))**2)/AK**2
SAL(IPASS,IL)=4*PI*WABS*(2*AL+1)*SUMA*del/AK**3
ST=STL(IPASS,IL)*10.0
SR=SRL(IPASS,IL)*10.0
SA=SAL(IPASS,IL)*10.0
SUMAB=SUMAB+SA
sumr=sumr+sr
sumt=sumt+st
322 write (6,710)l,s,scl(il),ST,SR,SA
c now convert the wave function for finite range
c for the incident and final waves only
confr=(alp1**2+ak**2)/alp1
do 891 i=1,nppp
a1(i)=psip(i+1)*qj(il,i)
a2(i)=psip(i+1)*qh(il,i)
891 continue
do 892 i=1,nppp
b2(nppp+1-i)=b2(nppp+2-i)+(a2(nppp+1-i)+a2(nppp+2-i))* .5*del
b1(i)=b1(i-1)+(a1(i)+a1(i-1))* .5*del
892 continue
do 893 i=1,npp+2
psip(i+1)=(qj(il,i)*b2(i)+qh(il,i)*b1(i))*confr
893 continue
do 335 i=1,npp
uz(l,i,ipass)=psip(i+1)*td(i)/ak
uzz(l,i,ipass)=psip(i+1)/ak
uzdd(l,i,ipass)=psip(i+1)*tdd(i)/ak
uz2(l,i,ipass)=(psip(i)-2.*psip(i+1)+psip(i+2))*td(i)/ak*deli**2
uzd(l,i,ipass)=psip(i+1)*td1(i)/ak
335 continue
goto 440
205 confr=(alp1**2+ak**2)/alp1
t(n1,n1)=t(n1,n1)+deli**2*y(ak*del*n,l,eta)/y(ak*del*n1,l,eta)

```

```

call invert (t,n1,160,mtem,ts)
do 650 i=1,llm+1
lam=1+2*i-llm-2
if(lam.lt.0) goto 650
if(lam.gt.lmax-1) goto 650
alam=lam
do 655 id=1,2
a2(npp+1)=0.
a4(npp+1)=0.
a6(npp+1)=0.
a8(npp+1)=0.
b2(npp+1)=0.
b4(npp+1)=0.
b6(npp+1)=0.
b8(npp+1)=0.
do 894 j=1,npp
a1(j)=uz(lam,j,id)*qj(il,j)
a2(j)=uz(lam,j,id)*qh(il,j)
a3(j)=uzdd(lam,j,id)*qj(il,j)
a4(j)=uzdd(lam,j,id)*qh(il,j)
a5(j)=uz2(lam,j,id)*qj(il,j)
a6(j)=uz2(lam,j,id)*qh(il,j)
a7(j)=uz(lam,j,id)*qj(il,j)/r(j)**2
a8(j)=uz(lam,j,id)*qh(il,j)/r(j)**2
894 continue
do 895 j=1,npp
b2(npp+1-j)=b2(npp+2-j)+(a2(npp+1-j)+a2(npp+2-j))* .5*del
b1(j)=b1(j-1)+(a1(j)+a1(j-1))* .5*del
b4(npp+1-j)=b4(npp+2-j)+(a4(npp+1-j)+a4(npp+2-j))* .5*del
b3(j)=b3(j-1)+(a3(j)+a3(j-1))* .5*del
b6(npp+1-j)=b6(npp+2-j)+(a6(npp+1-j)+a6(npp+2-j))* .5*del
b5(j)=b5(j-1)+(a5(j)+a5(j-1))* .5*del
b8(npp+1-j)=b8(npp+2-j)+(a8(npp+1-j)+a8(npp+2-j))* .5*del
b7(j)=b7(j-1)+(a7(j)+a7(j-1))* .5*del
895 continue
do 896 j=1,npp
vz(j,id)=(qj(il,j)*b2(j)+qh(il,j)*b1(j))*confr
vzdd(j,id)=(qj(il,j)*b4(j)+qh(il,j)*b3(j))*confr
vz2(j,id)=(qj(il,j)*b6(j)+qh(il,j)*b5(j))*confr
vzm2(j,id)=(qj(il,j)*b8(j)+qh(il,j)*b7(j))*confr
896 continue

```

```

v22(1,id)=0.
do 897 j=2,npp-1
v22(j,id)=(vz(j-1,id)-2.*vz(j,id)+vz(j+1,id))*deli**2
897 continue
655 continue
do 420 ll=0,llm
all=ll
coef=cg(all,alam,al,0.,0.,0.)*2
if (coef.eq.0) goto 420
dll=-all*(all+1.)+lam*(lam+1)
do 222 id=1,2
do 223 j=1,n1
vdel(j,id)=vzdd(j,id)-vz2(j,id)-v22(j,id)
1 +vz(j,id)*c11/r(j)**2+dll*vzm2(j,id)
223 continue
222 continue
do 219 j=1,n1
tv1(j)=0.
tv2(j)=0.
219 continue
do 218 k=1,n1
do 218 j=1,n1
tv1(j)=vz(k,2)*t(j,k)+tv1(j)
tv2(j)=vdel(k,2)*t(j,k)+tv2(j)
218 continue
tema=0.
temb=0.
tembp=0.
temc=0.
do 217 j=1,n1
tema=tema+vz(j,1)*tv1(j)
temb=temb+vz(j,1)*tv2(j)
tembp=tembp+vdel(j,1)*tv1(j)
temc=temc+vdel(j,1)*tv2(j)
217 continue
a(ll,lam)=-tema*del*coef+a(ll,lam)
b(ll,lam)=-temb*del*coef*.5+b(ll,lam)
bp(ll,lam)=-tembp*del*coef*.5+bp(ll,lam)
c(ll,lam)=-temc*del*coef*.25+c(ll,lam)
213 format(3i5,f10.5)
c multipole loop

```

```

420 continue
c end lam loop (on i)
650 continue
do 1650 i=1,lls
lam=l+2*i-lls-1
if(lam.lt.0) go to 1650
if(lam.gt.lmax-1) go to 1650
alam=lam
do 1655 id=1,2
a4(npp+1)=0.
a8(npp+1)=0.
b4(npp+1)=0.
b8(npp+1)=0.
do 1894 j=1,npp
a3(j)=uzd(lam,j,id)*qj(il,j)/r(j)
a4(j)=uzd(lam,j,id)*qh(il,j)/r(j)
a7(j)=uz(lam,j,id)*qj(il,j)/r(j)**2
a8(j)=uz(lam,j,id)*qh(il,j)/r(j)**2
1894 continue
do 1895 j=1,npp
b4(npp+1-j)=b4(npp+2-j)+(a4(npp+1-j)+a4(npp+2-j))* .5*del
b3(j)=b3(j-1)+(a3(j)+a3(j-1))* .5*del
b8(npp+1-j)=b8(npp+2-j)+(a8(npp+1-j)+a8(npp+2-j))* .5*del
b7(j)=b7(j-1)+(a7(j)+a7(j-1))* .5*del
1895 continue
do 1896 j=1,npp
vzdd(j,id)=(qj(il,j)*b4(j)+qh(il,j)*b3(j))*confr
vzm2(j,id)=(qj(il,j)*b8(j)+qh(il,j)*b7(j))*confr
1896 continue
1655 continue
do 1420 ll=1,lls,2
if(ll.lt.iabs(lam-1)) go to 1420
if (ll.gt. lam+1) go to 1420
elb=ll
q1=cg(elb,alam+1,al,zer,zer,zer)
if (q1.eq.0.) go to 1420
app=sqrt((lam+1.)*(2.*lam+3.))*q1*cf(ll)
x *cof6j(elb,alam+1,al,alam,elb,one)
app2=app**2*(2*lam+1)
do 1222 id=1,2
do 1223 j=1,n1

```

```

vdel(j,id)=(-vzdd(j,id)+vzm2(j,id)*(ll-1))
vdelp(j,id)=(-vzdd(j,id)-vzm2(j,id)*(ll+2))*sq(ll)
1223 continue
1222 continue
do 1219 j=1,n1
tv1(j)=0.
tv2(j)=0.
1219 continue
do 1218 k=1,n1
do 1218 j=1,n1
tv1(j)=vdel(k,2)*t(j,k)+tv1(j)
tv2(j)=vdelp(k,2)*t(j,k)+tv2(j)
1218 continue
tmm=0.
tpm=0.
tmp=0.
tpp=0.
do 1217 j=1,n1
tmm=tmm+vdel(j,1)*tv1(j)
tpm=tpm+vdel(j,1)*tv2(j)
tmp=tmp+vdelp(j,1)*tv1(j)
tpp=tpp+vdelp(j,1)*tv2(j)
1217 continue
a(ll,lam)=-tmm*del*app2+a(ll,lam)
b(ll,lam)=-tpm*del*app2+b(ll,lam)
bp(ll,lam)=-tmp*del*app2+bp(ll,lam)
c(ll,lam)=-tpp*del*app2+c(ll,lam)
asf(ll,lam)=(dm(ll)**2*a(ll,lam)+dp(ll)**2*c(ll,lam)
x +dm(ll)*dp(ll)*(b(ll,lam)+bp(ll,lam)))*6.
1420 continue
1650 continue
c end il loop
440 continue
if (ipass.eq.3) goto 557
if (ipass.eq.1) tek=-tek
if (ipass.eq.2) tek=0.
if (ipass.eq.2 .and. ipi0.ne.1) ifac=0
ipass=ipass+1
write(6,715) sumt,sumr,SUMAB
715 format (' sigt ',f10.4,' sigr ',f10.4,' SIGAB ',F10.4)
goto 441

```

```

557 continue
if (npr1.ne.1) goto 662
write (6,799)
799 format(' partial waves for ss term')
do 425 ll=0,lmax-1
425 write (6,485) ll,(a(1,ll)*200.,l=0,llm,2)
485 format(i5,8f10.5)
write (6,585)
585 format(' partial waves for sp term')
do 528 ll=0,lmax-1
528 write (6,485) ll,(b(1,ll)*200.,l=0,llm,2)
write (6,669)
669 format(' partial waves for ps term')
do 668 ll=0,lmax-1
668 write (6,485) ll,(bp(1,ll)*200.,l=0,llm,2)
write (6,672)
672 format(' partial waves for pp term')
do 670 ll=0,lmax-1
670 write (6,485) ll,(c(1,ll)*200.,l=0,llm,2)
write(6,1672)
1672 format(' partial waves for tmm')
do 1670 ll=0,lmax-1
1670 write (6,485) ll,(a(1,ll)*200.,l=1,lls,2)
write (6,1673)
1673 format(' partial waves for tpm')
do 1674 ll=0,lmax-1
1674 write (6,485) ll,(b(1,ll)*200.,l=1,lls,2)
write (6,1675)
1675 format(' partial waves for tmp')
do 1676 ll=0,lmax-1
1676 write (6,485) ll,(bp(1,ll)*200.,l=1,lls,2)
write (6,1677)
1677 format(' partial waves for tpp')
do 1678 ll=0,lmax-1
1678 write (6,485) ll,(c(1,ll)*200.,l=1,lls,2)
662 continue
c*****
C THIS IS A SUBROUTINE TO CALCULATE THE CORRECTION
C DUE TO THE DELTA FUNCTION
C FOR PION DOUBLE CHARGE EXCHANGE AMPLITUDE
c*****

```



```

FACT=(ALP1**2+AK**2)**2/(2.0*ALP1)
PI=3.1415927
NMAX=N
C*****
C CALCULATE THE BESSEL FUNCTION FOR IMAGINARY
ARGUMENT
C (J AND H) FOR DIFFERENT L AND r
C*****
DO I=1,NMAX
XX=I*ALP1*DEL
EP=EXP(XX)
CALL CJH(XX,EP,CJ,CH,LMAX)
DO L=1,LMAX+1
AJK(L-1,I)=CJ(L)/XX
AH(L-1,I)=CH(L)/XX
END DO
DO L=0,LMAX-1
AJP(L,I)=(L*AJK(L-1,I)-(L+1)*AJK(L+1,I))/(2.0*L+1)
AHP(L,I)=(L*AH(L-1,I)-(L+1)*AH(L+1,I))/(2.0*L+1)
ENDDO
ENDDO
C*****
C CALCULATE THE FUNCTION g(L',r1,r2) FROM THE ANALYTIC
C*****
DO I=1,NMAX
DO J=1,NMAX
DO L=0,LMAX-1
IF(I.LT.J) then
GK(L,I,J)=-FACT*(AJK(L,I)*AH(L,J)
& +AI*ALP1*I*DEL*AJP(L,I)*AH(L,J)
& +AI*ALP1*DEL*J*AJK(L,I)*AHP(L,J))
ELSE
GK(L,I,J)=-FACT*(AJK(L,J)*AH(L,I)
& +AI*ALP1*J*DEL*AJP(L,J)*AH(L,I)
& +AI*ALP1*I*DEL*AJK(L,J)*AHP(L,I))
END IF
c if (l.eq.5.and.i.le.20.and.j.le.20) then
c print 880, l,i,j,r(i),r(j),gk(l,i,j)
c 880 format(3i4,2f6.2,2f12.7)
c endif
END DO

```

```

END DO
END DO
C*****
C THIS WILL CALCULATE THE FUNCTION G(L,r) AND F(L,r) FOR r1
C AND r2 , IT CALCULATES THE DERIVATIVE OF THE PION WAVE
C FUNCTION
C*****
c test with explicit plane waves
c do lam=0,lmax-1
c do i=1,nmax
c zz=ak*r(i)
c gp(lam,i,1)=sj(lam+1,zz)
c gp(lam,i,2)=gp(lam,i,1)
c enddo
c enddo
c end explicit plane wave test
DO IPASS=1,2
DO lam=0,LMAX-1
DO I=1,NMAX
gp(lam,I,IPASS)=uzz(lam,i,ipass)/r(i)
END DO
END DO
enddo
DO IPASS=1,2
DO lam=0,LMAX-1
fp(lam,1,ipass)=(gp(lam,2,ipass)-gp(lam,1,ipass))/del
fp(lam,nmax,ipass)=(gp(lam,nmax,ipass)-gp(lam,nmax-1,ipass))/del
DO I=2,NMAX-1
FP(lam,I,IPASS)=(gp(lam,I+1,IPASS)-gp(lam,I-1,IPASS))/(2.*DEL)
END DO
END DO
DO lam=0,LMAX-1
DO I=1,NMAX
FK(lam,I,IPASS)=(FP(lam,I,IPASS)-(lam/r(i))*
1 gp(lam,I,IPASS))*r(i)**2
GR(lam,I,IPASS)=(fP(lam,I,IPASS)+((lam+1)/r(i))*
1 gp(lam,I,IPASS))*r(i)**2
c if (lam.eq.0.and.ipass.eq.1.and.i.lt.50)
c 1 print 881,i,r(i),gp(lam,i,ipass),fp(lam,i,ipass),
c 2 fk(0,i,1),gr(0,i,1)
c 881 format(i4,f6.2,8f8.4)

```

```

END DO
END DO
END DO
C*****
C INTEGRATION OVER r1 AND r2 FOR THE CORRECTION
C X(r1) AND Y(r2) IS THE NUCEAR WAVE FUNCTION FOR NUCLEONS
C 1 AND 2.
C*****
DO LP=0,LMAX-1
DO M=0,LMAX-1
SUMKG=0.0
SUMKF=0.0
DO I=1,NMAX
DO J=1,NMAX
SUMKG=SUMKG+GK(LP,I,J)*TD(I)*TD(J)*GR(M,I,1)*GR(M,J,2)
SUMKF=SUMKF+GK(LP,I,J)*TD(I)*TD(J)*FK(M,I,1)*FK(M,J,2)
END DO
END DO
glml(m,lp)=sumkg*del**2
flml(m,lp)=sumkf*del**2
END DO
END DO
DO ITH=1,imax
TH=(ITH-1)*5.0*PI/180.0
XX=COS(TH)
CALL PLEG(XX,PL,15)
DO L=0,7
al=1
DELC(L,ITH)=0.0
DO lam=0,LMAX-1
alam=lam
do 232 lp=0,lmax-1
if (lp.gt.l+lam+1) goto 232
if((-1)**(1+lp+lam).gt.0.) goto 232
alp=lp
COEFP=CG(alp,al,alam+1.,0.,0.,0.)**2*(alam+1.)/(2.*alam+3.)
coefm=0.
if (lam.gt.0)
1 COEFM=CG(alp,al,alam-1.,0.,0.,0.)**2*alam/(2.*alam-1.)
if (coefp.eq.0..and.coefm.eq.0.) goto 232
c print 339,lp,l,lam,coefp,coefm,flml(lam,lp),glml(lam,lp)

```

```

c 339 format(3i5,6f9.5)
DELAMP=PL(lam+1)*(COEFP*FLML(lam,LP)+COEFM*GLML(lam,LP)) ×
1 (2.*alp+1.)
DELC(L,ITH)=DELC(L,ITH)+DELAMP
c print 445,ith,lp,lam,l,lmax-1,delc(l,ith)*200.,delamp*200.
232 continue ! lp loop
END DO !lambda loop
DELC(L,ITH)=- (1.0/3.0)*DELC(L,ITH)
END DO !L loop
END DO !ith loop
C*****
do 525 ith=1,jmax
th=(ith-1)*idel*pi/180.
xx=cos(th)
call pleg(xx,pl,15)
do 526 l=0,llm,2
aa(l,ith)=0.
bb(l,ith)=0.
bbp(l,ith)=0.
cc(l,ith)=0.
do 529 ll=0,lmax-1
529 cc(l,ith)=cc(l,ith)+(2*ll+1)*pl(ll+1)*(c(l,ll))
ccd(L,ITH)=CC(L,ITH)+DELC(L,ITH)
C PRINT 445,(ITH-1)*5,L,DELC(L,ITH)*200.,cc(l,ith)*200.
C 1 ,ccd(l,ith)*200.
445 format(2i5,6f10.5)
do 526 lp=1,lmax
bb(l,ith)=bb(l,ith)+(2*lp-1)*pl(lp)*b(l,lp-1)
bbp(l,ith)=bbp(l,ith)+(2*lp-1)*pl(lp)*bp(l,lp-1)
526 aa(l,ith)=aa(l,ith)+(2*lp-1)*pl(lp)*a(l,lp-1)
do 1527 l=1,lls,2
sf(l,ith)=0.
do 1526 ll=0,lmax-1
sf(l,ith)=sf(l,ith)+(2*ll+1)*pl(ll+1)*asf(l,ll)
1526 continue
c sfd(l,ith)=sf(l,ith)+delc(l,ith)
c PRINT 445,(ITH-1)*5,L,DELC(L,ITH)*200.,sf(l,ith)*200.
c 1 ,sfd(l,ith)*200.
1527 continue
525 continue ! end theta loop

```

```

c write (6,835)
835 format(' s-s s-p')
c do 565 i=1,imax
c 565 write (6,527) (i-1)*idel,(aa(1,i)*200.,l=0,llm,2),
c 1 (bb(1,i)*200.,l=0,llm,2)
c write (6,836)
836 format(' p-s p-p')
c 673 write (6,527) (i-1)*idel,(bbp(1,i)*200.,l=0,llm,2),
c 1 (cc(1,i)*200.,l=0,llm,2)
527 format(i4,16f8.3)
write (6,839)
write (6,1839)
839 format(' a b asf bsf',
1 ' A2 B2 ASF2 BSF2')
1839 format(' alpha beta',
1 ' al2 be2')
do 791 i=1,imax
do 1792 l=1,lls,2
c sfd(1,i)=sfd(1,i)*cff*200.
1792 sf(1,i)=sf(1,i)*cff*200.
do 792 m=1,4
l=2*(m-1)
amp(m,i)=c00*aa(1,i)+c10*bb(1,i)+c01*bbp(1,i)+c11*(cc(1,i))
ampd(m,i)=c00*aa(1,i)+c10*bb(1,i)+c01*bbp(1,i)+c11*(ccd(1,i))
ampd(m,i)=ampd(m,i)*200.
792 amp(m,i)=amp(m,i)*200.
amp(2,i)=amp(2,i)*25./21.
amp(3,i)=amp(3,i)*81./77.
amp(4,i)=amp(4,i)*25./33.
ampd(2,i)=ampd(2,i)*25./21.
ampd(3,i)=ampd(3,i)*81./77.
ampd(4,i)=ampd(4,i)*25./33.
write (6,789) (i-1)*idel,amp(1,i),amp(2,i),amp(3,i),amp(4,i)
write (6,789) (i-1)*idel,ampd(1,i),ampd(2,i),ampd(3,i),ampd(4,i)
789 format(i5,8f7.2,' amps')
c do 1801,ij=0,6,2
c gee(ij,i)=gc(ij,0)*amp(1,i)+gc(ij,2)*amp(2,i)+gc(ij,4)*amp(3,i)
c x +gc(ij,6)*amp(4,i)
c gsf(ij,i)=gc(ij,1)*sf(1,i)+gc(ij,3)*sf(3,i)+gc(ij,5)*sf(5,i)
c 1 +gc(ij,7)*sf(7,i)
c1801 continue

```

```

aodd=sf(1,i)+sf(3,i)+sf(5,i)+sf(7,i)
alow=amp(1,i)
alowd=ampd(1,i)
ahi=amp(2,i)+amp(3,i)+amp(4,i)
ahid=ampd(2,i)+ampd(3,i)+ampd(4,i)
alof=alow-aodd/omegj
alofd=alowd-aodd/omegj
ahf=ahi-aodd*(omegj-1)/omegj
ahfd=ahid-aodd*(omegj-1)/omegj
xalpha=alof-(1./3.)*ahf
xbeta=(4./3.)*ahf
write (6,793) (i-1)*idel,amp(1,i),ahi,alof,ahf,cabs(amp(1,i))**2,
1 cabs(ahi)**2,cabs(alof)**2,cabs(ahf)**2
write (6,793) (i-1)*idel,ampd(1,i),ahid,alofd,ahfd,
1 cabs(ampd(1,i))**2,cabs(ahid)**2,cabs(alofd)**2,cabs(ahfd)**2
791 write (6,1793) xalpha,xbeta,cabs(xalpha)**2,cabs(xbeta)**2
1793 format( 32x,4f7.3,10x,2f5.2)
793 format (i4,8f7.3,4f5.2)
c write (6,1803)
c1803 format(' th,g0,g2,g4,g6')
c do 1802 i=1,imax
c1802 write (6,1793) (i-1)*idel,(gee(ij,i),ij=0,6,2)
c 1 ,((gee(ij,i)+gsf(ij,i)),ij=0,6,2)
c1793 format(i4,16f7.3)
write (6,640) e,zpi,alphap
write (6,641) wabs0,alz,alp1,qvalue,atgt
641 format(' wabs0= ',f6.2,' al0= ',f6.2,' al1= ',f6.2,
x ' qvalue= ',f6.2,' distortion core= ',f4.0)
write (6,*) ' Explanation of results to follow'
write (6,*) ' Seniority model with DSF no delta correction'
write (6,*) ' Seniority model with DSF with delta correction'
write (6,*) ' Seniority model no DSF no delta correction'
write (6,*) ' Seniority model no DSF with delta correction'
write (6,*) ' BMZ model with DSF no delta correction'
write (6,*) ' BMZ model with DSF with delta correction'
write (6,*) ' BMZ model without DSF no delta correction'
write (6,*) ' BMZ model without DSF with delta correction'
write (6,796)
796 format(' th ca42a ca44a ca46a ti46a ca48a ti48a ',
1 'ca44g ca46g ca48g ti48g xph b/a')
write (6,1990)

```

```

1990 format(' fe54 cr52 ti50 cr50 '
1 , 'cr52 ti50')
do 794 i=1,imax
aodd=sf(1,i)+sf(3,i)+sf(5,i)+sf(7,i)
alow=amp(1,i)
alofd=ampd(1,i)
ahi=amp(2,i)+amp(3,i)+amp(4,i)
ahid=ampd(2,i)+ampd(3,i)+ampd(4,i)
alof=alow-aodd/omegj
alofd=alofd-aodd/omegj
ahf=ahi-aodd*(omegj-1)/omegj
ahfd=ahid-aodd*(omegj-1)/omegj
ampgc=ahi+alow
amptot=cabs(ampgc)
C PRINT*,e,(i-1)*IDEL,ampgc,amptot
boa=cabs(ahf/alof) ! start amps with dsf and no delta correction
ca2=alof+ahf
ca4=alof+ahf/9.
ca6=alof-ahf/15.
ca8=alof-ahf/7.
akrt=akf/aki
aa2=cabs(ca2)**2*akrt
aa4=6.*cabs(ca4)**2*akrt
aa6=15.*cabs(ca6)**2*akrt
aa8=28.*cabs(ca8)**2*akrt
tig48=cabs(1.5147*ahf)**2*akrt
tia48=cabs(2.4495*(alof+.1675*ahf))**2*akrt
sen48=cabs(1.1638*ahf)**2*akrt
sen44=cabs(1.2571*ahf)**2*akrt
sen46=cabs(1.3771*ahf)**2*akrt
bmz44=cabs(.7977*amp(2,i)+1.1286*amp(3,i)+1.2057*amp(4,i))**2*akrt
bmz46=cabs(.6574*amp(2,i)+1.2617*amp(3,i)+1.353*amp(4,i))**2*akrt
bmz48=cabs(.4922*amp(2,i)+1.1923*amp(3,i)+1.2343*amp(4,i))**2*akrt
bmz44sf=cabs(.7977*amp(2,i)+1.1286*amp(3,i)+1.2057*amp(4,i)
1 -0.428*sf(1,i)-0.9558*sf(3,i)-1.0939*sf(5,i)-0.6539*sf(7,i)
2 )**2*akrt
bmz46sf=cabs(.6574*amp(2,i)+1.2617*amp(3,i)+1.353*amp(4,i)
1 -0.2360*sf(1,i)-1.0630*sf(3,i)-1.379*sf(5,i)-0.5945*sf(7,i)
2 )**2*akrt
bmz48sf=cabs(.4922*amp(2,i)+1.1923*amp(3,i)+1.2343*amp(4,i)
1 -0.14*sf(1,i)-.9232*sf(3,i)-1.3692*sf(5,i)-0.4861*sf(7,i)

```

```

2 )**2*akrt
tia46=cabs(alof+1.4741*ahf)**2*akrt
bti46=cabs(amp(1,i)+.7973*amp(2,i)+1.311*amp(3,i)+
x 1.269*amp(4,i))**2*akrt
btia48=cabs(2.45*amp(1,i)+.2067*amp(2,i)+.3790*amp(3,i)+
x .3366*amp(4,i))**2*akrt
temc=ahf/alof
ph=atan(aimag(temc)/real(temc))*180./pi
phx=real(temc)/boa
boad=cabs(ahfd/alofd) ! start amps with dsf and delta correction
ca2d=alofd+ahfd
ca4d=alofd+ahfd/9.
ca6d=alofd-ahfd/15.
ca8d=alofd-ahfd/7.
aa2d=cabs(ca2d)**2*akrt
aa4d=6.*cabs(ca4d)**2*akrt
aa6d=15.*cabs(ca6d)**2*akrt
aa8d=28.*cabs(ca8d)**2*akrt
tig48d=cabs(1.5147*ahfd)**2*akrt
tia48d=cabs(2.4495*(alofd+.1675*ahfd))**2*akrt
sen48d=cabs(1.1638*ahfd)**2*akrt
sen44d=cabs(1.2571*ahfd)**2*akrt
sen46d=cabs(1.3771*ahfd)**2*akrt
bmz44d=cabs(.7977*ampd(2,i)+1.1286*ampd(3,i)+1.2057*
1 ampd(4,i))**2*akrt
bmz46d=cabs(.6574*ampd(2,i)+1.2617*ampd(3,i)+1.353*
1 ampd(4,i))**2*akrt
bmz48d=cabs(.4922*ampd(2,i)+1.1923*ampd(3,i)+1.2343*
1 ampd(4,i))**2*akrt
bmz44sfd=cabs(.7977*ampd(2,i)+1.1286*ampd(3,i)+1.2057*ampd(4,i)
1 -0.428*sf(1,i)-0.9558*sf(3,i)-1.0939*sf(5,i)-0.6539*sf(7,i)
2 )**2*akrt
bmz46sfd=cabs(.6574*ampd(2,i)+1.2617*ampd(3,i)+1.353*ampd(4,i)
1 -0.2360*sf(1,i)-1.0630*sf(3,i)-1.379*sf(5,i)-0.5945*sf(7,i)
2 )**2*akrt
bmz48sfd=cabs(.4922*ampd(2,i)+1.1923*ampd(3,i)+1.2343*ampd(4,i)
1 -0.14*sf(1,i)-.9232*sf(3,i)-1.3692*sf(5,i)-0.4861*sf(7,i)
2 )**2*akrt
tia46d=cabs(alofd+1.4741*ahfd)**2*akrt
bti46d=cabs(ampd(1,i)+.7973*ampd(2,i)+1.311*ampd(3,i)+
x 1.269*ampd(4,i))**2*akrt

```



```

btia48d=cabs(2.45*ampd(1,i)+.2067*ampd(2,i)+.3790*ampd(3,i)+
x .3366*ampd(4,i))**2*akrt
temc=ahfd/alofd
phd=atan(aimag(temc)/real(temc))*180./pi
phxd=real(temc)/boa
c print results with dsf and no delta correction
write (6,795) (i-1)*idel,aa2,aa4,aa6,tia46,aa8,tia48,sen44,
x sen46,sen48,tig48,phx,boa
c print results with dsf and delta correction
write (6,795) (i-1)*idel,aa2d,aa4d,aa6d,tia46d,aa8d,tia48d,sen44d,
x sen46d,sen48d,tig48d,phxd,boad
IF((i-1)*IDEL.eq.10)then
PRINT*,e,aa2,aa4,aa6,aa8
PRINT*,e,aa2d,aa4d,aa6d,aa8d
PRINT*,e,sen44,sen46,sen48
PRINT*,e,sen44d,sen46d,sen48d
else
end if
795 format(i4,10f6.3,f7.3,f6.3)
boa=cabs(ahi/alow) ! start amps without DSF and no delta correction
ca2=alow+ahi
ca4=alow+ahi/9.
ca6=alow-ahi/15.
ca8=alow-ahi/7.
akrt=akf/aki
aa2=cabs(ca2)**2*akrt
aa4=6.*cabs(ca4)**2*akrt
aa6=15.*cabs(ca6)**2*akrt
aa8=28.*cabs(ca8)**2*akrt
tig48=cabs(1.5147*ahi)**2*akrt
tia48=cabs(2.4495*(alow+.1675*ahi))**2*akrt
sen48=cabs(1.1638*ahi)**2*akrt
sen44=cabs(1.2571*ahi)**2*akrt
sen46=cabs(1.3771*ahi)**2*akrt
tia46=cabs(alow+1.4741*ahi)**2*akrt
temc=ahi/alow
ph=atan(aimag(temc)/real(temc))*180./pi
phx=real(temc)/boa
boad=cabs(ahid/alowd) ! start amps without DSF with delta correction
ca2d=alowd+ahid
ca4d=alowd+ahid/9.

```

```

ca6d=alowd-ahid/15.
ca8d=alowd-ahid/7.
aa2d=cabs(ca2d)**2*akrt
aa4d=6.*cabs(ca4d)**2*akrt
aa6d=15.*cabs(ca6d)**2*akrt
aa8d=28.*cabs(ca8d)**2*akrt
tig48d=cabs(1.5147*ahid)**2*akrt
tia48d=cabs(2.4495*(alowd+.1675*ahid))**2*akrt
sen48d=cabs(1.1638*ahid)**2*akrt
sen44d=cabs(1.2571*ahid)**2*akrt
sen46d=cabs(1.3771*ahid)**2*akrt
tia46d=cabs(alowd+1.4741*ahid)**2*akrt
temc=ahid/alowd
phxd=real(temc)/boad
c print results without DSF and no delta correction
write (6,795) (i-1)*idel,aa2,aa4,aa6,tia46,aa8,tia48,sen44,
x sen46,sen48,tig48 ,phx,boa
c print results without DSF with delta correction
write (6,795) (i-1)*idel,aa2d,aa4d,aa6d,tia46d,aa8d,tia48d,sen44d,
x sen46d,sen48d,tig48d,phxd,boad
c print bmz results with DSF with no delta correction
write (6,798) bmz44sf,bmz46sf,bmz48sf
c print bmz results with DSF with delta correction
write (6,798) bmz44sfd,bmz46sfd,bmz48sfd
798 format(40x,3f6.3)
c print bmz results without DSF no delta correction
write (6,797) bti46,btia48,bmz44,bmz46,bmz48
c print bmz results without DSF with delta correction
write (6,797) bti46d,btia48d,bmz44d,bmz46d,bmz48d
797 format(22x,f6.3,6x,4f6.3)
IF((i-1)*IDEL.eq.10)then
PRINT*,e,aa2,aa4,aa6,aa8
PRINT*,e,aa2d,aa4d,aa6d,aa8d
PRINT*,e,sen44,sen46,sen48
PRINT*,e,sen44d,sen46d,sen48d
PRINT*,e,bmz44sf,bmz46sf,bmz48sf
PRINT*,e,bmz44sfd,bmz46sfd,bmz48sfd
PRINT*,e,bti46,btia48,bmz44,bmz48
PRINT*,e,bti46d,btia48d,bmz44d,bmz48d
else
end if

```

794 continue

stop

490 format (7f10.4,i2)

500 format (8i5,f5.3)

510 format (3i5,4f10.4,2f5.1,5x,i2)

520 format (f5.1)

530 format (' wabs=',f9.3,' aki=',f7.4,' akf=',f7.4,' akcmi=',f7.4  
1 ,'akcmf=',f7.4)

570 format (3f10.5)

580 format (2i5,2f5.2)

590 format (a72)

600 format (i3,a72)

610 format (i3,8f7.4)

620 format (' chg density from sick and mccarthy for a=',f3.0)

630 format (' z=',f4.0,' a=',f4.0,'as=',f5.2,  
1 ' ap=',f5.2,' pcm=',f7.3)

640 format (' e lab=',f5.1,' charge ',f3.0,'alpha ',f5.0)

671 format (' n=',i3,' to ',f6.2,' fm')

660 format (' l s-matrix coul s ST SR  
1 SA')

680 format (2e15.5)

690 format (i5,3f10.5)

700 format (f7.3,2e11.4,4e11.4)

710 format (i3,6f8.3,4f10.4,F9.3,F9.3,F9.3)

end

C\*\*\*\*\*

C PILOT NEW . FOR

SUBROUTINE PILOT (ALPHA,DR,IL,NR,AK)

IMPLICIT REAL \*4 (A-H,O-Z)

COMPLEX\*8 CI

COMPLEX\*16 CJ,CH,CJR,CHR

COMMON /VEES/ VS(160,160), VP(160,160)

DIMENSION RV(160),B1(160),B2(160),B3(160)

REAL \*8 A1,A2,A3,B1,B2,B3

DIMENSION A1(160),A2(160),A3(160),PHI(160,160),PHIR(160,160)

1 ,PHI2(160,160),VTEM(160,160)

DIMENSION CH(30), CJ(30),CJR(160),CHR(160)

DR2=DR\*\*2

ALPH2=ALPHA\*\*2

CONAL=(ALPH2+AK\*AK)/ALPHA

CLL=IL\*(IL-1)

```

DO 20 IR=1,NR
20 RV(IR)=DR*IR
DO 30 IR=1,NR
Z=ALPHA*RV(IR)
Y=EXP(Z)
CALL CJH (Z,Y,CJ,CH,IL)
CJR(IR)=CJ(IL)
CHR(IR)=CH(IL)
30 CONTINUE
TEST=1.E-10
DO 31 IR=1,NR
DO 31 JR=IR,NR
PHI(IR,JR)=CJR(IR)*CHR(JR)*CONAL
IF (ABS(PHI(IR,JR)).LT.TEST) PHI(IR,JR)=0.
PHI(JR,IR)=PHI(IR,JR)
31 CONTINUE
C DO 32 IR=1,NR,10
C 32 WRITE (11,33) RV(IR),(PHI(IR,JR),JR=IR,IR+7)
C 33 FORMAT(F6.2,1P10E9.2)
DO 42 IR=1,NR
TEM=RHO(RV(IR))
TEM2=RHOPP(RV(IR))
DO 42 JR=1,NR
PHI2(IR,JR)=TEM2*PHI(IR,JR)
42 PHIR(IR,JR)=TEM*PHI(IR,JR)
CALL SMM(PHI,PHIR,VS,NR,160)
CALL SMM(PHI,PHI2,VP,NR,160)
C DO 34 IR=1,NR
C DO 34 JR=IR,NR
c VS(IR,JR)=0.
C VP(IR,JR)=0.
C DO 35 K=1,NR
C VS(IR,JR)=VS(IR,JR)+PHI(IR,K)*PHIR(K,JR)
C VP(IR,JR)=VP(IR,JR)+PHI(IR,K)*PHI2(K,JR)
C 35 CONTINUE
C 34 CONTINUE
C CORRECT THE DIAGONAL ELEMENTS
DO 51 K=2,NR-2 ! correct above the diagonal
VS(K,K)=VS(K,K)-PHI(K,K)*PHIR(K,K)*.3333333333
1 +PHI(K,K+1)*PHIR(K+1,K)*.25
2 -PHI(K,K+2)*PHIR(K+2,K)*.0833333333

```

```

VP(K,K)=VP(K,K)-PHI(K,K)*PHI2(K,K)*.333333333
1 +PHI(K,K+1)*PHI2(K+1,K)*.25
2 -PHI(K,K+2)*PHI2(K+2,K)*.0833333333
51 CONTINUE
DO 510 K=4,NR ! correct below the diagonal
VS(K,K)=VS(K,K)+PHI(K,K-1)*PHIR(K-1,K)*.25
1 -PHI(K,K-2)*PHIR(K-2,K)*.0833333333
2 +PHI(K,1)*PHIR(1,K)*.0833333333
VP(K,K)=VP(K,K)+PHI(K,K-1)*PHI2(K-1,K)*.25
1 -PHI(K,K-2)*PHI2(K-2,K)*.0833333333
2 +PHI(K,1)*PHI2(1,K)*.0833333333
510 CONTINUE
VS(3,3)=VS(3,3)+PHI(3,2)*PHIR(2,3)*.25
VP(3,3)=VP(3,3)+PHI(3,2)*PHI2(2,3)*.25
VS(2,2)=VS(2,2)+PHI(2,1)*PHIR(1,2)*.333333333
VP(2,2)=VP(2,2)+PHI(2,1)*PHI2(1,2)*.333333333
VS(1,1)=VS(1,1)-PHI(1,1)*PHIR(1,1)*.166666666
1 +PHI(1,2)*PHIR(2,1)*.25-PHI(1,3)*PHIR(3,1)*.08333333
VP(1,1)=VP(1,1)-PHI(1,1)*PHI2(1,1)*.166666666
1 +PHI(1,2)*PHI2(2,1)*.25-PHI(1,3)*PHI2(3,1)*.08333333
C CORRECT I,I+1
DO 77 K=3,NR-3
VS(K,K+1)=VS(K,K+1)-(PHI(K,K)*PHIR(K,K)
1 +PHI(K,K+1)*PHIR(K+1,K))* .16666666
2 +(PHI(K,K-1)*PHIR(K-1,K)+PHI(K,K+2)*PHIR(K+2,K))* .25
3 -(PHI(K,K-2)*PHIR(K-2,K)+PHI(K,K+3)*PHIR(K+3,K))* .0833333
VP(K,K+1)=VP(K,K+1)-(PHI(K,K)*PHI2(K,K)
1 +PHI(K,K+1)*PHI2(K+1,K))* .16666666
2 +(PHI(K,K-1)*PHIR(K-1,K)+PHI(K,K+2)*PHI2(K+2,K))* .25
3 -(PHI(K,K-2)*PHIR(K-2,K)+PHI(K,K+3)*PHI2(K+3,K))* .0833333
77 CONTINUE
VS(2,3)=VS(2,3)+PHI(2,1)*PHIR(1,3)*.33333333
1 -(PHI(2,2)*PHIR(2,3)+PHI(2,3)*PHIR(3,3))* .1666666
2 +PHI(2,4)*PHIR(4,3)*.25
3 -PHI(2,5)*PHIR(5,2)*.083333333
VP(2,3)=VP(2,3)+PHI(2,1)*PHI2(1,3)*.33333333
1 -(PHI(2,2)*PHI2(2,3)+PHI(2,3)*PHI2(3,3))* .1666666
2 +PHI(2,4)*PHI2(4,3)*.25
3 -PHI(2,5)*PHI2(5,2)*.083333333
VS(1,2)=VS(1,2)-PHI(1,2)*PHIR(2,2)*.16666666
1 +PHI(1,3)*PHIR(3,2)*.25

```

```

2 -PHI(1,4)*PHIR(4,2)*.083333333
VP(1,2)=VP(1,2)-PHI(1,2)*PHI2(2,2)*.1666666
1 +PHI(1,3)*PHI2(3,2)*.25
2 -PHI(1,4)*PHI2(4,2)*.083333333
C CORRECT ELEMENTS I,I+2
DO 78 K=3,NR-4
VS(K,K+2)=VS(K,K+2)-(PHI(K,K)*PHIR(K,K+2)
1 +PHI(K,K+2)*PHIR(K+2,K+2))* .3333333
2 +PHI(K,K+1)*PHIR(K+1,K+2)*.333333
3 +(PHI(K,K-1)*PHIR(K-1,K+2)+PHI(K,K+3)*PHIR(K+3,K+2))* .25
4 -(PHI(K,K-2)*PHIR(K-2,K+2)+PHI(K,K+4)*PHIR(K+4,K+2))* .0833333
VP(K,K+2)=VP(K,K+2)-(PHI(K,K)*PHI2(K,K+2)
1 +PHI(K,K+2)*PHI2(K+2,K+2))* .3333333
2 +PHI(K,K+1)*PHI2(K+1,K+2)*.333333
3 +(PHI(K,K-1)*PHI2(K-1,K+2)+PHI(K,K+3)*PHI2(K+3,K+2))* .25
4 -(PHI(K,K-2)*PHI2(K-2,K+2)+PHI(K,K+4)*PHI2(K+4,K+2))* .0833333
78 CONTINUE
VS(2,4)=VS(2,4)+(PHI(2,1)*PHIR(1,4)+PHI(2,3)*PHIR(3,4))* .333333
1 -(PHI(2,2)*PHIR(2,4)+PHI(2,4)*PHIR(4,4))* .333333
2 +PHI(2,5)*PHIR(5,4)*.25-PHI(2,6)*PHIR(6,4)*.0833333
VP(2,4)=VP(2,4)+(PHI(2,1)*PHI2(1,4)+PHI(2,3)*PHI2(3,4))* .333333
1 -(PHI(2,2)*PHI2(2,4)+PHI(2,4)*PHI2(4,4))* .333333
2 +PHI(2,5)*PHI2(5,4)*.25-PHI(2,6)*PHI2(6,4)*.0833333
VS(1,3)=VS(1,3)-PHI(1,1)*PHIR(1,3)*.166666
1 +(PHI(1,2)*PHIR(2,3)-PHI(1,3)*PHIR(3,3))* .333333
2 +PHI(1,4)*PHIR(4,3)*.25-PHI(1,5)*PHIR(5,3)*.0833333
VP(1,3)=VP(1,3)-PHI(1,1)*PHI2(1,3)*.166666
1 +(PHI(1,2)*PHI2(2,3)-PHI(1,3)*PHI2(3,3))* .333333
2 +PHI(1,4)*PHI2(4,3)*.25-PHI(1,5)*PHI2(5,3)*.0833333
C CORRECT I,I+3
DO 79 K=3,NR-5
VS(K,K+3)=VS(K,K+3)-(PHI(K,K-2)*PHIR(K-2,K+3)
1 +PHI(K,K+5)*PHIR(K+5,K+3))* .0833333
2 +(PHI(K,K-1)*PHIR(K-1,K+3)+PHI(K,K+4)*PHIR(K+4,K+3))* .25
3 -(PHI(K,K)*PHIR(K,K+3)+PHI(K,K+3)*PHIR(K+3,K+3))* .29166666
4 +(PHI(K,K+1)*PHIR(K+1,K+3)+PHI(K,K+2)*PHIR(K+2,K+3))* .125
VP(K,K+3)=VP(K,K+3)-(PHI(K,K-2)*PHI2(K-2,K+3)
1 +PHI(K,K+5)*PHI2(K+5,K+3))* .0833333
2 +(PHI(K,K-1)*PHI2(K-1,K+3)+PHI(K,K+4)*PHI2(K+4,K+3))* .25
3 -(PHI(K,K)*PHI2(K,K+3)+PHI(K,K+3)*PHI2(K+3,K+3))* .29166666
4 +(PHI(K,K+1)*PHI2(K+1,K+3)+PHI(K,K+2)*PHI2(K+2,K+3))* .125

```

79 CONTINUE

C CORRECT I,I+4

DO 81 K=3, NR-6

VS(K,K+4)=VS(K,K+4)-(PHI(K,K-2)\*PHIR(K-2,K+4)

1 +PHI(K,K+6)\*PHIR(K+6,K+4))\* .08333333

2 +(PHI(K,K-1)\*PHIR(K-1,K+4)+PHI(K,K+5)\*PHIR(K+5,K+4))\* .25

3 -(PHI(K,K)\*PHIR(K,K+4)+PHI(K,K+2)\*PHIR(K+2,K+4)

4 +PHI(K,K+4)\*PHIR(K+4,K+4))\* .33333333

5

+(PHI(K,K+1)\*PHIR(K+1,K+4)+PHI(K,K+3)\*PHIR(K+3,K+4))\* .33333333

VP(K,K+4)=VP(K,K+4)-(PHI(K,K-2)\*PHI2(K-2,K+4)

1 +PHI(K,K+6)\*PHI2(K+6,K+4))\* .08333333

2 +(PHI(K,K-1)\*PHI2(K-1,K+4)+PHI(K,K+5)\*PHI2(K+5,K+4))\* .25

3 -(PHI(K,K)\*PHI2(K,K+4)+PHI(K,K+2)\*PHI2(K+2,K+4)

4 +PHI(K,K+4)\*PHI2(K+4,K+4))\* .33333333

5

+(PHI(K,K+1)\*PHI2(K+1,K+4)+PHI(K,K+3)\*PHI2(K+3,K+4))\* .33333333

81 CONTINUE

DO 9995 IR=1, NR-1

9995 VS(IR+1,IR)=VS(IR,IR+1)

CONCON=1./DR\*\*2

DO 1117 IR=2, NR-1

DO 1117 JR=2, NR-1

VP(IR,JR)=VP(IR,JR)+CLL\*VS(IR,JR)/RV(IR)\*\*2

1 +CLL\*VS(IR,JR)/RV(JR)\*\*2

1 -(VS(IR,JR-1)-2.\*VS(IR,JR)+VS(IR,JR+1))\*CONCON

1 -(VS(IR-1,JR)-2.\*VS(IR,JR)+VS(IR+1,JR))\*CONCON

1117 CONTINUE

DO 1118 IR=2, NR-1

VP(1,IR)=VP(1,IR)+CLL\*VS(1,IR)/RV(1)\*\*2

1 +CLL\*VS(1,IR)/RV(IR)\*\*2

1 -(-2.\*VS(1,IR)+VS(2,IR))\*CONCON

1 -(VS(1,IR-1)-2.\*VS(1,IR)+VS(1,IR+1))\*CONCON

VP(IR,1)=VP(IR,1)+CLL\*VS(IR,1)/RV(IR)\*\*2

1 +CLL\*VS(IR,1)/RV(1)\*\*2

1 -(-2.\*VS(IR,1)+VS(IR,2))\*CONCON

1 -(VS(IR-1,1)-2.\*VS(IR,1)+VS(IR+1,1))\*CONCON

1118 CONTINUE

VP(1,1)=VP(1,1)+2.\*CLL\*VS(1,1)/RV(1)\*\*2

1 -(-2.\*VS(1,1)+VS(2,1))\*CONCON

1 -(-2.\*VS(1,1)+VS(1,2))\*CONCON

```

DO 697 IR=1,NR
DO 697 JR=IR,NR
VP(IR,JR)=-VP(IR,JR)*.5*DR2
697 VP(JR,IR)=VP(IR,JR)
DO 45 IR=1,NR
DO 45 JR=IR,NR
VS(IR,JR)=VS(IR,JR)*DR2
VS(JR,IR)=VS(IR,JR)
45 CONTINUE
C DO 36 IR=1,31,10
C 36 WRITE (11,37) (VS(IR,JR),JR=IR,IR+5)
C 37 FORMAT(2P10F9.4)
C DO 698 IR=1,31,10
C 698 WRITE (11,37) (VP(IR,JR),JR=IR,IR+5)
RETURN
END
SUBROUTINE VCAL (ALPHA,DR,N,LP)
IMPLICIT REAL *4 (A-H,O-Z)
COMMON /VEES/ VS(160,160), VP(160,160)
COMMON /ATGT/ ATGT, PI, ZMULT, ANMULT, FACT
COMMON /VT/ VT, AK, DW, RZ
COMPLEX*8 VT(160,160)
COMMON /OPT/ CB0,CB1
COMPLEX*8 CB0,CB1
FAC=AK**2
FPI=1/(4.*PI)
CALL PIPOT (ALPHA,DR,LP,N,AK)
TEST=.0000000001
DO 5577 I=1,N
DO 5577 J=1,N
IF (ABS(VS(I,J)).LT.TEST) VS(I,J)=0.
IF (ABS(VP(I,J)).LT.TEST) VP(I,J)=0.
5577 CONTINUE
DO 10 I=1,N
R=DR*I
DO 10 J=1,N
VT(I,J)=-FPI*(-CB0*VS(I,J)*FAC+CB1*VP(I,J))
10 CONTINUE
RETURN
END
FUNCTION ST(F,S,C,N)

```



```
IMPLICIT REAL *4 (A-H,O-Z)
DIMENSION F(501)
SN=S
CN=C
CON=SN*F(2)
DO 1 I=3,N
CT=CN
CN=CN*C-SN*S
SN=CT*S+SN*C
1 CON=CON+SN*F(I)
ST=CON
RETURN
END
end
```

APPENDIX C  
SAMPLE OUTPUT RESULTS OF CALCIUM CODE

```

idel,imax= 5 37 iat(=1 for angle xf)= lipi0 (=1 for pi0 distorts)= 1
20.0000 40.0000 0.0000 3.0000 4.0000 300.0000 0.0000 1
0 0 0 0 0 0
120 0 14 8.0000 60.0000 1.0000 3.0000
using siegel-gibbs amplitudes
pion lab momen= 142.66 exitat energy= 0.00 tlab= 60.00
initial kcm= 141.91 final kcm= 141.91 141.91
li= 141.9074 lf= 141.9052 cmi= 118.5882 cmf= 118.5865
cpl0= -0.22009 -0.01376 cpl1= 0.79065 0.13028 cplf= 0.46729 0.06262
cz0= -0.21841 -0.01401 cz1= 0.76958 0.11232 czf= 0.45783 0.05259
L= 3 EB= 11.4660 RMS= 3.8337 VV= 54.50
C= 4.4826 SA= 0.5000 A= 41.0 Z= 0.0
L= 3 EB= 3.8211 RMS= 3.9177 VV= 54.50
C= 4.4826 SA= 0.5000 A= 41.0 Z= 21.0
transition density normalization 0.99978
transition density normalization 0.99975
norm of revised density 0.9998
rrmax 0.00 nnmax 0
c:00,01,10,11 0.0686 0.0087 -0.1678 -0.0353 -0.1709 -0.0395 0.4147 0.1320
using l dependent optical model strengths
4 0 1.00 1.00
wabs= 29.927 aki= 0.7191 akf= 0.7191 akcmi= 0.6009akcmf= 0.6009
q= 1 z= 20 n= 20 a= 40 paul 1
20 tlab 60.0 r 6.6 rms 4.2
-2-0.2140-0.0030 0.2880 0.0380 0.000060.0000 0.0030 0.3200
-1-1.4520 0.6070
0-1.7010 0.2680 5.2500 0.5330
1-1.7960 0.2520 5.4990 0.5320
2-1.7370 0.2920 5.5730 0.6020
3-1.4920 0.4340 5.6620 0.5910
4-1.2620 0.4330 6.6870 0.8310
5-0.9730 0.4410 6.8090 0.6920
6-0.7170 0.3510 7.0460 0.6390
7-0.5120 0.2780 6.6660 0.3890
8-0.5120 0.2780 6.6660 0.3890
9-0.5120 0.2780 6.6660 0.3890
10-0.5120 0.2780 6.6660 0.3890
11-0.5120 0.2780 6.6660 0.3890
12-0.5120 0.2780 6.6660 0.3890
13-0.5120 0.2780 6.6660 0.3890
z= 20. a= 40.as= 3.00 ap= 4.00 pcm= 0.719

```

chg density from sick and mccarthy for a=40.  
 e lab= 60.0 charge 1.alpha 300.  
 n=120 to 8.00 fm  
 k 0.71911 eta 0.20471  
*l s - matrix couls ST SR SA*  
 0 -0.208 0.146 0.974 -0.228 146.811 56.818 29.4024  
 1 0.275 0.378 0.985 0.173 264.412 142.404 71.6853  
 2 0.356 0.647 0.929 0.369 391.259 138.137 46.3714  
 3 0.654 0.657 0.871 0.492 294.154 59.852 11.5095  
 4 0.765 0.622 0.816 0.578 256.886 15.044 1.3342  
 5 0.759 0.649 0.766 0.643 322.322 1.741 0.0952  
 6 0.719 0.694 0.720 0.694 443.311 0.175 0.0058  
 7 0.678 0.735 0.678 0.735 586.366 0.011 0.0003  
 8 0.640 0.768 0.640 0.768 743.880 0.000 0.0000  
 9 0.604 0.797 0.604 0.797 913.578 0.000 0.0000  
 10 0.571 0.821 0.571 0.821 1094.237 0.001 0.0000  
 11 0.540 0.842 0.540 0.842 1284.906 0.001 0.0000  
 12 0.511 0.859 0.511 0.859 1484.778 -0.001 0.0000  
 13 0.484 0.875 0.484 0.875 1693.171 0.001 0.0000  
 sigt 9920.0703 sigr 414.1851 SIGAB 160.4040  
 k 0.71908 eta -0.20472  
*l s - matrix couls ST SR SA*  
 0 -0.176 0.527 0.974 0.228 142.924 41.992 18.9014  
 1 0.166 0.375 0.985 -0.173 304.065 151.652 75.2704  
 2 0.542 0.355 0.929 -0.369 278.429 176.368 66.0039  
 3 0.866 -0.040 0.871 -0.492 114.403 106.022 23.7092  
 4 0.858 -0.455 0.816 -0.578 155.255 31.078 3.2427  
 5 0.776 -0.627 0.766 -0.643 299.983 3.707 0.2359  
 6 0.721 -0.692 0.720 -0.694 440.028 0.387 0.0145  
 7 0.678 -0.735 0.678 -0.735 586.095 0.025 0.0007  
 8 0.640 -0.768 0.640 -0.769 743.952 0.001 0.0000  
 9 0.604 -0.797 0.604 -0.797 913.704 0.001 0.0000  
 10 0.571 -0.821 0.571 -0.821 1094.392 0.001 0.0000  
 11 0.540 -0.842 0.540 -0.842 1285.087 0.000 0.0000  
 12 0.511 -0.859 0.511 -0.859 1484.990 0.000 0.0000  
 13 0.484 -0.875 0.484 -0.875 1693.407 -0.001 0.0000  
 sigt 9536.7158 sigr 511.2329 SIGAB 187.3788  
*a b asf bsf A2 B2 ASF2 BSF2*  
*alpha beta al2 be2*  
 0 -0.34 0.27 -0.23 0.33 -0.46 0.72 0.11 0.51 amps  
 0 -0.46 -0.13 -0.37 -0.11 -0.57 0.37 0.04 0.30 amps

0 -0.336 0.266 -0.585 1.559 -0.422 0.022 -0.843 0.824 0.18 2.77 0.18 1.39  
 0 -0.458 -0.135 -0.900 0.555 -0.543 -0.380 -1.157 -0.179 0.23 1.12 0.44 1.37  
 -0.141 -0.253 -1.124 1.099 0.08 2.47  
 5 -0.34 0.26 -0.23 0.33 -0.45 0.71 0.10 0.50 amps  
 5 -0.45 -0.14 -0.37 -0.11 -0.56 0.37 0.04 0.29 amps  
 5 -0.335 0.259 -0.582 1.537 -0.419 0.019 -0.833 0.816 0.18 2.70 0.18 1.36  
 5 -0.454 -0.137 -0.888 0.546 -0.537 -0.377 -1.139 -0.175 0.22 1.09 0.43 1.33  
 -0.141 -0.253 -1.110 1.088 0.08 2.42  
 10 -0.33 0.24 -0.23 0.31 -0.44 0.68 0.10 0.47 amps  
 10 -0.44 -0.14 -0.36 -0.11 -0.53 0.35 0.04 0.28 amps  
 10 -0.334 0.237 -0.573 1.471 -0.411 0.010 -0.803 0.790 0.17 2.49 0.17 1.27  
 10 -0.442 -0.144 -0.853 0.519 -0.519 -0.370 -1.083 -0.162 0.22 1.00 0.41 1.20  
 -0.143 -0.253 -1.071 1.054 0.08 2.26  
 15 -0.33 0.20 -0.24 0.29 -0.41 0.64 0.09 0.44 amps  
 15 -0.42 -0.15 -0.34 -0.11 -0.49 0.33 0.04 0.25 amps  
 15 -0.331 0.203 -0.558 1.366 -0.397 -0.003 -0.756 0.749 0.15 2.18 0.16 1.13  
 15 -0.423 -0.154 -0.797 0.475 -0.489 -0.359 -0.994 -0.142 0.20 0.86 0.37 1.01  
 -0.145 -0.252 -1.007 0.999 0.08 2.01  
 20 -0.33 0.16 -0.24 0.26 -0.38 0.59 0.07 0.39 amps  
 20 -0.40 -0.17 -0.32 -0.11 -0.44 0.31 0.04 0.22 amps  
 20 -0.326 0.159 -0.536 1.228 -0.378 -0.019 -0.692 0.694 0.13 1.79 0.14 0.96  
 20 -0.397 -0.166 -0.721 0.418 -0.449 -0.344 -0.878 -0.116 0.19 0.70 0.32 0.78  
 -0.147 -0.251 -0.923 0.925 0.08 1.71  
 25 -0.32 0.11 -0.23 0.22 -0.33 0.52 0.06 0.33 amps  
 25 -0.37 -0.18 -0.29 -0.10 -0.38 0.27 0.03 0.18 amps  
 25 -0.318 0.107 -0.507 1.064 -0.355 -0.038 -0.616 0.627 0.11 1.39 0.13 0.77  
 25 -0.366 -0.179 -0.631 0.351 -0.403 -0.324 -0.741 -0.086 0.17 0.52 0.27 0.56  
 -0.149 -0.247 -0.822 0.837 0.08 1.38  
 30 -0.31 0.05 -0.23 0.18 -0.28 0.45 0.04 0.26 amps  
 30 -0.33 -0.19 -0.26 -0.10 -0.31 0.24 0.03 0.14 amps  
 30 -0.307 0.053 -0.469 0.883 -0.327 -0.057 -0.531 0.552 0.10 1.00 0.11 0.59  
 30 -0.330 -0.191 -0.530 0.277 -0.351 -0.301 -0.592 -0.054 0.15 0.36 0.21 0.35  
 -0.150 -0.241 -0.708 0.736 0.08 1.04  
 35 -0.29 0.00 -0.22 0.13 -0.23 0.37 0.03 0.19 amps  
 35 -0.29 -0.20 -0.22 -0.09 -0.23 0.20 0.03 0.09 amps  
 35 -0.292 -0.001 -0.424 0.696 -0.297 -0.075 -0.440 0.472 0.09 0.66 0.09 0.42  
 35 -0.291 -0.200 -0.423 0.202 -0.296 -0.275 -0.439 -0.023 0.12 0.22 0.16 0.19  
 -0.150 -0.233 -0.587 0.629 0.08 0.74  
 40 -0.27 -0.05 -0.21 0.10 -0.17 0.29 0.01 0.13 amps  
 40 -0.25 -0.21 -0.18 -0.08 -0.15 0.16 0.02 0.05 amps  
 40 -0.273 -0.051 -0.372 0.510 -0.265 -0.091 -0.347 0.388 0.08 0.40 0.08 0.27

40 -0.250 -0.206 -0.315 0.128 -0.242 -0.246 -0.290 0.006 0.10 0.12 0.12 0.08  
 -0.149 -0.220 -0.463 0.518 0.07 0.48  
 45 -0.25 -0.09 -0.19 0.06 -0.12 0.21 0.00 0.06 amps  
 45 -0.21 -0.21 -0.15 -0.06 -0.08 0.11 0.02 0.01 amps  
 45 -0.250 -0.093 -0.314 0.334 -0.231 -0.103 -0.256 0.306 0.07 0.21 0.06 0.16  
 45 -0.209 -0.206 -0.209 0.059 -0.190 -0.215 -0.152 0.031 0.09 0.05 0.08 0.02  
 -0.146 -0.205 -0.342 0.408 0.06 0.28  
 50 -0.22 -0.13 -0.18 0.03 -0.06 0.14 -0.01 0.01 amps  
 50 -0.17 -0.20 -0.11 -0.05 -0.01 0.07 0.02 -0.03 amps  
 50 -0.225 -0.127 -0.251 0.176 -0.198 -0.110 -0.170 0.228 0.07 0.09 0.05 0.08  
 50 -0.169 -0.201 -0.110 -0.002 -0.142 -0.183 -0.030 0.050 0.07 0.01 0.05 0.00  
 -0.141 -0.185 -0.227 0.304 0.05 0.14  
 55 -0.20 -0.15 -0.15 0.01 -0.01 0.07 -0.02 -0.04 amps  
 55 -0.13 -0.19 -0.08 -0.03 0.05 0.04 0.01 -0.05 amps  
 55 -0.197 -0.150 -0.184 0.040 -0.165 -0.111 -0.091 0.155 0.06 0.04 0.04 0.03  
 55 -0.132 -0.189 -0.021 -0.052 -0.101 -0.151 0.072 0.063 0.05 0.00 0.03 0.01  
 -0.135 -0.163 -0.121 0.207 0.04 0.06  
 60 -0.17 -0.16 -0.13 -0.01 0.04 0.01 -0.03 -0.07 amps  
 60 -0.10 -0.17 -0.05 -0.02 0.10 0.00 0.01 -0.08 amps  
 60 -0.168 -0.161 -0.117 -0.070 -0.135 -0.108 -0.021 0.091 0.05 0.02 0.03 0.01  
 60 -0.099 -0.172 0.055 -0.091 -0.067 -0.119 0.151 0.070 0.04 0.01 0.02 0.03  
 -0.128 -0.138 -0.028 0.122 0.04 0.02  
 65 -0.14 -0.16 -0.10 -0.01 0.08 -0.04 -0.03 -0.10 amps  
 65 -0.07 -0.15 -0.02 0.00 0.14 -0.03 0.00 -0.09 amps  
 65 -0.139 -0.162 -0.052 -0.152 -0.109 -0.099 0.038 0.037 0.05 0.03 0.02 0.00  
 65 -0.071 -0.151 0.118 -0.118 -0.041 -0.088 0.208 0.070 0.03 0.03 0.01 0.05  
 -0.122 -0.111 0.051 0.049 0.03 0.00  
 70 -0.11 -0.15 -0.07 -0.01 0.11 -0.08 -0.03 -0.11 amps  
 70 -0.05 -0.13 0.00 0.02 0.16 -0.05 0.00 -0.10 amps  
 70 -0.112 -0.153 0.009 -0.206 -0.086 -0.087 0.086 -0.007 0.04 0.04 0.01 0.01  
 70 -0.049 -0.126 0.165 -0.134 -0.024 -0.060 0.242 0.065 0.02 0.05 0.00 0.06  
 -0.115 -0.084 0.115 -0.010 0.02 0.01  
 75 -0.09 -0.14 -0.04 -0.01 0.13 -0.11 -0.03 -0.12 amps  
 75 -0.03 -0.10 0.02 0.03 0.18 -0.07 0.00 -0.10 amps  
 75 -0.087 -0.137 0.064 -0.235 -0.068 -0.072 0.123 -0.041 0.03 0.06 0.01 0.02  
 75 -0.033 -0.100 0.198 -0.139 -0.014 -0.035 0.257 0.055 0.01 0.06 0.00 0.07  
 -0.109 -0.058 0.164 -0.054 0.02 0.03  
 80 -0.07 -0.11 -0.01 0.00 0.15 -0.12 -0.02 -0.12 amps  
 80 -0.02 -0.07 0.03 0.05 0.18 -0.09 0.00 -0.09 amps  
 80 -0.067 -0.115 0.111 -0.242 -0.054 -0.056 0.148 -0.064 0.02 0.07 0.01 0.03  
 80 -0.023 -0.074 0.217 -0.136 -0.011 -0.014 0.255 0.042 0.01 0.07 0.00 0.07

-0.104 -0.034 0.198 -0.085 0.01 0.05  
85 -0.05 -0.09 0.01 0.01 0.15 -0.13 -0.02 -0.11 amps  
85 -0.02 -0.05 0.05 0.06 0.18 -0.10 0.00 -0.09 amps  
85 -0.051 -0.090 0.148 -0.230 -0.045 -0.039 0.164 -0.078 0.01 0.07 0.00 0.03  
85 -0.019 -0.049 0.224 -0.125 -0.014 0.002 0.240 0.027 0.00 0.07 0.00 0.06  
-0.100 -0.014 0.218 -0.103 0.01 0.06  
90 -0.04 -0.07 0.03 0.03 0.15 -0.14 -0.01 -0.09 amps  
90 -0.02 -0.03 0.05 0.07 0.17 -0.10 0.00 -0.07 amps  
90 -0.039 -0.065 0.174 -0.203 -0.041 -0.025 0.170 -0.083 0.01 0.07 0.00 0.04  
90 -0.020 -0.028 0.219 -0.110 -0.021 0.012 0.215 0.010 0.00 0.06 0.00 0.05  
-0.097 0.003 0.226 -0.111 0.01 0.06  
95 -0.03 -0.04 0.05 0.04 0.14 -0.13 0.00 -0.08 amps  
95 -0.02 -0.01 0.06 0.07 0.15 -0.11 0.00 -0.06 amps  
95 -0.032 -0.042 0.190 -0.167 -0.039 -0.013 0.168 -0.082 0.00 0.06 0.00 0.03  
95 -0.024 -0.012 0.205 -0.092 -0.031 0.017 0.184 -0.006 0.00 0.05 0.00 0.03  
-0.095 0.014 0.224 -0.109 0.01 0.06  
100 -0.03 -0.02 0.07 0.05 0.13 -0.12 0.00 -0.06 amps  
100 -0.03 0.00 0.06 0.08 0.12 -0.10 0.00 -0.05 amps  
100 -0.028 -0.023 0.194 -0.126 -0.040 -0.006 0.159 -0.075 0.00 0.05 0.00 0.03  
100 -0.030 -0.001 0.185 -0.073 -0.042 0.016 0.149 -0.022 0.00 0.04 0.00 0.02  
-0.093 0.019 0.212 -0.100 0.01 0.05  
105 -0.03 -0.01 0.08 0.06 0.11 -0.11 0.01 -0.04 amps  
105 -0.04 0.00 0.06 0.08 0.09 -0.10 0.00 -0.03 amps  
105 -0.028 -0.009 0.189 -0.084 -0.043 -0.003 0.144 -0.065 0.00 0.04 0.00 0.03  
105 -0.038 0.003 0.159 -0.055 -0.053 0.009 0.114 -0.036 0.00 0.03 0.00 0.01  
-0.091 0.019 0.192 -0.087 0.01 0.04  
110 -0.03 0.00 0.08 0.07 0.08 -0.10 0.01 -0.02 amps  
110 -0.05 0.00 0.06 0.07 0.07 -0.09 0.00 -0.02 amps  
110 -0.029 -0.002 0.175 -0.044 -0.046 -0.005 0.125 -0.054 0.00 0.03 0.00 0.02  
110 -0.045 0.000 0.130 -0.039 -0.062 -0.003 0.081 -0.048 0.00 0.02 0.00 0.01  
-0.088 0.013 0.167 -0.071 0.01 0.03  
115 -0.03 0.00 0.08 0.08 0.05 -0.08 0.01 -0.01 amps  
115 -0.05 -0.01 0.06 0.07 0.04 -0.09 0.00 -0.01 amps  
115 -0.032 -0.002 0.153 -0.009 -0.049 -0.013 0.103 -0.041 0.00 0.02 0.00 0.01  
115 -0.051 -0.009 0.100 -0.026 -0.068 -0.020 0.050 -0.058 0.00 0.01 0.00 0.01  
-0.083 0.001 0.138 -0.055 0.01 0.02  
120 -0.03 -0.01 0.08 0.08 0.03 -0.06 0.01 0.01 amps  
120 -0.06 -0.02 0.06 0.06 0.01 -0.08 0.00 0.00 amps  
120 -0.034 -0.009 0.126 0.019 -0.050 -0.025 0.079 -0.030 0.00 0.02 0.00 0.01  
120 -0.055 -0.024 0.070 -0.018 -0.071 -0.040 0.023 -0.066 0.00 0.01 0.01 0.00  
-0.076 -0.015 0.106 -0.040 0.01 0.01

125 -0.04 -0.02 0.08 0.07 0.00 -0.05 0.01 0.02 amps  
125 -0.06 -0.04 0.06 0.05 -0.02 -0.07 0.00 0.01 amps  
125 -0.036 -0.022 0.094 0.039 -0.050 -0.042 0.054 -0.020 0.00 0.01 0.00 0.00  
125 -0.056 -0.044 0.041 -0.014 -0.069 -0.063 0.001 -0.073 0.01 0.00 0.01 0.01  
-0.068 -0.035 0.072 -0.026 0.01 0.01  
130 -0.04 -0.04 0.07 0.06 -0.02 -0.04 0.01 0.03 amps  
130 -0.05 -0.07 0.05 0.03 -0.04 -0.06 0.00 0.01 amps  
130 -0.036 -0.041 0.061 0.051 -0.047 -0.062 0.029 -0.012 0.00 0.01 0.01 0.00  
130 -0.053 -0.068 0.014 -0.014 -0.064 -0.089 -0.018 -0.077 0.01 0.00 0.01 0.01  
-0.056 -0.058 0.038 -0.016 0.01 0.00  
135 -0.03 -0.06 0.07 0.05 -0.04 -0.03 0.00 0.03 amps  
135 -0.05 -0.09 0.05 0.02 -0.06 -0.05 0.00 0.02 amps  
135 -0.034 -0.064 0.027 0.055 -0.042 -0.084 0.004 -0.007 0.01 0.00 0.01 0.00  
135 -0.048 -0.094 -0.010 -0.018 -0.055 -0.115 -0.032 -0.080 0.01 0.00 0.02 0.01  
-0.043 -0.082 0.005 -0.009 0.01 0.00  
140 -0.03 -0.09 0.06 0.04 -0.06 -0.02 0.00 0.03 amps  
140 -0.04 -0.12 0.05 0.00 -0.07 -0.05 -0.01 0.02 amps  
140 -0.030 -0.089 -0.007 0.052 -0.034 -0.108 -0.019 -0.004 0.01 0.00 0.01 0.00  
140 -0.039 -0.123 -0.031 -0.026 -0.043 -0.141 -0.044 -0.082 0.02 0.00 0.02 0.01  
-0.028 -0.107 -0.026 -0.006 0.01 0.00  
145 -0.02 -0.12 0.05 0.02 -0.08 -0.01 -0.01 0.03 amps  
145 -0.03 -0.15 0.05 -0.01 -0.08 -0.04 -0.01 0.02 amps  
145 -0.025 -0.117 -0.039 0.043 -0.025 -0.132 -0.041 -0.004 0.01 0.00 0.02 0.00  
145 -0.028 -0.151 -0.049 -0.036 -0.029 -0.167 -0.052 -0.083 0.02 0.00 0.03 0.01  
-0.012 -0.131 -0.055 -0.005 0.02 0.00  
150 -0.02 -0.14 0.04 0.01 -0.09 -0.01 -0.01 0.03 amps  
150 -0.02 -0.18 0.04 -0.03 -0.09 -0.04 -0.01 0.02 amps  
150 -0.017 -0.144 -0.067 0.031 -0.015 -0.156 -0.061 -0.006 0.02 0.01 0.02 0.00  
150 -0.015 -0.178 -0.064 -0.047 -0.013 -0.190 -0.057 -0.084 0.03 0.01 0.04 0.01  
0.005 -0.154 -0.081 -0.007 0.02 0.01  
155 -0.01 -0.17 0.03 -0.01 -0.11 -0.01 -0.02 0.03 amps  
155 0.00 -0.20 0.04 -0.04 -0.10 -0.03 -0.02 0.02 amps  
155 -0.010 -0.169 -0.093 0.017 -0.005 -0.178 -0.078 -0.008 0.03 0.01 0.03 0.01  
155 -0.002 -0.203 -0.076 -0.060 0.003 -0.211 -0.061 -0.085 0.04 0.01 0.04 0.01  
0.021 -0.175 -0.104 -0.011 0.03 0.01  
160 0.00 -0.19 0.03 -0.02 -0.11 -0.01 -0.03 0.03 amps  
160 0.01 -0.22 0.04 -0.06 -0.10 -0.03 -0.02 0.02 amps  
160 -0.002 -0.192 -0.114 0.002 0.005 -0.196 -0.092 -0.012 0.04 0.01 0.04 0.01  
160 0.010 -0.225 -0.085 -0.071 0.017 -0.229 -0.063 -0.085 0.05 0.01 0.05 0.01  
0.036 -0.193 -0.122 -0.016 0.04 0.02  
165 0.01 -0.21 0.02 -0.03 -0.12 -0.01 -0.03 0.03 amps

165 0.02 -0.24 0.04 -0.07 -0.11 -0.03 -0.02 0.02 amps  
 165 0.005 -0.211 -0.130 -0.012 0.014 -0.212 -0.103 -0.015 0.04 0.02 0.05 0.01  
 165 0.021 -0.242 -0.092 -0.081 0.030 -0.244 -0.064 -0.085 0.06 0.02 0.06 0.01  
 0.049 -0.207 -0.137 -0.021 0.05 0.02  
 170 0.01 -0.22 0.02 -0.04 -0.12 -0.01 -0.03 0.03 amps  
 170 0.03 -0.26 0.04 -0.07 -0.11 -0.03 -0.02 0.01 amps  
 170 0.011 -0.225 -0.142 -0.023 0.021 -0.224 -0.111 -0.018 0.05 0.02 0.05 0.01  
 170 0.029 -0.255 -0.097 -0.089 0.040 -0.254 -0.065 -0.085 0.07 0.02 0.07 0.01  
 0.058 -0.217 -0.148 -0.025 0.05 0.02  
 175 0.01 -0.23 0.01 -0.05 -0.13 -0.01 -0.04 0.02 amps  
 175 0.03 -0.26 0.04 -0.08 -0.11 -0.03 -0.03 0.01 amps  
 175 0.014 -0.234 -0.150 -0.029 0.026 -0.231 -0.116 -0.020 0.05 0.02 0.05 0.01  
 175 0.035 -0.263 -0.099 -0.094 0.046 -0.260 -0.065 -0.085 0.07 0.02 0.07 0.01  
 0.064 -0.224 -0.155 -0.027 0.05 0.02  
 180 0.02 -0.24 0.01 -0.05 -0.13 -0.01 -0.04 0.02 amps  
 180 0.04 -0.27 0.04 -0.08 -0.11 -0.03 -0.03 0.01 amps  
 180 0.016 -0.237 -0.152 -0.032 0.027 -0.233 -0.118 -0.021 0.06 0.02 0.06 0.01  
 180 0.037 -0.266 -0.100 -0.096 0.048 -0.263 -0.065 -0.085 0.07 0.02 0.07 0.01  
 0.066 -0.226 -0.157 -0.028 0.06 0.03

e lab= 60.0 charge 1.alpha 300.

wabs0= 29.93 al0= 3.00 al1= 4.00 qvalue= 0.00 distortion core= 40.

Explanation of results to follow

Seniority model with DSF no delta correction

Seniority model with DSF with delta correction

Seniority model no DSF no delta correction

Seniority model no DSF with delta correction

BMZ model with DSF no delta correction

BMZ model with DSF with delta correction

BMZ model without DSF no delta correction

BMZ model without DSF with delta correction

th ca42a ca44a ca46a ti46a ca48a ti48a ca44g ca46g ca48g ti48g xph b/a

fe54 cr52 ti50 cr50 cr52 ti50

0 2.314 1.670 2.021 4.298 2.802 2.054 2.196 2.636 1.882 3.189 0.750 2.792

0 3.205 5.418 5.286 5.474 7.508 4.267 2.168 2.601 1.858 3.147 0.568 1.767

0 4.180 2.124 1.718 8.013 1.836 2.800 4.382 5.258 3.756 6.362 0.857 3.884

0 2.020 1.897 2.813 3.652 4.313 2.231 1.768 2.122 1.515 2.567 0.668 2.218

1.586 1.815 1.510

1.367 1.447 1.165

5.457 2.374 3.179 3.625 2.990

2.507 1.972 1.265 1.460 1.229

5 2.263 1.641 2.000 4.202 2.787 2.016 2.147 2.577 1.841 3.118 0.745 2.780



5 3.112 5.283 5.195 5.310 7.400 4.169 2.097 2.516 1.797 3.044 0.566 1.755  
5 4.067 2.069 1.688 7.797 1.826 2.725 4.267 5.121 3.657 6.196 0.852 3.877  
5 1.968 1.865 2.784 3.555 4.283 2.190 1.718 2.062 1.473 2.495 0.664 2.201  
1.550 1.774 1.476  
1.321 1.399 1.126  
5.308 2.311 3.095 3.529 2.910  
2.438 1.936 1.229 1.417 1.193  
10 2.114 1.557 1.938 3.924 2.744 1.905 2.007 2.408 1.720 2.913 0.730 2.744  
10 2.848 4.897 4.928 4.843 7.084 3.887 1.894 2.273 1.623 2.750 0.558 1.718  
10 3.742 1.913 1.603 7.179 1.799 2.513 3.940 4.728 3.376 5.720 0.836 3.854  
10 1.818 1.773 2.700 3.275 4.195 2.072 1.576 1.891 1.350 2.288 0.652 2.149  
1.448 1.657 1.379  
1.193 1.263 1.017  
4.880 2.133 2.854 3.253 2.683  
2.240 1.834 1.124 1.295 1.090  
15 1.885 1.426 1.842 3.496 2.673 1.734 1.789 2.147 1.533 2.597 0.705 2.682  
15 2.450 4.309 4.513 4.141 6.585 3.456 1.593 1.912 1.365 2.313 0.544 1.655  
15 3.253 1.682 1.483 6.245 1.769 2.200 3.442 4.130 2.950 4.997 0.806 3.801  
15 1.591 1.631 2.567 2.850 4.050 1.890 1.360 1.632 1.165 1.974 0.632 2.061  
1.291 1.477 1.228  
1.002 1.061 0.854  
4.235 1.868 2.488 2.833 2.337  
1.942 1.677 0.966 1.110 0.934  
20 1.601 1.262 1.716 2.964 2.574 1.521 1.519 1.822 1.302 2.205 0.669 2.590  
20 1.972 3.590 3.987 3.303 5.940 2.926 1.238 1.486 1.061 1.798 0.524 1.564  
20 2.665 1.414 1.352 5.121 1.749 1.833 2.836 3.404 2.431 4.118 0.761 3.696  
20 1.315 1.454 2.393 2.337 3.851 1.666 1.099 1.318 0.942 1.595 0.605 1.936  
1.095 1.252 1.040  
0.777 0.823 0.663  
3.458 1.560 2.043 2.323 1.916  
1.581 1.482 0.775 0.888 0.746  
25 1.290 1.080 1.571 2.382 2.447 1.285 1.222 1.467 1.048 1.775 0.621 2.466  
25 1.476 2.822 3.394 2.438 5.194 2.353 0.879 1.055 0.754 1.276 0.495 1.443  
25 2.052 1.147 1.233 3.942 1.746 1.464 2.194 2.633 1.881 3.186 0.696 3.509  
25 1.024 1.259 2.188 1.795 3.599 1.422 0.824 0.989 0.706 1.197 0.572 1.773  
0.880 1.005 0.835  
0.550 0.582 0.469  
2.644 1.250 1.572 1.783 1.469  
1.203 1.270 0.575 0.656 0.550  
30 0.982 0.896 1.412 1.805 2.292 1.048 0.927 1.113 0.795 1.347 0.559 2.305  
30 1.015 2.080 2.782 1.641 4.396 1.792 0.558 0.670 0.479 0.811 0.454 1.286

30 1.480 0.911 1.140 2.835 1.760 1.134 1.582 1.898 1.355 2.296 0.613 3.212  
30 0.748 1.062 1.961 1.284 3.299 1.178 0.566 0.679 0.485 0.822 0.535 1.569  
0.666 0.759 0.630  
0.348 0.369 0.297  
1.882 0.975 1.122 1.267 1.044  
0.848 1.059 0.388 0.439 0.368  
35 0.700 0.722 1.247 1.279 2.108 0.825 0.657 0.789 0.563 0.954 0.481 2.104  
35 0.629 1.427 2.191 0.985 3.594 1.286 0.305 0.366 0.262 0.443 0.396 1.088  
35 0.996 0.725 1.076 1.892 1.778 0.871 1.050 1.260 0.900 1.524 0.519 2.792  
35 0.510 0.875 1.720 0.846 2.957 0.952 0.347 0.417 0.298 0.504 0.500 1.327  
0.470 0.535 0.443  
0.190 0.201 0.163  
1.237 0.757 0.734 0.822 0.675  
0.549 0.862 0.232 0.258 0.215  
40 0.463 0.566 1.080 0.835 1.896 0.629 0.429 0.515 0.368 0.623 0.388 1.862  
40 0.340 0.900 1.654 0.504 2.832 0.866 0.133 0.159 0.114 0.193 0.309 0.840  
40 0.627 0.593 1.031 1.167 1.779 0.682 0.630 0.756 0.540 0.915 0.433 2.274  
40 0.325 0.707 1.475 0.510 2.581 0.754 0.182 0.219 0.156 0.265 0.477 1.049  
0.305 0.345 0.285  
0.082 0.088 0.072  
0.745 0.602 0.429 0.473 0.386  
0.324 0.689 0.115 0.125 0.103  
45 0.279 0.433 0.914 0.493 1.659 0.466 0.252 0.302 0.216 0.366 0.275 1.579  
45 0.150 0.511 1.192 0.199 2.142 0.542 0.038 0.045 0.032 0.055 0.170 0.539  
45 0.376 0.507 0.990 0.668 1.739 0.559 0.332 0.399 0.285 0.482 0.387 1.716  
45 0.196 0.562 1.230 0.282 2.183 0.587 0.075 0.089 0.064 0.108 0.495 0.741  
0.177 0.199 0.163  
0.024 0.028 0.024  
0.412 0.501 0.215 0.230 0.185  
0.175 0.543 0.042 0.043 0.034  
50 0.149 0.324 0.754 0.252 1.407 0.337 0.128 0.153 0.109 0.185 0.135 1.258  
50 0.047 0.254 0.816 0.046 1.547 0.313 0.005 0.006 0.005 0.008 -0.073 0.251  
50 0.228 0.451 0.936 0.370 1.644 0.483 0.148 0.178 0.127 0.215 0.430 1.187  
50 0.119 0.439 0.994 0.151 1.780 0.453 0.019 0.023 0.016 0.028 0.657 0.420  
0.088 0.097 0.079  
0.006 0.009 0.010  
0.221 0.440 0.087 0.086 0.067  
0.097 0.423 0.007 0.005 0.004  
55 0.068 0.238 0.602 0.104 1.148 0.239 0.051 0.061 0.044 0.074 -0.062 0.904  
55 0.009 0.103 0.527 0.003 1.060 0.165 0.014 0.017 0.012 0.021 -0.564 0.528  
55 0.157 0.409 0.857 0.227 1.487 0.433 0.056 0.067 0.048 0.082 0.649 0.764

55 0.082 0.336 0.772 0.098 1.389 0.345 0.005 0.006 0.004 0.007 0.975 0.245  
0.034 0.037 0.030  
0.014 0.019 0.018  
0.139 0.398 0.027 0.022 0.015  
0.071 0.327 0.003 0.003 0.003  
60 0.025 0.171 0.463 0.029 0.899 0.167 0.014 0.017 0.012 0.020 -0.429 0.542  
60 0.010 0.030 0.317 0.025 0.683 0.079 0.044 0.053 0.038 0.064 -1.829 1.222  
60 0.134 0.367 0.750 0.185 1.277 0.389 0.029 0.035 0.025 0.043 0.974 0.586  
60 0.071 0.251 0.572 0.094 1.030 0.259 0.018 0.022 0.015 0.026 0.484 0.537  
0.009 0.010 0.008  
0.034 0.041 0.036  
0.126 0.361 0.015 0.014 0.009  
0.078 0.248 0.017 0.023 0.020  
65 0.009 0.120 0.341 0.005 0.671 0.115 0.004 0.005 0.004 0.006 -1.000 0.360  
65 0.028 0.004 0.174 0.070 0.410 0.035 0.076 0.091 0.065 0.110 -4.333 2.254  
65 0.135 0.317 0.621 0.195 1.035 0.341 0.041 0.049 0.035 0.059 0.929 0.751  
65 0.075 0.182 0.400 0.116 0.719 0.191 0.044 0.053 0.038 0.064 0.341 1.001  
0.004 0.006 0.007  
0.055 0.064 0.056  
0.146 0.317 0.031 0.037 0.031  
0.100 0.185 0.040 0.051 0.045  
70 0.009 0.081 0.239 0.011 0.478 0.077 0.012 0.014 0.010 0.017 -0.642 0.706  
70 0.048 0.000 0.085 0.112 0.229 0.016 0.099 0.119 0.085 0.144 -3.289 3.897  
70 0.140 0.260 0.481 0.219 0.787 0.284 0.067 0.081 0.058 0.098 0.780 1.089  
70 0.081 0.125 0.261 0.143 0.469 0.135 0.072 0.086 0.061 0.104 0.305 1.572  
0.012 0.017 0.017  
0.070 0.081 0.070  
0.173 0.265 0.057 0.071 0.061  
0.122 0.132 0.062 0.079 0.070  
75 0.016 0.053 0.159 0.030 0.327 0.051 0.026 0.032 0.023 0.038 -0.424 1.307  
75 0.059 0.003 0.037 0.135 0.123 0.009 0.109 0.131 0.093 0.158 -2.969 6.989  
75 0.139 0.198 0.346 0.234 0.560 0.222 0.094 0.113 0.081 0.137 0.671 1.503  
75 0.085 0.081 0.156 0.160 0.285 0.091 0.093 0.112 0.080 0.135 0.287 2.304  
0.024 0.033 0.031  
0.076 0.088 0.076  
0.190 0.208 0.081 0.102 0.089  
0.134 0.089 0.078 0.099 0.087  
80 0.023 0.032 0.102 0.049 0.221 0.032 0.041 0.049 0.035 0.060 -0.361 2.075  
80 0.060 0.004 0.016 0.135 0.074 0.006 0.105 0.127 0.090 0.153 -5.05714.368  
80 0.129 0.139 0.229 0.232 0.373 0.159 0.112 0.134 0.096 0.163 0.576 2.001  
80 0.082 0.047 0.084 0.163 0.165 0.057 0.104 0.125 0.089 0.151 0.248 3.319

0.036 0.048 0.044  
 0.074 0.085 0.073  
 0.190 0.150 0.096 0.121 0.106  
 0.133 0.056 0.086 0.108 0.095  
 85 0.028 0.018 0.065 0.062 0.155 0.018 0.052 0.062 0.044 0.075 -0.402 3.007  
 85 0.052 0.002 0.013 0.117 0.065 0.004 0.092 0.110 0.079 0.133 -5.61817.330  
 85 0.112 0.087 0.139 0.212 0.237 0.103 0.118 0.142 0.101 0.171 0.467 2.640  
 85 0.072 0.024 0.042 0.151 0.100 0.032 0.104 0.125 0.089 0.151 0.140 4.863  
 0.044 0.058 0.053  
 0.065 0.076 0.066  
 0.174 0.098 0.100 0.126 0.111  
 0.121 0.031 0.084 0.105 0.093  
 90 0.028 0.010 0.046 0.066 0.123 0.010 0.056 0.068 0.048 0.082 -0.535 3.964  
 90 0.038 0.000 0.021 0.088 0.078 0.002 0.073 0.088 0.063 0.106 -1.891 8.887  
 90 0.090 0.049 0.078 0.181 0.151 0.060 0.113 0.136 0.097 0.165 0.316 3.526  
 90 0.059 0.010 0.024 0.128 0.077 0.015 0.095 0.114 0.081 0.138 -0.140 7.157  
 0.048 0.062 0.056  
 0.052 0.062 0.054  
 0.147 0.058 0.095 0.119 0.104  
 0.099 0.015 0.076 0.094 0.083  
 95 0.026 0.006 0.039 0.061 0.112 0.005 0.055 0.066 0.047 0.080 -0.709 4.510  
 95 0.023 0.001 0.032 0.057 0.100 0.001 0.053 0.064 0.046 0.077 -1.037 5.226  
 95 0.069 0.023 0.044 0.145 0.106 0.029 0.101 0.121 0.087 0.147 0.075 4.801  
 95 0.044 0.003 0.021 0.100 0.079 0.005 0.080 0.096 0.069 0.116 -0.631 8.507  
 0.046 0.059 0.054  
 0.039 0.048 0.043  
 0.114 0.029 0.082 0.102 0.090  
 0.074 0.006 0.063 0.077 0.068  
 100 0.021 0.004 0.039 0.051 0.111 0.003 0.049 0.059 0.042 0.071 -0.833 4.326  
 100 0.012 0.008 0.045 0.032 0.122 0.003 0.036 0.043 0.031 0.052 -0.761 3.368  
 100 0.050 0.008 0.029 0.110 0.089 0.012 0.085 0.102 0.073 0.123 -0.310 6.363  
 100 0.029 0.001 0.027 0.071 0.092 0.001 0.062 0.075 0.053 0.090 -0.912 6.577  
 0.040 0.052 0.047  
 0.028 0.036 0.032  
 0.083 0.012 0.066 0.081 0.071  
 0.051 0.002 0.048 0.059 0.052  
 105 0.015 0.005 0.041 0.039 0.114 0.003 0.040 0.048 0.034 0.058 -0.880 3.691  
 105 0.005 0.019 0.056 0.015 0.139 0.007 0.023 0.027 0.019 0.033 -0.602 2.245  
 105 0.035 0.002 0.025 0.081 0.085 0.003 0.068 0.081 0.058 0.098 -0.739 7.035  
 105 0.017 0.003 0.036 0.045 0.106 0.001 0.045 0.054 0.038 0.065 -0.966 4.440  
 0.033 0.042 0.038

0.019 0.026 0.024  
0.055 0.004 0.050 0.059 0.051  
0.031 0.003 0.033 0.040 0.036  
110 0.010 0.007 0.044 0.026 0.114 0.005 0.029 0.035 0.025 0.043 -0.869 2.950  
110 0.003 0.033 0.067 0.009 0.151 0.015 0.014 0.017 0.012 0.020 -0.431 1.526  
110 0.023 0.001 0.025 0.057 0.083 0.001 0.051 0.062 0.044 0.074 -0.949 6.098  
110 0.009 0.006 0.044 0.025 0.115 0.004 0.029 0.035 0.025 0.042 -0.958 3.006  
0.024 0.031 0.028  
0.014 0.020 0.019  
0.034 0.002 0.035 0.040 0.034  
0.016 0.006 0.021 0.025 0.022  
115 0.006 0.010 0.048 0.016 0.114 0.008 0.020 0.023 0.017 0.028 -0.805 2.217  
115 0.006 0.047 0.080 0.011 0.161 0.026 0.009 0.011 0.008 0.014 -0.205 1.091  
115 0.015 0.001 0.027 0.038 0.081 0.000 0.037 0.045 0.032 0.054 -0.992 4.782  
115 0.004 0.011 0.051 0.012 0.121 0.008 0.017 0.020 0.015 0.025 -0.908 1.987  
0.016 0.021 0.019  
0.011 0.016 0.016  
0.018 0.002 0.023 0.024 0.020  
0.008 0.012 0.011 0.014 0.012  
120 0.004 0.015 0.054 0.009 0.117 0.013 0.011 0.014 0.010 0.016 -0.680 1.515  
120 0.014 0.055 0.097 0.020 0.179 0.042 0.008 0.009 0.007 0.011 0.101 0.868  
120 0.008 0.003 0.029 0.023 0.081 0.001 0.026 0.031 0.022 0.037 -0.995 3.571  
120 0.002 0.017 0.061 0.005 0.131 0.016 0.008 0.010 0.007 0.012 -0.789 1.203  
0.009 0.012 0.011  
0.010 0.015 0.015  
0.008 0.003 0.013 0.012 0.009  
0.006 0.020 0.005 0.006 0.006  
125 0.004 0.023 0.067 0.006 0.134 0.022 0.005 0.006 0.005 0.008 -0.497 0.892  
125 0.023 0.058 0.124 0.034 0.214 0.063 0.008 0.010 0.007 0.012 0.578 0.773  
125 0.004 0.006 0.036 0.012 0.090 0.004 0.016 0.020 0.014 0.024 -0.987 2.417  
125 0.004 0.028 0.079 0.004 0.156 0.027 0.003 0.004 0.003 0.004 -0.547 0.610  
0.004 0.006 0.006  
0.010 0.015 0.015  
0.002 0.007 0.007 0.005 0.003  
0.008 0.032 0.002 0.002 0.003  
130 0.006 0.035 0.091 0.006 0.173 0.035 0.002 0.002 0.001 0.002 -0.246 0.404  
130 0.034 0.052 0.164 0.049 0.275 0.089 0.010 0.012 0.008 0.014 1.647 0.723  
130 0.001 0.013 0.053 0.004 0.121 0.010 0.010 0.012 0.009 0.014 -0.989 1.457  
130 0.008 0.045 0.111 0.009 0.207 0.045 0.001 0.001 0.001 0.001 0.115 0.232  
0.002 0.003 0.003  
0.011 0.015 0.015

0.000 0.015 0.003 0.002 0.001  
0.015 0.050 0.001 0.002 0.002  
135 0.010 0.054 0.132 0.010 0.244 0.054 0.000 0.000 0.000 0.000 0.552 0.087  
135 0.046 0.041 0.223 0.065 0.372 0.121 0.012 0.014 0.010 0.017 7.807 0.678  
135 0.000 0.026 0.087 0.000 0.183 0.023 0.006 0.007 0.005 0.009 -0.999 0.843  
135 0.016 0.070 0.163 0.019 0.296 0.072 0.001 0.001 0.001 0.001 1.000 0.197  
0.001 0.002 0.003  
0.011 0.016 0.015  
0.002 0.028 0.002 0.002 0.001  
0.024 0.075 0.001 0.003 0.003  
140 0.016 0.079 0.191 0.017 0.352 0.080 0.001 0.001 0.001 0.001 0.507 0.175  
140 0.057 0.028 0.301 0.080 0.508 0.160 0.014 0.016 0.012 0.020 3.526 0.630  
140 0.003 0.048 0.143 0.002 0.287 0.045 0.004 0.005 0.004 0.006 -0.897 0.555  
140 0.027 0.105 0.239 0.033 0.429 0.108 0.003 0.003 0.002 0.004 0.843 0.314  
0.001 0.003 0.003  
0.012 0.016 0.015  
0.007 0.051 0.003 0.004 0.004  
0.036 0.110 0.003 0.006 0.006  
145 0.023 0.111 0.270 0.027 0.498 0.113 0.003 0.003 0.002 0.004 0.284 0.307  
145 0.069 0.014 0.399 0.095 0.683 0.204 0.015 0.018 0.013 0.022 1.756 0.580  
145 0.009 0.080 0.222 0.009 0.433 0.078 0.005 0.006 0.005 0.008 -0.595 0.488  
145 0.041 0.150 0.339 0.052 0.606 0.155 0.006 0.007 0.005 0.008 0.728 0.396  
0.003 0.005 0.005  
0.013 0.016 0.015  
0.015 0.082 0.006 0.008 0.008  
0.050 0.154 0.006 0.009 0.009  
150 0.032 0.150 0.365 0.038 0.675 0.151 0.006 0.007 0.005 0.009 0.189 0.389  
150 0.080 0.005 0.512 0.108 0.889 0.253 0.016 0.020 0.014 0.024 1.186 0.534  
150 0.020 0.122 0.321 0.023 0.616 0.120 0.009 0.010 0.007 0.013 -0.306 0.513  
150 0.057 0.204 0.460 0.073 0.821 0.211 0.010 0.012 0.009 0.015 0.663 0.446  
0.005 0.007 0.007  
0.013 0.016 0.014  
0.028 0.123 0.009 0.014 0.013  
0.066 0.207 0.009 0.013 0.013  
155 0.041 0.192 0.470 0.050 0.872 0.194 0.010 0.012 0.008 0.014 0.134 0.440  
155 0.091 0.000 0.634 0.120 1.113 0.305 0.017 0.021 0.015 0.025 0.902 0.493  
155 0.034 0.170 0.435 0.042 0.825 0.170 0.014 0.017 0.012 0.020 -0.120 0.555  
155 0.075 0.264 0.593 0.097 1.059 0.273 0.015 0.018 0.013 0.021 0.627 0.475  
0.008 0.010 0.010  
0.013 0.015 0.014  
0.043 0.171 0.014 0.020 0.019

0.082 0.265 0.013 0.017 0.016  
160 0.051 0.235 0.576 0.063 1.072 0.237 0.014 0.016 0.012 0.020 0.101 0.471  
160 0.101 0.001 0.756 0.131 1.338 0.355 0.018 0.021 0.015 0.026 0.737 0.460  
160 0.050 0.222 0.554 0.065 1.040 0.223 0.020 0.025 0.018 0.030 -0.005 0.593  
160 0.093 0.324 0.728 0.122 1.301 0.336 0.019 0.023 0.017 0.028 0.606 0.493  
0.010 0.013 0.012  
0.012 0.015 0.013  
0.059 0.221 0.019 0.026 0.024  
0.098 0.323 0.016 0.021 0.019  
165 0.060 0.274 0.674 0.074 1.256 0.276 0.017 0.021 0.015 0.025 0.081 0.490  
165 0.109 0.006 0.866 0.140 1.542 0.401 0.018 0.022 0.015 0.026 0.635 0.434  
165 0.065 0.270 0.664 0.087 1.240 0.273 0.027 0.033 0.023 0.039 0.066 0.621  
165 0.110 0.380 0.853 0.144 1.523 0.393 0.024 0.029 0.020 0.035 0.595 0.504  
0.012 0.015 0.014  
0.012 0.014 0.012  
0.075 0.268 0.024 0.032 0.029  
0.113 0.377 0.019 0.023 0.021  
170 0.067 0.306 0.753 0.083 1.405 0.308 0.020 0.024 0.017 0.029 0.069 0.501  
170 0.116 0.013 0.955 0.147 1.706 0.437 0.018 0.022 0.016 0.026 0.572 0.416  
170 0.079 0.310 0.755 0.106 1.403 0.315 0.033 0.039 0.028 0.048 0.109 0.641  
170 0.123 0.425 0.953 0.162 1.702 0.440 0.027 0.033 0.023 0.040 0.590 0.511  
0.014 0.017 0.015  
0.012 0.013 0.012  
0.088 0.307 0.029 0.037 0.033  
0.125 0.420 0.021 0.026 0.023  
175 0.071 0.326 0.805 0.089 1.501 0.329 0.022 0.026 0.019 0.032 0.063 0.507  
175 0.120 0.018 1.012 0.151 1.813 0.460 0.018 0.022 0.016 0.026 0.538 0.405  
175 0.088 0.337 0.814 0.119 1.509 0.342 0.037 0.044 0.032 0.053 0.133 0.652  
175 0.132 0.454 1.018 0.174 1.818 0.470 0.030 0.035 0.025 0.043 0.587 0.514  
0.015 0.018 0.016  
0.012 0.013 0.011  
0.097 0.333 0.031 0.040 0.036  
0.133 0.448 0.022 0.027 0.024  
180 0.073 0.333 0.823 0.091 1.535 0.336 0.023 0.027 0.019 0.033 0.061 0.509  
180 0.121 0.020 1.032 0.153 1.849 0.468 0.018 0.022 0.016 0.026 0.528 0.402  
180 0.091 0.346 0.834 0.124 1.546 0.352 0.038 0.046 0.033 0.055 0.140 0.656  
180 0.135 0.464 1.041 0.178 1.858 0.480 0.030 0.036 0.026 0.044 0.586 0.515  
0.016 0.018 0.017  
0.012 0.013 0.011  
0.100 0.342 0.032 0.041 0.037  
0.136 0.458 0.023 0.028 0.024

APPENDIX D  
CARBON CODE

```

c.....has operator form of the angle transform
c....set up for full angular distribution
c.....has expanded dimension to allow l=3 and j=7/2
c program gin (wfin,tape4=wfin,
c 1 pout,tape8=pout,ginout,tape6=ginout,ca40den,tape2=ca40den,
c 2 ingin,input=ingin,wfout,tape1=wfout,wfn14,tape3=wfn14)
c..... for ca isotopes 1f7/2, 1f5/2, 2p3/2 2p1/2
common /vees/ vs(120,120), vp(120,120)
common /rhoc/ rc, as, anr,rrmax,nnmax
common /ifac/ ifac, om
common /atgt/ atgt, pi, zmult, anmult, fact
common /vt/ t, ak, dw, rz
common /rhonew/ drrr, rhos, rpp, rhop,rhoin(200)
common/ampblk/e,cpl0,cpl1,cplf,czf,cz0,cz1,iat,qvalue,atfs
common /bigrho/ delta,deltai,brho(0:20000)
common /opt/ cb0, cb1
dimension rh(100),rhop(500),rhos(501),rpp(501)
dimension fsick(120),rrs(200),mtem(120,120)
dimension sq(20),cf(20)
dimension sp(20),sm(20)
dimension psi(120),r(120),x(120),lm(40)
2 ,qj(15,200),qh(15,200)
dimension sgc(51), pl(200)
dimension ssn(4),ssl(4),ssj(4),ssp(4),ssmat(4,4)
dimension tr(0:1001,4,4),trd(0:1001,4,4),trdd(0:1001,4,4)
1 ,twi(0:1001,4),twf(0:1001,4),rwf(1001)
dimension ti(0:200,4,4),tid(0:200,4,4),tidd(0:200,4,4),rmst(4,4)
dimension anf(4,4,0:6),af(4,4,0:7,0:6,0:6)
character *72 head
character *10 angl
complex cpl0,cpl1,cplf,czf,cz0,cz1,c00,c01,c10,c11,cff
1 ,f1,f2,f3,f4,xn1,ampnf,ampf
complex tv1(120),tv2(120)
1 ,vz(200,2),vzdd(200,2),vz2(200,2)
2 ,v22(200,2),vdel(200,2),vdelp(200,2),asx
complex scl(40),p1h,p3h,alsz,akc,z(0:15,100),blsz,bkc
complex psip(201),ts(120,120),f(800),sumf,ahi,ahf
complex ca2,ca4,ca6,ca8
complex a1(0:200),a2(0:200)
1 ,b2(0:200),b1(0:200),a3(0:200),a4(0:200)
2 ,b3(0:200),b4(0:200),b5(0:200),b6(0:200),a5(0:200),a6(0:200)

```



```

3 ,b7(0:200),b8(0:200),a7(0:200),a8(0:200),vzm2(200,2)
complex uz2(0:15,121,2,4,4),uzdd(0:15,121,2,4,4)
1 ,uz1(0:15,121,2,4,4),uz(0:15,121,2,4,4),uzd(0:15,121,2,4,4)
complex fpp(0:7,0:15,4,4),fpm(0:7,0:15,4,4),fmp(0:7,0:15,4,4),
1 fmm(0:7,0:15,4,4),azz(0:7,0:15,4,4)
complex sl(40),fsk, fpk
complex a(0:6,0:15,4,4),b(0:6,0:15,4,4),c(0:6,0:15,4,4)
complex bp(0:6,0:15,4,4)
complex cb0, cb1,temc,temb,tembp
complex b0cex,b1cex,b0v(40),b1v(40),temd(2),tema,
1 tem(2),temm2(2),tmm,tmp,tpm,tpm,tpm
complex princ,alow,aodd,alof
complex aa(0:6,51,4,4),bbp(0:6,51,4,4),cc(0:6,51,4,4)
1 ,bb(0:6,51,4,4),amp(0:6,51,4,4)
3 ,ffpp(0:7,51,4,4),ffpm(0:7,51,4,4),ffmp(0:7,51,4,4)
4 ,ffmm(0:7,51,4,4),aazz(0:7,51,4,4)
complex ai,sh1,sh2,cap,t(120,120),x,sb,psi,det,y,s
complex*16 cj(30),ch(30)
open (4,file='wfin.dat',status='unknown')
open (8,file='pout.dat',status='unknown')
open (6,file='ginout.dat',status='unknown')
open (2,file='c12den.dat',status='unknown')
open (5,file='ingin.dat',status='unknown')
open (1,file='wfout.dat',status='unknown')
c open (3,file='wfn14.dat',status='unknown')
c.....assorted constants
zer=0.
one=1.
oh=0.5
ai=(0.,1.)
hc=197.33
pi=3.14159265358979
fsc=1./137.035982
apm=139.57
apmf=apm/hc
c.....
c.....read in the shell structure
c.....the largest j must be first
c.....
read (5, 571)nc
write (6,1489) nc

```

```

1489 format(' number of shells = ',i3)
read (5,490) ssj(1), ssj(2), ssj(3), ssj(4)
read (5,490) ssl(1), ssl(2), ssl(3), ssl(4)
write (6,1490) ssj(1),ssj(2),ssj(3),ssj(4)
write (6,1491) ssl(1),ssl(2),ssl(3),ssl(4)
1490 format(' ssj= ',4f10.4)
1491 format(' ssl= ',4f10.4)
c.....llm and lls are maximum multipoles in nflip and flip cases
lls=2*ssj(1)+.001
llm=2*ssl(1)+.001
write (6,1493) llm, lls
1493 format(' llm= ',i4, ' lls= ',i4)
c.....zero the arrays (not needed on the cray)
call zeroary(a,b,c,bp,ti,tid,tidd,twi,twf,fmm,
1 fmp,fpm,fpp,azz,a1,a2,a3,a4,a5,a6,a7,a8,
2 b1,b2,b3,b4,b5,b6,b7,b8,nc)
c.....calcs overall racah coefficients
call cgstuf(ssl,ssj,anf,af,nc)
do 1651 l=1,20
elb=l
sq(1)=sqrt(elb/(elb+1))
c.....sp,sm for l=lambda=2 case
sp(1)=cof6j(one,one,one,elb,elb,elb+1)
x *sqrt(3*(elb+1)*(2*elb+3))
sm(1)=cof6j(one,one,one,elb,elb,elb-1)
x *sqrt(3*elb*(2*elb-1))
1651 cf(1)=cof6j(one,one,one,elb,elb-1,elb)
x *sqrt(3*elb*(2*elb+1))
c..... input parameters
write (6,333)char(15)
333 format(a2)
read (5,571) idel,imax,iat,ipi0
write(6,572) idel,imax,iat,ipi0
571 format(4i5)
572 format(' delta theta=',i3,' number ang pts=',i3,
x /,' iat (=1 for angle xf)=' ,i3,' ipi0 (=1 for pi0 dist)=' ,i3)
read (5,490) ztgt,atgt,del,alz,alp1,alphap,qvalue,nsick
write (6,490) ztgt,atgt,del,alz,alp1,alphap,qvalue,nsick
nnuc=atgt
acore=nnuc
if(nnuc.gt.39) acore=40

```

```

C print 3000, acore
C 3000 format(' acore=',f6.1)
read (5,500) npr1,npr2,npr3,npr4,npr5,npr6
write (6,500) npr1,npr2,npr3,npr4,npr5,npr6,npp
c.....npr1, npr4 unused
c npr2 causes the wave function to be printed
c npr3 causes the full non-local potential to be printed
read (5,510) n,nkmt,lmax,rz,e,zpi,rq
write (6,510) n,nkmt,lmax,rz,e,zpi,rq
c n is the number of mesh points,
c rz is the matching radius, e is the incident energy and zpi the charg
c of the incident pion
c rq=radius of equivalent charged sphere
c.....read in core density for distorted waves
do 41 i=1,200
read (2,42) rrs(i),rhoin(i)
41 continue
42 format(2f10.4)
del=rz/n
n1=n-1
npp=n1
c.....evaluate pion-nucleon scx amplitudes
irowe=0
if (e.gt.80.)irowe=1
if (irowe.eq.1) write(6,777)
if (irowe.eq.0) write(6,778)
777 format(' using rowe-saloman amplitudes')
778 format(' using siegel-gibbs amplitudes')
call sgampx(irowe,nnuc)
write (6,779) cpl0,cpl1,cplf
779 format(' cpl0=',2f10.5,' cpl1=',2f10.5,' cplf=',2f10.5)
write (6,780) cz0,cz1,czf
780 format(' cz0=',2f10.5,' cz1=',2f10.5,' czf=',2f10.5)
c create tables of spherical bessels of imag arg for finite-range
c.....transforms.
nppp=npp+39
do 885 i=1,nppp
xx=i*del*alp1
ep=exp(xx)
call cjh(xx,ep,cj,ch,lmax)
do 886 il=1,lmax,2

```

```

qj(il,i)=-dimag(cj(il))
qh(il,i)=dimag(ch(il))
qj(il+1,i)=cj(il+1)
qh(il+1,i)=ch(il+1)
886 continue
885 continue
c.....read in nuclear wave functions: twi(initial),
c.... twf(final)
do 143 ii=1,nc
do 43 i=1,800
read (4,44) rwf(i),twi(i,ii)
twf(i,ii)=twi(i,ii)
43 continue
read (4,590) head
write (6,590) head
read (4,590) head
write (6,590) head
read (4,590) head
write (6,590) head
143 continue
do 147 ii=1,nc
do 47 i=1,800
47 read (1,44) rwf(i),twf(i,ii)
read (1,590) head
write (6,590) head
read (1,590) head
write (6,590) head
read (1,590) head
write (6,590) head
147 continue
44 format(f8.2,e15.8)
c.....make transition densities (tr) and calc norms
do 171 j=1,nc
do 171 k=1,nc
rmst(j,k)=0.
171 continue
do 151 j=1,nc
do 151 k=1,nc
do 51 i=1,800
tr(i,j,k)=twi(i,j)*twf(i,k)
rmst(j,k)=rmst(j,k)+tr(i,j,k)*rwf(i)**2

```

```

51 continue
151 continue
eps=rwf(1)
do 172 j=1,nc
do 172 k=1,nc
172 rmst(j,k)=rmst(j,k)*eps
c do 173 j=1,nc
c do 173 k=1,nc
c 173 write (6,52)j,k,rmst(j,k)
52 format(' transition density norm ',2i4,f10.5)
c.....laplacian (trdd) and 1st deriv (trd) of transition densities
do 176 k=1,nc
do 176 j=1,nc
tr(0,k,j)=0.
if(ssl(j).eq.0. .and. ssl(k).eq.0.) tr(0,k,j)=tr(1,k,j)
do 55 i=1,799
trdd(i,k,j)=(tr(i+1,k,j)-2.*tr(i,k,j)+tr(i-1,k,j))/eps**2
1 +(tr(i+1,k,j)-tr(i-1,k,j))/(eps*rwf(i))
trd(i,k,j)=(tr(i+1,k,j)-tr(i-1,k,j))/(eps*2)
55 continue
176 continue
c.....interpolate trans density to solution mesh (del)
do 175 j=1,nc
do 175 k=1,nc
sum=0.
do 45 i=1,n
rr=del*i
r(i)=rr
dd=rr/eps
ii=dd
if (ii.gt.798) goto 45
dd=dd-ii
ti(i,k,j)=(1.-dd)*tr(ii,k,j)+dd*tr(ii+1,k,j)
tid(i,k,j)=(1.-dd)*trd(ii,k,j)+dd*trd(ii+1,k,j)
tidd(i,k,j)=(1.-dd)*trdd(ii,k,j)+dd*trdd(ii+1,k,j)
sum=sum+ti(i,k,j)*rr**2
45 continue
sum=sum*del
c write(6,152)k,j,sum
152 format(' trans den norm on soln mesh ',2i4,f10.5)
175 continue

```

```

sum=0.
call clrho
write (6,444) rrmx,nnmx
444 format(' rrmx',f6.2,' nnmx',i5)
delta=.001
deltai=1./delta
jj=rrmx*deltai
do 471 i=1,jj
rr=delta*i
brho(i)=rho(rr)
471 continue
brho(0)=brho(1)
c.....evaluate pion-nucleon scx parameters
alpha=alphap/hc
aias=atgt*938.9
om=apm+e
aklab=sqrt(om**2-apm**2)/hc
epn=sqrt(139.57**2+938.9**2+2.*om*938.9)
akcmi=aklab*938.9/epn
ep=sqrt(139.57**2+aias**2+2.*om*aias)
anuc=aias+qvalue
omf=(ep**2-apm**2-anuc**2)/2./anuc
ak=sqrt(om**2-apm**2)/197.32
ak=ak*aias/ep
aki=ak
akf=sqrt(omf**2-apm**2)/hc
enpf=sqrt(139.57**2+938.9**2+2.*omf*938.9)
akcmf=akf*938.9/enpf
akf=akf*anuc/ep
rati=aki/akcmi
ratf=akf/akcmf
cpl0=cpl0*rati
cz0=cz0*ratf
cpl1=cpl1/rati
cz1=cz1/ratf
cplf=cplf/rati
czf=czf/ratf
c.....cff=*cplf*czf is put below for quenching
c00=cpl0*cz0
c01=cpl0*cz1
c10=cpl1*cz0

```

```

c11=cpl1*cz1
write(6,3333) c00,c01,c10,c11
3333 format(' c00,c01,c10,c11 ',8f10.4)
cfact=ep/anuc
read (5,580) ifac,idat,zf,rad
c....ifac=0 plane wave
c.... 2 free b's
c.... 4 l-dependent b's
c.... all else l=0 used for all b's
if (ifac.eq.0) write (6,837)
837 format(' doing plane wave calculation')
if (ifac.eq.4) write (6,838)
838 format(' using l dependent optical model strengths')
write (6,580) ifac,idat,zf,rad
read (5,570) wabs,delm,sperc,quench
gm=77.0**2
wabs=wabs*((515*gm/4.0)/((E-215.)**2+gm/4.))*(14./40.)**2
write (6,1570) wabs,delm,sperc,quench
1570 format(' wabs=',f7.3,'delm=',f7.3, ' sperc=',f7.3,' quench=',f5.2)
delm=delm/hc
cpl0=(1.+sperc)*cpl0
cz0=(1.+sperc)*cz0
akz=sqrt((sqrt(ak**2+apmf**2)-delm)**2-apmf**2)
cff=cplf*czf*quench
write (6,1571) akz
1571 format(' interm momentum=',f10.5)
c.....optical model parameters
wabs0=wabs
write (6,530) wabs,aki,akf,akcmi,akcmf,xf
read (8,590) head
write (6,590) head
read (8,600) lampx,head
write (6,600) lampx,head
read (8,610) lb,b0cex,b1cex,fsk,fpk
write (6,610) lb,b0cex,b1cex,fsk,fpk
c.....free b's read in here
read (8,610) lb,cb0,cb1
write (6,610) lb,cb0,cb1
cb0=cb0*cfact
cb1=cb1/cfact
c.....l-dependent b's read in here

```

```

do 60 lp=1,lampx
read (8,610) lm(lp),b0v(lp),b1v(lp)
if (lp.le.lmax) write (6,610) lm(lp),b0v(lp),b1v(lp)
b0v(lp)=b0v(lp)*cfact
b1v(lp)=b1v(lp)/cfact
60 continue
write (6,630) ztgt,atgt,alz,alp1,ak
write (6,1491) ssl(1),ssl(2),ssl(3),ssl(4)
if (nsick.ne.1) go to 70
call chg (acore,fsick,n,del)
write (6,620) atgt
70 continue
write (6,640) e,zpi,alphap
write (6,671) n,rz
deli=1./del
n2=n-2
ipass=1
tek=2*zpi*ztgt*fsc*sqrt(apm**2+(hc*aki)**2)/hc
c start 1 loop
c.....pass1=pi+ pass2=pi- pass3=pi0
c.....for passes 1 and 2 l=l(pion); for pass3 l=l(green fcn)
441 do 440 il=1,lmax
if (ipass.lt.3.and.il.eq.1) write (6,660)
if(ipass.eq.2)ak=akf
if(ipass.eq.3)ak=akz
eta=tek/(2.*ak)
l=il-1
al=l
if (ifac.eq.2) go to 130
k=1
if (ifac.eq.4) k=il
cb0=b0v(k)
cb1=b1v(k)
130 continue
if (ifac.eq.0) cb0=0.
if (ifac.eq.0) cb1=0.
c.....ak0 doesn't seem to be used. arg to vcal.
ak0=1.
C print *,'calling vcal'
938 call vcal (alpha,del,ak0,n,il)
C print *,'back from vcal'

```



```

if (npr3.eq.1) call potpr (r,n,il,alphap)
do 211 i=1,n1
211 t(i,i)=t(i,i)-2.*deli**2
do 212 i=1,n2
t(i,i+1)=t(i,i+1)+deli**2
t(i+1,i)=t(i+1,i)+deli**2
212 continue
c11=al*(al+1.)
do 220 i=1,n1
facc=1./r(i)
if (r(i).lt.rq) facc=(3./rq-r(i)**2/rq**3)/2.
if (nsick.eq.1) facc=fsick(i)
220 t(i,i)=t(i,i)-c11/r(i)**2-tek*facc+ai*wabs*rho(r(i))**2+ak**2
if (ipass.le.2) then
c.....1st and 2nd pass calculate distorted waves.
do 230 i=1,n2
230 x(i)=-t(i,n1)
call cls (n2,1,t,120,x,120)
x(n1)=1.
else
c.....3rd pass: t becomes the green function.
c..... t(n1,n1) line is b.c.
confr=(alp1**2+ak**2)/alp1
t(n1,n1)=t(n1,n1)+deli**2*y(ak*del*n1,eta)/y(ak*del*n1,eta)
call invert (t,n1,120,mtem,ts)
do 1230 i=1,n1
1230 x(i)=t(n1,i)
xn1=2*x(n2)-x(n-3)+del**2*(c11/r(i)**2-ak**2)*x(n2)
endif
if(npr2.ne.1)goto 241
write (6,242)(r(i),x(i)/x(20),i=1,n1)
242 format(3f10.5)
241 continue
c..... evaluate pion wave fcns and s-matrix
do 240 i=1,n1
c if (l.eq.10) write (6,936) r(i),x(i)
c 936 format(' r,x ',3e18.7)
240 psi(i)=x(i)
call sigcou (eta,sgc)
do 80 jl=1,lmax
80 scl(jl)=cexp(2.*ai*sgc(jl))

```

```

sh1=y(ak*r(n1),l,eta)
sh2=y(ak*r(n2),l,eta)
det=psi(n1)*sh2-psi(n2)*sh1
cap=.5*(sh2*conjg(sh1)-sh1*conjg(sh2))/det
s=-(psi(n1)*conjg(sh2)-psi(n2)*conjg(sh1))/det
c write(6,1513) det,cap,psi(n1)
1513 format(' det ',6e12.3)
939 sl(il)=s
do 275 i=1,n1
psi(i)=cap*psi(i)
psip(i+1)=psi(i)
275 continue
if (npr2.ne.2) go to 1275
write (6,242) (r(i),psip(i),i=1,n1)
1275 continue
do 323 jj=n1-1,nppp+1
rt=del*(jj-1)
sh1=y(ak*rt,l,eta)
psip(jj)=(conjg(sh1)+s*sh1)*.5
323 continue
322 write (6,710)l,ak,eta,s,scl(il),cap
c.....take v-transform of wave functions
confr=(alp1**2+ak**2)/alp1
do 891 i=1,nppp
a1(i)=psip(i+1)*qj(il,i)
a2(i)=psip(i+1)*qh(il,i)
891 continue
do 892 i=1,nppp
b2(nppp+1-i)=b2(nppp+2-i)+(a2(nppp+1-i)+a2(nppp+2-i))* .5*del
b1(i)=b1(i-1)+(a1(i)+a1(i-1))* .5*del
892 continue
do 893 i=1,npp+2
psip(i+1)=(qj(il,i)*b2(i)+qh(il,i)*b1(i))*confr
893 continue
if (ipass.eq.3) go to 205
c.....pass 1 and 2: multiply by transition density to get uz's
do 1335 k=1,nc
do 1335 j=1,nc
do 335 i=1,npp
uz(l,i,ipass,j,k)=psip(i+1)*ti(i,j,k)/ak
uzdd(l,i,ipass,j,k)=psip(i+1)*tidd(i,j,k)/ak

```

```

uz2(l,i,ipass,j,k)=(psip(i)-2.*psip(i+1)+psip(i+2))*ti(i,j,k)
1 /ak*deli**2
uzd(l,i,ipass,j,k)=psip(i+1)*tid(i,j,k)/ak
uz1(l,i,ipass,j,k)=(psip(i+2)-psip(i))*deli*ti(i,j,k)/(2*ak)
uz1(l,i,ipass,j,k)=uz1(l,i,ipass,j,k)-psip(i+1)*ti(i,j,k)
1 /(ak*r(i))
335 continue
1335 continue
c.....return for next pass
goto 440
c.....pass 3: construct multipole amplitudes
205 continue
if(npr2.ne.1)go to 1241
c write (6,242) (r(i),t(n1,i)/t(n1,20),i=1,n1)
1241 continue
c....nonflip part
c.... l is ang mom for the green function
c.... lpi is pion angular momentum
c.... lpi= l-llm,....,l+llm
llmt=llm*2+1
do 650 k1=1,nc
do 650 k2=1,nc
do 650 i=1,llmt
lpi=1+i-llm-1
if(lpi.lt.0) goto 650
if(lpi.gt.lmax-1) goto 650
c.....take v-transform of uz to get each scx stage (id=1,2)
alpi=lpi
do 655 id=1,2
a2(npp+1)=0.
a4(npp+1)=0.
a6(npp+1)=0.
a8(npp+1)=0.
b2(npp+1)=0.
b4(npp+1)=0.
b6(npp+1)=0.
b8(npp+1)=0.
do 894 j=1,npp
a1(j)=uz(lpi,j,id,k1,k2)*qj(il,j)
a2(j)=uz(lpi,j,id,k1,k2)*qh(il,j)
a3(j)=uzdd(lpi,j,id,k1,k2)*qj(il,j)

```

```

a4(j)=uzdd(lpi,j,id,k1,k2)*qh(il,j)
a5(j)=uz2(lpi,j,id,k1,k2)*qj(il,j)
a6(j)=uz2(lpi,j,id,k1,k2)*qh(il,j)
a7(j)=uz(lpi,j,id,k1,k2)*qj(il,j)/r(j)**2
a8(j)=uz(lpi,j,id,k1,k2)*qh(il,j)/r(j)**2
894 continue
do 895 j=1,npp
b2(npp+1-j)=b2(npp+2-j)+(a2(npp+1-j)+a2(npp+2-j))* .5*del
b1(j)=b1(j-1)+(a1(j)+a1(j-1))* .5*del
b4(npp+1-j)=b4(npp+2-j)+(a4(npp+1-j)+a4(npp+2-j))* .5*del
b3(j)=b3(j-1)+(a3(j)+a3(j-1))* .5*del
b6(npp+1-j)=b6(npp+2-j)+(a6(npp+1-j)+a6(npp+2-j))* .5*del
b5(j)=b5(j-1)+(a5(j)+a5(j-1))* .5*del
b8(npp+1-j)=b8(npp+2-j)+(a8(npp+1-j)+a8(npp+2-j))* .5*del
b7(j)=b7(j-1)+(a7(j)+a7(j-1))* .5*del
895 continue
do 896 j=1,npp
vz(j,id)=(qj(il,j)*b2(j)+qh(il,j)*b1(j))*confr
vzdd(j,id)=(qj(il,j)*b4(j)+qh(il,j)*b3(j))*confr
vz2(j,id)=(qj(il,j)*b6(j)+qh(il,j)*b5(j))*confr
vzm2(j,id)=(qj(il,j)*b8(j)+qh(il,j)*b7(j))*confr
896 continue
v22(1,id)=0.
do 897 j=2,npp-1
v22(j,id)=(vz(j-1,id)-2.*vz(j,id)+vz(j+1,id))*deli**2
897 continue
655 continue
c.....construct dcx amp by combining vz*t*vz
c.....ll is multipole (cap l) and l is l(green function)
c.....the factor atfs is the s-wave part of the angle transform
do 420 ll=0,llm
if (anf(k1,k2,ll).eq.0.) go to 420
all=ll
coef=cg(all,alpi,al,0.,0.,0.)***2
if (coef.eq.0) goto 420
dll=-all*(all+1.)+lpi*(lpi+1)*atfs
do 222 id=1,2
do 223 j=1,n1
vdel(j,id)=vzdd(j,id)-(vz2(j,id)+v22(j,id))*atfs
1 +vz(j,id)*atfs*c1l/r(j)**2+dll*vzm2(j,id)
223 continue
222 continue

```

```

222 continue
do 219 j=1,n1
tv1(j)=0.
tv2(j)=0.
219 continue
do 218 k=1,n1
do 218 j=1,n1
tv1(j)=vz(k,2)*t(j,k)+tv1(j)
tv2(j)=vdel(k,2)*t(j,k)+tv2(j)
218 continue
tema=0.
temb=0.
tembp=0.
temc=0.
do 217 j=1,n1
tema=tema+vz(j,1)*tv1(j)
temb=temb+vz(j,1)*tv2(j)
tembp=tembp+vdel(j,1)*tv1(j)
temc=temc+vdel(j,1)*tv2(j)
217 continue
a(ll,lpi,k1,k2)=-tema*del*coef+a(ll,lpi,k1,k2)
b(ll,lpi,k1,k2)=-temb*del*coef*.5+b(ll,lpi,k1,k2)
bp(ll,lpi,k1,k2)=-tembp*del*coef*.5+bp(ll,lpi,k1,k2)
c(ll,lpi,k1,k2)=-temc*del*coef*.25+c(ll,lpi,k1,k2)
213 format(3i5,f10.5)
420 continue
c.....end lpi loop (on i) for non-flip amplitudes
650 continue
c.... begin lpi loop (on i) for flip amplitudes
llst=2*lls+1
do 1650 k1=1,nc
do 1650 k2=1,nc
do 1650 i=1,llst
lpi=1+i-lls-1
if(lpi.lt.0) go to 1650
if(lpi.gt.lmax-1) go to 1650
c.....v-transform of uz. to get scx factors (flip case)
alpi=lpi
do 1655 id=1,2
a2(npp+1)=0.
b2(npp+1)=0.

```

```

a4(npp+1)=0.
a8(npp+1)=0.
b4(npp+1)=0.
b8(npp+1)=0.
do 1894 j=1,npp
a1(j)=uz1(lpi,j,id,k1,k2)*qj(il,j)/r(j)
a2(j)=uz1(lpi,j,id,k1,k2)*qh(il,j)/r(j)
a3(j)=uzd(lpi,j,id,k1,k2)*qj(il,j)/r(j)
a4(j)=uzd(lpi,j,id,k1,k2)*qh(il,j)/r(j)
a7(j)=uz(lpi,j,id,k1,k2)*qj(il,j)/r(j)**2
a8(j)=uz(lpi,j,id,k1,k2)*qh(il,j)/r(j)**2
1894 continue
do 1895 j=1,npp
b2(npp+1-j)=b2(npp+2-j)+(a2(npp+1-j)+a2(npp+2-j))* .5*del
b1(j)=b1(j-1)+(a1(j)+a1(j-1))* .5*del
b4(npp+1-j)=b4(npp+2-j)+(a4(npp+1-j)+a4(npp+2-j))* .5*del
b3(j)=b3(j-1)+(a3(j)+a3(j-1))* .5*del
b8(npp+1-j)=b8(npp+2-j)+(a8(npp+1-j)+a8(npp+2-j))* .5*del
b7(j)=b7(j-1)+(a7(j)+a7(j-1))* .5*del
1895 continue
do 1896 j=1,npp
vzdd(j,id)=(qj(il,j)*b4(j)+qh(il,j)*b3(j))*confr
vzm2(j,id)=(qj(il,j)*b8(j)+qh(il,j)*b7(j))*confr
vz(j,id)=(qj(il,j)*b2(j)+qh(il,j)*b1(j))*confr
1896 continue
1655 continue
c...ll, flip, lambda=ll(+-)1 (built from lambda=ll-1)
c.....construct dcx amplitude by combining scx*g*scx
do 1420 ll=1,lls
if(ll.lt.iabs(lpi-1)) go to 1420
if (ll.gt. lpi+1) go to 1420
if(abs(af(k1,k2,ll,ll-1,ll-1)).lt.1.e-6 .and.
x abs(af(k1,k2,ll,ll-1,ll+1)).lt.1.e-6 .and.
x abs(af(k1,k2,ll,ll+1,ll-1)).lt.1.e-6 .and.
x abs(af(k1,k2,ll,ll+1,ll+1)).lt.1.e-6 .and.
x ll.gt.0) go to 1420
elb=ll
q1=cg(elb,alpi+1,al,zer,zer,zer)
if (q1.eq.0.) go to 1420
app=sqrt((lpi+1.)*(2.*lpi+3.))*q1*cf(ll)
x *cof6j(elb,alpi+1,al,alpi,elb,one)

```

```

app2=app**2*(2*lpi+1)*6.
do 1222 id=1,2
do 1223 j=1,n1
vdel(j,id)=(-vzdd(j,id)+vzm2(j,id)*(ll-1))
vdelp(j,id)=(-vzdd(j,id)-vzm2(j,id)*(ll+2))*sq(ll)
1223 continue
1222 continue
do 1219 j=1,n1
tv1(j)=0.
tv2(j)=0.
1219 continue
do 1218 k=1,n1
do 1218 j=1,n1
tv1(j)=vdel(k,2)*t(j,k)+tv1(j)
tv2(j)=vdelp(k,2)*t(j,k)+tv2(j)
1218 continue
tmm=0.
tpm=0.
tmp=0.
tpp=0.
do 1217 j=1,n1
tmm=tmm+vdel(j,1)*tv1(j)
tpm=tpm+vdel(j,1)*tv2(j)
tmp=tmp+vdelp(j,1)*tv1(j)
tpp=tpp+vdelp(j,1)*tv2(j)
1217 continue
c.....p means lambda=l+1 m means lambda=l-1
fmm(ll,lpi,k1,k2)=-tmm*del*app2+fmm(ll,lpi,k1,k2)
fpm(ll,lpi,k1,k2)=-tpm*del*app2+fpm(ll,lpi,k1,k2)
fmp(ll,lpi,k1,k2)=-tmp*del*app2+fmp(ll,lpi,k1,k2)
fpp(ll,lpi,k1,k2)=-tpp*del*app2+fpp(ll,lpi,k1,k2)
c.... end ll multipole loop
1420 continue
c.....begin ll flip. lambda=ll
do 2420 ll=1,llm
if(abs(af(k1,k2,ll,ll)).lt.1.e-6) go to 2420
elb=ll
stl=6./(2*lpi+1)
q1=sqrt((alpi+1.)*(2.*alpi+3.))
q2=sqrt(alpi*(2*alpi-1.))
spp= cg(elb+1,alpi+1,al,zer,zer,zer)*sp(ll)*q1

```

```

x *cof6j(elb+1,alpi+1,al,alpi,elb,one)
spm=-cg(elb+1,alpi-1,al,zer,zer,zer)*sp(ll)*q2
x *cof6j(elb+1,alpi-1,al,alpi,elb,one)
smp=-cg(elb-1,alpi+1,al,zer,zer,zer)*sm(ll)*q1
x *cof6j(elb-1,alpi+1,al,alpi,elb,one)
smm= cg(elb-1,alpi-1,al,zer,zer,zer)*sm(ll)*q2
x *cof6j(elb-1,alpi-1,al,alpi,elb,one)
afgp=-elb*(spp+spm)+(elb+1)*(smp+smm)
afpg=-alpi*(spp+smp)+(alpi+1)*(spm+smm)
afg=alpi*elb*spp-elb*(alpi+1)*spm-(elb+1)*alpi*smp
x +(elb+1)*(alpi+1)*smm
c...as a check. remove if works!
if(abs(spp+spm+smp+smm) .gt. 0.0001)
x write (6,1833) elb,alpi,al,spp,spm,smp,smm
1833 format(' spp etc',3f6.1,5f10.5)
do 2222 id=1,2
do 2223 j=1,n1
vdel(j,id)=afgp*vz(j,id)+afpg*vzdd(j,id)+afg*vzm2(j,id)
2223 continue
2222 continue
do 2219 j=1,n1
2219 tv1(j)=0.
do 2218 k=1,n1
do 2218 j=1,n1
tv1(j)=vdel(k,2)*t(j,k)+tv1(j)
2218 continue
tmm=0.
do 2217 j=1,n1
2217 tmm=vdel(j,1)*tv1(j)+tmm
c.....sign reversal relative to fmm,fpm,fmp,fpp because of the
c.....phase factor (-1)**(1+L+lamp)
c.....there is another phase of (-1)**L in cgstuf
azz(ll,lpi,k1,k2)=azz(ll,lpi,k1,k2)+tmm*del*stl
c.....end ll loop
2420 continue
c.....end lpi loop (on i) for flip amplitudes
1650 continue
c.....end il loop
440 continue
if (ipass.eq.3) goto 557
if (ipass.eq.1) tek=-tek

```



```

if (ipass.eq.2) tek=0.
if (ipass.eq.2 .and. ipi0.ne.1) ifac=0
ipass=ipass+1
c.....go back for pi0 and pi- passes.
goto 441
557 continue
nprt=0
if (nprt.ne.1) go to 1799
write (6,799)
799 format(' partial waves for ss term')
do 425 ll=0,lmax-1
write (6,485) ll,(a(1,ll,1,1)*200.,l=0,llm)
write (6,485) ll,(a(1,ll,1,2)*200.,l=0,llm)
425 write (6,485) ll,(a(1,ll,2,2)*200.,l=0,llm)
485 format(i5,10f8.3)
write (6,585)
585 format(' partial waves for sp term')
do 528 ll=0,lmax-1
write (6,485) ll,(b(1,ll,1,1)*200.,l=0,llm)
write (6,485) ll,(b(1,ll,1,2)*200.,l=0,llm)
528 write (6,485) ll,(b(1,ll,2,2)*200.,l=0,llm)
write (6,669)
669 format(' partial waves for ps term')
do 668 ll=0,lmax-1
write (6,485) ll,(bp(1,ll,1,1)*200.,l=0,llm)
write (6,485) ll,(bp(1,ll,1,2)*200.,l=0,llm)
668 write (6,485) ll,(bp(1,ll,2,2)*200.,l=0,llm)
write (6,672)
672 format(' partial waves for pp term')
do 670 ll=0,lmax-1
write (6,485) ll,(c(1,ll,1,1)*200.,l=0,llm)
write (6,485) ll,(c(1,ll,1,2)*200.,l=0,llm)
670 write (6,485) ll,(c(1,ll,2,2)*200.,l=0,llm)
write(6,1672)
1672 format(' partial waves for tmm')
do 1670 ll=0,lmax-1
write (6,485) ll,(fmm(1,ll,1,1)*200.,l=1,lls)
write (6,485) ll,(fmm(1,ll,1,2)*200.,l=1,lls)
1670 write (6,485) ll,(fmm(1,ll,2,2)*200.,l=1,lls)
write (6,1673)
1673 format(' partial waves for tpm')

```

```

do 1674 ll=0,lmax-1
write (6,485) ll,(fpm(1,ll,1,1)*200.,l=1,lls)
write (6,485) ll,(fpm(1,ll,1,2)*200.,l=1,lls)
1674 write (6,485) ll,(fpm(1,ll,2,2)*200.,l=1,lls)
write (6,1675)
1675 format(' partial waves for tmp')
do 1676 ll=0,lmax-1
write (6,485) ll,(fmp(1,ll,1,1)*200.,l=1,lls)
write (6,485) ll,(fmp(1,ll,1,2)*200.,l=1,lls)
1676 write (6,485) ll,(fmp(1,ll,2,2)*200.,l=1,lls)
write (6,1677)
1677 format(' partial waves for tpp')
do 1785 ll=0,lmax-1
write (6,485) ll,(fpp(1,ll,1,1)*200.,l=1,lls)
write (6,485) ll,(fpp(1,ll,1,2)*200.,l=1,lls)
1785 write (6,485) ll,(fpp(1,ll,2,2)*200.,l=1,lls)
write (6,486)
486 format(' partial waves for azz')
do 1679 ll=0,lmax-1
write (6,485) ll,(azz(1,ll,1,1),l=1,lls)
write (6,485) ll,(azz(1,ll,1,2),l=1,lls)
1679 write (6,485) ll,(azz(1,ll,2,2),l=1,lls)
1799 continue
c.....sum partial wave series
do 525 k1=1,nc
do 525 k2=1,nc
do 525 ith=1,imax
th=(ith-1)*idel*pi/180.
xx=cos(th)
call pleg(xx,pl,15)
c.....non flip
do 526 l=0,llm
aa(l,ith,k1,k2)=0.
bb(l,ith,k1,k2)=0.
bbp(l,ith,k1,k2)=0.
cc(l,ith,k1,k2)=0.
do 529 ll=0,lmax-1
529 cc(l,ith,k1,k2)=cc(l,ith,k1,k2)+(2*ll+1)*pl(ll+1)*c(l,ll,k1,k2)
do 526 lp=1,lmax
bb(l,ith,k1,k2)=bb(l,ith,k1,k2)+(2*lp-1)*pl(lp)*b(l,lp-1,k1,k2)
bbp(l,ith,k1,k2)=bbp(l,ith,k1,k2)+(2*lp-1)*pl(lp)*bp(l,lp-1,k1,k2)

```

```

526 aa(l,ith,k1,k2)=aa(l,ith,k1,k2)+(2*lp-1)*pl(lp)*a(l,lp-1,k1,k2)
c.....flip
do 2526 l=0,lls
ffpp(l,ith,k1,k2)=0.
ffpm(l,ith,k1,k2)=0.
ffmp(l,ith,k1,k2)=0.
ffmm(l,ith,k1,k2)=0.
aazz(l,ith,k1,k2)=0.
do 2526 ll=0,llmax-1
ffpp(l,ith,k1,k2)=ffpp(l,ith,k1,k2)+(2*ll+1)*pl(ll+1)*
x fpp(l,ll,k1,k2)
ffpm(l,ith,k1,k2)=ffpm(l,ith,k1,k2)+(2*ll+1)*pl(ll+1)*
x fpm(l,ll,k1,k2)
ffmp(l,ith,k1,k2)=ffmp(l,ith,k1,k2)+(2*ll+1)*pl(ll+1)*
x fmp(l,ll,k1,k2)
ffmm(l,ith,k1,k2)=ffmm(l,ith,k1,k2)+(2*ll+1)*pl(ll+1)*
x fmm(l,ll,k1,k2)
aazz(l,ith,k1,k2)=aazz(l,ith,k1,k2)+(2*ll+1)*pl(ll+1)*
x azz(l,ll,k1,k2)
2526 continue
525 continue
c write (6,835)
835 format(' s-s s-p')
c do 565 i=1,imax
c 565 write (6,527) (i-1)*idel,(aa(l,i)*200.,l=0,llm),
c 1 (bb(l,i)*200.,l=0,llm)
c write (6,836)
836 format(' p-s p-p')
c do 673 i=1,imax
c 673 write (6,527) (i-1)*idel,(bbp(l,i)*200.,l=0,llm),
c 1 (cc(l,i)*200.,l=0,llm)
527 format(i4,16f8.3)
write (6,333) char(12)
c write (6,839)
839 format(' multipoles: a,b')
c.....include transition amplitudes. ll=multipole, i=angle k's chan
do 791 k1=1,nc
do 791 k2=1,nc
do 791 i=1,imax
do 792 ll=0,llm
amp(ll,i,k1,k2)=c00*aa(ll,i,k1,k2)+c10*bb(ll,i,k1,k2)

```

```

1 +c01*bbp(ll,i,k1,k2)+c11*cc(ll,i,k1,k2)
792 amp(ll,i,k1,k2)=amp(ll,i,k1,k2)*200.
do 1892 ll=0,lls
ffpp(ll,i,k1,k2)=-ffpp(ll,i,k1,k2)*cff*200.
ffpm(ll,i,k1,k2)=-ffpm(ll,i,k1,k2)*cff*200.
ffmp(ll,i,k1,k2)=-ffmp(ll,i,k1,k2)*cff*200.
ffmm(ll,i,k1,k2)=-ffmm(ll,i,k1,k2)*cff*200.
1892 aazz(ll,i,k1,k2)=-aazz(ll,i,k1,k2)*cff*200.
791 continue
write (6,640) e,zpi,alphap
write (6,641) wabs0,alz,alp1,qvalue,atgt
641 format(' wabs0= ',f6.2,' al0= ',f6.2,' all= ',f6.2,
x ' qvalue= ',f6.2,' distortion core= ',f4.0)
c write (6,796)
796 format(' th p1/2 p3/2 l=s=0 k-c ',
x ' cosx a b')
797 format(' th p1/2 p3/2 l=s=0 k-c ',
x ' a b(ls0) cos(ls0) b(k-c) cos(k=c)')
write (6,793)
793 format(' th cs(nf) real imag cs real',
x ' imag')
c.....construct dcx amplitudes by summing over multipoles
1495 continue
read (5,491) ssp(1), ssp(2), ssp(3), ssp(4), it,ip
491 format(4f10. 5,2i5)
if (ssp(1).lt.-1.001) stop
c if(it.lt.0) iangmx=imax
c if(it.ge.0) iangmx=1
iangmx=imax
fulnorm=0.
do 177 k1=1,nc
fulnorm=fulnorm+ssp(k1)**2*rmst(k1,k1)
177 continue
do 794 i=1,iangmx
ampnf=0.
ampf=0.
do 795 k1=1,nc
do 795 k2=1,nc
sss=ssp(k1)*ssp(k2)
do 2794 ll=0,llm
ampnf=ampnf+sss*anf(k1,k2,ll)*amp(ll,i,k1,k2)

```

```

ampf=ampf+sss*af(k1,k2,ll,ll)*aazz(ll,i,k1,k2)
2794 continue
do 2796 ll=0,lls
lp1=ll+1
lm1=ll-1
if (lm1.gt.llm) go to 2796
if (lp1.le.llm)
x ampf=ampf+sss*af(k1,k2,ll,lp1,lp1)*ffpp(ll,i,k1,k2)
if (lm1.ge.0)
x ampf=ampf+sss*af(k1,k2,ll,lm1,lm1)*ffmm(ll,i,k1,k2)
if (lm1.ge.0 .and. lp1.le.llm)
x ampf=ampf+sss*(af(k1,k2,ll,lp1,lm1)*ffpm(ll,i,k1,k2)
x +af(k1,k2,ll,lm1,lp1)*ffmp(ll,i,k1,k2))
2796 continue
795 continue
akrt=akf/aki
cnf=cabs(ampnf)**2*akrt
cflp=cabs(ampf-ampnf)**2*akrt
write(6,1500) (i-1)*idel,cnf,ampnf,cflp,-ampf+ampnf,it,ip
1500 format(i5,f9.3,2f9.3,f9.3,2f9.3,2i5)
c.....ampnf=sum(k1,k2) ssp(k1)*ssp(k2) sum(l) anf(k1,k2,l)*amp(l,i,k1,k2)
c.....ampf=sum(k1,k2) ssp(k1)*ssp(k2) sum(l,lam,lamp)af(k1,k2,l,lam,lamp)
794 continue
go to 1495
490 format (7f10.4,i2)
500 format (8i5,f5.3)
510 format (3i5,4f10.4,2f5.1,5x,i2)
520 format (f5.1)
530 format (' wabs=',f9.3,' aki=',f8.3,' akf=',f8.3,' akcmi=',f8.3
1 ,'akcmf=',f8.3,' xf=',f7.2)
570 format (4f10.5)
580 format (2i5,2f5.2)
590 format (a72)
600 format (i3,a72)
610 format (i3,8f7.4)
620 format (' chg density from sick and mccarthy for a=',f3.0)
630 format (' z=',f4.0,' a=',f4.0,'as=',f5.2,
1 ' ap=',f5.2,' pcm=',f7.3)
640 format (' e lab=',f5.1,' charge ',f3.0,'alpha ',f5.0)
671 format (' n=',i3,' to ',f6.2,' fm')
660 format (' l k eta s-matrix coul s '

```

```
1 , ' cap ' )  
680 format (2e15.5)  
690 format (i5,3f10.5)  
700 format (f7.3,2e11.4,4e11.4)  
710 format (i3,6f7.4,4f10.4)  
end
```

APPENDIX E  
SAMPLE OUTPUT RESULTS OF CARBON CODE

```

number of shells = 2
ssj= 1.5000 0.5000 0.0000 0.0000
ssl= 1.0000 1.0000 0.0000 0.0000
llm= 2 lls= 3
delta theta= 5 number ang pts= 19
iat (=1 for angle xf)= 1 ipi0 (=1 for pi0 dist)= 1
6.0000 12.0000 0.0800 3.5000 3.5000 500.0000 4.0000 1
0 0 0 0 0 0
100 0 10 8.0000 120.0000 1.0000 3.8000
using rowe-saloman amplitudes
pion lab momen= 218.87 exitat energy= 4.00 tlab= 120.00 initial kcm= 213.98
final kcm= 209.29 209.29
li= 213.9800 lf= 209.2944 cmi= 174.4015 cmf= 170.9957
operator angle transform, atfs= 0.8
operator angle transform, atfs= 0.8
cpl0= -0.18010 -0.00034 cpl1= 0.78491 0.50921 cplf= 0.42340 0.25250
cz0= -0.18037 -0.00095 cz1= 0.79785 0.46845 czf= 0.42744 0.23233
L= 1 EB= 8.2509 RMS= 2.9285 VV=37.4
C= 3.1332 SA= 0.5000 A= 14.0 Z= 0.0
this is an extra line
L= 1 EB= 8.2509 RMS= 2.9285 VV=37.4
C= 3.1332 SA= 0.5000 A= 14.0 Z= 0.0
this is an extra line
L= 1 EB= 4.7960 RMS= 3.0198 VV= 37.50
C= 3.1332 SA= 0.5000 A= 14.0 Z= 7.0
this is another extra line
L= 1 EB= 4.7960 RMS= 3.0198 VV= 37.50
C= 3.1332 SA= 0.5000 A= 14.0 Z= 7.0
this is another extra line
rrmax 6.48 nnmax 325
c00,c01,c10,c11 0.0488 0.0003 -0.1439 -0.0848 -0.1407 -0.0924 0.2581 0.5153
using l dependent optical model strengths
4 0 4.50 3.88
wabs= 8.900delm= 0.000 sperc= 0.000 quench= 1.00
interm momentum= 1.08435
wabs= 8.900 aki= 1.084 akf= 1.061 akcmi= 0.884akcmf= 0.866 xf=0.00
q= 1 z= 8 n= 8 a= 16 paul 1
20 tlab120.0 r 4.5 rms 2.7
-2-0.2170 0.0070 0.6120 0.4000-0.1000 0.0000 0.0040 0.7800
-1-1.0070 0.4320 8.4250 6.0910
0-0.9900 0.2240 5.4980 3.4050

```

1-1.0330 0.2350 6.3830 3.0640  
 2-1.0010 0.2850 5.9670 3.6280  
 3-0.9230 0.3920 6.7880 3.6060  
 4-0.7860 0.3290 8.2190 4.6230  
 5-0.6060 0.2580 8.0210 2.9160  
 6-0.3930 0.1810 7.3900 1.5710  
 7-0.2210 0.1180 6.5750 0.6920  
 8-0.2210 0.1180 6.5750 0.6920  
 9-0.2210 0.1180 6.5750 0.6920

z= 6. a= 12.as= 3.50 ap= 3.50 pcm= 1.084

ssl= 1.0000 1.0000 0.0000 0.0000

chg density from sick and mccarthy for a=12.

e lab=120.0 charge 1.alpha 500.

n=100 to 8.00 fm

*l k eta s - matrix couls cap*

0 1.0843 0.0523-0.1220-0.1365 0.9982-0.0602 0.4048 -0.3680  
 1 1.0843 0.0523 0.0699-0.0260 0.9990 0.0442 0.3387 0.3503  
 2 1.0843 0.0523 0.2501 0.1446 0.9953 0.0963 -0.3202 0.2652  
 3 1.0843 0.0523 0.5810 0.2916 0.9914 0.1310 -0.8383 -0.2076  
 4 1.0843 0.0523 0.8621 0.2463 0.9876 0.1568 -0.3314 -0.0998  
 5 1.0843 0.0523 0.9688 0.2001 0.9841 0.1774 0.6860 0.0652  
 6 1.0843 0.0523 0.9793 0.1981 0.9809 0.1946 1.2070 0.1208  
 7 1.0843 0.0523 0.9778 0.2094 0.9779 0.2092 1.1464 0.1214  
 8 1.0843 0.0523 0.9751 0.2219 0.9751 0.2219 0.8105 0.0911  
 9 1.0843 0.0523 0.9724 0.2332 0.9724 0.2333 0.4687 0.0554

*l k eta s - matrix couls cap*

0 1.0605-0.0534-0.1433-0.0959 0.9981 0.0615 0.3582 -0.4024  
 1 1.0605-0.0534 0.0452-0.0316 0.9990-0.0452 0.3708 0.3172  
 2 1.0605-0.0534 0.2565 0.0915 0.9951-0.0985 -0.2764 0.3058  
 3 1.0605-0.0534 0.6261 0.1321 0.9910-0.1339 -0.8478 -0.0986  
 4 1.0605-0.0534 0.8946-0.0350 0.9871-0.1603 -0.3145 -0.0476  
 5 1.0605-0.0534 0.9771-0.1552 0.9834-0.1814 0.7187 -0.0614  
 6 1.0605-0.0534 0.9799-0.1952 0.9800-0.1989 1.2104 -0.1194  
 7 1.0605-0.0534 0.9769-0.2136 0.9769-0.2138 1.1209 -0.1211  
 8 1.0605-0.0534 0.9739-0.2269 0.9739-0.2268 0.7750 -0.0891  
 9 1.0605-0.0534 0.9712-0.2384 0.9712-0.2384 0.4385 -0.0530  
 0 1.0843 0.0000-0.1376-0.1102 1.0000 0.0000 9.0687 10.0508  
 1 1.0843 0.0000 0.0495-0.0332 1.0000 0.0000 -8.8748 10.1024  
 2 1.0843 0.0000 0.2416 0.1136 1.0000 0.0000 -11.7161 -6.2119  
 3 1.0843 0.0000 0.5904 0.2157 1.0000 0.0000 1.7299 -12.8521  
 4 1.0843 0.0000 0.8803 0.1146 1.0000 0.0000 11.8077 -4.2459



```
5 1.0843 0.0000 0.9875 0.0277 1.0000 0.0000 9.7818 6.8960
6 1.0843 0.0000 0.9990 0.0044 1.0000 0.0000 1.5597 11.0656
7 1.0843 0.0000 0.9999 0.0004 1.0000 0.0000 -5.0222 8.7476
8 1.0843 0.0000 1.0000-0.0001 1.0000 0.0000 -7.2948 4.5512
9 1.0843 0.0000 1.0000 0.0000 1.0000 0.0000 -6.4615 1.5895
e lab=120.0 charge 1.alpha 500.
wabs0= 8.90 al0= 3.50 al1= 3.50 qvalue= 4.00 distortion core= 12.
th cs(nf) real imag cs real imag
0 7.286 -2.125 -1.713 2.723 -1.003 -1.334 0 0
5 7.008 -2.061 -1.708 2.619 -0.961 -1.324 0 0
10 6.233 -1.874 -1.692 2.330 -0.840 -1.295 0 0
15 5.131 -1.579 -1.659 1.926 -0.650 -1.244 0 0
20 3.927 -1.201 -1.604 1.499 -0.407 -1.170 0 0
25 2.838 -0.768 -1.520 1.137 -0.132 -1.070 0 0
30 2.022 -0.315 -1.403 0.896 0.153 -0.945 0 0
35 1.541 0.125 -1.249 0.794 0.423 -0.795 0 0
40 1.366 0.522 -1.060 0.808 0.660 -0.626 0 0
45 1.397 0.848 -0.842 0.889 0.845 -0.442 0 0
50 1.508 1.085 -0.605 0.977 0.967 -0.253 0 0
55 1.587 1.222 -0.360 1.022 1.020 -0.069 0 0
60 1.560 1.257 -0.123 0.996 1.004 0.101 0 0
65 1.408 1.196 0.092 0.897 0.926 0.246 0 0
70 1.157 1.053 0.272 0.743 0.795 0.358 0 0
75 0.861 0.845 0.407 0.565 0.625 0.433 0 0
80 0.582 0.595 0.491 0.397 0.432 0.468 0 0
85 0.370 0.324 0.523 0.263 0.232 0.464 0 0
90 0.252 0.055 0.504 0.178 0.040 0.424 0 0
```

